Author:
Beh, Kian Chung

Title:
Resource Allocation for the Long Term Evolution (LTE)of3G

Resource Allocation for the Long Term Evolution (LTE) of 3G

Kian Chung Beh

A thesis submitted to the University of Bristol in accordance with the requirements of the Degree of Doctor of Philosophy in the Faculty of Engineering

Department of Electrical and Electronic Engineering

November 2009

Abstract

Long Term Evolution (LTE) is the next major step in mobile radio communications and is currently introduced as Release 8 in the 3rd Generation Partnership Project (3GPP). The new evolution aims to reduce delay, improve spectrum flexibility and further reduce the cost for operators and end users. In order to fulfil the target of achieving high throughput, LTE employs Orthogonal Frequency Division Multiplexing (OFDM) as the physical layer transmission technique in the downlink. OFDM is suitable for high data rate transmission in wideband wireless systems due to its spectral efficiency and good immunity to multipath fading.

LTE enables multiple user access through an Orthogonal Frequency Division Multiple Access (OFDMA) scheme. In OFDMA, multiple user access is enabled by sharing the subcarriers among different users. The division of the system bandwidth between multiple users opens up an additional dimension in the frequency domain which can be exploited for diversity purposes. In addition to that, two MIMO techniques are adopted in LTE, namely space frequency block coding (SFBC) and Spatial Multiplexing (SM). The adaptation of the spatial multiplexing technique in LTE creates additional freedom in the resource allocation in the downlink. By employing a transmit precoding technique, spatial layers can be scheduled to different users and an additional layer of diversity in the space domain can be achieved. The additional layer of diversity can further increase the diversity gain that be achieved in the frequency and time domains.

This thesis mainly addresses the gain that can be achieved by resource allocation in the time, frequency and spatial domains in LTE. A detailed performance analysis on the physical layer of LTE downlink will be presented for both SISO and MIMO scenarios. A unitary precoding technique is also considered. Some well known and commonly used scheduling and resource allocations algorithms are investigated and presented. In addition to that, several novel scheduling and resource allocation algorithms are proposed and presented. Simulation results have shown that considerable improvement in terms of throughput performance or complexity can be observed. In particular, a diversity gain of up to 10dB can be achieved in the downlink when resource allocation algorithms are employed for a MU-MIMO scenario. In short, this thesis aims to give a detailed analysis on the diversity gain that can be achieved in the OFDMA system and the possible trade-off between the diversity gain in three dimensions as well as the signalling overhead.

Dedication

To my grandfather, late Beh Kai Phong

To my parents, Beh Kok Hai and Hey Soy Moy

Acknowledgements

First of all, I would like to express my heartfelt gratitude to both of my supervisors, Dr. Angela Doufexi and Dr. Simon Armour. Without them, I will not come to a stage where I am standing now, completing my PhD and expressing my appreciations. Especially, I would like to thank Dr. Angela Doufexi for her dedication and patience over the past few years. She has been absolutely a devoted supervisor, whom embraces me with valuable insights to guide me through my PhD. I would also like to show same amount of thankfulness to Dr. Simon Armour for all his dedication and encouragements throughout my studies. His insightful and enlightening supervision has been of great importance in the completion of my PhD.

I would like to take this opportunity to thank Professor Joe McGeehan and Professor Mark Beach for their help at providing financial supports (by Mobile VCE and EPSRC) for my PhD studies. Besides that, my appreciation also goes to coordinators and colleagues from MVCE, including Dr. Walter Tuttlebee, Prof. Rahim Tafazolli, Dr Tim Moulsley, Dr. Vasilis Friderikos, Dr. John Thompson and Dr. Tim Harrold for all their helps. In addition to that, I would also like to expression my gratefulness to my CCR colleagues. They have been very helpful at my work. Among them are Yugang Jia, Bernice Han, Mai Tran, Xiaolin Chen, Yuwen Pan, Marios Nicolaou and Gillian Huang.

I would also like to mention some of my friends whom have given supports and care selflessly. I must say their care and love strengthen my belief to accomplish my PhD. Among them are Jianru Yu, Jie Ma, Xinlun Cai and Seiw Li Yap.

Last not but least, I would like to thank everyone including departmental staffs, CCR colleagues and friends from Hodgkin House, who made my PhD life a pleasant and an enjoyable one.

Author's Declaration

I declare that the work in this dissertation was carried out in accordance with the Regulations of the University of Bristol. The work is original, except where indicated by special reference in the text, and no part of the dissertation has been submitted for any other academic award. Any views expressed in the dissertation are those of the author.

SIGNED: ..... DATE:.....

Table of Contents

List of Figures

List of Tables

List of Abbreviations

1G	First Generation
2G	Second Generation
3G	Third Generation
3GPP	3rd Generation Partnership Project
3GPP2	Third Generation Partnership Project 2
4G	Fourth Generation
ACK	Acknowledgement
AMC	Adaptive Modulation and Coding
AMPS	Analogue Mobile Phone System
ARQ	Automatic Retransmission Request
AWGN	AWGN
BER	Bit Error Rate
BS	Base Station
CC	Chase Combining
CP	Cyclic Prefix
CDF	Cumulative Distribution Function.
CDMA	Code Division Multiple Access
CRC	Cyclic Redundancy Check
CSI	Channel State Information
DSA	Dynamic Sub-carrier Allocation
DVB	Digital Video Broadcasting
E_b/N_o	Bit Energy to Noise Power
EDGE	Enhanced Data rates for GSM Evolution
DFT	Discrete Fourier Transform
DPC	Dirty paper coding
ETSI	European Telecommunications Standards Institute
EV-DO	Evolution-Data Optimised
FD	Frequency Domain
FDD	Frequency Division Duplex
FEC	Forward error correction
FFT	Fast Fourier Transform

FSA	Fixed Subcarrier Allocation
GA	Greedy Algorithm
GPRS	General Packet Radio Service
GSM	Global System for Mobile Communications
HARQ	Hybrid Automatic Retransmission Request
HSDPA	High-Speed Downlink Packet Access
HSPA	High Speed Packet Access
HTTP	Hypertext Transfer Protocol
ICI	Inter Carrier Interference
IFFT	Inverse Fast Fourier Transform
IMT	International Mobile Telecommunications
IR	Incremental Redundancy
ISI	Inter-Symbol Interference
ITU	International Telecommunication Union
JTAC	Japanese Total Access Communication System
LAN	Local Area Network
LOS	Line of Sight
LTE	Long Term Evolution
MAC	Medium Access Control
MAP	Maximum a Posteriori
MCS	Modulation and Coding Scheme
MGSS	Maximum Gain Sort-Swap
MIMO	Multiple Input Multiple Output
MMSE	Minimum Mean Square Error
MRC	Maximal Ratio Combining
MRW	Maximum Ratio Weighted
NACK	Negative Acknowledgement
NMT	Nordic Mobile Telephone
OFDM	Orthogonal Frequency Division Multiplexing
OFDMA	Orthogonal Frequency Division Multiple Access
PDF	Probability Density Function
PDP	Power Delay Profile
PER	Packet Error Rate
PF	Proportional Fair

PHY	Physical
PL	Path Loss
PRB	Physical Resource Block
PU2RC	Per User Unitary and Rate Control
QAM	Quadrature Amplitude Modulation
QoS	Quality of Service
QPSK	Quadrature Phase Shift Keying
RCPC	Rate Compatible Punctured Convolutional
RCPT	Rate Compatible Punctured Turbo
RMS	Root Mean Square
RR	Round Robin
SC-FDMA	Single Carrier – Frequency Division Multiple Access
SCM(E)	Spatial Channel Model (Extension)
SINR	Signal to Interference and Noise Ratio
SISO	Single Input Single Output
SM	Spatial Multiplexing
SNR	Signal to Noise Ratio
STBC	Space-Time Block Code
SVD	Singular Value Decomposition
TACS	Total Access Communication Systems
TD	Time Domain
TDD	Time Division Duplex
TDMA	Time Division Multiple Access
TD-SCDMA	Time Division – Synchronous Code Division Multiple Access
UE	User Equipment
UMTS	Universal Mobile Telecommunications System
V-BLAST	Vertical Bell Labs Layered Space-Time
WCDMA	Wideband Code Division Multiple Access
WIMAX	Worldwide Interoperability for Microwave Access
WLAN	Wireless Local Area Network
ZF	Zero Forcing

List of Publications

K.C.Beh, A.Doufexi, S.Armour, 'Performance Evaluation of Hybrid ARQ Schemes of 3GPP LTE ODFMA System', *in Proceedings of International Symposium on Personal, Indoor and Mobile Radio Communications* (PIMRC), September 2007, pp 1-5

K.C.Beh, S.Armour ,A.Doufexi, 'Joint Time-Frequency Domain Proportional Fair Scheduler with HARQ for 3GPP LTE Systems', *in Proceedings of Vehicular Technology Conference*, Calgary, October 2008, pp1-5

K.C.Beh, A.Doufexi, S.Armour, 'A Low Complexity Dynamic Resource Allocation Algorithm for 3GPP LTE Based on a Maximal Ratio Weighted Metric with Limited Feedback', *in Proceedings of NEWCOM++/COST2100 Workshop on Radio Resource Assignment for LTE'*, Vienna, September 2009

K.C.Beh, C.Han, M.Nicolaou, S.Armour, A.Doufexi, "Power Efficient MIMO Techniques for 3GPP LTE and Beyond," *invited paper at special session on Green Radio at Vehicular Technology Conference*, Alaska, September 2009

K.C.Beh, A.Doufexi, S.Armour, 'On the Performance of SU-MIMO and MU-MIMO in 3GPP LTE Downlink', *in Proceedings of International Symposium on Personal, Indoor and Mobile Radio Communications* (PIMRC), Tokyo, September 2009

K.C.Beh, S.Armour ,A.Doufexi, 'A Modified Partial Feedback scheme for Multi-User MIMO' *submitted to VTC 2010 Spring*

C.Han, K.C.Beh, M.Nicolaou, S.Armour, A.Doufexi, 'Dynamic Resource Scheduling and Allocation Algorithms for LTE', *submitted to VTC 2010 Spring*

M.Nicolaou, C.Han, K.C.Beh, S.Armour, A.Doufexi, 'MIMO Techniques for Green Radio Guaranteeing QoS', *Accepted in Journal of Communications and Networks (JCN) Special Issue On Green Radio: Energy Efficiency In Wireless*

Chapter 1

Introduction

1.1 Current and Next Generation Wireless Communication Technology

Over the last decade, the growth of wireless services such as mobile internet telephony, multimedia services and mobile broadband has laid a higher expectation on wireless networks. However, a wireless link is not able to achieve the same performance as a wired network, especially in terms of throughput and reliability. The wireless link becomes the performance bottleneck for several reasons. Mostly, it is due to the dynamic nature of wireless medium where the channels condition changes rapidly due to time-varying fading, distance and interference. The inherent problems of wireless channels have imposed great challenges to the researchers and system engineers.

In the late 1980s, some large scale commercial cellular networks were deployed across different continents in the world. These cellular networks include Analogue Mobile Phone System (AMPS-used in America), Total Access Communication Systems (TACS –used in parts of Europe), Nordic Mobile Telephone (NMT- used in parts of Europe), and Japanese Total Access Communication System (J-TACS – used in Japan and Hong Kong)[1][2]. These cellular standards were often known as first generation (1G) systems and were developed independently across different continents. The first generation systems mainly used analogue technology and suffered from some weaknesses, especially in terms of security. Since it was an analog standard, it was very susceptible to static and noise and has no protection from eavesdropping using a scanner. The mobile industry suffered losses due to cloning problems with the first generation phones.

The inherent drawbacks of the analogue first generation system drove development of digital second generation systems, such as GSM (Global System for Mobile Communications) [2][3]. Most development and standardization work on GSM was done under the auspices of European Telecommunications Standards Institute (ETSI). GSM is

the most the successful cellular system to date. It is estimated that 80% of the current mobile market is using GSM [4]. GSM is used by over 3 billion people across more than 212 countries and territories. The ubiquity of GSM makes international roaming very simple and common between mobile phone operators. This enables subscribers to use their phones in many parts of the world seamlessly. The market for GSM is still growing, especially in third world developing countries, where fixed line connectivity is non-existent and it would be cost effective to deploy a cellular network rather than a fixed line network.

In the mid 1990s, an evolution path for the GSM was establishd, which is known as General Packet Radio Service (GPRS), also known as 2.5G. GPRS supports a much better data rate of up to a theoretical maximum of 140.8 kbps. GPRS is packet switched rather than a conventional (at that time) connection oriented circuit switched network. It is deployed in many places where GSM is used since it is fully backward compatible. Not long after that, an enhanced GPRS (E-GPRS), or Enhanced Data rates for GSM Evolution (EDGE) was introduced to further increase the data rate by using more efficient coding and modulation schemes.

However, the demand for higher speed connectivity continued to increase, especially due to the rise of multimedia services and mobile internet. The second generation systems at that time were not able to cope with the ever increasing speed requirement. At the end of the 1990s, a third generation system was first proposed by 3rd Generation Partnership Project (3GPP). 3GPP is a collaboration between groups of telecommunications associations to produce a globally applicable third generation (3G) mobile phone system specification within the scope of the International Mobile Telecommunications-2000 (IMT-2000) project of the International Telecommunication Union (ITU). ITU is one of the specialised agencies of the United Nations and plays a most central role in standardization, allocation of the radio spectrum and organizing interconnection arrangements between different countries to allow international phone calls.

Universal Mobile Telecommunications System (UMTS) is one of the third-generation (3G) mobile telecommunications technologies. The name UMTS, introduced by ETSI, is mainly used in Europe but it is more widely known as W-CDMA across the world. Most UMTS handsets support GSM, which allow seamless dual-mode operation between 2G and 3G operations. This is an important feature of 3G systems, which supports backward compatibility with older generation system. Other third generation systems include

CDMA2000 [5] which is mainly used in North America and TD-SCDMA [6] which is being deployed in China.

3GPP standards are structured as *Releases*. The first release of the UMTS is called *Release 99* (*R99*). *R99* can support up to 384kbps at the downlink, which is a tremendous improvement compared to the second generation system. Several releases have been specified as enhancements to the first release. Among them are *Release 5* (High-Speed Downlink Packet Access- HSDPA) and *Release 6* (High-Speed Uplink Packet Access- HSUPA). HSDPA supports high speed connectivity in the downlink, with a peak data rate of 14.4 Mbps. HSUPA was introduced later than HSDPA, with a maximum uplink speed of 5.76Mbps. HSDPA and HSUPA together are known as High Speed Packet Access (HSPA). The latest release from 3GPP, *Release 7* is known as Evolved High-Speed Packet Access (HSPA+). *Release 7* can support up to 44Mbps in the downlink and 22 Mbps in the uplink. HSPA+ is gradually being deployed in certain parts of Europe, Australia and USA to provide a truly high speed cellular network.

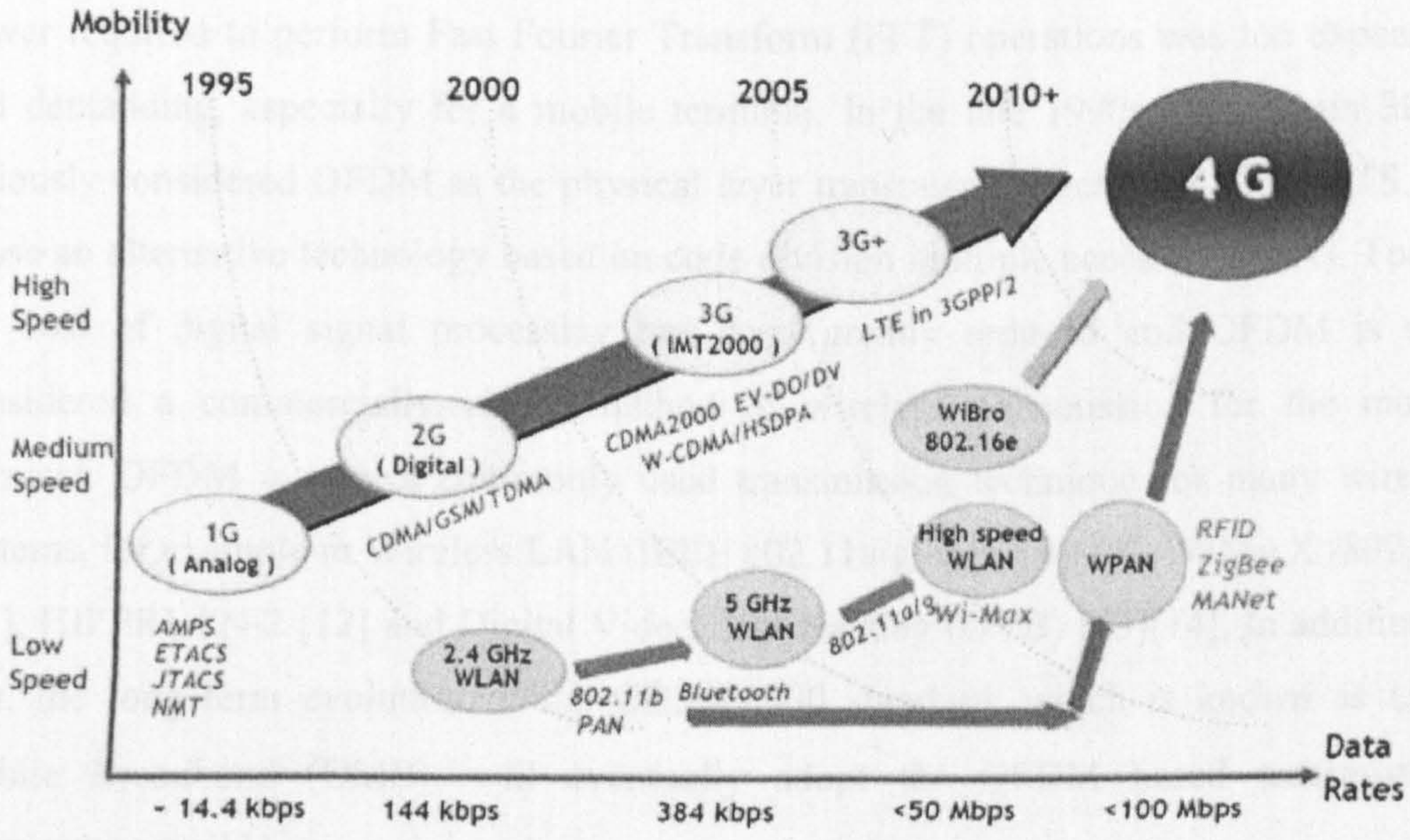

Figure 1-1: Mobile Communication Roadmap [25]

However, facing stiff competition from other wireless technology such as IEEE 802.16 based broadband wireless access standard (or more widely known as WIMAX), there is a need to further improve the speed and versatility of the network. A long term evolution of the current 3G system was proposed in the year 2004. The Long Term Evolution, often known as LTE, is a last step toward a fourth generation (4G) of radio technologies designed to increase the capacity and speed of mobile telephone networks. LTE will be

introduced as *Release 8* in the 3GPP. One of the main targets of LTE is to achieve at least 100Mbps in the downlink and 50Mbps in the uplink. However, LTE still does not meet the requirement of a fourth generation (4G) system defined by the IMT-Advanced project. An enhancement to LTE, known as LTE-Advanced will be released as 4G, but it will only occur in the year 2011. A roadmap showing the history of mobile radio communication is illustrated in Figure 1-1.

1.2 Cross-Layer Resource Allocation in LTE

Feasibility studies of LTE started in 2005. Several physical layer transmission techniques have been proposed to the 3GPP. However, it very was soon decided an that an Orthogonal Frequency Division Multiplexing (OFDM) [7] based physical layer transmission technique would be used. Although OFDM existed for many years in communication systems, its use in mobile devices only occurs very recently. The European Telecommunications Standards Institute (ETSI) first looked at OFDM as a possible candidate for GSM back in the late 1980s. However at that time, the processing power required to perform Fast Fourier Transform (FFT) operations was too expensive and demanding, especially for a mobile terminal. In the late 1990s, once again 3GPP seriously considered OFDM as the physical layer transmission technique for UMTS, but chose an alternative technology based on code division multiple access (CDMA). Today, the cost of digital signal processing has been greatly reduced and OFDM is now considered a commercially viable method of wireless transmission for the mobile terminal. OFDM is now a commonly used transmission technique for many wireless systems, for example in Wireless LAN (IEEE 802.11a/g/n) [8][9][10], WIMAX (802.16e) [11], HIPERLAN-2 [12] and Digital Video Broadcasting (DVB) [13][14]. In addition to that, the long term evolution of the CDMA2000 standard, which is known as Ultra Mobile Broadband (UMB), will eventually adopt the OFDM based transmission technique as well [1].

OFDM appears to be a very attractive choice for LTE as this technique can help to fulfil the target of achieving high throughput. OFDM is suitable for high data rate transmission in wideband wireless systems due to its spectral efficiency and good immunity to multipath fading. OFDM converts a wideband channel into several parallel narrowband subcarriers through an IFFT/FFT processing in the transmitter and receiver. The use of the narrowband subcarriers in combination with a cyclic prefix makes OFDM

transmission robust to frequency selective fading [7] as well as eliminating the need for a complex equalization process at the receiver side.

In HSDPA, a fast packet scheduling over the radio interface was already enabled. Transmission of short packets with a duration of a same order as the coherence time of the fading channel is possible, as shown in Figure 1-2. In HSDPA, several new techniques have been introduced, such as fast channel state information, dynamic link adaptation, scheduling exploiting multiuser diversity and fast retransmission protocol (Hybrid Automatic Retransmission Request) [15][16]. These features bring a high throughput capability to the existing 3G network. However in HSDPA, a conventional circuit switch resource allocation is still maintained alongside the fast adaptive packet scheduling. LTE is a completely packet-switched network, without the support for the circuit-switch connection-oriented protocols as seen in previous releases [17].

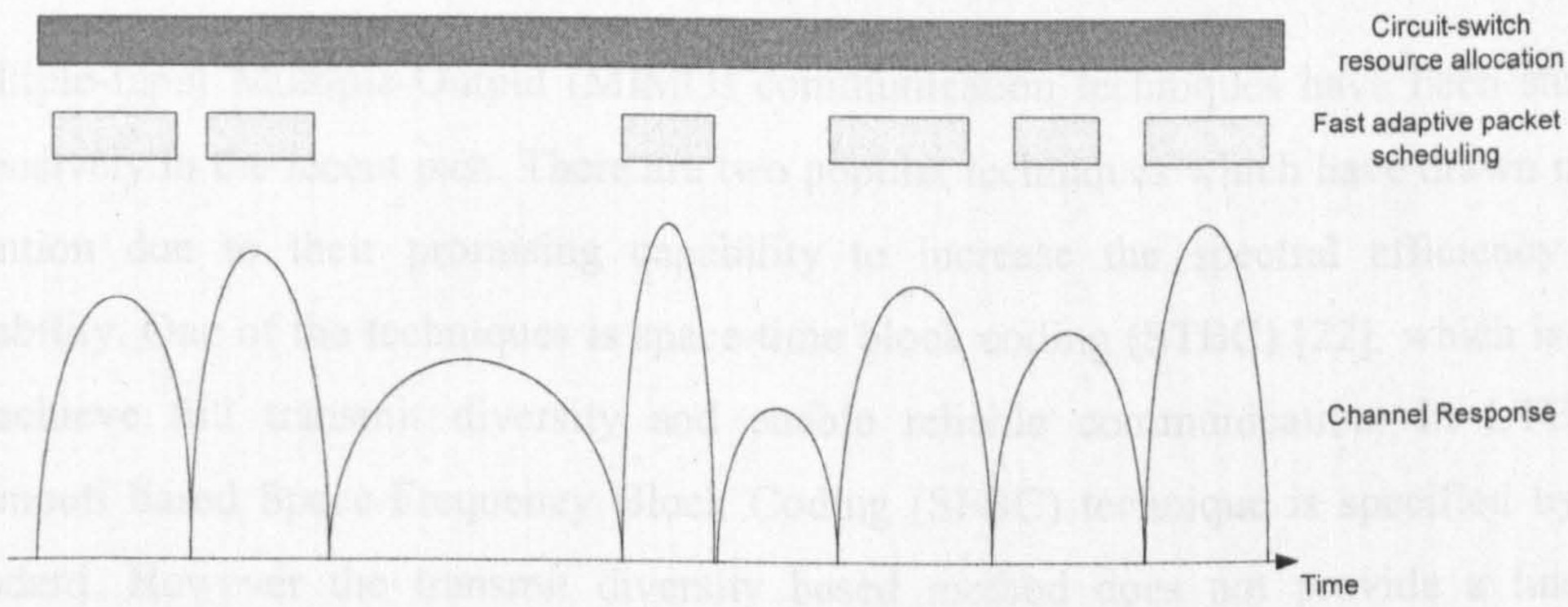

Figure 1-2: Fast Packet Scheduling

LTE enables multiple user access through an Orthogonal Frequency Division Multiple Access (OFDMA) [18][19] scheme. OFDMA is an extension of the OFDM technique. In a convention OFDM system, all the available subcarriers will be allocated to a single user. Multiple user access is only possible in the time domain e.g. via Time Division Multiple Access (TDMA) scheme as in a wireless LAN (e.g. 802.11a) network. However in OFDMA, multiple user access is enabled by sharing the subcarriers among different users. The division of the system bandwidth between multiple users opens up an additional dimension in frequency domain which can be exploited for diversity purposes.

The OFDMA based physical layer transmission technique has been considered as the most promising technique recently and this technique will be heavily used for the

foreseeable future. The OFDMA based physical layer transmission technique selected for a number of different reasons. First of all, resources of variable bandwidth can be allocated to different users and this leads to a better resource management and better quality of service (QoS) control. On top of the diversity in the time domain, an additional layer of diversity can be achieved in the frequency domain by allocating subcarriers to user who is experiencing good channels. An example of resource allocation in OFDMA based system is shown in Figure 1-3. In addition to that, the packet duration was further reduced from 2ms in HSDPA down to 1ms in LTE [17][20]. The short transmission interval can better capture the benefits of time and/or frequency selectivity of the channel fading. The short transmission interval coupled with the new dimension of frequency diversity has further consolidated the need for a cross layer interaction [21] between Medium Access Control (MAC) and physical (PHY) layers. Through cross layer interaction, the MAC layer can exploit and/or mitigate features of the physical environment of the air interface and thus improve the system performance.

Multiple-Input Multiple-Output (MIMO) communication techniques have been studied extensively in the recent past. There are two popular techniques which have drawn much attention due to their promising capability to increase the spectral efficiency and reliability. One of the techniques is space-time block coding (STBC) [22], which is able to achieve full transmit diversity and enable reliable communication. In LTE, an Alamouti based Space-Frequency Block Coding (SFBC) technique is specified by the standard. However the transmit diversity based method does not provide a linearly increasing channel capacity with the number of transmit and receive antennas. Another technique that is also included in the LTE standard is spatial multiplexing (SM) [23], which aims to increase the ultimate spectral efficiency by transmitting independent parallel data streams over multiple antennas.

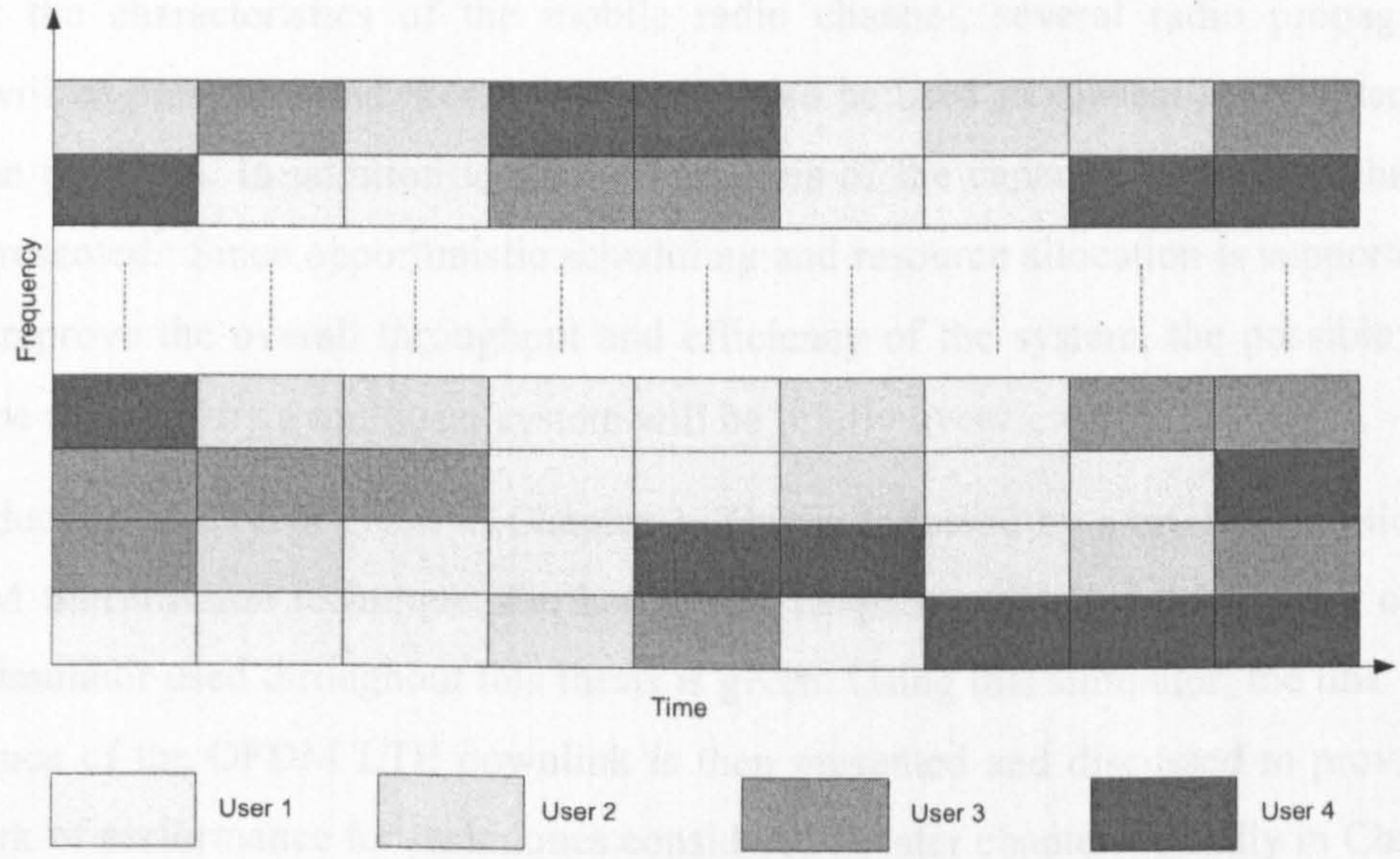

Figure 1-3: Example of resource allocation in an OFDMA system

The adaptation of the spatial multiplexing technique in LTE creates additional freedom in the resource allocation in the downlink. By employing a transmit precoding technique [24], spatial layers can be scheduled to different users and an additional layer of diversity in space domain can be achieved. The additional layer of diversity can further increase the diversity gain that be achieved in the frequency and time domains. This further extended the need for cross layer interaction between the MAC and PHY layers. However, the gain of resource allocation in frequency, time and space domains can only be achieved by very sophisticated control signalling in the uplink. The control signalling in the uplink is an important research challenges in LTE, to make resource allocation in LTE a viable working model.

1.3 Thesis Outline

This thesis mainly addresses the gain that can be achieved by resource allocation in an OFDMA system. As mentioned earlier, diversity gain in three dimensions can be exploited. LTE is chosen as the evaluation platform since this is the latest release of the cellular network and is widely considered by the research community at the moment. This thesis aims to give a detailed analysis on the diversity gain that can be achieved in the ODFMA system and the possible trade-off between the diversity gain in three dimensions as well as the signalling overhead.

Chapter 2 presents the fundamentals of mobile radio propagation. Some interesting properties of the mobile radio propagation will be characterised. In order to accurately

represent the characteristics of the mobile radio channel, several radio propagation models will be presented and these models will also be used in subsequent chapters for evaluation purposes. In addition to that, an analysis of the capacity of a radio channel will be presented. Since opportunistic scheduling and resource allocation is supported in LTE to improve the overall throughput and efficiency of the system, the possible gain that can be achieved by a multiuser system will be briefly overviewed.

An introduction to LTE is given in Chapter 3. This is followed by a brief description of an OFDM transmission technique. Further in that chapter, a detailed description of the OFDM simulator used throughout this thesis is given. Using this simulator, the link level performance of the OFDM LTE downlink is then presented and discussed to provide a benchmark of performance for techniques considered in later chapters. Finally in Chapter 3, some popular Hybrid Automatic Retransmission Request (ARQ) techniques are presented together with performance analysis.

Chapter 4 presents some popular scheduling algorithms that are commonly used in a cellular network. Firstly, the performance of a conventional proportionally fair scheduler is evaluated in the downlink of LTE. A modified joint time-frequency proportional scheduler is proposed. The proposed scheduler aims to strike a balance between diversity gain in time and frequency domains. A detailed performance analysis of the proposed algorithm is presented. In addition to that, a performance of various mapping strategies in link adaptation is considered. Based on the performance of different mapping strategies, a modified proportional fair scheduler which takes into account the HARQ mechanism is proposed. Detailed simulation results and analysis are again presented.

Since Chapter 4 mainly considers a joint time and frequency domain scheduling strategy, the focus is shifted to the resource allocation strategy in the frequency domain only in Chapter 5. In particular, attention has been given on how to achieve a near optimum resource allocation performance. It is well known that an optimum resource allocation strategy is computationally expensive and not practical for actual implementation. In order to achieve a near optimal performance, two heuristic but simple resource allocation algorithms are proposed. In particular, a maximal ratio weighted metric is proposed to help achieve the goal. Some popular techniques including optimal and sub-optimal algorithms are also presented for comparison purposes.

Chapter 6 provides an overview of the MIMO techniques that are adopted in LTE, such as space frequency block coding (SFBC) and Spatial Multiplexing (SM). A detailed link

level performance for both MIMO techniques is given. In particular, the performance of both schemes in different spatial correlated channels will be evaluated. An analysis on the throughput performance with ideal link adaptation will also be presented. It aims to examine how some of the LTE's targets such as peak data rate can be achieved. Lastly in this chapter, the performance of HARQ in MIMO schemes is investigated.

Chapter 7 will investigate the performance of a Single User MIMO (SU-MIMO) scheme and a Multi User MIMO(MU-MIMO) scheme in the downlink of LTE. A unitary[+] precoding method based on Discrete Fourier Transform is proposed in the downlink of LTE. The performance of this precoding technique will be evaluated and compared to a singular value decomposition (SVD) method in this thesis. In addition to that, performance of both the SU-MIMO and the MU-MIMO using frequency domain resource allocation will be analysed. Two feedback schemes, namely full feedback and partial feedback scheme are considered, modified partial feedback scheme is proposed and the performance is evaluated.

Last but not least, Chapter 8 will give a conclusion of the thesis. Important analysis and research findings will be summarized and presented. Future work will be outlined as a possible extension to the current work.

1.4 Key Contributions

It is anticipated that the output of this thesis could contribute to the development of LTE especially in the aspect of resource allocation and scheduling. In this section, some of the significant research outputs are highlighted as possible contributions.

- A detailed performance analysis of the physical layer of LTE downlink is presented. The performance analysis is useful in helping the design of the link budget, network planning, and resource management.
- A detailed performance analysis of several popular HARQ schemes is investigated in the downlink of LTE for both SISO and MIMO scenarios.

[+] A unitary matrix is an n by n complex matrix U satisfying the condition $U^*U = UU^* = I_n$, where I_n is the identity matrix in n dimension and U^* is the conjugate transpose of U.

- A modified proportionally fair scheduler which considers the retransmission information is proposed.

- A joint time-frequency domain scheduler is proposed. The proposed scheduler combines a proportionally fair scheduler in the time domain with an aggressive frequency domain resource allocation algorithm.

- Two heuristic resource allocation algorithms are proposed to maximise the throughput given an equal share constraint. The algorithms works on a maximal ratio weighted metric and achieve a near optimal performance with low computational complexity.

- A detailed performance analysis on the performance of SU-MIMO and MU-MIMO in the downlink of LTE is presented.

- A modified partial feedback scheme for MU-MIMO which exploits the difference of the received SINR of different precoding matrices is proposed.

References

[1] Theodore S.Rapport, ' Wireless Communications: Principles and Practise', 2nd Edition, Prentice Hall PTR , 2002

[2] S.Sesia, I.Toufik, M.Baker, ' LTE The Long Term Evolution: From Theory to Practice,' John Wiley & Sons Ltd., 2009, pp243-282

[3] Online: http://www.3gpp.org/ftp/Specs/html-info/45-series.htm

[4] GSM Association, "GSM World statistics", 2007. Online: http://www.gsmworld.com/newsroom/market-data/market_data_summary.htm

[5] 3GPP2, 'Introduction to cdma2000 Standards for Spread Spectrum Systems', 2002, Online: http://www.3gpp2.org/Public_html/specs/C.S0001-C_v1.0.pdf

[6] Zheng Wenfu; Ma Yuanyuan; Kalle, L., "From Manufacturer-Driven to Carrier-Driven: Towards China's TD-SCDMA Commercialization Strategies," *Business and Information Management, 2008. ISBIM '08. International Seminar on* , vol.1, no., pp.93-97, 19-19 Dec. 2008

[7] OFDM for Wireless Multimedia Communications, Richard van Nee and Ramjee Prasad, Artech House, Boston and London, 2000.

[8] "IEEE Standard for Information technology--Telecommunications and information exchange between systems--Local and metropolitan area networks--Specific requirements Part 11: Wireless LAN Medium Access Control (MAC) and Physical Layer (PHY) Specifications Amendment 5: Enhancements for Higher Throughput," *IEEE Std 802.11n-2009*, vol., no., pp.c1-502, Oct. 29 2009

[9] "Supplement to IEEE standard for information technology telecommunications and information exchange between systems - local and metropolitan area networks - specific requirements. Part 11: wireless LAN Medium Access Control (MAC) and Physical Layer (PHY) specifications: high-speed physical layer in the 5 GHz band," *IEEE Std 802.11a-1999* , vol., no., pp.-, 1999

[10] "IEEE standard for information technology- telecommunications and information exchange between systems- local and metropolitan area networks- specific requirements Part II: wireless LAN medium access control (MAC) and physical layer (PHY) specifications," *IEEE Std 802.11g-2003*, vol., no., pp.i-67, 2003

[11] "IEEE Standard for Local and metropolitan area networks Part 16: Air Interface for Fixed and Mobile Broadband Wireless Access Systems Amendment 2: Physical and Medium Access Control Layers for Combined Fixed and Mobile

Operation in Licensed Bands and Corrigendum 1," *IEEE Std 802.16e-2005 and IEEE Std 802.16-2004/Cor 1-2005 (Amendment and Corrigendum to IEEE Std 802.16-2004)* , vol., no., pp.0_1-822, 2006

[12] ETSI, "Broadband Radio Access Networks (BRAN); HIPERLAN type 2 technical specification; Physical (PHY) layer," August 1999. <DTS/BRAN-0023003> V0.k.

[13] ETSI, "Digital Video Broadcasting (DVB); Framing structure, channel coding and modulation for digital terrestrial television", June 2004.

[14] ETSI, "Digital Video Broadcasting (DVB); Transmission System for Handheld Terminals (DVB-H) ", Nov. 2004

[15] H. Holma, A. Toskala, ' WCDMA for UMTS – HSPA Evolution and LTE', 4th Edition, John Wiley & Sons, 2007

[16] E. Dahlman,S. Parkvall, J. Skold, P. Beming,' 3G Evolution: HSPA and LTE for Mobile Broadband', Academic Press, 2008

[17] 'Technical Specification Group Radio Access Network; (E-UTRA) and (E-UTRAN): Overall Description', 3GPP TS 36.300 V8.8.0, April 09. [Online]. Available: http://www.3gpp.org/ftp/Specs/html-info/36300.htm

[18] H. Sari, Y. Levy, and G. Karam, "An analysis of orthogonal frequency division multiple access," in *Proc. IEEE GLOBECOM*, vol. 3, Nov. 1997, pp. 1635–1642.

[19] Yin, Hujun; Alamouti, Siavash, "OFDMA: A Broadband Wireless Access Technology," *Sarnoff Symposium, 2006 IEEE* , vol., no., pp.1-4, 27-28 March 2006

[20] 'Technical Specification Group Radio Access Network;High Speed Downlink Packet Access (HSDPA);Overall description', 3GPP TS 25.308 V5.7.0, Dec. 04. [Online]. Available: http://www.3gpp.org/ftp/Specs/html-info/25308.htm

[21] Srivastava, V.; Motani, M., "Cross-layer design: a survey and the road ahead," *Communications Magazine, IEEE* , vol.43, no.12, pp. 112-119, Dec. 2005

[22] S. Alamouti, "A simple transmit diversity technique for wireless communications", IEEE JSAC, Vol. 16, No. 8, pp. 1451-1458, 1998

[23] Gerard J. Foschini, Glen D. Golden, Reinaldo A. Valenzuela, and Peter W. Wolniansky, "Simplified Processing for High Spectral Efficiency Wireless Communication Employing Multi-Element Arrays", IEEE Transactions on Selected Areas in Communications, Vol. 17, No. 11, Nov 1999

[24] S. J. Kim, H. J. Kim, C. S. Park, and K. B. Lee, "On the Performance of Multiuser MIMO Systems in WCDMA/HSDPA: Beamforming, Feedback and User Diversity," IEICE Transactions on Communications, vol. E98-B, no. 8, pp. 2161–2169, Aug. 2006.

[25] H. W. Lee, ' 3G LTE & IMT-Advance' , Presented at HSN 2006, Feb 2006

Chapter 2

Mobile Radio Propagation: Theory and Channels

In wireless transmission, a signal is transmitted from a transmitter to a receiver through wireless channels as a result of electromagnetic wave propagation. Different from a wired transmission, the wireless transmission is unstable and unpredictable due to the dynamic nature of the environment. The signal experiences various mechanisms of radio propagation such as attenuation, reflection, diffraction and scattering. A realistic channel propagation modelling is thus very important to evaluate a wireless system. In this chapter, a brief description of radio propagation will be presented and discussed.

Different scenarios such as rural, suburban, urban and indoor environments have different channel propagation characteristics. Different scenarios set different requirements for network planning, link budget, antenna configuration and preferred transmission mode. In this chapter, several commonly used radio propagation models will be presented. These models will then be used in the subsequent chapters for evaluation purposes.

For a radio channel with a single input signal and a single output signal (SISO) with a given bandwidth and transmit power, Shannon has shown that the performance limitation of a reliable communication is the channel capacity [1]. Firstly SISO channel capacity will be presented. Secondly, since Multiple input and Multiple output (MIMO) architecture has been included in LTE, channel capacity for the MIMO channels will also be presented. Finally, since opportunistic scheduling and resource allocation is also supported in LTE to improve the overall throughput and efficiency of the system, the possible gain that can be achieved by a multiuser system will be briefly overviewed.

2.1 Mobile Radio Propagation

Radiowave propagation and the associated fading characteristics need to be carefully considered when designing a modern mobile radio communications system. There are

two main fading phenomena than can be identified which affect the received signal properties. These fading effects can often be categorised into: large scale fading and small scale fading. These phenomena will be discussed in detail in the following section.

2.1.1 Large Scale Fading

Large scale fading refers to the average signal power attenuation or path loss due to motion over large areas. The large-scale fading is very much dependent on the distance of a receiver from a transmitter and its geographical location. This phenomenon is very much affected by prominent terrain contours, e.g. hills, buildings etc. between the transmitter and receiver. According to [2][3], large scale fading can mainly be categorised into two sub-parts: propagation path loss and shadowing.

2.1.1.1 Propagation Path Loss

Propagation path loss is a very important characteristic of the wireless channel. It significantly affects the average signal level at the receiver. If a receiver is far from a transmitter, the path loss will be large and vice versa. This is attributed to the nature of radio propagation. When a wireless signal is transmitted from a point source it travels in all directions, like a surface of a sphere. As the radius of the sphere increases, the surface area increases too. Since the transmit power is spread uniformly over the surface area, the power density (in terms of Watts per metre squared) reduces when the signal travels further from the source. The received power density is inversely proportional to the square of the receiver's distance from the transmitter (i.e. proportional to $1/d^2$, where d is the distance between transmitter and receiver).

In order to compute the received power from the received power density, an effective area of the receiving antenna needs to be calculated. The effective area is related to the operating frequency, and the physical construction of the antenna. The effective area of an antenna is given by:

$$A_i = G\lambda^2/4\pi \qquad (2\text{-}1)$$

where G represents the antenna gain (relative to an *isotropic* source), and λ represents the carrier wavelength. The carrier's frequency and wavelength are related by $c = f\lambda$, where f represents the carrier frequency and c the speed of light. The term isotropic means 'equal in all directions', and in this context an isotropic antenna is one that emits radiation equally and spherically. It should be noted that practical antennas tend to direct

radiation in particular directions (such as a sectorised antenna). When the transmit power is focused in particular directions, compared to an isotropic antenna, the received power density in those directions is higher. This results in an antenna gain G in these directions and the gain is usually greater than one.

Given P_T is the total transmit power, the following equation shows the received power P_R at a distance d from the transmitter:

$$P_R = \frac{P_T}{4\pi d^2} A_i = \frac{P_T}{4\pi d^2} \frac{\lambda^2}{4\pi} = P_T \left(\frac{\lambda}{4\pi d} \right)^2 \qquad (2\text{-}2)$$

This equation assumes that the power is transmitted isotropically. When a directional antenna is used, antenna gain can be achieved. G_T and G_R are used to represent the antenna gains (relative to an isotropic source) at the transmitter and receiver respectively. Thus the received power at the receiver, also known as Friss free space equation [2], can be rewritten as:

$$P_R = P_T G_T G_R \left(\frac{\lambda}{4\pi d} \right)^2 \qquad (2\text{-}3)$$

The propagation path loss is defined as the ratio or the transmitted power P_T to the receiver power P_R, and it can be represented (in dBs) as:

$$PL = \frac{P_T}{P_R} = 10 \log \left[G_T G_R \left(\frac{\lambda}{4\pi d} \right)^2 \right]^{-1} \qquad (2\text{-}4)$$

Since the path loss equation is commonly quoted for isotropic antennas, in which case the antenna gain terms can be omitted (since they are equal to unity), it can be given by:

$$PL = 10 \log \left(\frac{4\pi d}{\lambda} \right)^2 = 10 \log \left(\frac{4\pi df}{c} \right)^2 . \qquad (2\text{-}5)$$

However, the free space path loss model alone is not suitable to model the radio propagation in the real world. Free space path loss as its name suggests, can only accurately model the propagation loss when the transmit and receive antennas are in unobstructed free space, or with no multipath. These ideal conditions are almost never achieved in ordinary terrestrial or cellular communications, due to obstructions, reflections from buildings, and reflections from the ground. This equation can however

model the propagation in satellite communications or in anechoic chambers with reasonably accuracy [2].

In reality, the strength of the signal decays faster than a free space model, usually in an order of up to inverse power of 3 or 4, depending on the propagation environment. Several path loss models such as Walfish-Ikegami and Hata urban propagation model [10] have been suggested. In particular, these models are currently used in SCM, which will be explained in detail in a later section.

2.1.1.2 Shadowing

Diffraction is often termed shadowing because the diffracted field can reach the receiver even when shadowed by an impenetrable obstruction. Diffraction occurs when the propagation path between a transmitter and a receiver is obstructed by an impenetrable object, which dimension is large relative to the wavelength λ. This causes secondary waves to be formed behind the obstructing body [2][3].

Measurements have shown that at any value of *d*, (the distance of a transmitter from the receiver) the path loss at a particular location is random and log-normally distributed (normal in dB). That is given by:

$$PL_{(d)}^{shadow} = PL_{(d)} + X_{\sigma} \qquad (2\text{-}6)$$

where $PL_{(d)}$ is the path loss experienced at the receiver given a distance *d*. The path loss might follow a different path loss exponent *n*, depending on the path loss model. X_{σ} is a zero-mean Gaussian distributed random variable (in dB) with standard deviation σ (also in dB). The log-normal distribution [4] describes the random shadowing effect which is observed over a large number of measurement locations, which have the same distance from the transmitter, but with different terrain contours. Therefore, the shadowing phenomena is simply known as log-normal shadowing.

2.1.2 Small Scale Fading

Small scale fading is often used to describe the rapid fluctuations of the amplitudes, phases or multipath propagation of a radio signal over a very short period of time or travel distance. Small scale fading is caused by interference of two or more transmitted signals which arrive at the receiver at slightly different times due to different propagation paths, as shown in Figure 2-1. These multipath waves will be combined at the receiver and the resultant signal can vary considerably in amplitude and phase. The variation very

much depends on the distribution of the intensity and the relative propagation time of the multipath waves as well as the bandwidth of the transmitted signal.

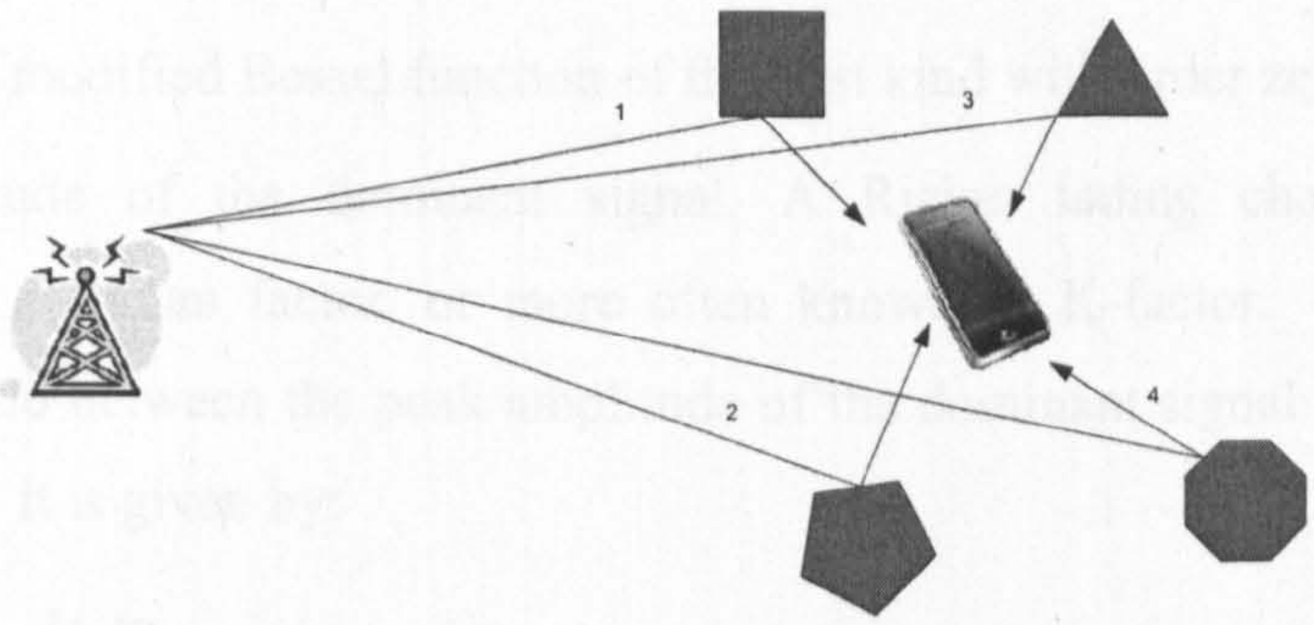

Figure 2-1: Multipath propagation at the receiver

In the case of a constructive vector summation of the signals, a channel gain of higher than mean is obtained, and it is often known as peak. On the other hand, a fade occurs when a destructive vector summation of signals happens. Therefore, maintaining a reliable wireless communication can become very difficult. In this section, the fading caused by multipath will be further characterised.

Firstly, in a scenario when there is no line of sight (NLOS) component between a transmitter and receiver, the multipath rays will all have similar amplitudes. This type of fading is often known as Rayleigh fading [5]. The multipath is said to be Rayleigh distributed and the Rayleigh distribution has a probability density function (*pdf*) of:

$$p(r) = \left(\frac{r}{\sigma^2}\right)\exp\left(\frac{-r^2}{2\sigma^2}\right) \tag{2-7}$$

where σ^2 represents the variance of the quadrature Gaussian processes and r represents the output random variable. It is well known that the envelope of the sum of two quadrature Gaussian noise signal obeys a Rayleigh distribution. Therefore the received signal envelope can be defined as $r = \sqrt{X_1^2 + X_2^2}$, where X_1 and X_2 are zero-mean Gaussian random variables which correspond to the quadrature and in-phase component of the signal envelope r, with mean power of σ^2.

In the case where a LOS or strong wave exists, the fading characteristic is different from Rayleigh fading. It is often known as Rician fading [5] when a LOS or strong wave exists between the transmitter and receiver. The probability density function of the Rician distribution can be given as:

$$p(r) = \left(\frac{r}{\sigma^2}\right)\exp\left(\frac{A^2 - r^2}{2\sigma^2}\right) I_o\left(\frac{rA}{2}\right) \qquad (2\text{-}8)$$

where $I_O(.)$ is the modified Bessel function of the first kind with order zero and A denotes the peak amplitude of the dominant signal. A Rician fading channel is usually characterised by a Rician factor, or more often known as K-factor. The K-factor is defined as the ratio between the peak amplitude of the dominant signal and the variance of the multi-path. It is given by:

$$K = 10\log(A^2/2\sigma^2)dB \qquad (2\text{-}9)$$

The K factor is often quoted in dB value. From this equation it can be seen that if no strong component exists, i.e. $A_c \rightarrow 0$, the equation simplifies to the Rayleigh distribution. In contrast, if the power of the strong component dominates over the random power then the constructive and destructive resultant signal will only fluctuate slightly around the average power of the strong component. The Rician *pdf* for two values of K-factor are plotted in Figure 2-2 together with the Rayleigh *pdf*. The *pdf* plots clearly show the more deterministic nature of the Rician channel compared to the Rayleigh channel, especially for higher K-factors.

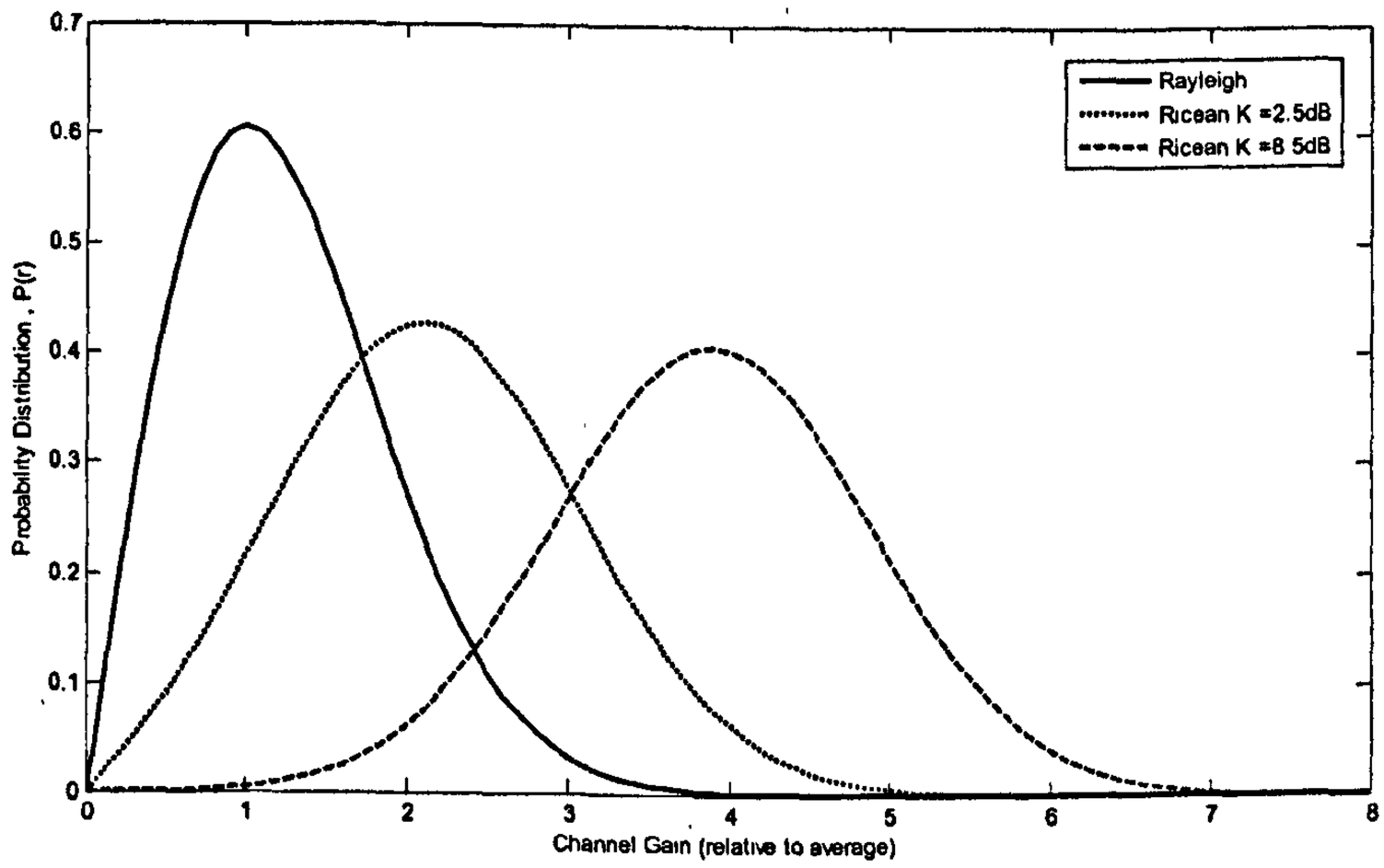

Figure 2-2: Probability density functions for Rayleigh and Ricean distribution

To further illustrate these fading channels, two typical fading envelopes of Rayleigh and Rician fading channels are shown in Figure 2-3 and Figure 2-4 respectively. A receiver speed of 10m/s and a carrier frequency of 2GHz are assumed. It can be seen that in

Rayleigh fading channels, some very deep fades can be observed. This is mainly due to the absence of a strong dominant path. Deep fades of up to -30db are visible in this example. In the case of Rician fading with a K-factor of 5dB, a strong dominant path prevents a disastrous destructive summation at the receiver. Therefore very deep fades can be avoided, however variation in the received signal is still inevitable, but at a smaller magnitude.

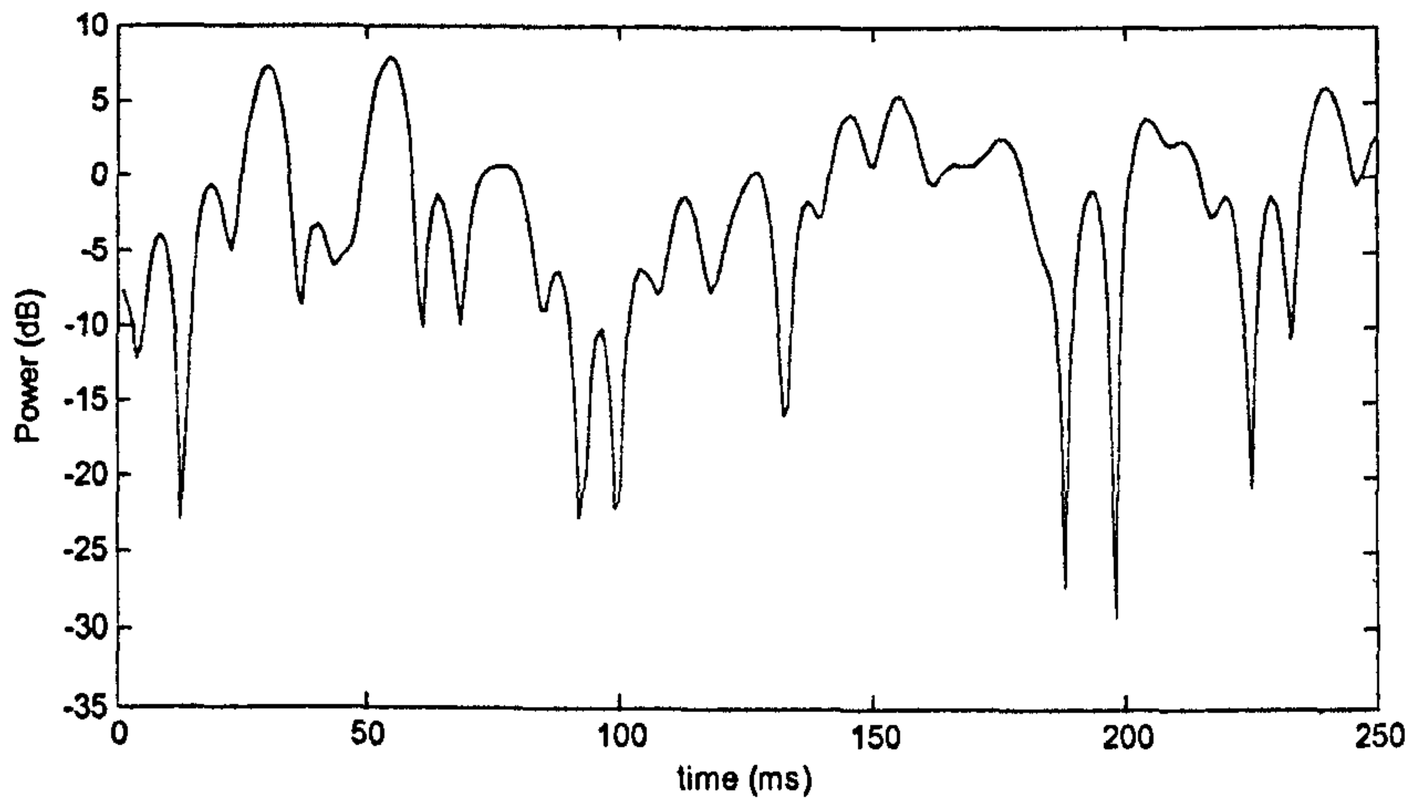

Figure 2-3: An example Rayleigh fading envelope

Figure 2-4: An example Rician fading envelope for K-factor of 5dB

In the following section, the two mechanisms that cause small scale fading are further characterised. Firstly, the multipath propagation that leads to time domain dispersion will be further described. This will be followed by the frequency domain dispersion that is due to the relative transmitter and/or receiver motion, or environmental changes.

2.1.2.1 Time domain dispersion

Since LOS communication does not always exist in a wireless communication, a wireless signal often travels to the mobile receiver through several paths due to reflections, diffraction and scattering. Reflection refers to the mechanism where a propagating electromagnetic wave impinges upon a smooth surface with very large dimension, relative to the radio frequency signal wavelength, λ. Scattering occurs when a radio wave impinges on a large, rough surface or surface whose dimension is in the order of λ or less. This causes the energy to spread out (or scattered in all directions). Diffraction on the other hand occurs when there is a dense body, whose dimension is large relative to λ within a transmitter and a receiver. This causes secondary waves to be formed behind the obstructing body.

These fundamental mechanisms cause the wireless signal to reach the receiver via multipaths, each with unique paths, as for example in Figure 2-1. The time of flight will be different for each path, resulting in time dispersion at the receiver. The received energy of the propagation waves are different, due to the unique travelling paths (length) as well as energy lost due to distinct diffractions or scatterings. The time dispersion mechanism due to multipath propagation is often best described in a power delay profile (PDP). A PDP is obtained by calculating the power of each path and plotting its value against the propagation delay, which is usually normalised to the time of the first received path. A typical PDP is shown in Figure 2-5. A PDP usually follows an exponential decay in power, which follows the fundamental law of Friss space equation, where the received power is inversely proportional to the propagation distance.

It is possible to quantify the degree of dispersion in a channel by evaluating its root mean square (*rms*) delay spread. This value can be calculated from Equation 2-10, where α_k represents the received amplitude of the k-th ray after a time delay of τ_k seconds, and τ_a represents the time for half the power to arrive.

$$\tau_a = \frac{\sum_{k=1}^{N} \tau_k \alpha_k^2}{\sum_{k=1}^{N} \alpha_k^2}, \qquad \tau_{rms} = \sqrt{\frac{\sum_{k=1}^{N} [\tau_k - \tau_a]^2 \alpha_k^2}{\sum_{k=1}^{N} \alpha_k^2}} \tag{2-10}$$

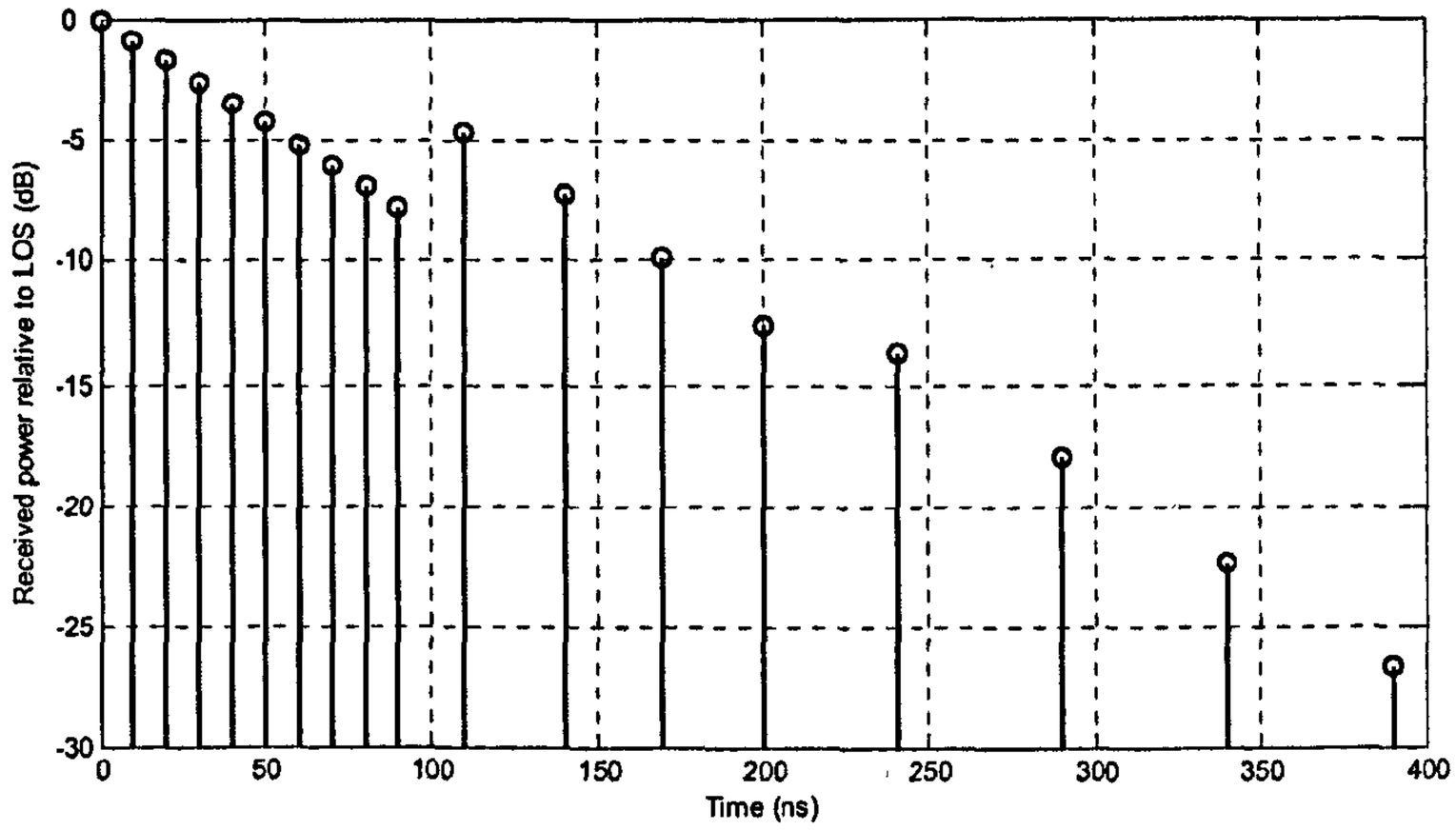

Figure 2-5: An example power delay profile

This is an important indicator since it incorporates all the information from a power delay profile and expresses it as a single value which easily allows direct comparisons between differing channels and environments. In practice, since weak paths (which are not really significant at the receiver) with long delays can result in large *rms* delay spreads, it is common to discard ray paths below a power threshold relative to the strongest path. A threshold of 20dB is commonly used [2]. Another useful parameter, the normalized (with respect to symbol period, T_s) *rms* delay spread, τ_n is commonly used in radio propagation. This parameter is useful at characterising type of channels, and this will be discussed shortly. The parameter is given by:

$$\tau_n = \frac{\tau_{rms}}{T_s} \tag{2-11}$$

Time dispersion due to multipath propagation causes the transmitted signal to undergo either flat or frequency selective fading. If the mobile radio channel has a relatively constant gain and linear phase response over a bandwidth which is greater than the bandwidth of the transmitted signal, then the received signal is said to have undergone flat fading. Flat fading channels are also known as narrowband channels, since the bandwidth of the transmitted signal is narrower compared to the flat fading bandwidth of the channel as shown in Figure 2-6. Flat fading usually occurs when the symbol period T_s is long compared to the delay spread. This is usually the case when the normalized *rms* delay spread is less than 0.1[8][9].

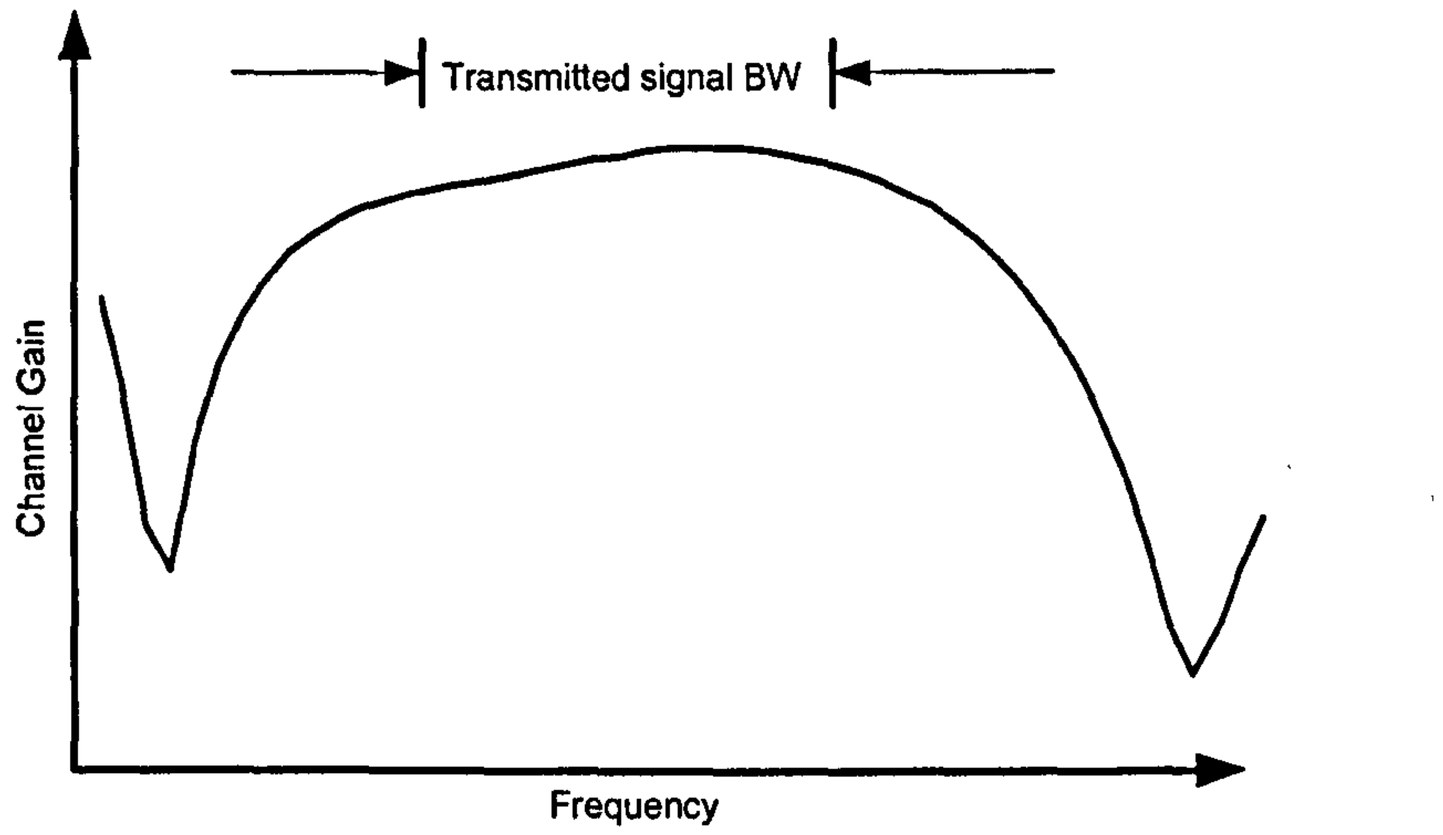

Figure 2-6: A typical Flat Fading scenario

Another useful parameter that is used to characterize the fading channel is called the correlation bandwidth or coherence bandwidth, B_c. Correlation bandwidth refers to the width of a bandwidth where the frequency response is considered flat. In other words, the correlation bandwidth refers to the range of frequencies where two frequency components have a strong amplitude correlation. The correlation bandwidth is often defined as the bandwidth where the frequency correlation is above 0.5. In this case, correlation bandwidth is approximately given by [2][3]:

$$B_c = \frac{1}{5\tau_{rms}} \tag{2-12}$$

The equation above shows that the correlation bandwidth is inversely proportional to the τ_{rms}. Thus it can be easily inferred that for a fading channel with large *rms* delay spread, the correlation bandwidth will be small and vice versa.

When the transmitted signal is larger than the correlation bandwidth, then the received signal is said to have undergone a frequency selective fading. Frequency selective fading channels are also known as wideband channels, since the bandwidth of the transmitted signal is wider compared to the flat fading (correlation) bandwidth of the channel, as shown in Figure 2-7. In contrast to flat fading, frequency selective fading usually occurs when the symbol period T_s is relatively short compared to the delay spread.

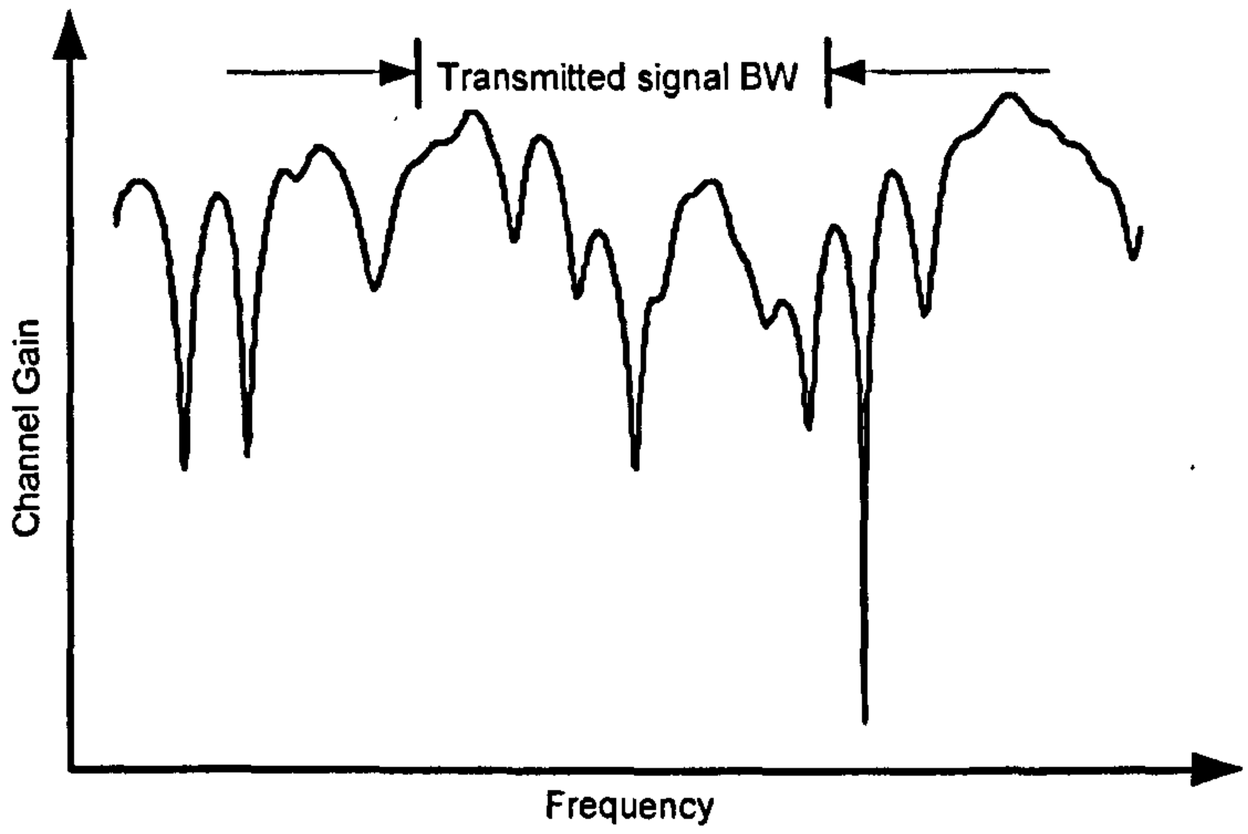

Figure 2-7: A typical Frequency Selective scenario

Frequency selective fading is predominantly due to the severe time dispersion of the transmitted symbol and induces inter-symbol interference (ISI). Frequency selective fading channels are much more difficult to handle than flat fading channels. More complex equalisation at the receiver is needed to overcome the harmful effects of delay spread. For a very wideband system, equalisation processes can become very complex. Multi-carrier transmission techniques, such as OFDM, can convert the wideband channel into parallel narrowband channels and effectively reduce implementation complexity by utilizing frequency domain equalization [10]. This multi-carrier technique is the core transmission technique that will be investigated in this thesis and it will be discussed in detail in Chapter 3.

2.1.2.2 Frequency domain dispersion

In the previous section, time dispersion due to multipath propagation has been described. As a matter of fact, the phenomenon can be similarly characterised in the frequency domain [2]. In this section, frequency dispersion due to Doppler spreading will be briefly described.

Two useful parameters, Doppler spread and correlation time are often used to characterise the time varying nature of the channel, in a small-scale region. Doppler spread is a measure of the spectral broadening caused by the time rate of change of a mobile radio channel. It is defined as the range of frequencies over which Doppler spectrum remains non-zero. The sharpness and the steepness of the boundaries of

Doppler spectrum are very much decided by the upper limit of the Doppler shift. Therefore, the amount of the spectral broadening depends on the frequency shift f_d, which is a function of the velocity of the terminal relative to the base station. This frequency shift is better known as the *Doppler* frequency. As a terminal moves away from the base station, the signal experiences a negative Doppler frequency whereas when the terminal moves towards the base station, it experiences a positive Doppler frequency. The maximum value of the Doppler shift, f_m is given by [2][3]:

$$f_m = \frac{vf}{c} \tag{2-13}$$

Another important parameter, the correlation time, is in fact the time domain dual of Doppler spread and is often used to characterize the time varying nature of the frequency domain dispersiveness. Similarly to the correlation bandwidth, correlation time is actually a statistical measure of the time duration over which the channel impulse response remains invariant. The correlation time is often defined as the duration over which a channel's response maintains a correlation of at least 0.5. Thus the correlation time can be approximately given in terms of f_m as [2]:

$$T_c \approx \frac{9}{16\pi f_m} \tag{2-14}$$

From the equation above, it can be seen that the correlation time is inversely proportionally to the maximum Doppler shift of the channel. Thus, when a mobile receiver is travelling at high speed (thus high Doppler shift), the correlation time will be small and vice versa.

Similarly to dispersion in the time domain, a channel may be classified either as fast fading or slow fading channel by considering the correlation time. When the correlation time of the channel is smaller than the symbol period of the transmitted signal, a fast fading is said to have occurred. In this case, the channel impulse response changes rapidly within the symbol duration. The Doppler spreading leads to frequency dispersion, or time selective fading and essentially causes signal distortion [2].

In the case where the correlation time is larger than the transmitted signal or when the channel impulse response is changing at a rate much slower than the transmitted signal, a slow fading occurs. In short, the velocity of the mobile receiver and the baseband signalling determines whether a signal undergoes fast fading or slow fading. Given a

fixed symbol period, when a mobile is travelling at high speed, fast fading tends to happen and vice versa.

Although flat fading is often desired where complex equalization is not needed, this is not always the case. [19] has shown that diversity gain can be achieved in frequency selective channels. Multiuser diversity can be further exploited to achieve more gain than an AWGN only channel. Multiuser diversity gain will be discussed later in the chapter.

2.2 Channel Modelling

2.2.1 SISO: ITU Channel Models

Realistic modelling of radio channel propagation requires extensive measurement campaigns. In the 1980s and 1990s, several research projects such as COST 231[11] and COST 259[12] have been carried out to measure the wideband channels for SISO. These channels model form a basis for the ITU models which where largely used in the research and development of the third generation of wireless communications systems. ITU channel models consider several user scenarios such as indoor office, outdoor-to-indoor, pedestrian and vehicular radio environments. The ITU channel model uses a simple tapped-delay line model to model the radio channel propagation. Several key parameters that are used to describe the propagations are time delay spread, path loss and shadowing, multipath characteristics as well as operating frequency. Several channel models such as the ITU Pedestrian A, Pedestrian B and Vehicular A were proposed. The key parameters for ITU channel modelling can be found in [6]. The ITU models were further extended [7] to cater for higher bandwidth channel models and more complicated channel scenarios.

2.2.2 MIMO: Spatial Channel Model (Extension) (SCM(E))

There is an ever increasing demand for higher download speed for mobile devices, due to new services that can be provided by new mobile devices, such as audio/video streaming and mobile internet. These services require a higher spectral efficiency to achieve the target. Thus MIMO techniques have been proposed to increase the spectral efficiency and to provide a high throughput. However, MIMO was not introduced in UMTS until Release 7, and MIMO channel modelling was not included in the ITU channel models.

Therefore, in order to have a realistic channel model for MIMO systems, 3GPP and 3GPP2 jointly developed a geometry based SCM [17]. SCM was originally intended for the evaluation of different MIMO schemes for High Speed Downlink Packet Access (HSDPA). SCM includes a simple tapped-delay line model that can be used for link level simulation as well as a geometry-based stochastic model for system-level simulations. However the SCM was only defined for a 5 MHz bandwidth CDMA (HSDPA) system in the 2 GHz band, whereas the currently defined LTE system requires a wider bandwidth of up to 20 MHz. Other issues of the SCM include a lack of short-term system-level time-variability in the model, a lack of Ricean K-factor models (LOS support) for macro scenarios, and a lack of a wider range of scenarios. However, these issues have been addressed in the SCM Extension (SCME) Channel Model [15]. SCME is fully backward compatible with SCM but with some practical and necessary add-ons. [16] has provided a publicly available matrix generator for SCME channels and this is used throughout this thesis.

The SCME simulator can generate system level simulation of multiple cells/ sectors, with multiple base stations and UEs. The SCME can support a large number of simulation runs, often called 'drops', which can be predefined. During a drop, the large-scale parameters, e.g. path loss are fixed but the channel undergoes fast fading according to selected scenarios and the motion of the UEs. The geometry framework for spatial parameters for the MIMO channels is shown in Figure 2-8.

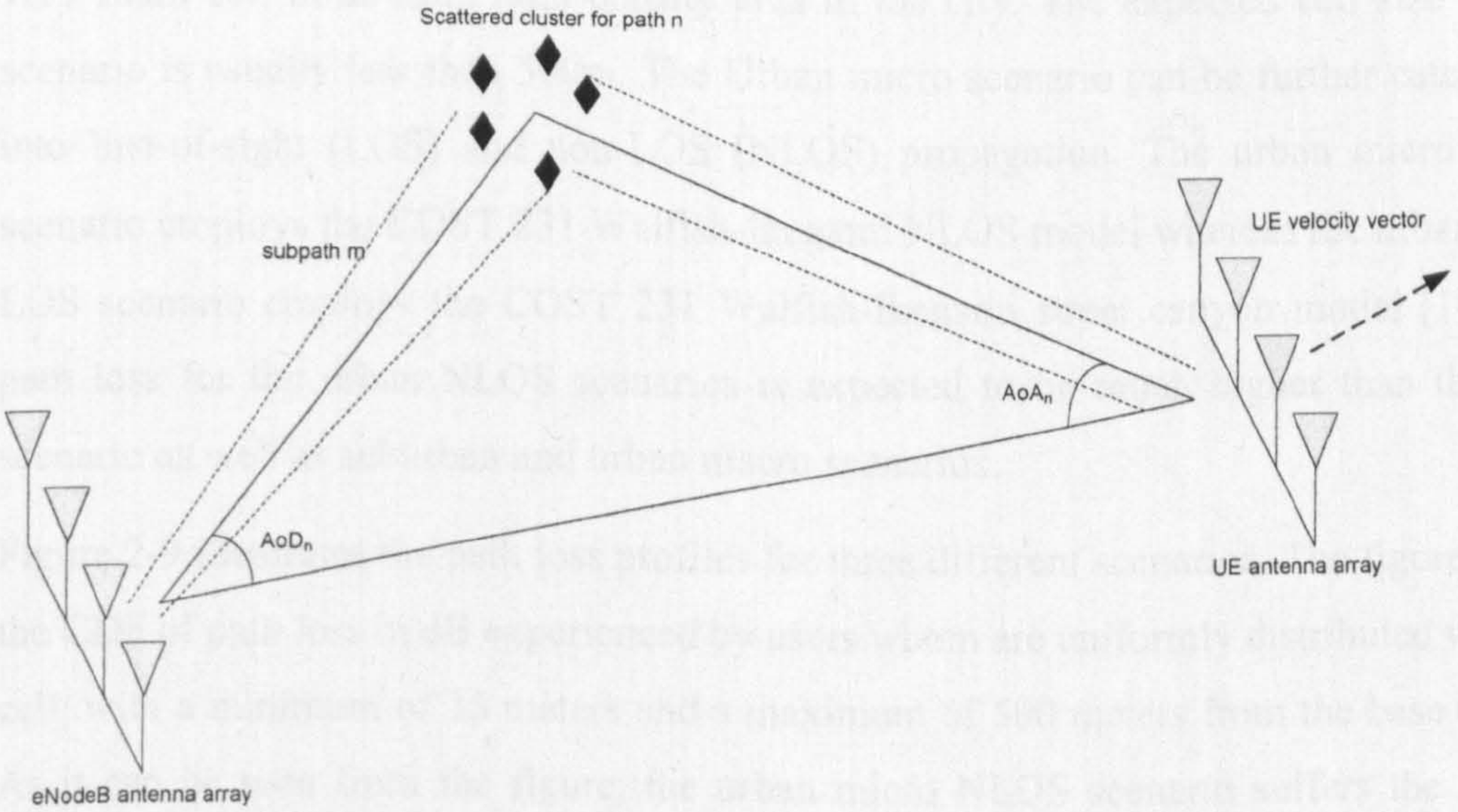

Figure 2-8: Geometry for generating spatial parameters for base station (eNodeB) and UE

The time-delay properties of the SCME link level model are similar to the ITU channel models for the case of SISO. There is a fixed number of 6 "paths" in every scenario. The fixed values for the power and delays parameters of the paths are tabulated in Table 2-1. However for MIMO channel models, SCME defines the spatial characteristics of the MIMO channels by including angular spread as well as the directional distribution of the propagation paths at both the base station and the UE. In contrast to a fixed link level simulation, path powers, path delays, and angular properties are modelled as random variables which are defined through probability density functions (PDFs) and cross-correlations. The per-path angular spread at both the base station and UE follows a Laplacian distribution. Each multipath is made up of 20 spatially separated "sub-paths" according to the sum-of-sinusoids method [14]. The main parameters for the SCME models are shown in Table 2-2.

Three main propagation environments are defined in SCME: Suburban Macro, Urban Macro, and Urban Micro. As the name suggests, suburban macro can be used to model the radio propagation in suburb area, where less buildings and moving vehicles can be expected. This model has a smaller *rms* delay spread and a smaller path loss than the urban macro and urban micro scenarios. The Urban scenario is used to model a typical city area, with reasonably high density of scatterers, such as building, vehicles etc. Both the suburban macro and urban macro scenarios employ the modified COST231 Hata urban propagation model [13]. The Urban micro on the other hand is used to model a very small cell in an ultra high density area in the city. The expected cell size for this scenario is usually less than 500m. The Urban micro scenario can be further categorised into line-of-sight (LOS) and non-LOS (NLOS) propagation. The urban micro NLOS scenario employs the COST 231 Walfish-Ikegami NLOS model whereas the urban micro LOS scenario employs the COST 231 Walfish-Ikegami street canyon model [17]. The path loss for the urban NLOS scenarios is expected to be much higher than the LOS scenario as well as suburban and urban macro scenarios.

Figure 2-9 illustrates the path loss profiles for three different scenarios. The figure shows the CDF of path loss in dB experienced by users whom are uniformly distributed within a cell, with a minimum of 35 meters and a maximum of 500 meters from the base station. As it can be seen from the figure, the urban micro NLOS scenario suffers the highest path loss on average, approximately 10dB worse than the Suburban macro scenario. This is well expected due to very high density of obstruction objects and scatterers. The urban

micro LOS scenario on the other hand has a relatively low path loss compared to others, due to its advantage of geographical location.

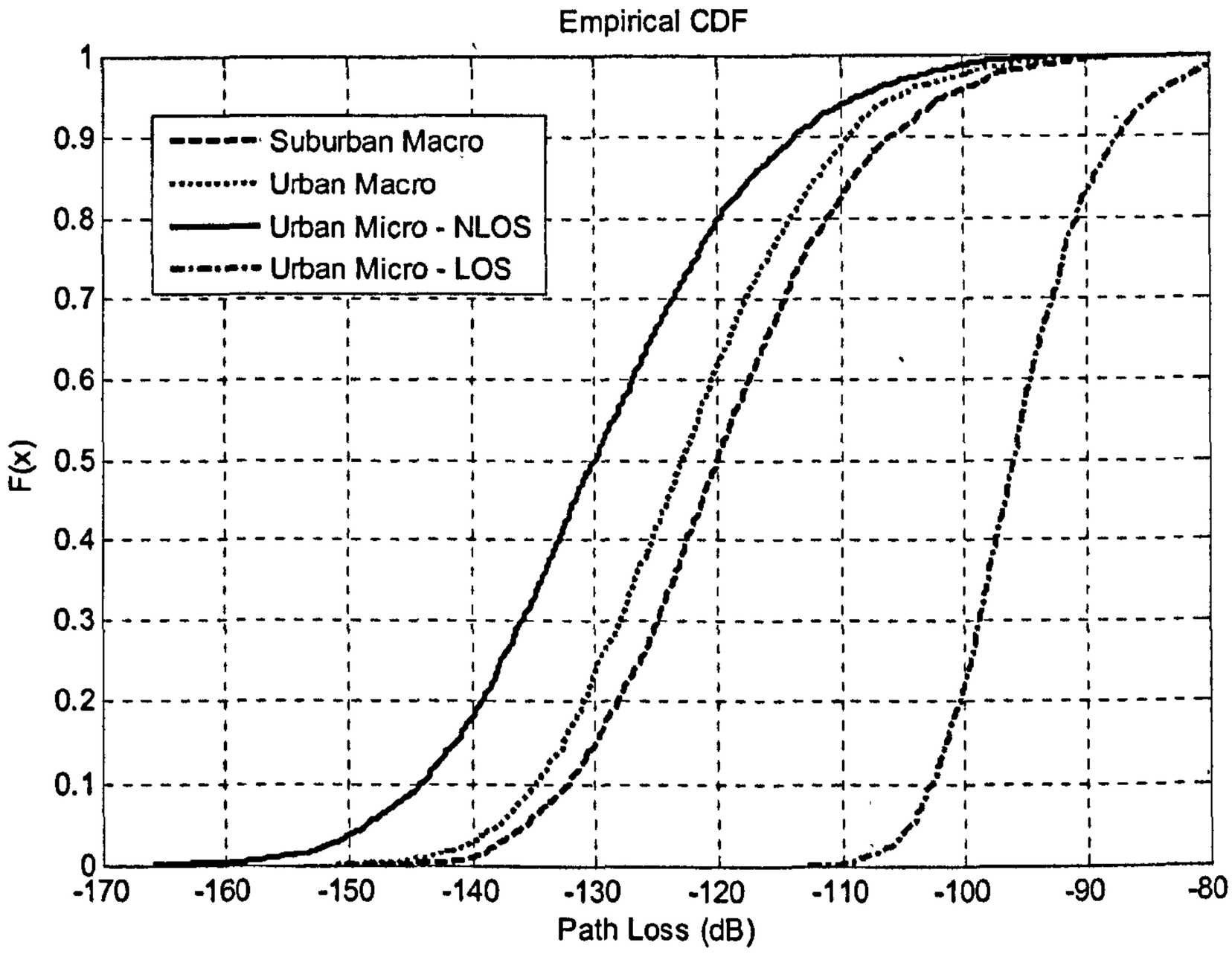

Figure 2-9: CDF plot of Path loss for three scenarios

Table 2-1: Tapped delay-line parameters for SCME

Scenario		Suburban Macro		Urban Macro		Urban Micro	
Power-delay parameters: Relative path power(dB) /delay(μs)	1	0	0	0	0	0	0
	2	-2.6682	0.1408	-2.2204	0.3600	-1.2661	0.2840
	3	-6.2147	0.0626	-1.7184	0.2527	-2.7201	0.2047
	4	-10.4132	0.4015	-5.1896	1.0387	-4.2973	0.6623
	5	-16.4735	1.3820	-9.0516	2.7300	-6.0140	0.8066
	6	-22.1898	2.8280	-12.5013	4.5977	-8.4306	0.9227
rms delay spread(μs)		0.17		0.65		0.25	

Table 2-2: Main parameter for SCME

Scenario		Suburban Macro	Urban Macro	Urban Micro
Number of paths		6	6	6
Number of sub-paths (M) per-path		20	20	20
Mean AS at base station (degree)		5	8, 15	19
Mean AS at the receiver (degree)		68	68	68
SCM path-loss(dB) (d is in meter)	NLOS	31.5+35log10(d)	34.5+35log10(d)	34.53+38log10(d)
	LOS			30.18+26log10(d)
SCM shadowing standard deviation (dB)	NLOS	8	8	10
	LOS	-	-	4

2.3 Capacity of wireless channel

In the end of 1940s, Claude Shannon made a breakthrough in wireless communications [19] by characterizing the limits of reliable communication. Shannon showed that by more intelligent coding of the information, one can in fact communicate at a strictly positive rate but with as small an error possibility as desired [1]. However there is a maximal rate that this can be done and it is called the channel capacity. If one attempts to communicate above the channel capacity, then it is impossible to drive the error probability to zero.

In this section, the channel capacity of a SISO AWGN (Additive White Gaussian Noise) channel will be first discussed. This will be followed by the capacity of a MIMO fading channel. A point to point scenario will be first considered and a multiuser scenario will be followed in the next section.

2.3.1 SISO Channel Capacity

Given a channel, which can be characterised by a double-sided bandwidth of $2B$ Hertz, with additive noise described by a Gaussian distribution with zero mean (or simply Additive white Gaussian noise (AWGN)), the capacity, C of a SISO channel can be given as:

$$C = B\log 2\left(1+\frac{S}{BN_o}\right) bits/s \qquad (2\text{-}15)$$

where B is the bandwidth of the channel in Hertz, S is the total received signal power over the bandwidth and N_o is power spectral density of white Gaussian noise. The term S/BN_o is often known as the signal-to-noise ratio (SNR) of the communication signal to the Gaussian noise interference and is expressed as a linear power ratio in the equation. Thus, for any rate r smaller C, there exists an error correction code that allows error free communication, given that the code is sufficiently long. However, Equation 2-15 applies to a simple scenario of an ideal channel, where only additive noise in considered and this is not realistic in actual wireless communication. Realistic radio channels are affected by some fundamental mechanisms of radio propagation, such as reflection, scattering and diffraction, depending on surrounding environments. Thus it is impossible to characterise the wireless channel in a deterministic sense.

A statistical model is more appropriate to describe the channel capacity of a faded channel. Given that x is the transmitted symbol and y is the corresponding received signal, the input/out relationship for a faded channel can be easily expressed by:

$$y(n) = hx(n) + w(n) \tag{2-16}$$

where h is a random variable and $w(n)$ is additive noise. This is called a flat-fading model where the 'flat' attribute refers to the modelling of the channel transfer function with a constant modulus. Therefore, the capacity of a fading channel depends on the characteristic of h, and when h is known at the receiver side but not at the transmitter, the channel capacity can be given by[19][21]:

$$C = B\log 2\left(1 + |h|^2 \frac{S}{BN_o}\right) bits/s \tag{2-17}$$

The channel capacity is often given in a spectral efficiency form (in bits/s/Hz) where it is normalised by bandwidth. The capacity of a flat Rayleigh channel is given in Figure 2-10. As we can see, the capacity of a Rayleigh faded channel is lower than the AWGN channel. This is true only for a point to point scenario. However, in a multiuser scenario, this is no longer true when h is available at the transmitter. A multiuser gain can be achieved and a higher gain can be achieved. This will be discussed in more detailed in Section 2.4.

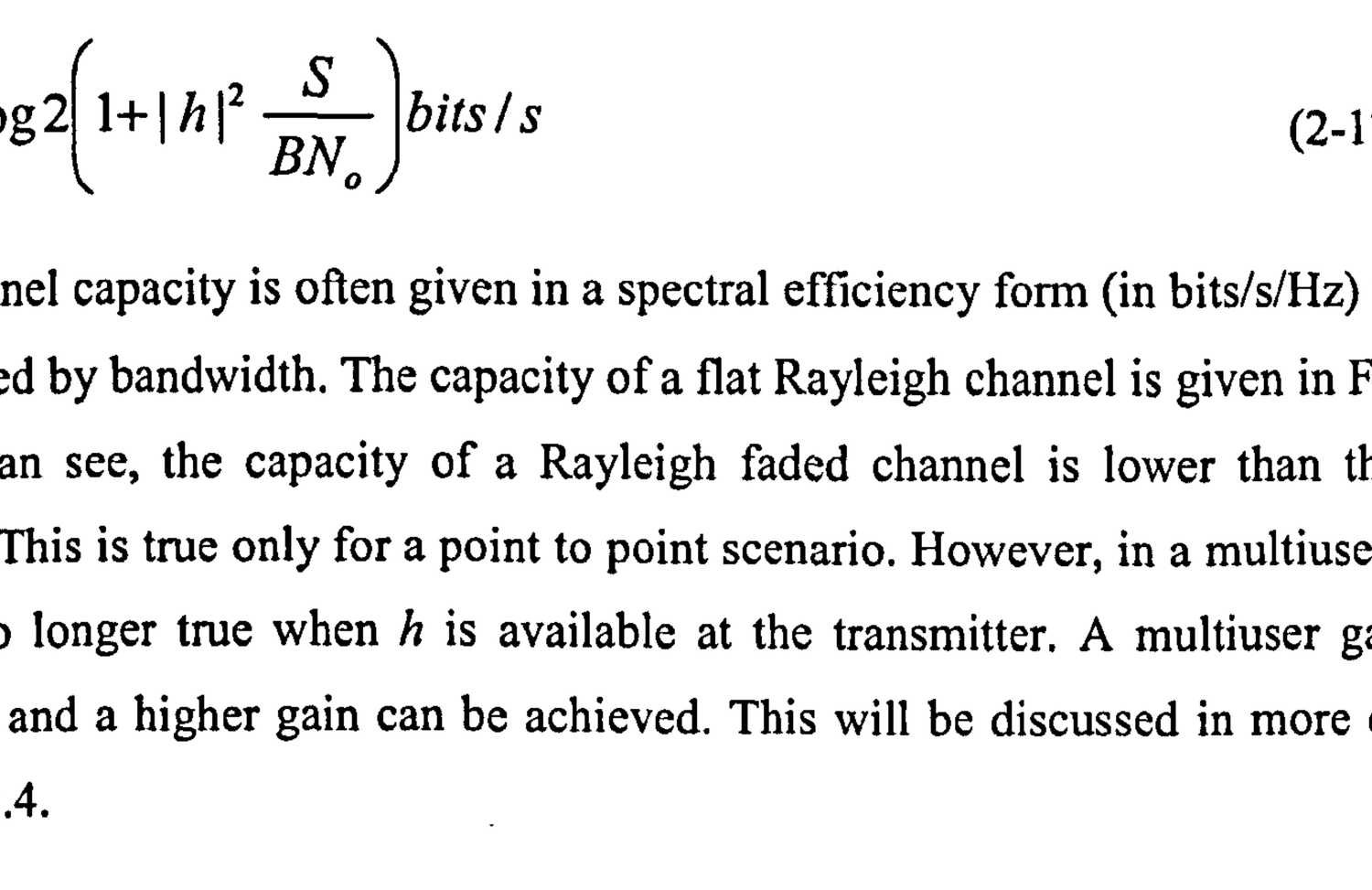

Figure 2-10: Channel capacity of a SISO Rayleigh fading channel compared to Shannon's channel capacity of a SISO AWGN channel

2.3.2 MIMO Channel Capacity

The generalized Shannon bound on capacity has been presented by Foschini in [22]. If the transmitter has no knowledge of the radio channel H, then the ergodic (mean) capacity that can be achieved is given by:

$$C = \log\left(\det(I_{N_R} + \frac{S}{N_T N_o} HH^H) \right) \tag{2-18}$$

where N_r and N_t are the number of receive antennas and transmit antenna respectively, I_{NR} is the identity matrix of size N_R, $\{.\}^H$ denotes a Hermitian transpose operation and H is the channel matrix between the N_t transmit and N_r receiver antennas and can be illustrated in Figure 2-11.

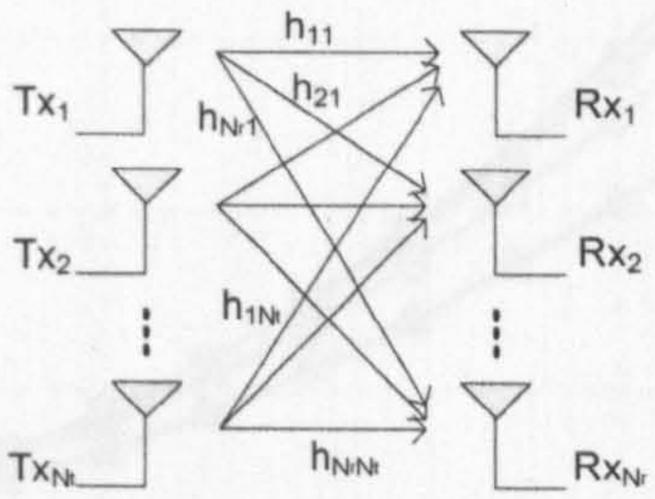

Figure 2-11: An example of MIMO channels

In a MIMO channel with rich scattering environment, the signal from each individual transmitter will appear highly uncorrelated from all the others. As a result, the signal corresponding to each transmitter will have a distinct spatial signature at the receiver. These different spatial signatures allow the receiver to effectively separate the data streams with some adequate signal processing. However, signals received by two antennas are correlated to certain extent. The correlation coefficient depends on the antenna separation as well as the angular spectrum of the incoming radio wave [23]. When the transmit antennas are not separated wide enough or there is no rich scattering environment between the transmitter and receiver, the channels will appear to be correlated at the receiver and MIMO capacity cannot be achieved. Therefore, the existence of spatial correlation has a strong impact on the capacity limit of the MIMO channel. [23] has shown that antenna separation of at least 4 λ is needed to achieve 80% of the capacity in the uncorrelated antenna case.

The channel capacity of a MIMO system without the knowledge of H in the transmitter is shown in Figure 2-12. In addition to that, the channel capacities for spatially correlated channels are also shown. In the figure, the channel capacity for the SCM Urban macro channel is generated using Equation 2-18. Three correlation factors are considered, very low correlation (0.1), low correlation (0.5) and high correlation (0.9). As shown in the figure, the MIMO channel capacity decreases significantly for highly correlated channels.

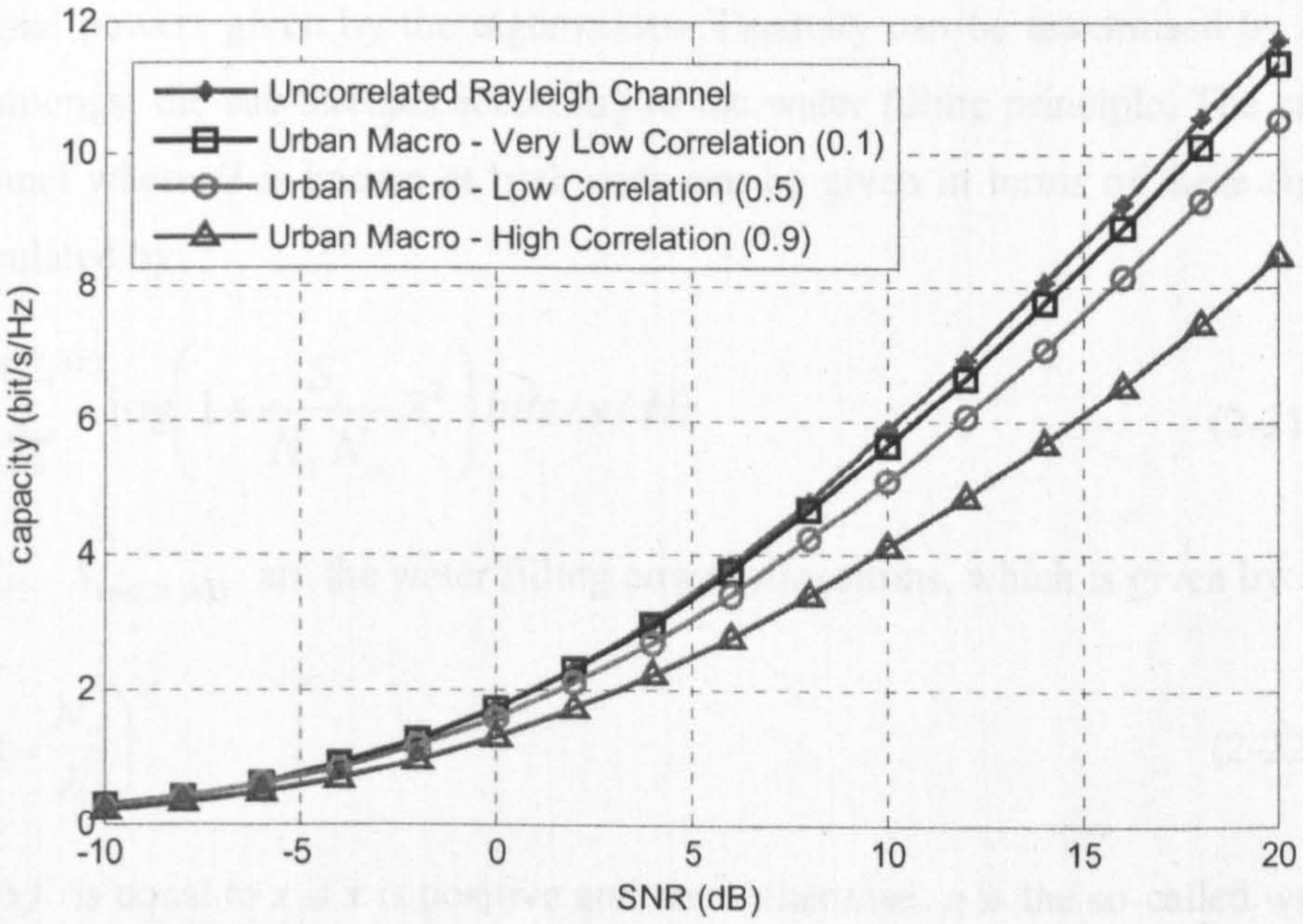

Figure 2-12: MIMO Channel Capacity for uncorrelated Rayleigh Channel and SCM Urban Macro channels with various correlation factors

In the case where the channel matrix H is available at the transmitter, the capacity of the channel can be computed by decomposing the vector channel into a set of parallel and independent sub-channels. A Singular Value Decomposition (SVD) method can be employed to evaluate the capacity of the MIMO channel. Using the SVD method, the complex channel between the transmitter and receiver antennas, H can be represented as:

$$H = U\Lambda V^H \tag{2-19}$$

where the $N_r \times N_r$ matrix U and the $N_t \times N_t$ matrix V are unitary matrices that represent the left and right singular vectors of H respectively. The diagonal elements $\lambda_1, \ldots, \lambda_Q$ of matrix Λ are the singular values of matrix H, where Q is the rank of H and $Q \leq min(N_r, N_t)$. The squared singular values λ_i^2 are the eigenvalues of the matrix HH^H and also $H^H H$.

To apply SVD, the transmitted signal vector x is multiplied by right singular matrix V and the receiver multiplies the conjugate transpose of the left singular matrix U^H to form an estimate $\hat{y}$ of the transmitted symbol vector.

$$\begin{aligned}\hat{y} &= U^H y = U^H (U\Lambda V^H Vx + w) \\ &= \Lambda\hat{x} + \hat{w}\end{aligned} \tag{2-20}$$

The equation above represents a system with Q equivalent parallel SISO eigen-channels with signal powers given by the eigenvalues. Capacity can be maximised by allocating power amongst the sub-streams according to the water filling principle. The capacity of the channel where H is known at both ends can be given in terms of these eigenvalues and calculated by:

$$C = \sum_{i=1}^{\min(Nt,Nr)} \log\left(1 + \frac{S_i}{N_T N_o}\lambda_i^2\right) bits/s/Hz \tag{2-21}$$

where $S_1 \ldots S_{\min(N_t,N_r)}$ are the water filling power allocations, which is given by:

$$S_i = \left(\mu - \frac{N_0}{\lambda_i^2}\right)^+ \tag{2-22}$$

Where $(x)^+$ is equal to x if x is positive and zero otherwise. μ is the so-called water-level, and is chosen such that total power constraint is satisfied $(\sum_i S_i = S)$ where S is the total power.

SVD-based beamforming is an optimal transmit and receive beamforming technique which can be deployed to decompose the MIMO channel into a number of parallel non-interfering subchannels, or eigen-channels. This method will render more power to better eigen-channels and allocate less power to weaker ones, since these subchannel are not contributing to the capacity. However, the benefit obtained by adaptive power allocation is only noticeable for lower SNRs, and it diminishes at high SNRs, as shown in Figure 2-13. When the number of the transmit antennas is the same or lower than the number of receiver antennas, the gain of adaptive power allocation is insignificant. However, when the number of transmit antennas is larger than the number of receive antennas there is a significant potential gain to be achieved by water-filling power allocation [18].

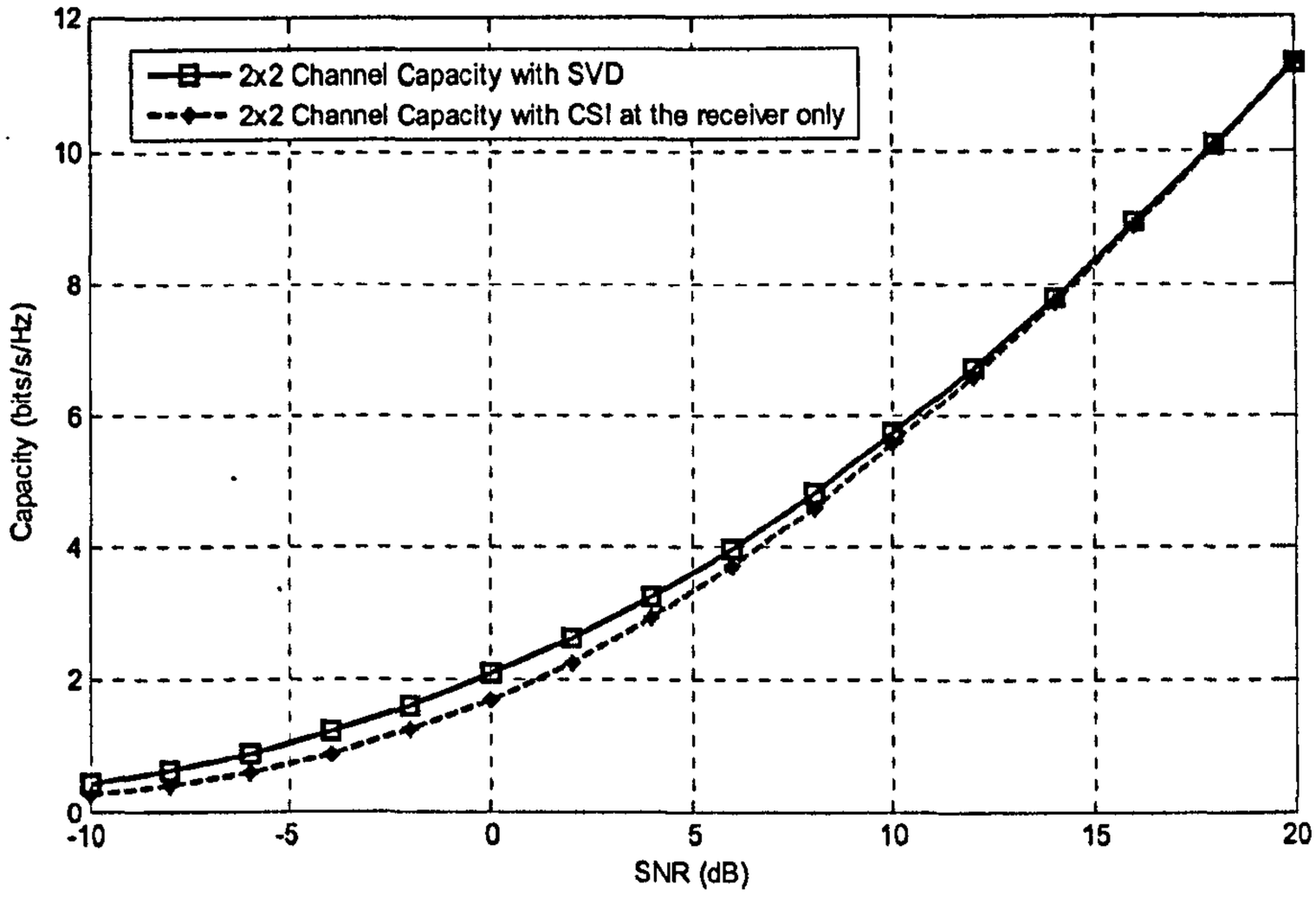

Figure 2-13: Channel Capacity with SVD

2.4 Multiuser Diversity

As explained in the previous section, fading can always be expected in a wireless transmission due to the fundamental mechanisms of radio propagation. Traditionally, fading is often seen as a problem and a challenge in wireless communication. For example, complex equalizers [24] have been proposed in the receiver to combat the effect of fading. The fading effect leads to a multiuser diversity concept, where when there is a sufficient number of users in a system, not only the effect of fading can be counteracted, but the multiuser diversity can improve the system performance by exploiting the channel fading.

Multiuser diversity exists when there are many users in the system and each fades independently, for example as shown in Figure 2-14. When this occurs, there is a high probability that one of the users will have a strong channel at any one time. By allowing that user to transmit at that instance, the shared channel resource can be used in a most efficient manner and it will maximise the total system throughput. When there are more users in the system, an even stronger channel can be selected and in this case, more multiuser gain is said to be achieved.

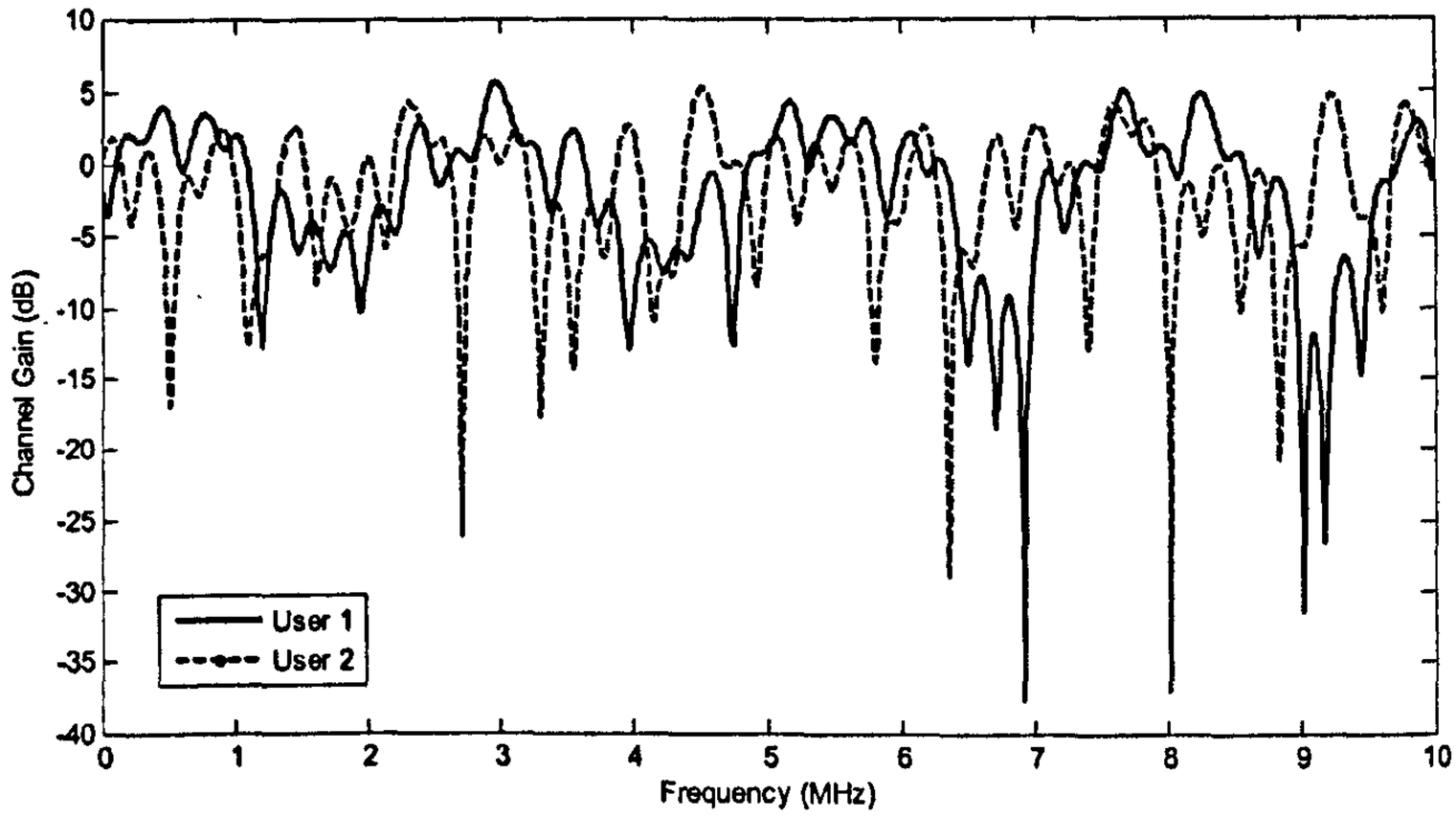

Figure 2-14: Independent fading channels for 2 users

When there is sufficient number of users in a system, the sum capacity of fading channel can exceed the AWGN channel capacity, provided full CSI is available at the transmitter [19]. This can be shown in Figure 2-15. The performance curves show the channel capacities as a function of the number of users for Rayleigh and Ricean faded channels in comparison to AWGN only channel, at an SNR of 0dB. No multiuser diversity can be achieved in an AWGN channel. However in the case of the Rayleigh channel, allowing the users to transmit at the peaks will result in a higher average gain at the receivers. For a Rayleigh faded channel, the capacity with 25 users is about a factor of 2.2 higher than the capacity of a single user. This is equivalent to 5.5dB gain over the AWGN channel. In other words, the AWGN channel needs an additional 5.5dB to achieved the same capacity achieved by Rayleigh channel with 25 users.

However, the amount of multiuser diversity that can be exploited depends crucially on the fading distribution. The more selective the channel, the more likely there is a user with a very strong channel and thus larger multiuser diversity gain. This can be seen also in Figure 2-15 that the gain of a Rician faded channel is much less than the Rayleigh faded channel, especially for a Rician channel with high K- factor. As mentioned in the previous section, a Rician faded channel occurs when there is a strong LOS component. The more dominant the strong component, the higher the K- factor. When a strong component exists, fading is less random or relatively flat. Thus it's less likely to have a very high peak nor a deep fade and thus less multiuser diversity can be achieved. As shown in the figure, a Rician channel with K-factor 8dB achieves less multiuser diversity

gain than a Rician channel with K-factor of 2.5dB. Even so, the Rician channel with 8dB K-factor still achieves a gain factor of 1.6, which is equivalent to 3dB gain compared to the AWGN channel.

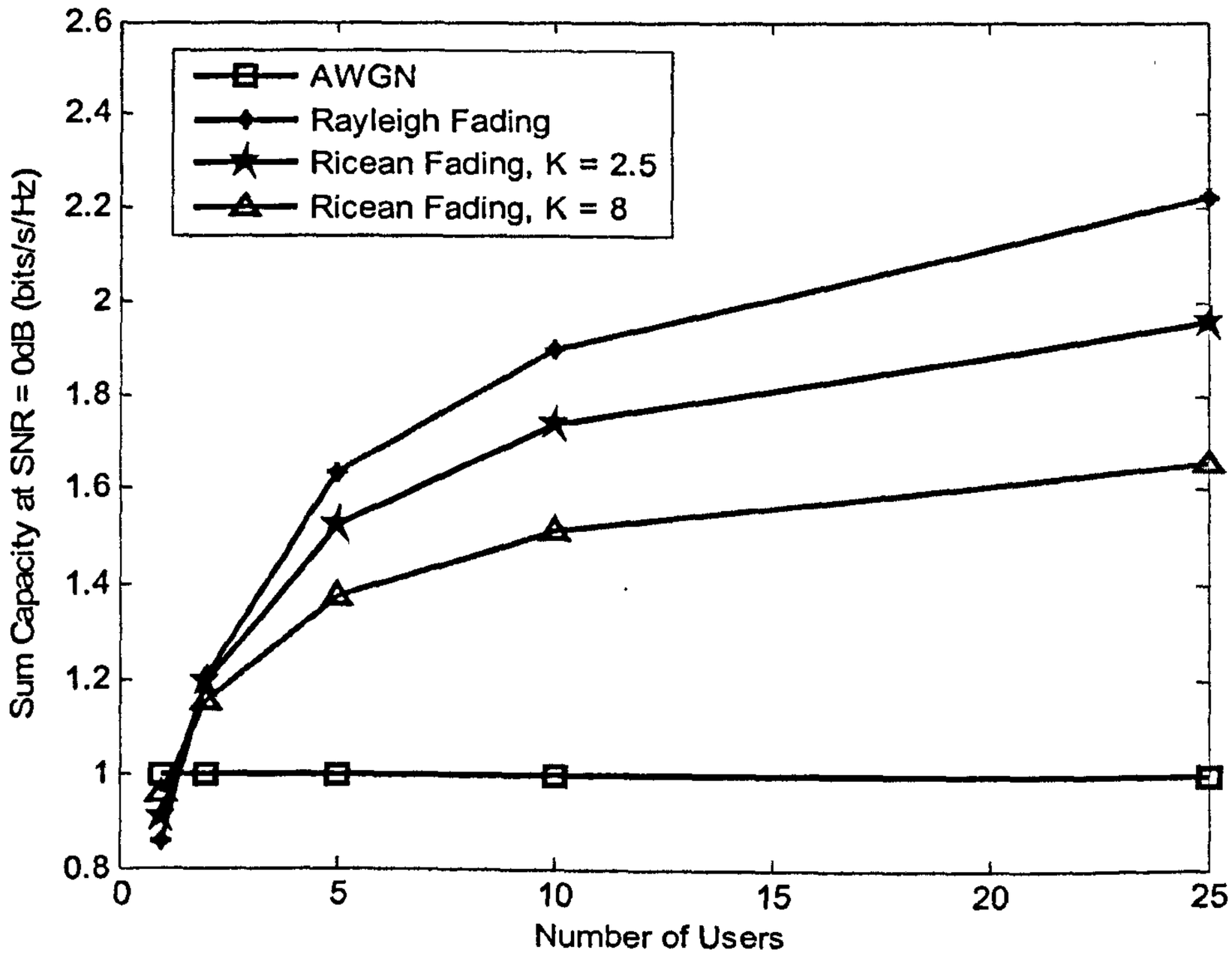

Figure 2-15: Multiuser diversity gain for Rayleigh and Rician fading channels, compared to AWGN only channel

However, there are issues that need to be taken into consideration while exploiting the multiuser diversity. These can be mainly categorised into:

- **Fairness and delay**: In an ideal scenario, all users are assumed to have a similar fading statistic. However, this is not always the case. Some users might have higher SNR or different fading distributions due to different geographical locations and slow fading conditions. One challenging issue is to allocate the resources to all the users fairly with different delay requirements. Several scheduling algorithms have been proposed in the literature to exploit the inherent multiuser diversity gain while maintaining fairness and delay constrains. These will be discussed in detail in Chapter 4.
- **Channel measurement and feedback**: One of the main requirements to achieve the multiuser diversity is to have CSI information at the transmitter. This requires a large amount of feedback information especially when there are many resource

units and number of users. In addition to that, CSI information is also subject to delay and measurement errors. These issues constitute a limitation on the ability to exploit multiuser diversity. Reduced feedback schemes will be discussed in Chapter 5.

- **Slow and limited fluctuation**: As mentioned earlier, the gain of multiuser diversity depends heavily upon the fading distribution of the channel. Fast variation in a channel is preferred over a slow fading channel. A LOS component creates a less dynamic channel with smaller fluctuation and consequently less multiuser gain. The total multiuser gain of the system will therefore be affected by those users with slow fading channels.

2.5 Conclusion

In this chapter, radiowave propagation and the associated fading characteristics have been briefly discussed. In order to investigate the performance of a wireless system, a practical channel model is needed to model the channel fading. The 3GPP Spatial Channel Model Extension (SCME) is discussed and this channel model is used throughout this thesis.

In addition to that, the channel capacity of SISO and MIMO channels has been presented. The effect of spatial correlation on the MIMO channel capacity is also presented. Lastly, the potential gain of a multiuser system is also discussed. When more users exist in a wireless system, multiuser diversity gain can be achieved. More gain can be achieved in Rayleigh fading channels when there are sufficient users in the system and the CSI information is available at the transmitter.

In the next chapter, we will briefly discuss about the development of 3GPP Long Term Evolution and its physical layer transmission technique, Orthogonal Frequency Division Multiplexing (OFDM). A physical layer link level simulation will also be presented.

References

[1] Claude Shannon, 'The zero error capacity of a noisy channel', IRE Transactions on Information Theory, vol. 2, Sept.1956 pp 8 – 19

[2] Theodore S.Rapport, ' Wireless Communications: Principles and Practise', 2nd Edition, Prentice Hall PTR , 2002

[3] Bernard Sklar, ' Digital Communications: Fundamentals and Applications' , 2nd Edition, Prentice Hall PTR, 2001

[4] E. Limpert, W. Stahel and M. Abbt ,'Log-normal Distributions across the Sciences: Keys and Clues,' BioScience, 51 (5), p. 341–352 (2001).

[5] John. G. Proakis, ' Digital Communications', 4th Edition, The McGraw-Hill Companies, 2001

[6] 3GPP Technical Specification 25.101, ' UE Radio Transmission and Reception (FDD) Release 7,' www.3gpp.org

[7] Ericsson, Nokia, Motorola, Rohde & Schwaz, ' R4-070572: Proposal for LTE Channel Models', www.3gpp.org, 3GPP TSG RAN WG4, meeting 43, Kobe, Japan May 2007.

[8] J. Parsons, The Mobile Radio Propagation Channel, Wiley, 2000.

[9] A. Nix, A Fundamental Investigation into Short Range, High Capacity Mobile Data Transmission, PhD Thesis, September 1999, University of Bristol.

[10] OFDM for Wireless Multimedia Communications, Richard van Nee and Ramjee Prasad, Artech House, Boston and London, 2000.

[11] Commission of the European Communities, ' Digital Land Mobile Radio Communications- COST 231 Final Report', 1993

[12] Commission of the European Communities, ' Wireless Flexible Personalised Communications- COST 259 Final Report', 2001

[13] Hata, Masaharu, 'Empirical Formula for Propagation Loss in Land Mobile Radio Services', *IEEE Transactions on Vehicular Technology*, Vol. VT-29, No. 3, pp. 317-325

[14] M. F. Pop, and N. C. Beaulieu, "Limitations of sum-of-sinusoids fading channel simulators," *IEEE Trans. Commun.*, vol. 49, no. 4, Apr. 2001, pp. 699–708.

[15] D.S.Baum, J.Hansen, J.Salo, "An interim channel model for beyond-3G systems: extending the 3GPP spatial channel model (SCM)", *VTC 2005 Spring*, Volume 5, Page 3132 – 3136

[16] J. Salo, G. Del Galdo, J. Salmi, P. Kyösti, M. Milojevic, D. Laselva, and C. Schneider. (2005, Jan.) MATLAB implementation of the 3GPP Spatial Channel Model (3GPP TR 25.996) [Online]. Available: http://www.tkk.fi/Units/Radio/scm/

[17] "Spatial channel model for MIMO simulations", 3GPP TR 25.996 V6.1.0, Sep'03. [Online]: http://www.3gpp.org/ftp/Specs/html-info/25996.htm

[18] Branka Vucetic, Jinhong Yuan, ' Space-Time Coding', John Wiley & Sons Ltd, 2003, pp 1-41

[19] D. Tse, P. Viswanath, Fundamentals of Wireless Communication, Cambridge University Press, June 27, 2005.

[20] S.Sesia, I.Toufik, M.Baker, ' LTE The Long Term Evolution: From Theory to Practice,' John Wiley & Sons Ltd., 2009, pp243-282

[21] Sergio Barbarossa, ' Multiantenna Wireless Communication Systems', Artech House, 2005

[22] G.J. Foshini ad M.J. Gans, ' On limits of wireless communications in a fading environment when using multiple antennas', Wireless pers. Commun., vol. 6, no. 3, p.311, Mar. 1998

[23] D.Chizhik, F.Rashid-Farrokhi, J.Ling, and A.Lozano, 'Effect of antenna separation on the capacity of BLAST in correlated channels', *IEEE Commun. Letters*, vol.4, no. 11, Nov. 2000, pp.337-339

[24] J.Proakis, 'Adaptive Equalization for TDMA Digital Mobile Radio', *IEEE Transactions on Vehicular Technology,* vol.40, no. 2, pp 333-341, May 1991

Chapter 3

3G and Beyond – 3GPP Long Term Evolution (LTE)

3G Universal Mobile Telecommunications System (UMTS) and later releases e.g. High-Speed Downlink Packet Access (HSDPA) has been a great success and is currently adopted in many countries in the world. But even so, in order to meet the stringent requirements for future mobile radio services, the industry must further improve the current infrastructure of mobile radio communications.

In 2004, 3rd Generation Partnership Project (3GPP) started to investigate a new evolution by identifying the requirements from all the different key players in the field. Following a workshop focused on this topic, it was agreed to start a feasibility study on a new packet-only radio system while continuing to work on the Wideband Code Division Multiple Access (WCDMA) based air interface at full speed. The feasibility study was started in March 2005, and some of the key requirements defined for the work are given in [1]. This new evolution is known as Long Term Evolution (LTE).

3.1 Introduction on Long Term Evolution (LTE)

Long Term Evolution (LTE) is the next major step in mobile radio communications and will be introduced as Release 8 in the 3rd Generation Partnership Project (3GPP). The new evolution aims to reduce delay, improve spectrum flexibility and further reduce the cost for operators and end users. In December 2008, the specifications of Release 8 have been locked and these specifications are sufficiently stable for commercial implementation. As of May 2009, Release 8 specifications have yet to be ratified as a standard.

Some of the targets of the standard include [2]:

- Peak download rates of 326.4 Mbit/s for 4x4 antennas, 172.8 Mbit/s for 2x2 antennas for every 20 MHz of spectrum
- Peak upload rates of 86.4 Mbit/s for every 20 MHz of spectrum
- At least 200 active users in every 5 MHz cell. (i.e., 200 active data clients)
- Sub-5ms latency for small IP packets
- Increased spectrum flexibility, ranging from 1.25MHz to 20MHz
- Optimal cell size of 5 km, 30 km sizes with reasonable performance, and up to 100 km cell sizes supported with acceptable performance
- Co-existence with legacy standards
- Support of MBSFN (Multicast Broadcast Single Frequency Network).

Several multiple access options were proposed to 3GPP, but it came rather quickly to the conclusion that Orthogonal Frequency Division Multiple Access (OFDMA) is to be used in the downlink. The core of the LTE downlink radio is essentially the conventional OFDM with data transmitted over several parallel narrowband subcarriers. The use of the narrowband subcarriers in combination with a cyclic prefix makes OFDM transmission inherently robust to multipath fading. The use of the narrowband subcarrier essentially eliminates the need for a complex equalization process at the receiver side. This greatly simplifies the baseband processing at the receiver and thus reduces the terminal cost and power consumption.

One of the most important considerations in the uplink of the LTE is the power efficiency. Relative to the downlink, the end user equipment has significantly less available transmission power, which is mainly due to the battery constraint. Therefore, instead of the conventional OFDM transmission scheme which is proposed in the downlink, a single carrier transmission in the form of DFT-spread OFDM (also known as Single Carrier FDMA (SC-FDMA)) is proposed. This scheme has a smaller peak to average power ratio than the conventional OFDM, thus resulting in more power efficient and less complex user terminals.

Depending on different geographical location and regulation aspects, the radio spectrum is available in different frequency bands and sizes. In addition, the spectrum might also come as both paired and unpaired spectrum. Therefore, spectrum flexibility in LTE is one of the key features of LTE radio access. In the proposed standard, LTE supports scalable bandwidth from approximately 1.25MHz up to 20MHz. The adoption of scalable bandwidth enables smooth migration of some earlier systems, e.g.

cdma2000/1xEVDo systems. The spectrum flexibility of scalable bandwidth also further enables allocation under scattered spectrum availability. In addition to that, LTE can also operate in both paired and unpaired spectrum by defining a single radio access technology that can operate in both frequency division duplex (FDD) and time division duplex operation (TDD). The support of both FDD and TDD operations enables better integration of some legacy systems and possible migration in the future.

One of the key enhancement features in HSDPA and now in LTE is the hybrid Automatic Retransmission reQuest (ARQ) [3]. Hybrid ARQ schemes are used to provide a reliable communication over noisy wireless channels. HARQ is able to compensate for link adaptation errors and provide a finer granularity of coding rate thus giving a better throughput performance. The details of the implementation of HARQ will be given in a later section.

Scheduling algorithms play a central role in determining the overall performance of high speed cellular data systems, where high throughput and fair resource allocation among all the mobile users is desirable. In LTE, dynamic scheduling is applied to both the uplink and downlink. Channel dependent scheduling is used to achieve high cell throughput [4]. Channel dependent scheduling will schedule a user to transmit on time or frequency resources with relatively good channel conditions. By using channel dependent scheduling, transmission can be carried out with higher data rate by using e.g. higher order modulation, lower coding rate, etc. The details of scheduling will be discussed in Chapter 5.

Multiple-Input Multiple-Output (MIMO) communication techniques have been studied extensively in the recent past. The use of multi-antenna transmission techniques can significantly improve the system performance, reliability or both. There are two popular techniques which have drawn much attention due to their promising capability to increase the spectral efficiency and reliability. One of the techniques is space-time block coding (STBC) [5], which is able to achieve full transmit diversity and enable reliable communication. Thus in LTE, an Alamouti based Space-Frequency Block Coding (SFBC) technique is proposed in the standard. However the transmit diversity based method does not provide a linearly increasing channel capacity as the number of transmit and receive element grows simultaneously. Another technique that is also proposed in the LTE standard is spatial multiplexing (SM), also known as Vertical Bell Labs Layered Space-Time (V-BLAST) [6] which aims to increase the spectral efficiency. However,

this technique is limited by the transmission environment and highly dependent on the channel characteristics, which are determined by antenna configuration and richness of scattering. The performance degrades severely when the spatial channel correlation is high, e.g. in a line of sight (LOS) scenario. The details of the MIMO implementation will be given in Chapter 6.

3.2 LTE OFDMA Downlink

OFDMA is a multiple access scheme based on OFDM where data is transmitted to different users on different subcarriers. It is a very attractive choice for LTE as it is suitable for high data rate transmission in wideband wireless systems due to its spectral efficiency and good immunity to multipath fading. In order to investigate the link level performance of LTE downlink, a baseband LTE link level simulator was implemented in MATLAB. Due to limited time and resource constrain, we are unable to come out with a simulator which can model a complete LTE system. Although the simulator is not standard compliant, it is made as close as the interim LTE specifications. In the simulator the key parameters of the OFDM system are made the same as the LTE. The procedures of the baseband processing at the physical layer also follow the specification. However, some implementation approaches, such as generator polynomials for Turbo coding and interleaving, puncturing pattern and etc might not be fully standard compliant. The key parameters of the LTE OFDMA downlink system assumed in this thesis are given in Table 3-1. Figure 1 shows the proposed system model of LTE OFDMA system which employs Hybrid ARQ.

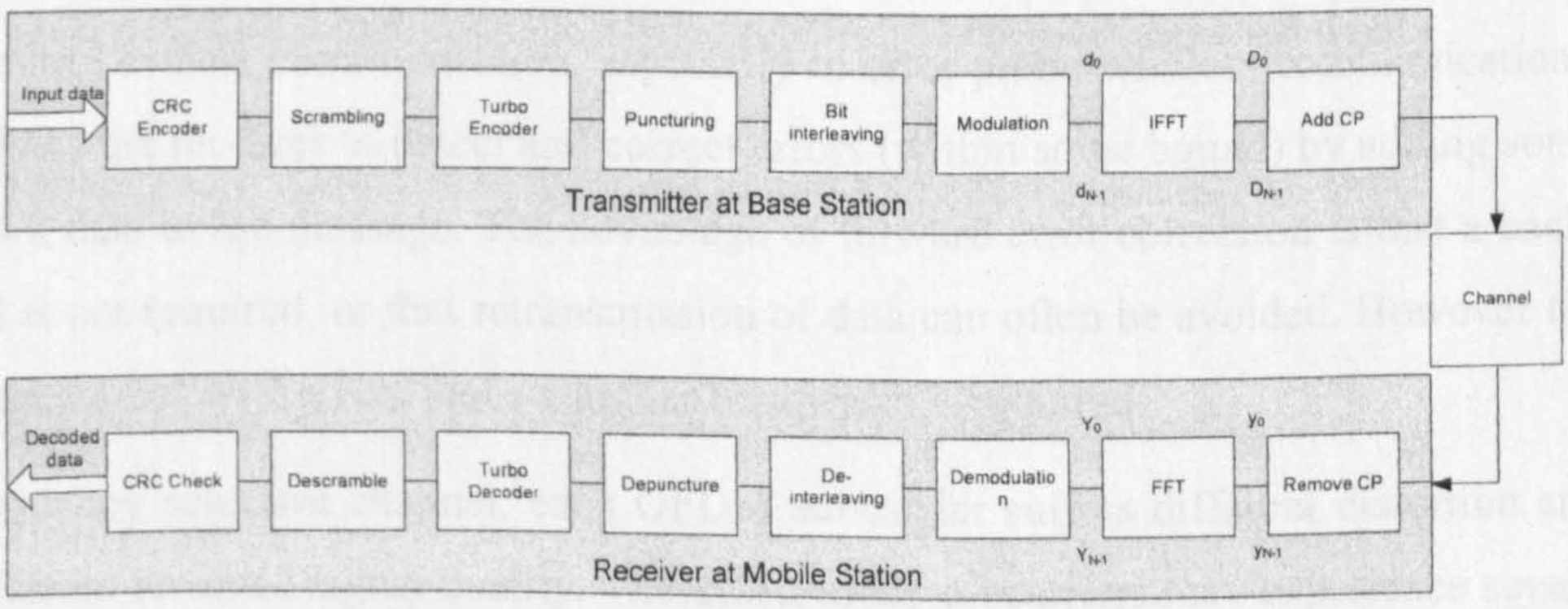

Figure 3-1 System Model for LTE OFDMA

Table 3-1: Parameters for LTE OFDMA downlink

Transmission Bandwidth		10 MHz
Time Slot/Sub-frame duration		0.5ms/1ms
Sub-carrier spacing		15kHz
Sampling frequency		15.36MHz (4x3.84MHz)
FFT size		1024
Number of occupied sub-carriers		601
Number of OFDM symbols per time slot (Short/Long CP)		7/6
CP length (μs/samples)	Short	(4.69/72)x6 (5.21/80)x1
	Long	(16.67/256)

3.2.1 Cyclic Redundancy Check

A Cyclic Redundancy Check (CRC) is an error detecting code. The CRC was invented by W. Wesley Peterson, and published in his 1961 paper [7]. The use of CRCs is popular because they are simple to implement in binary hardware and are particularly good at detecting common errors, e.g. errors caused by noise in transmission channels.

The CRC is used as a checksum to detect accidental or unintended alteration of data during a process of storage of transmission. The computation of the CRC resembles a long division operation in which the quotient is discarded and the remainder becomes the result. If the remainder is nonzero, an error has been detected. If the remainder is zero, either no error or an undetectable error has occurred. In the LTE link level simulator, a 32bit CRC is used to encode the data at the transmitter and to detect errors at the receiver. Please refer to Appendix A2 for the generator polynomial.

3.2.2 FEC Coding - Turbo Coding

A forward error correction (FEC) or error correction code plays a very important role in error control in data communication, especially in error prone wireless communications. FEC allows the receiver to detect and correct errors (within some bound) by adding some redundant data to the message. The advantage of forward error correction is that a back-channel is not required, or that retransmission of data can often be avoided. However the advantage comes with a cost since a higher bandwidth is required.

In a frequency selective channel, each OFDM subcarrier suffers different distortion and thus different received signal quality. Therefore, some subcarriers may experience severe fading and may affect the overall error performance of the system. If the OFDM system is uncoded, the performance will be dominated by these weak sub-carriers. Therefore, to

take advantage of a multi-carrier system, an efficient FEC is needed to correct the errors caused by the deeply faded subcarriers.

LTE employs the state-of-the-art Turbo coding [9] which pushes the current wireless communication efficiency near to the Shannon limit. Turbo codes were first introduced by Berrou, Glavieux and Thitimajshima in 1993. In the LTE link level simulator, the turbo codes are constructed using two simple recursive systematic convolutional (RSC) code in parallel. Each of the RSC codes has a code rate of ½ and thus the mother code of the turbo code is 1/3 and would generate 2 parity bits (1 bit from each RSC encoder) for each data bit. Please refer to Appendix A2 for the generator polynomial of the encoder. The turbo decoding employs the Log-MAP (Maximum a Posteriori) algorithm [11] and the maximum number of decoding iterations is limited to 8. The turbo inner interleaver is pseudorandom.

3.2.3 Puncturing

It is relatively easy to adapt the code rate for a Turbo code by puncturing. Puncturing is a process of omitting some of the parity bits or in some case systematic codes after encoding. By removing some of the encoded bits at pre-defined sequences, the code rate can be easily adapted to different coding rates and thus provide finer granularity of coding rates. Furthermore, the same encoder and decoder can be used regardless of the number of bits that have been punctured, and therefore increase the flexibility of the system without significantly increasing its complexity. At the receiver, the inverse operation, known as depuncturing, is implemented by inserting erasures at the pre-defined locations before decoding. The puncturing pattern that is used in the simulator will be given in Section 3.6. Puncturing rates that are supported in the simulator are 1/3, 1/2, 3/4 and 6/7.

3.2.4 Interleaving

The unreliable and error-prone nature of the wireless channel is often a major challenge in the wireless communication. In addition, the errors in wireless channels tend to be very bursty. In order to prevent error bursts, a widely used and important technique, interleaving is often employed. Interleaving aims to randomise the errors bursts and emulate the random errors for correction with error correction codes, e.g. Turbo codes. In the LTE link level simulator, a random interleaving is used.

3.2.5 Scrambling

A scrambling process can eliminate the occurrence of long sequences consisting of '0' or '1' only. In general, a scrambler uses a predefined generator polynomial at the transmitter. The manipulations are then reversed by the same scrambler at the receiving side. In the simulator, a random scrambler is used instead.

3.2.6 Modulation

A modulation process will takes binary digits, 0 or 1, as input and produce complex-valued modulation symbols, $d=I+jQ$, as output. In LTE, both the downlink and uplink will support data modulation schemes of QPSK, 16QAM, and 64QAM [13]. A robust BPSK scheme is mainly used for control signalling in both downlink and uplink. A Gray coded bit-assignment is used to facilitate error correction at the receiver. The constellation diagrams for these modulations schemes are given in Appendix A2.

3.2.7 FFT/IFFT

The success of OFDM lies in the use of the narrowband subcarriers which essentially eliminate the need for a complex equalization process. This can be made possible by modulating data symbols onto parallel frequency sub-carriers via an inverse discrete Fourier transform (IDFT) process. After the modulation, the complex data sequence $(D_0, D_1, \ldots, D_{N-1})$ will go through the IDFT process and can be represented as:

$$D_m = \frac{1}{N}\sum_{n=0}^{N-1} d_n e^{j(2\pi nm/N)} = \frac{1}{N}\sum_{n=0}^{N-1} d_n e^{j(2\pi f_n t_m)} \quad m = 0,1,2,\ldots N-1 \qquad (3\text{-}1)$$

where $f_n = n/(NT_s)$, $t_m = mT_s$ and T_s is the sampling time of the serial data sequence d_n. However for faster and practical implementation, an inverse fast Fourier transform (FFT) is used instead. The FFT exploits the symmetry and periodicity property of the DFT to reduce the repeated and unnecessarily operations. The complexity of the operations can be reduced from $O(N^2)$ to $O(N \log N)$[8] , which is particularly useful for large FFT size. In the LTE link level simulator, the IFFT/FFT size, N is 1024 unless otherwise stated. As a result, the computation complexity can be reduced significantly. At the receiver, an inverse operation (FFT) is applied to Y to determine the received frequency domain data symbols y_n. Thus:

$$y_n = \sum_{m=0}^{N-1} Y_m e^{-j(2\pi nm/N)} \quad n = 0,1,2\ldots N-1 \qquad (3\text{-}2)$$

The output data y_n will be equal to d_n for the case of a distortionless channel and noiseless receiver.

3.2.8 Cyclic Prefix

In order to prevent inter symbol interference (ISI) and inter carrier interference (ICI) due to delay spread and transmit/receiver filter group delay, a method called the Guard Interval or Cyclic Extension is deployed. This method precedes each OFDM symbol with periodic extension of the symbol itself. By doing this, the total OFDM symbol duration will be $T_{total} = T_g + T$, where T_g represents the guard interval and T represents the useful OFDM symbol duration.

When the guard interval is longer than the excess delay of the radio channel, the multipath components from the previous OFDM symbol will not interfere with the current OFDM symbol and thus ISI is eliminated [12]. Since the insertion of the guard interval will reduce the overall efficiency of the system, the length of the guard interval should be maintained at a minimum level, e.g. larger than the maximum excess delay of the radio channel [12].

LTE offers two choices of cyclic prefix, long and short cyclic prefix, with 4.69μs and 16.7 μs respectively [2]. For the case of short cyclic prefix, the useful symbol duration of an OFDM symbol is approximately 67μs and thus the cyclic prefix overhead is approximately 7%. While a short (normal) cyclic prefix does an adequate job for most of the users in the cell, long (extended) cyclic prefix is intended for users at the cell edges where the excess delay spread would be larger than the short cyclic prefix. When the extended cyclic prefix is employed, only 6 OFDM symbols will be transmitted per time slot instead of 7 OFDM symbols, when the normal cyclic prefix is used. The overall efficiency will be inevitably affected in order to provide a better protection against interference.

3.2.9 Channel Estimation

Frequency selective fading along with timing offset and frequency offset causes random phase and amplitude variation of the constellation on the sub-carriers. Therefore coherent detection using estimates of the reference amplitudes and phases is crucial to determine the best possible decision boundaries for the constellation of each sub-carrier. The channel estimation in OFDM systems is generally based on the use of pilot subcarriers in given positions of the frequency-time grid. For fast-varying channels, non-negligible

fluctuations of the channel gains are expected between consecutive subcarriers and OFDM symbols. Thus, in order to ensure adequate estimation accuracy, it is necessary to spread the pilot subcarriers across the OFDM subframe. According to [13], the pilot structure for the LTE downlink is shown in Figure 3-2. In the simulation, a linear interpolation technique is used to interpolate the channel gain in between the subcarriers. However in the time domain, the channel estimation is assumed to be constant for all the OFDM symbols, since a channel is assumed to remain the same during the transmission of a packet. In addition to that, an IEEE802.11a WLAN channel estimation strategy using preamble is considered for comparison. Pilots are spread across the entire frequency domain and by averaging over two OFDM symbols (as shown in Figure 3-3), the distorting effects of noise on the channel estimation process can also be reduced.

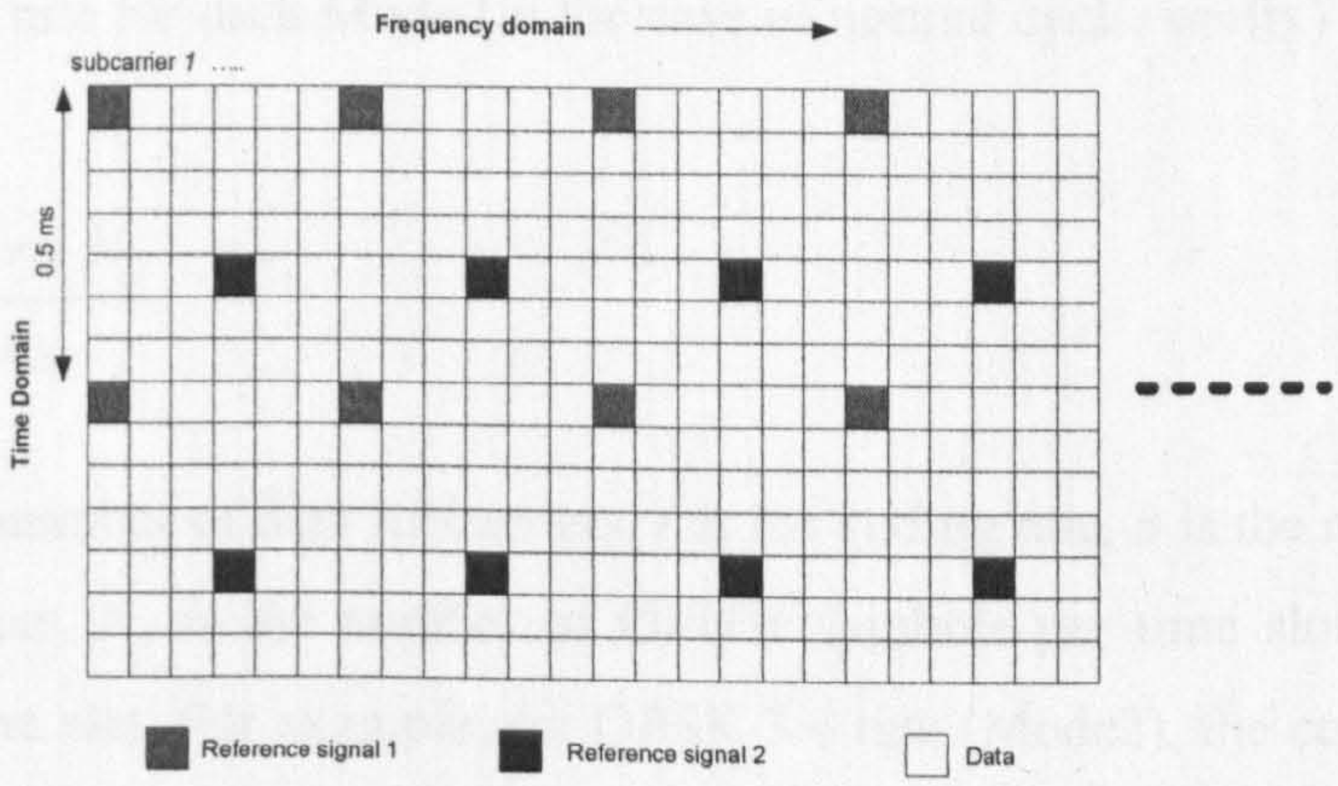

Figure 3-2: LTE pilot structure for SISO

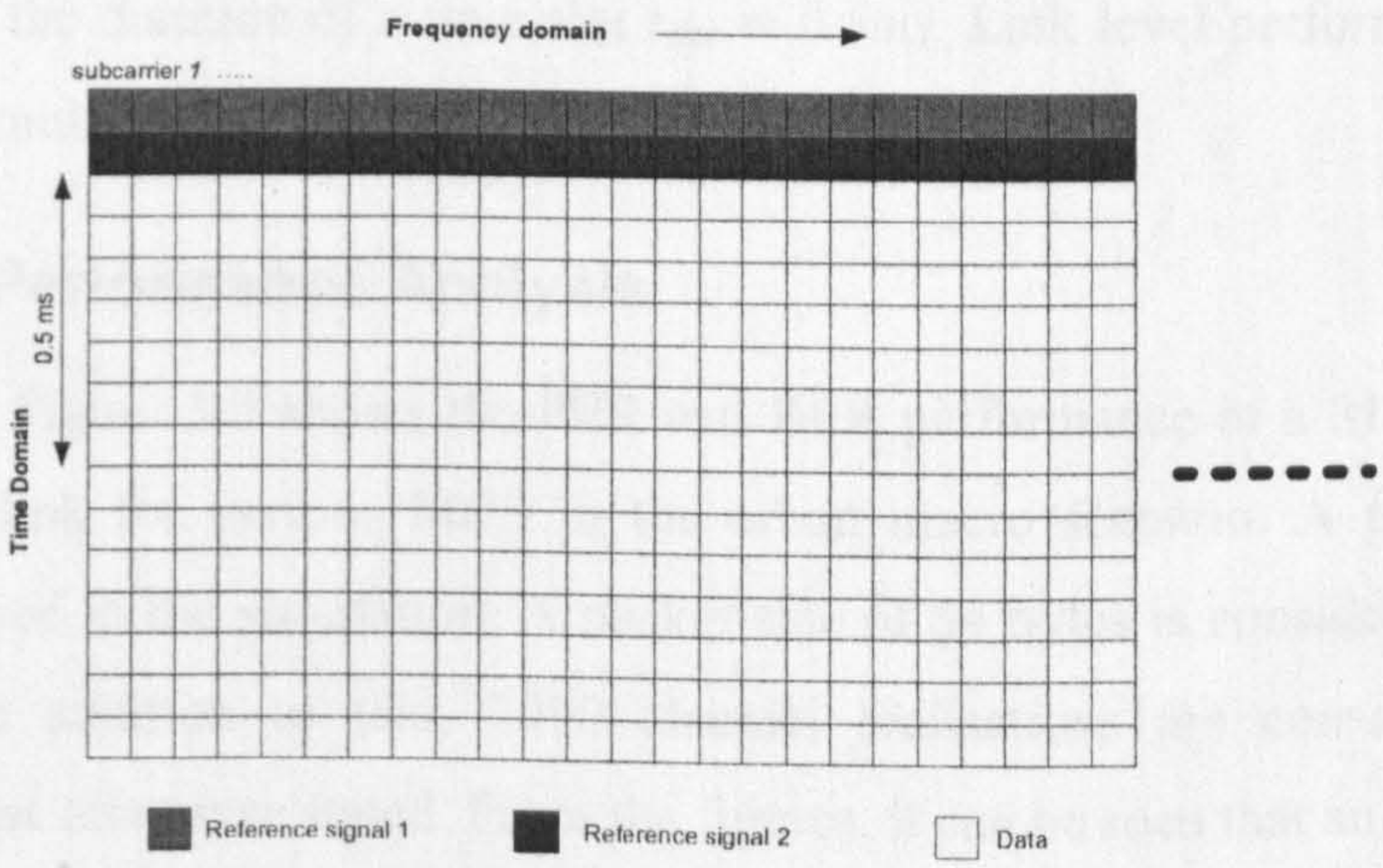

Figure 3-3: Channel estimation using preamble strategy

3.3 SISO Physical Layer performance for LTE Downlink

As mentioned in an earlier section, only three data modulation schemes are supported in the downlink. These are QPSK, 16QAM and 64QAM. In the simulation model, only six Modulation and Coding Schemes (MCS) levels are considered, as shown in Table 3-2. For a complete list of MCS levels in LTE, please refer to [10].

Table 3-2: Modulation and Coding Schemes

Mode	Modulation	Coding Rate,*r*	Coded bits per subcarrier,*b*	Data bits per time slot (0.5ms)	Nominal Bit Rate(Mbps)
1	QPSK	1/2	2	4200	8.4
2	QPSK	3/4	2	6300	12.6
3	16 QAM	1/2	4	8400	16.8
4	16 QAM	3/4	4	12600	25.2
5	64 QAM	1/2	6	12600	25.2
6	64 QAM	3/4	6	18900	37.8

The nominal bit rate for each Mode (in the case of normal cyclic prefix) can be obtained by:

$$Bit\ Rate, R = \frac{N_d r b\ N_o}{t_{slot}} \tag{3-3}$$

Where N_d is the number of data subcarriers, r is the coding rate, b is the number of coded bits per subcarrier, N_o is the number of OFDM symbols per time slot and t_{slot} is the duration of a time slot. For example, for QPSK 3/4 rate (Mode2), the coding rate r=3/4, the number of coded bits per subcarrier $b=2$, and the number of OFDM symbols per time slot $N_o = 7$ and the duration of a time slot $t_{slot} = 0.5ms$. Link level performance for each MCS will be simulated and investigated in the following section.

3.3.1 Error Performance Analysis

Figure 3-4 and Figure 3-5 shows the PER and BER performance of a SISO scenario in the LTE downlink for various MCS in the urban macro scenario. A perfect channel estimation is used in the simulation. A packet size of 54 bytes is considered throughout the chapter. In addition to that, 2000 channel realisations are considered in each simulation unless otherwise stated. From the figures, it can be seen that an UE will be out of service when the SNR is below 0dB while the UE will be at the highest MCS at approximately 24dB given that PER transmission target of 10% is often expected. It is also worth mentioning that Mode 4, i.e. 16QAM ¾ coding rate becomes obsolete for these channel conditions since it is outperformed by 64QAM ½ coding rate over the whole SNR range and gives the same nominal data rate. Since MIMO techniques are

supported in the LTE specifications and these techniques offer higher spectral efficiency, SISO performance is mainly simulated for comparison purposes.

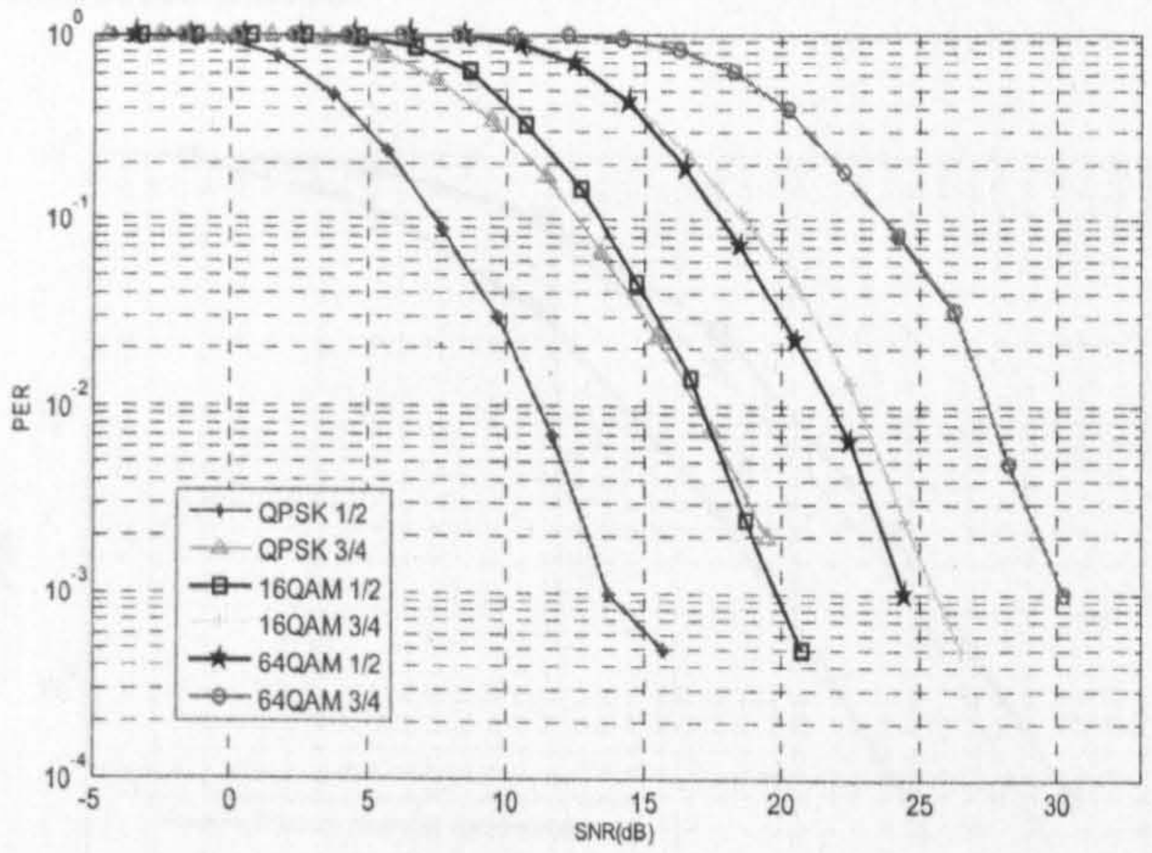

Figure 3-4: PER Performance for different MCS in Urban Macro channel

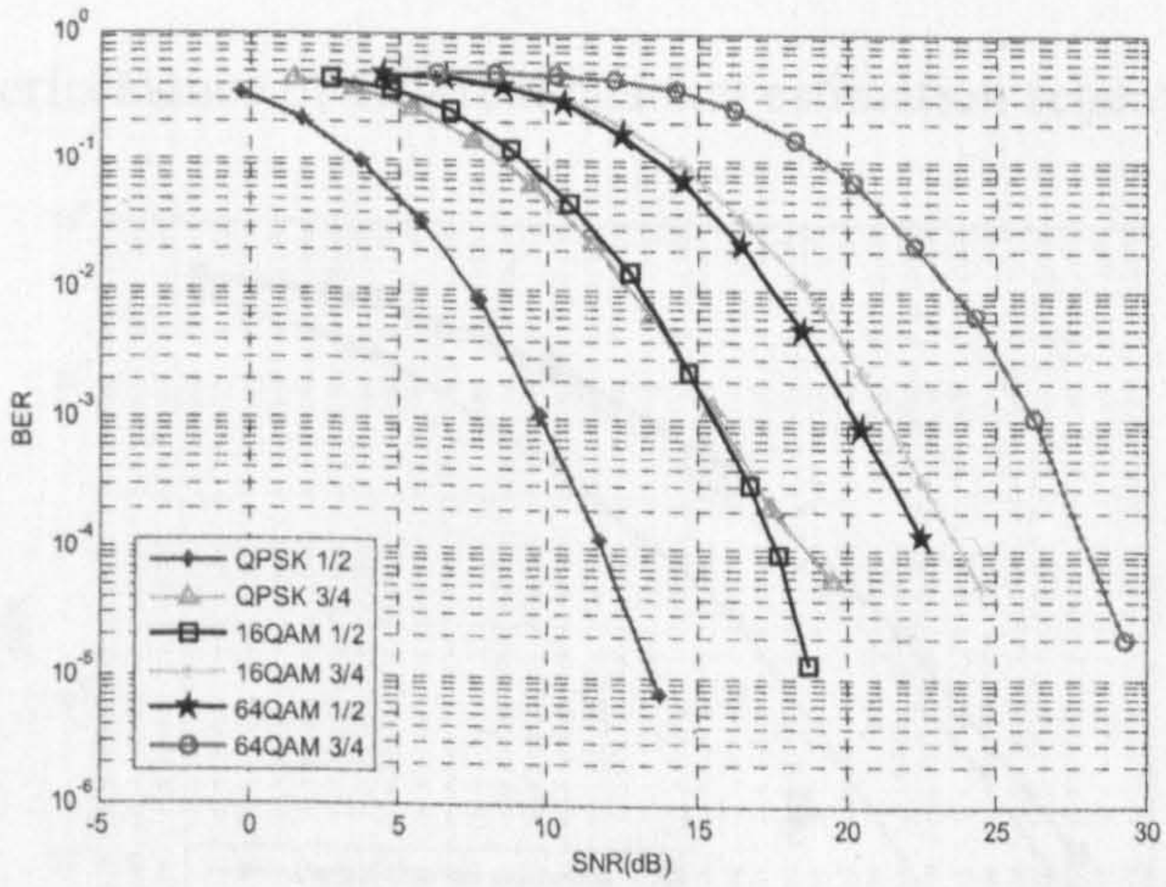

Figure 3-5: BER Performance for different MCS in Urban Macro channel

Figure 3-6 and Figure 3-7 show the PER and BER performance respectively for QPSK ½ rate in urban macro scenario for different channel estimation strategies. Perfect channel estimation, where the channel variation is perfectly known at the receiver performs superior to the channel estimation methods using preamble and the LTE pilot structure. It is worth noting that the LTE pilot structure is only marginally worse than the preamble strategy which spreads pilots across all the frequency sub-carriers. Thus, by carefully selecting the pilot structure such as the LTE pilot structure, the number of pilots can be reduced considerably but only with an expense of slight performance trade-off. However it should be kept in mind that a constant channel is assumed throughout a packet transmission and thus the preamble strategy will have an edge over the pilot strategy. In

the case of time- varying channel (in a packet transmission), this may not hold true. For consistency and comparison throughout the thesis, the perfect channel estimation strategy is assumed unless otherwise stated.

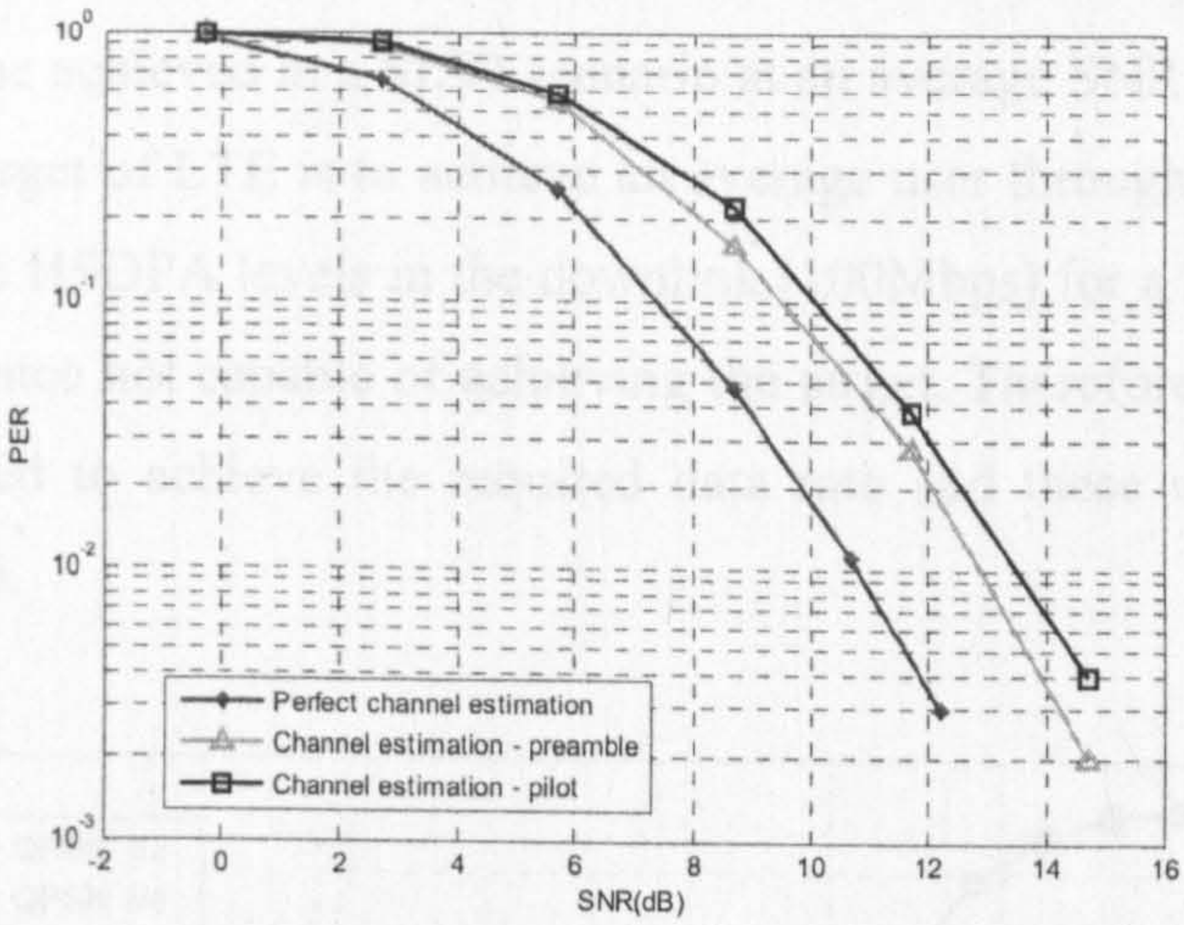

Figure 3-6: PER performance of different channel estimation schemes in QPSK 1/2 rate

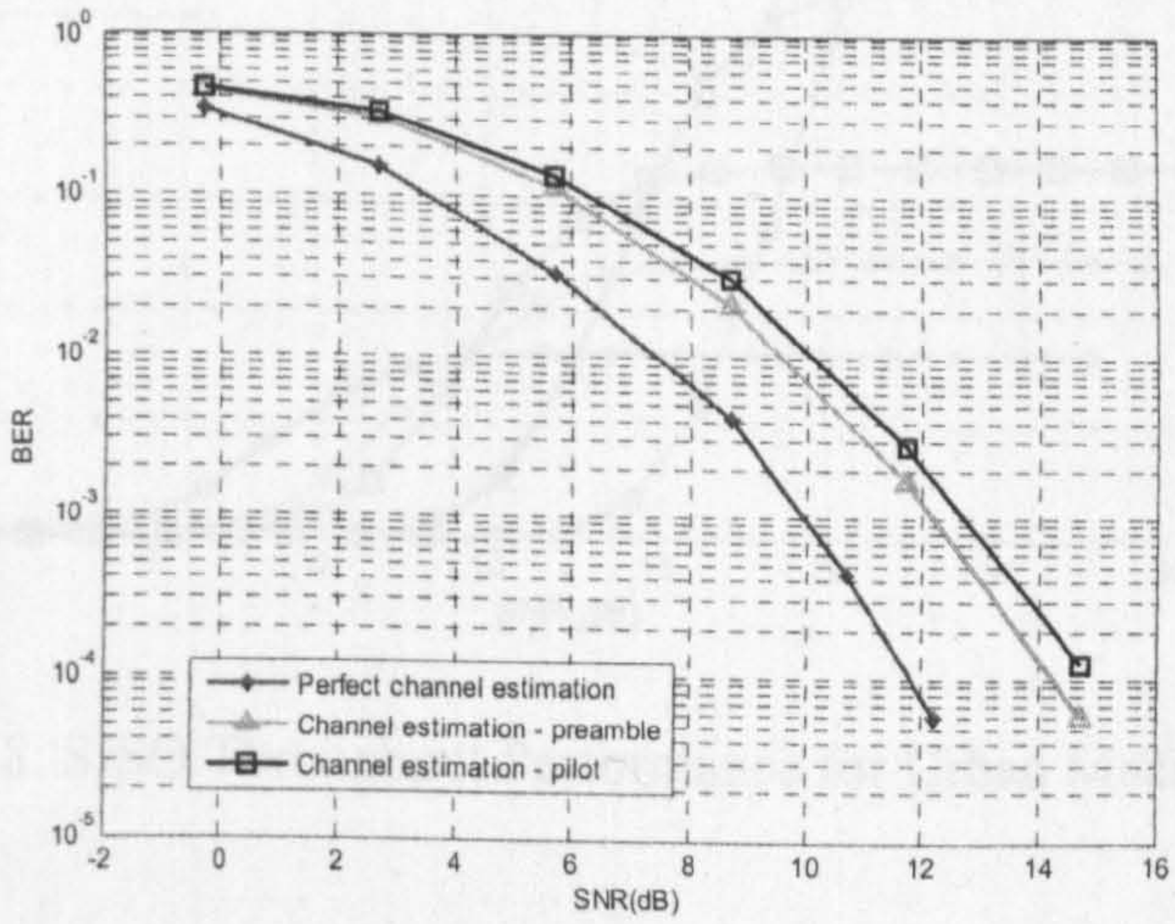

Figure 3-7: BER performance of different channel estimation schemes in QPSK 1/2 rate

3.3.2 Throughput Performance Analysis

The average achievable throughput for the SISO scheme in the urban macro scenario is presented in Figure 3-8. The achievable throughput is derived from the data rate and the residual packet error rate and thus measured in terms of bits per second. An approximation of the link throughput is given by:

$$Throughput \approx R(1 - PER) \qquad (3\text{-}4)$$

where R and PER are the bit rate and the residual packet error rate for a specific mode respectively. The throughput envelope is obtained by using ideal adaptive modulation and coding (AMC) based on the (throughput) optimum switching point. Given the system bandwidth of 10MHz, it can be seen that a maximum spectral efficiency of 3.78bits/Hz/s can be achieved in a SISO scenario at an average SNR of 27dB. However, the fundamental target of LTE is to achieve an average user throughput of three to four-times the Release 6 HSDPA levels in the downlink (100Mbps) for a 20MHz spectrum. A SISO scheme is hence not capable of achieving the target. Therefore, MIMO techniques will be incorporated to achieve the required data rate and these will be discussed in details in Chapter 6.

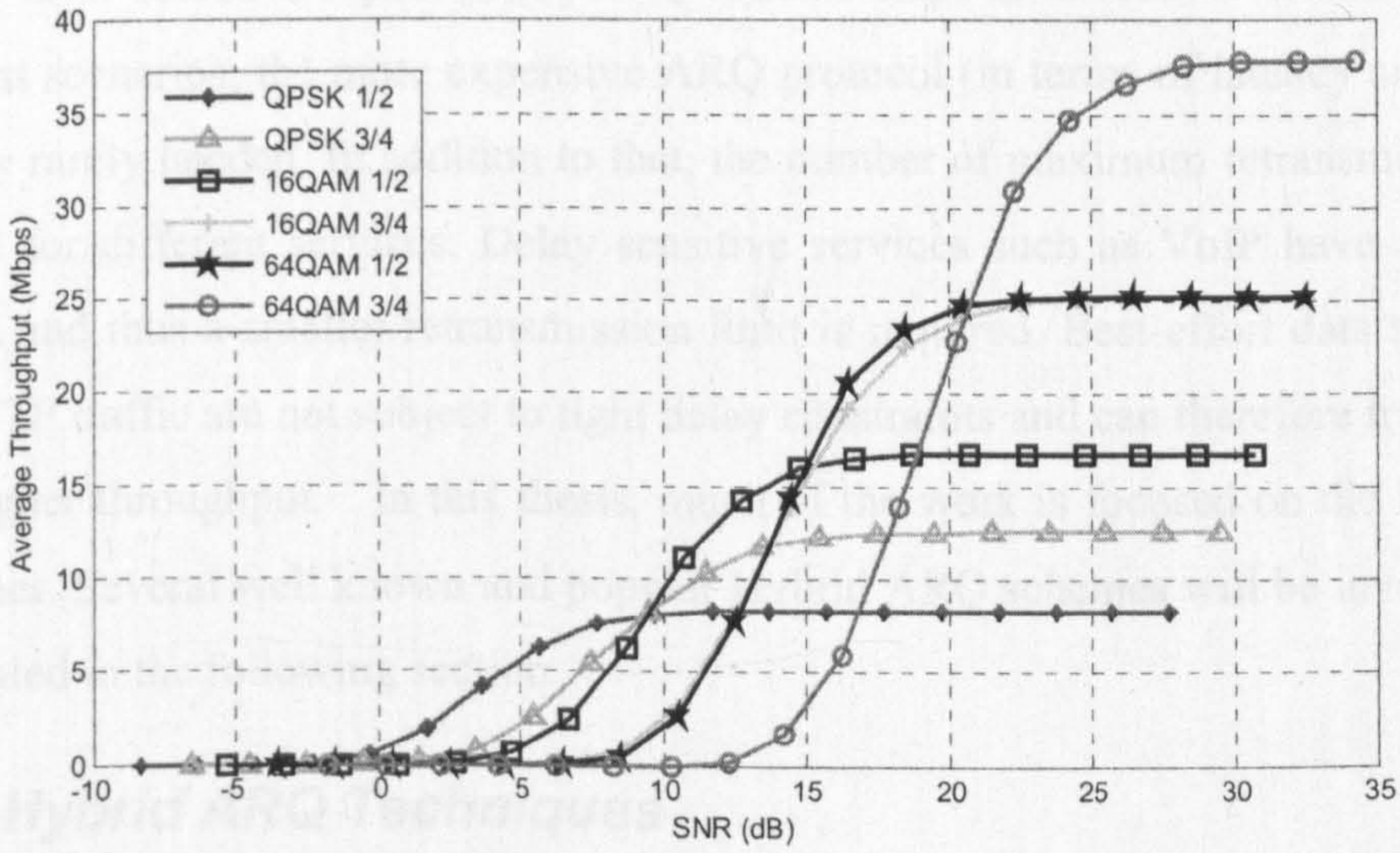

Figure 3-8: SISO Throughput Performance for Urban Macro channel

3.4 LTE Hybrid ARQ

The wireless communication channel is error prone in nature. Occasional data transfer errors which arise from noise, interference and fading are inevitable in any communications system, especially in a wireless system. Thus, a retransmission scheme is necessary to safeguard against these errors and to maintain the quality of data and services. In addition to that, a more efficient retransmission handling can further increase the radio capabilities and ultimately leads to throughput enhancement.

Hybrid ARQ is essentially a combination of Forward Error Correction (FEC) with Automatic Retransmission request in an enhanced manner. Hybrid ARQ schemes are

commonly used to provide a reliable communication over noisy wireless channels. Hybrid ARQ is able to compensate for link adaptation errors and provide a finer granularity of coding rate thus giving a better throughput performance.

LTE supports a dynamic and efficient two layered retransmission scheme: A fast hybrid ARQ protocol with low overhead feedback complemented by a highly reliable selective repeat ARQ protocol. This two layered retransmission scheme yields a low latency and overhead without compromising reliability. In general, most of the errors are captured and corrected by the lightweight Hybrid ARQ protocol. The lower layer Hybrid ARQ uses N-process Stop-And-Wait protocol [3][14]. However, when the Hybrid ARQ is not able to correct the error after some time, e.g. reaching the retransmission limit, then the higher layer selective repeat [2][3] ARQ scheme steps in to recover the data. Therefore, in most scenarios, the more expensive ARQ protocol (in terms of latency and overhead) is only rarely needed. In addition to that, the number of maximum retransmission can be varied for different services. Delay sensitive services such as VoIP have a tight delay bound and thus a smaller retransmission limit is required. Best-effort data services such as HTTP traffic are not subject to tight delay constraints and can therefore trade off delay for higher throughput. In this thesis, much of the work is focused on the Hybrid ARQ schemes. Several well known and popular Hybrid ARQ schemes will be investigated and presented in the following section.

3.5 Hybrid ARQ Techniques

3.5.1 Hybrid ARQ Type I

The simplest method is called Hybrid ARQ Type-I or Simple ARQ. When a packet is found to be in error though Cyclic Redundancy Check (CRC), a retransmission request will be sent to the transmitter and the erroneous packet will be discarded. The transmitter will then retransmit the same packet until the packet is successfully decoded at the receiver or a maximum retransmission limit is reached.

In the case where the erroneous packets are stored in a buffer and the corresponding soft values at bit level are combined according to the weights of received signal to noise ratio, this method is known as Hybrid ARQ Type I with Packet Combining or Chase Combining [15]. There are two popular methods to combine the information from each transmission depending on the location of combining in the receiver. The first method is bit-level combining. The combining for bit-level combining happens at the output of the

bit-metric calculator. The packets are combined at bit level by direct addition of the demodulation of soft bits. Demodulation of soft bit is equivalent to values of Log Likelihood Ratio (LLR) [16] given as:

$$LLR(b) = \log \frac{P_r\{b = 1|r\}}{P_r\{b = 0|r\}} \tag{3-5}$$

The second method is symbol-level combining, where the packets are combined before the demodulation of soft bits. Symbol level combining has better performance while requiring smaller buffer size at the receiver [19]. However the symbol level combining method has some limitations which make it unsuitable for practical implementation. For symbol level combining, the same modulation scheme should be used to ensure the same symbol location for maximal ratio combining which is not suitable for systems which employ adaptive modulation or constellation rearrangement [23] techniques. Additionally, Hybrid ARQ schemes such as incremental redundancy will be more difficult to implement using symbol level combining. On the other hand, combining at the bit level, which requires the same information bits but not necessarily the same symbol does not have this limitation.

Figure 3-9 gives a simple graphical illustration of the received bits at the receiver for each transmission. As can be seen in Figure 3-9, the coding rate remains the same after retransmissions, however the robustness is improved due to the maximal ratio combining process which increases the diversity gain and error performance.

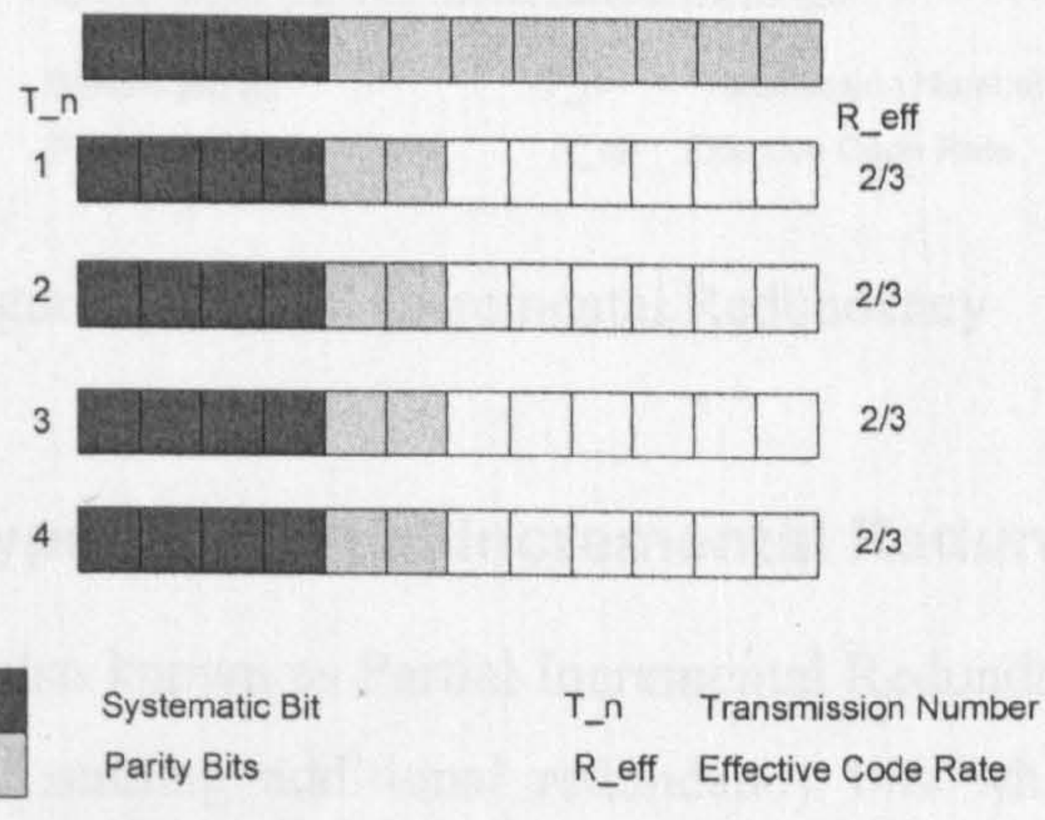

Figure 3-9: Chase Combining

3.5.2 Hybrid ARQ Type II - Full Incremental Redundancy

Hybrid ARQ Type II is known as Full Incremental Redundancy (IR). In incremental redundancy schemes, information bits are usually encoded by a low rate mother code. Based on the selected modulation and coding scheme, information bits and a selected number of parity bits are transmitted. If the transmission is not successful, Full IR decreases coding rate in each retransmission by sending additional redundancy (parity bits) only. The retransmitted packet can be chase combined with the previous packets to increase the diversity gain. This strategy can rapidly reduce the coding rate in the retransmission, thus more coding gain can be achieved. When the coding rate is reduced to the mother rate, e.g. 1/3, then a repetition code is used where the previously transmitted code is repeated. In comparison to Chase Combining, there is a higher implementation effort and buffer requirement [17]. Full IR can be illustrated in Figure 3-11 where the initial coding rate of 2/3 is rapidly decreased to coding rate of 1/3 coding after 1 retransmission. When the mother code is reached, repetition code is then used to exploit more diversity gain at the receiver.

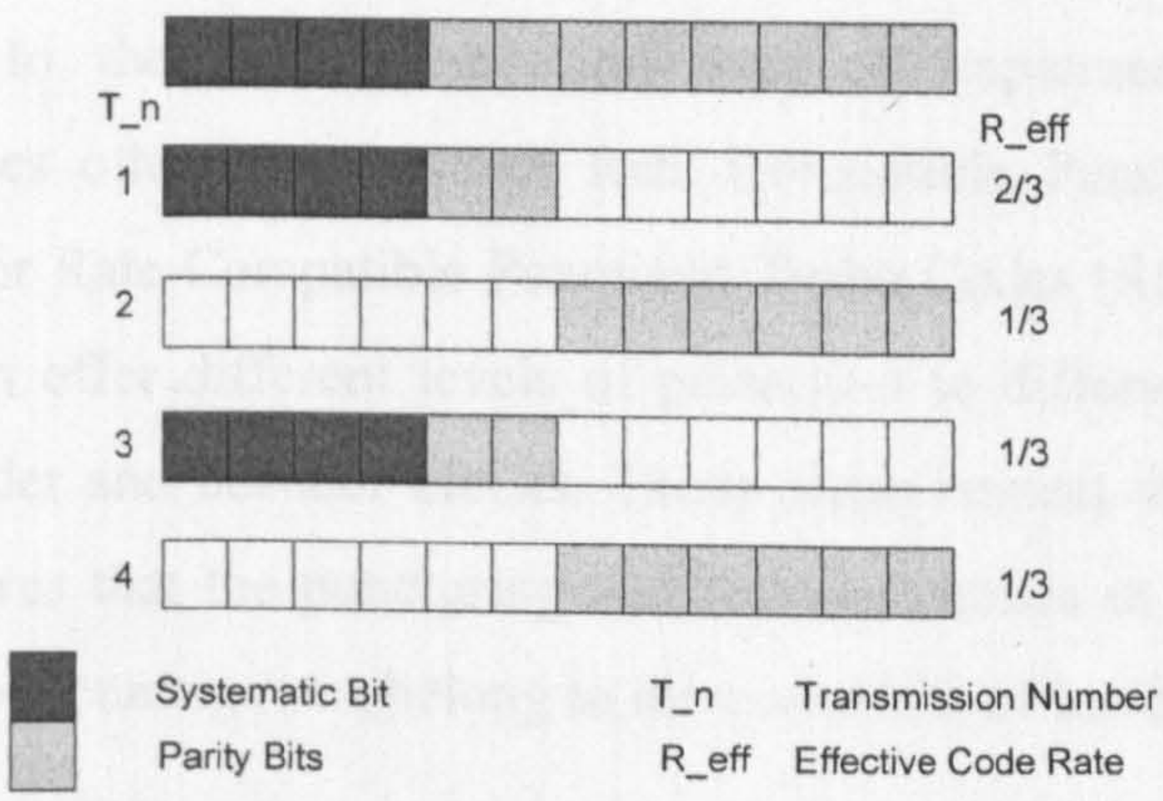

Figure 3-10: Full Incremental Redundancy

3.5.3 Hybrid ARQ Type-III - Partial Incremental Redundancy

Hybrid ARQ Type-III is also known as Partial Incremental Redundancy and this method decreases coding rate by sending additional redundancy bits while maintaining self-decodability in each retransmission These bits will then be combined with the previously received packets which were stored at the buffer of the receiver to form more powerful error correction codes. This can be illustrated in Figure 3-11 where the initial coding rate of 2/3 is gradually decreased to coding rate of 1/3 coding after 3 retransmissions. On top of the coding gain, the multiple copies of systematic bits can be chase combined to

further exploit the diversity gain. Thus, Partial IR can obtain considerable improvement over Chase combining due to additional coding gain. However, there is a trade-off of higher implementation effort and buffer requirement.

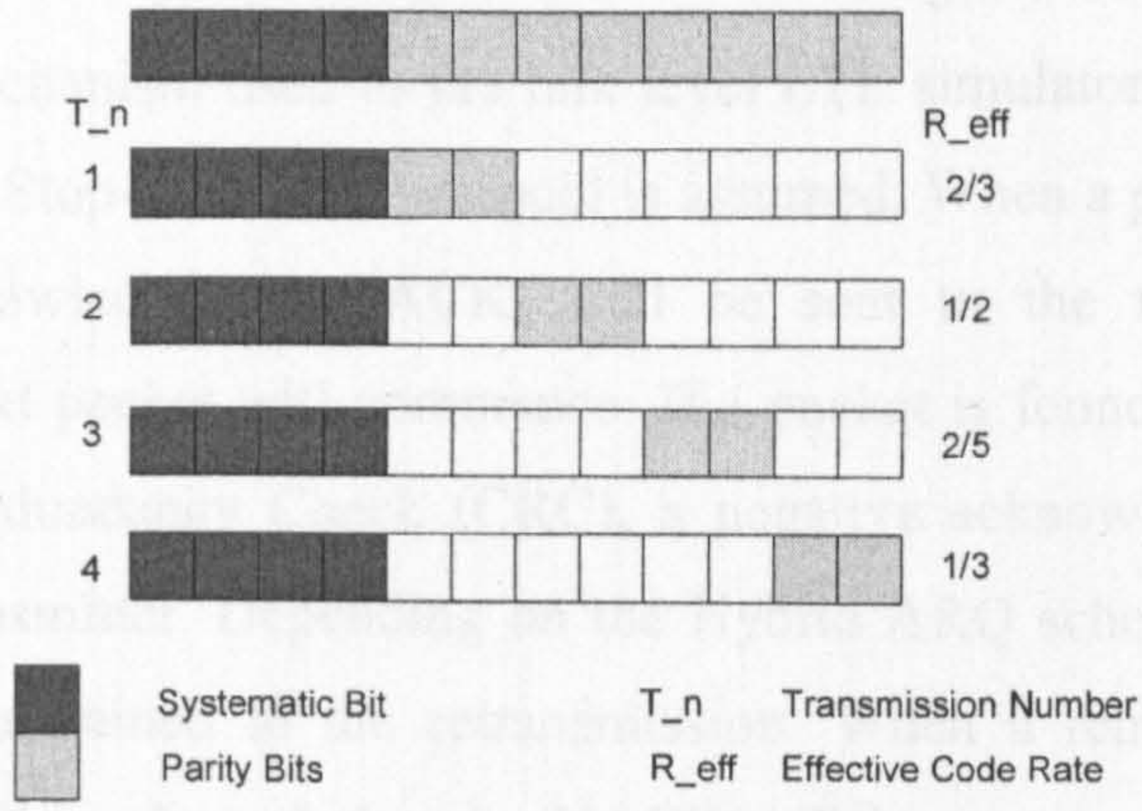

Figure 3-11: Partial Incremental Redundancy

3.6 Rate Compatible Puncturing Codes

The family of codes used in the incremental redundancy are obtained by puncturing the mother code. Due to the performance and ease of implementation, incremental redundancy techniques often make use of Rate Compatible Punctured Convolutional Codes (RCPC) [20] or Rate Compatible Punctured Turbo Codes (RCPT) [21]. The rate-compatible codes can offer different levels of protection to different blocks of bits by using the same encoder and decoder blocks. These codes respect the rate compatibility criterion which requires that the puncturing matrices are chosen in such a way that the coded bits of higher puncturing rates belong to the coded bits of lower puncturing rates.

In the simulation, the RCPT codes can be obtained by puncturing the parity bits of a rate 1/3 mother turbo code. A puncturing period of 6 is used in this simulation to form the code rates of 3/4 and 1/2. The puncturing matrix used in the simulation is shown in Table 3-3.

Table 3-3: RCPT Puncturing Table

RCPT Systematic Puncturing Table						
Systematic	1 1 1 1 1 1	1 1 1 1 1 1	1 1 1 1 1 1	1 1 1 1 1 1	1 1 1 1 1 1	1 1 1 1 1 1
Parity 1	1 0 0 0 0 0	1 0 1 0 0 0	1 0 1 0 1 0	1 1 1 0 1 0	1 1 1 1 1 0	1 1 1 1 1 1
Parity 2	0 0 0 1 0 0	0 0 0 1 0 1	0 1 0 1 0 1	0 1 0 1 1 1	1 1 0 1 1 1	1 1 1 1 1 1
Code Rate	3/4	3/5	1/2	3/7	3/8	1/3

3.7 Physical Layer performance of LTE with HARQ

The performance of these Hybrid ARQ schemes is investigated in the LTE downlink. The retransmission mechanism used in the link level LTE simulator is shown in Figure 3-12. A single channel Stop-And-Wait protocol is assumed. When a packet is transmitted successfully, an acknowledgement (ACK) will be sent to the transmitter and the transmission of the next packet will commence. If a packet is found to be in error, e.g. detected by Cyclic Redundancy Check (CRC), a negative acknowledgement (NACK) will be sent to the transmitter. Depending on the Hybrid ARQ scheme, the coding rate will be reduced or maintained in the retransmission. When a retransmission limit is reached, the packet will be discarded and a NACK will be sent to the transmitter. An error is logged, the counter will be reset, and the next packet will be transmitted. In the simulator, the maximum number of retransmissions is limited to 4.

In the analysis, a quasi-static fading channel is assumed where the channel gain is constant during one transmission block and changes independently from one block to another. In this investigation, a static environment is assumed where the channel condition remains constant over all the transmission blocks within one ARQ mechanism. In the static environment, there is no temporal diversity that can be achieved in the retransmissions. Therefore, the coding and combining gain that can be achieved by different HARQ schemes can be better reflected under this environment. A dynamic environment is also considered where a new channel condition is used in each retransmission. The results will be presented in Appendix A1.

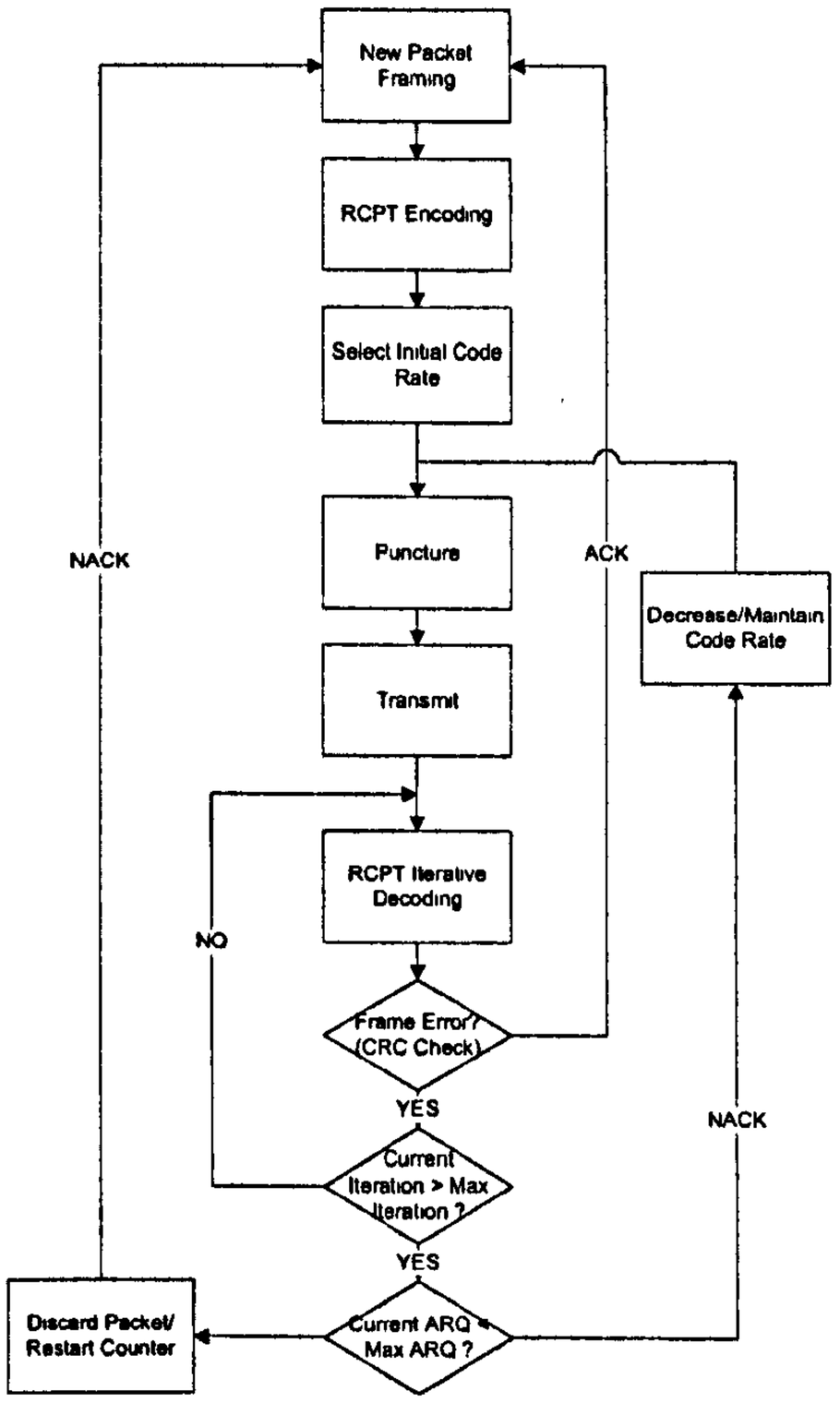

Figure 3-12: The flowchart for Hybrid ARQ Simulator

3.7.1 Error Performance Analysis

Figure 3-13 present the PER performance of various Hybrid ARQ schemes for 16QAM ¾ rate. From Figure 3-13a, it can be observed that very little gain is obtained in the retransmissions, where a static environment model is assumed. However, when a more dynamic environment is considered, the performance gain will be more significant. These results will be shown in Appendix A1. The simple ARQ scheme does not exploit any combining gain from each retransmission due to the fact the erroneous packets from the previous transmissions were discarded. In the case of Chase Combining, significant combining gain can be achieved in each subsequent retransmission. From Figure 3-13b, it can be seen that most significant gain is obtained in the first retransmission (2^{nd} transmission), where the combining gain is approximately 3dB. The combining gain in later retransmissions deceases gradually. Figure 3-13c shows that the Partial IR scheme achieves higher gain in the retransmissions. In the Partial IR scheme, a more robust error correction code is formed in each retransmission. Thus this scheme obtains more gain in each retransmission compared to Chase Combing scheme due to additional coding gain.

On the other hand, Full IR achieves the highest gain (up to 9dB at PER of 10^{-2}) in the first retransmission, which can be observed in Figure 3-13d. Since the Full IR scheme only transmits the parity bits in the retransmission, huge decoding gain can be obtained. When the coding rate is reduced to the mother code rate, a repetition code is used and more gain can also be obtained from the combining process.

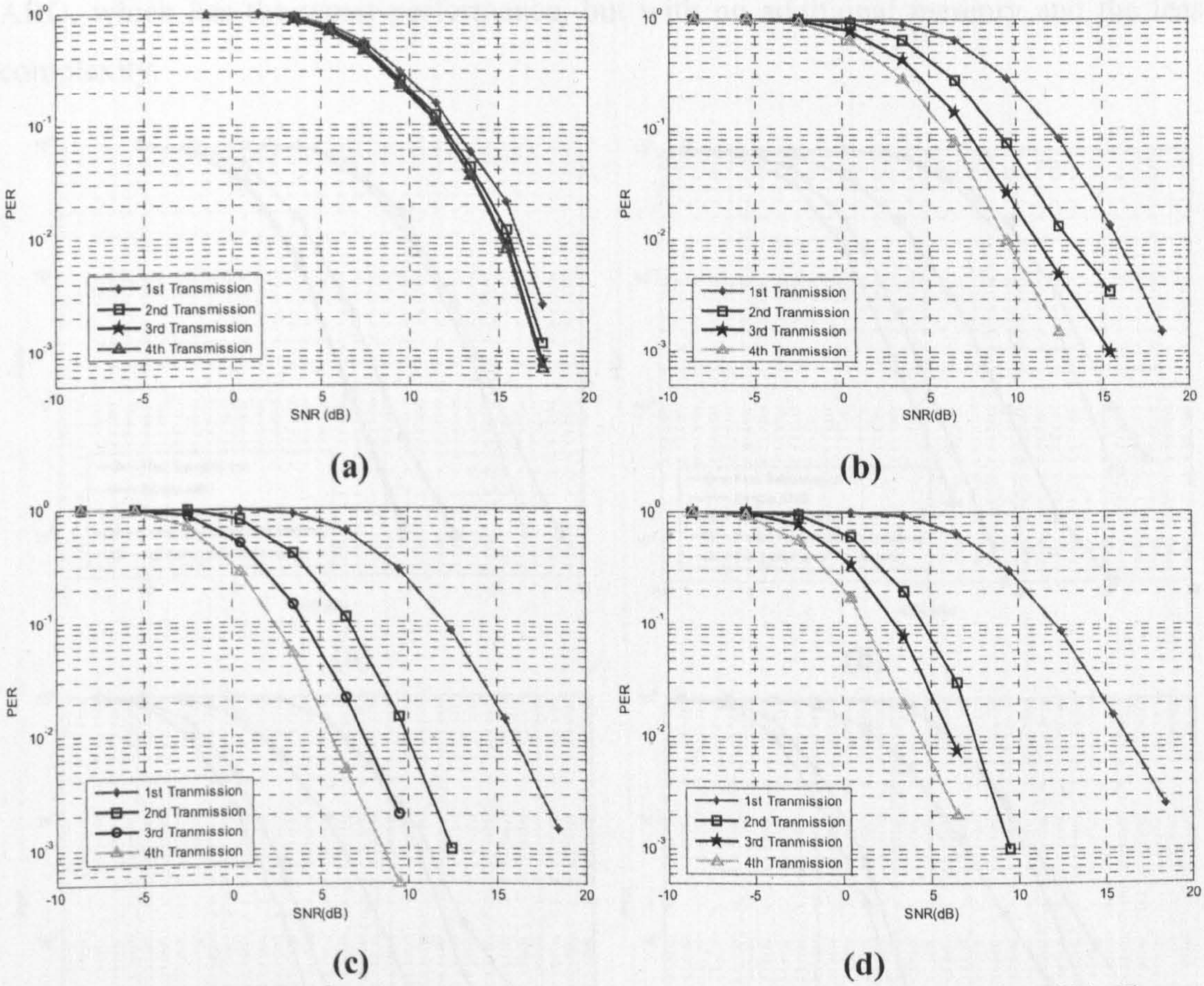

Figure 3-13: PER Performance over retransmissions for a) Simple ARQ and b) Chase Combining c) Partial Incremental Redundancy and d) Full Incremental Redundancy

Figure 3-14a-d present the PER performance of various Hybrid ARQ schemes for different MCS levels, with a packet size of 54 bytes. It can be clearly seen that Full IR outperforms other Hybrid ARQ schemes, especially for high MCS. Both IR techniques outperform Chase Combining due to the high decoding gain obtained over the retransmissions. For high coding rate (3/4), Partial IR require six retransmission to transmit all the redundancy bits and to reduce the effective coding rate down to 1/3 mother coding rate. On the contrary, Full IR can reduce the coding more rapidly as more redundancy bits are sent instead of systematic bit. For lower coding rate (1/2), Full IR no longer has decoding gain over Partial IR since both methods reduced the coding rate

down to 1/3 mother code with just one retransmission. Thus for Mode 1, both Full IR and Partial IR have identical performance.

Full IR offers maximum decoding gain among all schemes but at the expense of the highest soft combining buffer requirements. Chase Combining on the other hand is easier to implement and requires lower memory. It offers better performance than Simple ARQ, which has the worst performance, but with no additional memory and the least complexity.

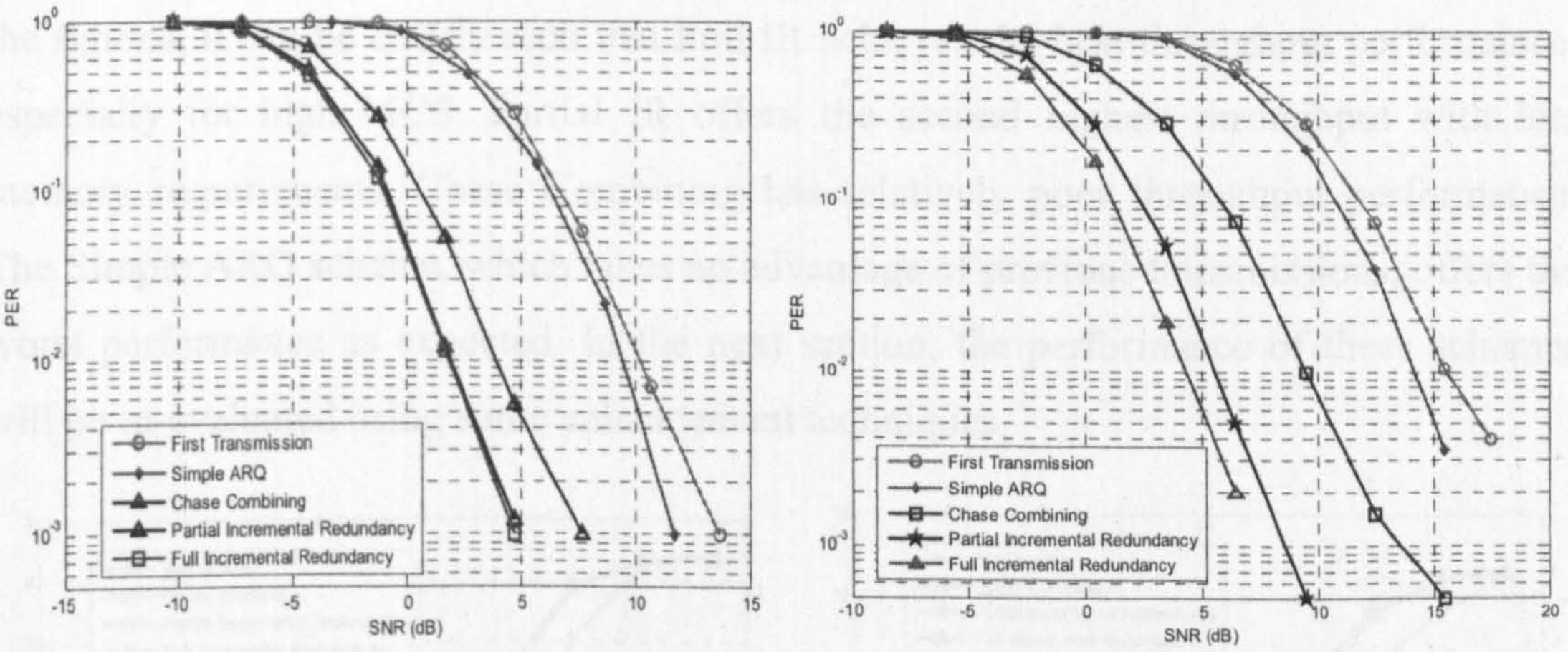

(a) (b)

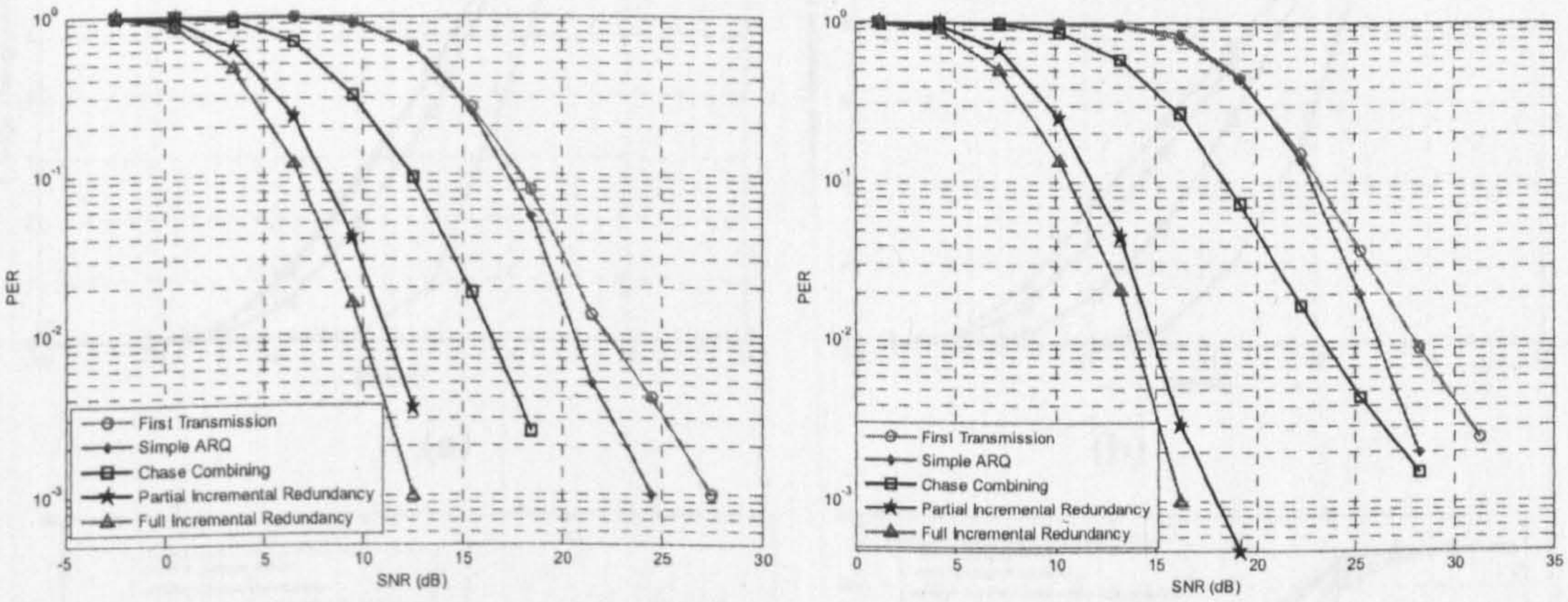

(c) (d)

Figure 3-14: PER Performance for different HARQ schemes for a) Mode 1, b) Mode 2, c) Mode 4 and d) Mode 6

3.7.2 Throughput Performance Analysis

Throughput is an important metric to measure the performance of different HARQ schemes. Throughput is defined as the expected number of correctly received information bits per time duration that it takes the transmitter to send only one data

packet. Thus to take into account the multiple transmissions of Hybrid ARQ, the throughput equation is given by [18]:

$$Throughput = \frac{R(1-PER)}{N_{ave}} \tag{3-6}$$

where R is the transmitted bit rate, PER is the residual packet error rate after maximum number of retransmissions and N_{ave} is the average number of transmissions. The throughput performance of the Hybrid ARQ schemes is given in Figure 3-15a-d. From the figures, it can be clearly seen that Full IR achieves the best throughput performance, especially for high MCS. Partial IR offers the second highest throughput with less memory requirements. Chase Combining has relatively poor throughput performance. The Simple ARQ scheme, which takes no advantage of previous transmissions, offers the worst performance as expected. In the next section, the performance of these schemes will be re-evaluated using some enhancement techniques.

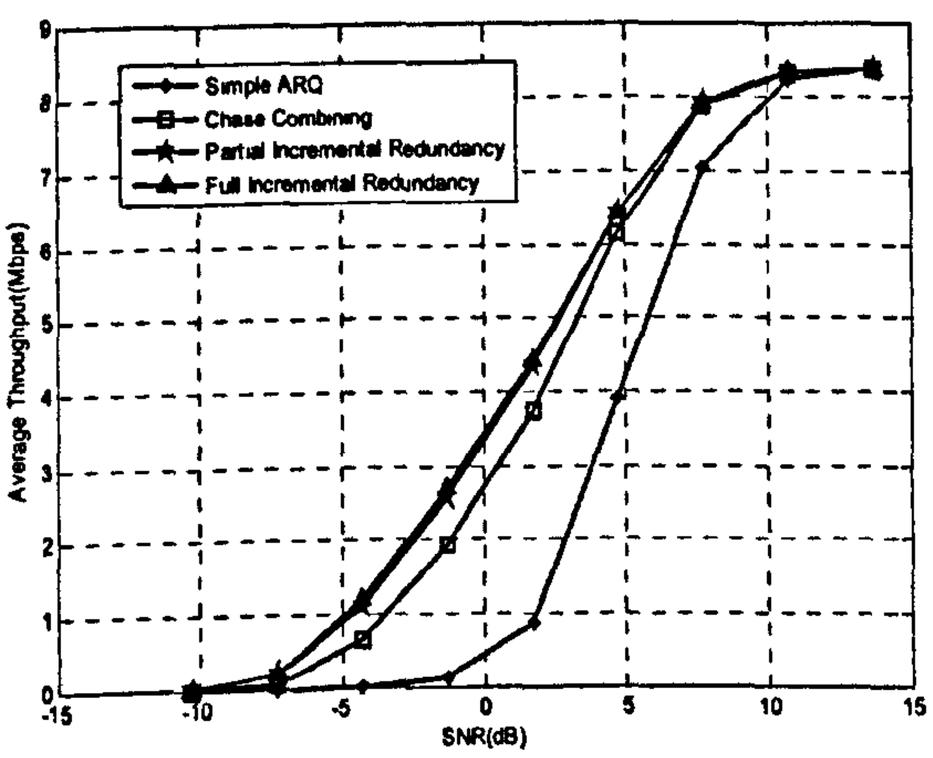

(a)

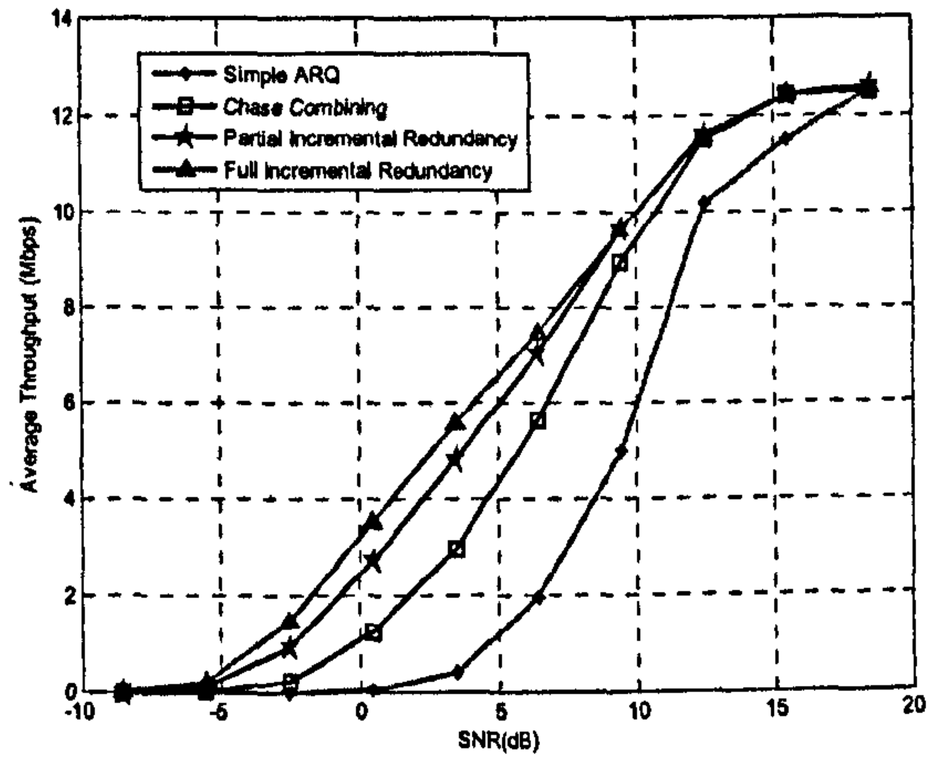

(b)

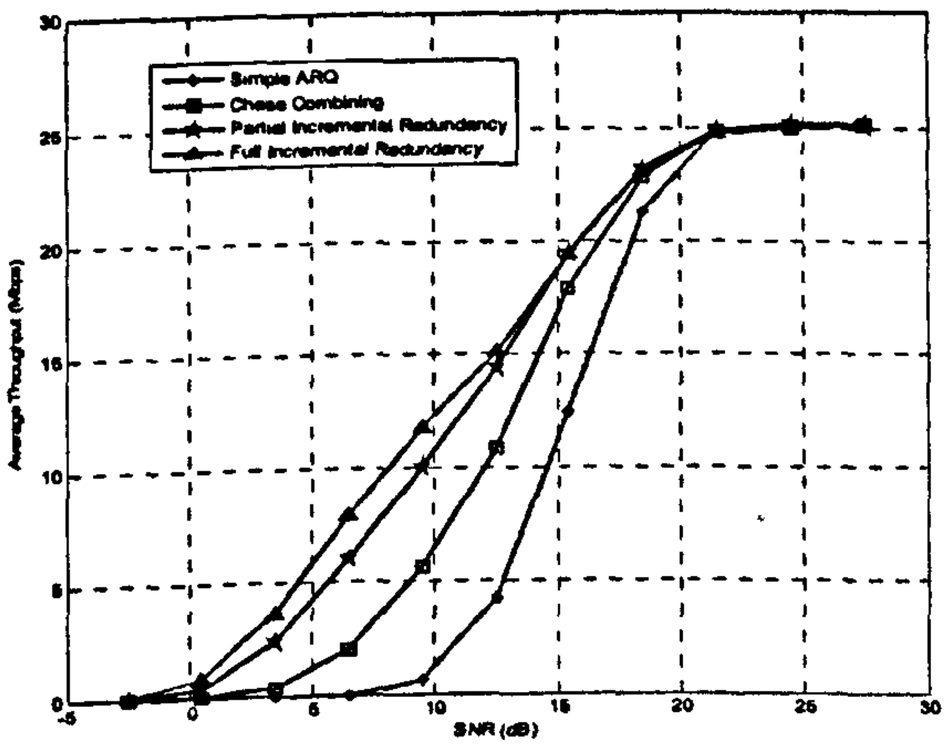

(c)

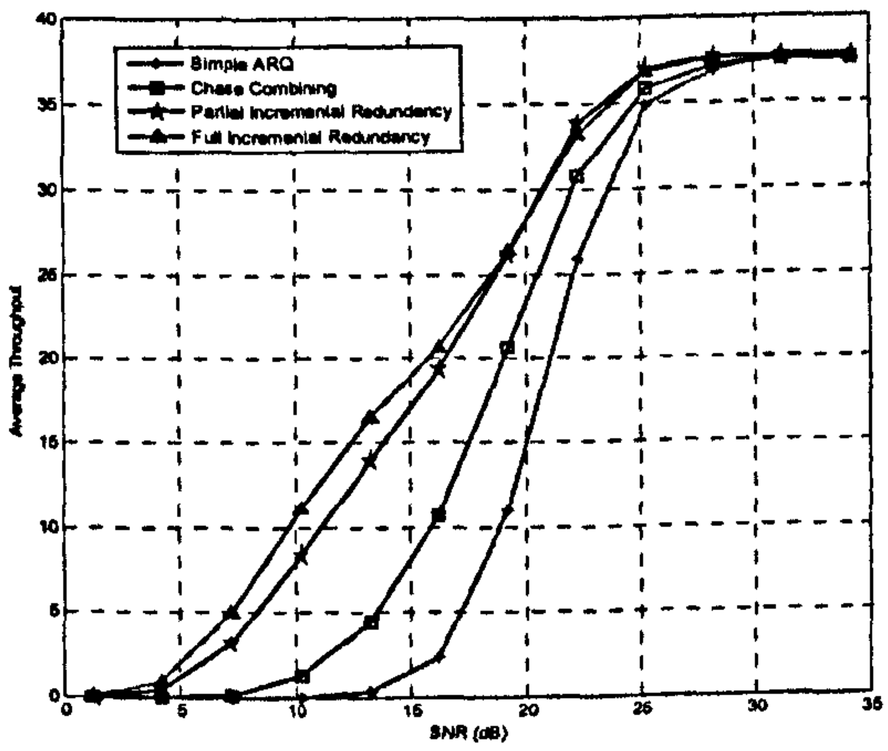

(d)

Figure 3-15: Throughput performance comparison for a) Mode 1, b) Mode 2, c) Mode 4 and d) Mode 6

3.8 Hybrid ARQ Enhancement Techniques

Several techniques have been proposed to further improve the system performance in the retransmissions on top of the gain by Hybrid ARQ techniques. [22] exploits the frequency diversity to obtain additional diversity gain, [23] exploits the inequality of unequal bit protection in higher order modulation schemes. In this section, both techniques will be investigated and the performance of these techniques in LTE will be evaluated and presented.

3.8.1 Subcarrier Rearrangement

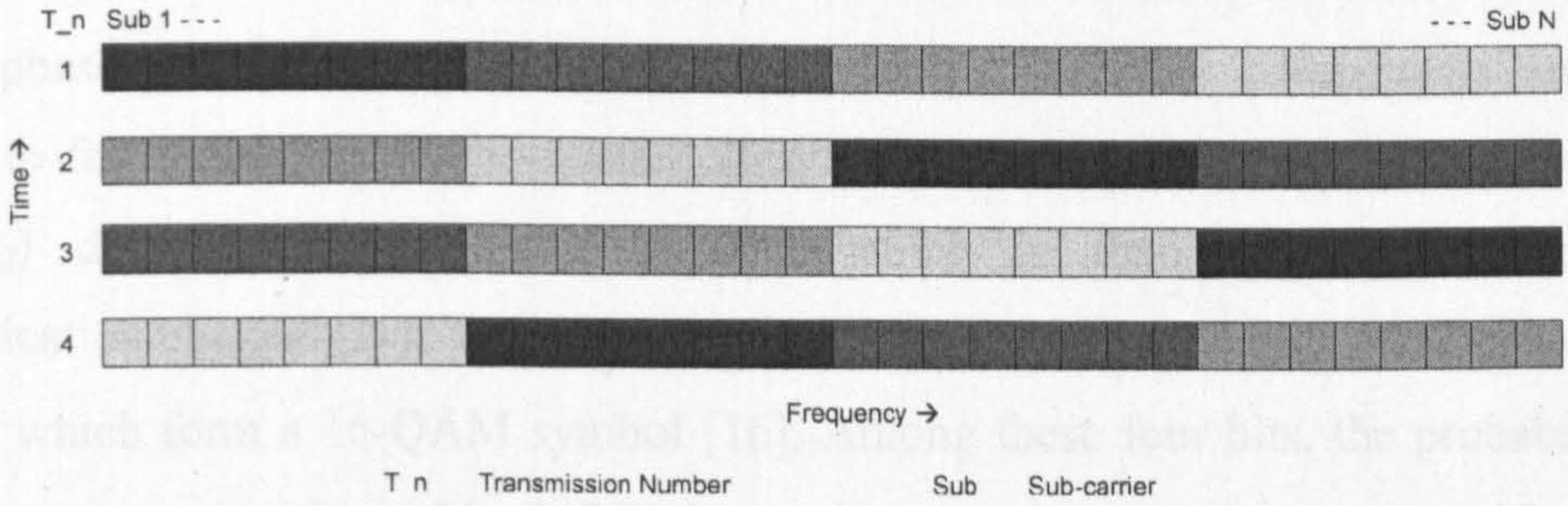

Figure 3-16: Subcarrier Rearrangement

In a frequency selective channel, each OFDM subcarrier suffers different distortion and thus different received signal quality. Fading in between pairs of subcarriers will be uncorrelated provided they are separated wider than the channel coherence bandwidth in the frequency domain. Therefore, frequency diversity can be achieved by assigning code bits to different subcarriers in retransmissions by shifting the code bits with an appropriate step – larger than the channel coherent bandwidth.

In this section, a subcarrier rearrangement scheme is employed as shown in Figure 3-16 [24]. In the first retransmission, the subcarriers are shifted by half of the useful data subcarriers, which correspond to half of the system bandwidth, 5MHz in this case. The shift in the frequency domain will be large enough to fully utilize the inherent frequency diversity effect. In the following retransmission, subcarriers are shifted by ¾ and ¼ of useful data carriers, relative to the first transmitted packet. The merit of this scheme is that no additional buffer is required, but only simple shifting operations are need in the retransmission.

3.8.2 Constellation Rearrangement

QAM (Quadrature Amplitude Modulation) is a very commonly used modulation scheme and has been defined as the key modulation scheme in LTE. In particular, a square QAM is proposed due to the relative ease of implementation and performance gain [25]. The use of square QAM enables an advanced hybrid ARQ technique namely signal constellation rearrangement [23]. This technique averages the variations in bit reliabilities caused by signal constellation of a multilevel modulation formats (QAM in this case) over retransmission.

For an M-ary QAM constellation, a serial data bit stream is serial-parallel converted into two (in-phase (I) and quadrature (Q)) bit streams. These two components are then mapped to form complex symbols using Gray encoding. For 16-QAM, every four bits ($I_1Q_1I_2Q_2$) defines a constellation symbol which is then transmitted over the communication channel. It is well known that unequal error protection exists among the four bits which form a 16-QAM symbol [16]. Among these four bits, the probability of error for a most significant bit (MSB) is considerably less than a least significant bit (LSB). For example, for the first bit of a 16 QAM symbol to be demodulated erroneously, it requires three times more perturbation in the real (or imaginary) part than the third bit of the 16 QAM symbol. In short, the MSBs have three times more reliability than the LSBs. However it should be noted that all these bits carry information which is equally important and unequal error protection is undesired. Therefore, in order to compensate for this problem, bits can be rearranged in such a manner that less protected bits will be given more protection in the retransmissions. This can be achieved by using different mappings at subsequent transmissions as shown in Figure 3-17.

The different mappings shown in Figure 3-17 can be achieved by using simple functionalities such as reordering and inversion of the logical bit values. Table 3-4 define the operations applied to the bits before constellation mapping. These rearrangement techniques average the error probability of each bit over the retransmissions. Maximum benefit from constellation rearrangement can be achieved with four retransmissions, each with different constellation mapping. In addition, constellation rearrangement does not require additional User Equipment (UE) buffer but only trivial operations to rearrange the output bit sequence to achieve a different constellation mapping. 64-QAM has a similar characteristic of unequal error protection as in 16-QAM. Similar rearrangement

techniques can be applied in the case of 64-QAM to achieve the maximum benefit of constellation rearrangement.

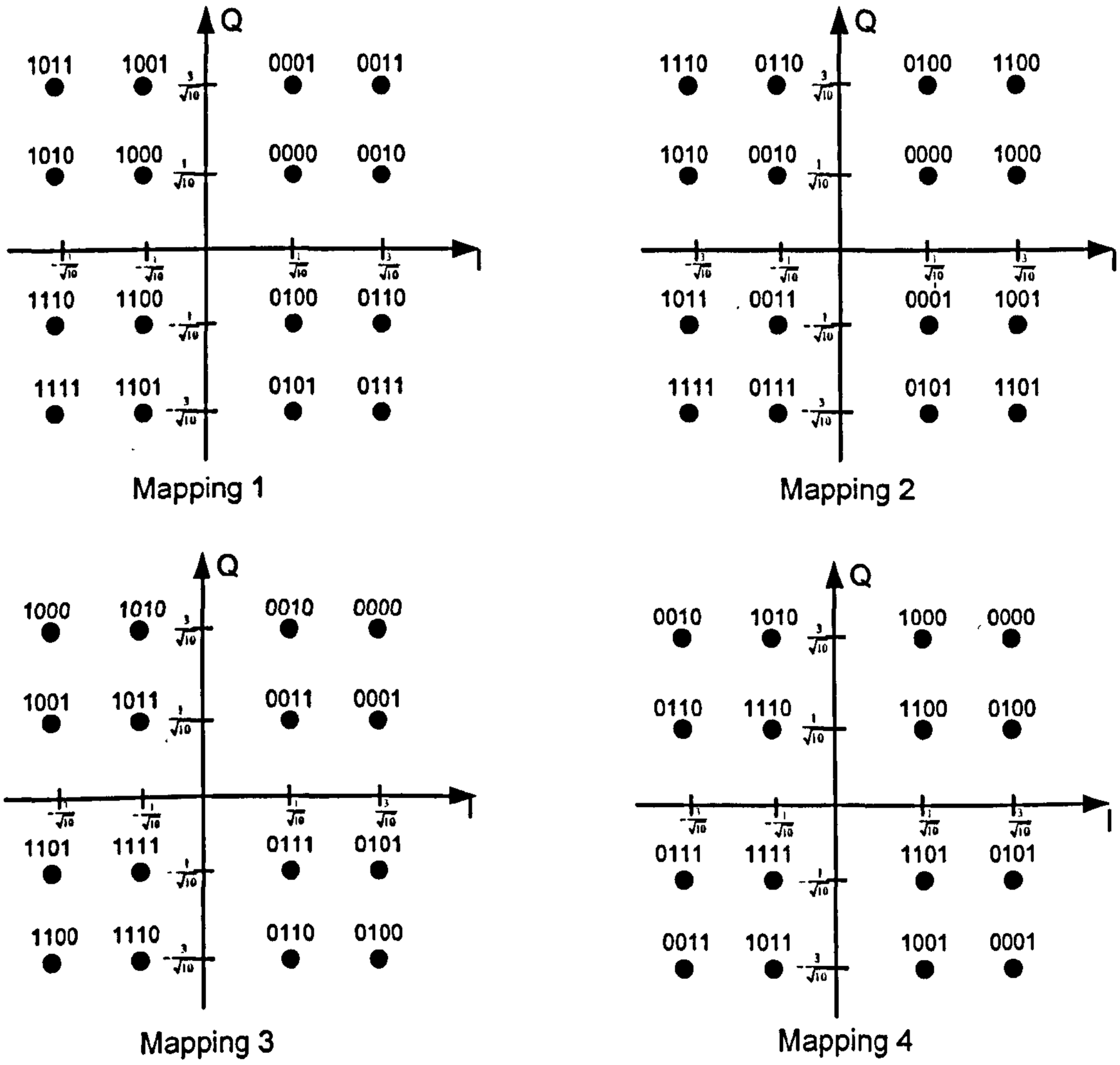

Figure 3-17: 16 QAM Signal Constellation with different mappings

Table 3-4: Constellation rearrangement for 16QAM

Transmission	Output bit sequence	Operation
1	*I1Q1I2Q2*	None
2	*I2Q2I1Q1*	Swapping MSBs with LSBs
3	*I1Q1I2Q2*	Inversion of LSBs' logical values
4	*I2Q2I1Q1*	Both Swapping and inversion

These two techniques can be combined to obtain both 'constellation' and frequency diversity. Code bits are modulated using different constellation mapping and then assigned to subcarriers which are shifted by a reasonably large step in frequency domain to further achieve frequency diversity in retransmissions. However, when QPSK is used as the modulation scheme, the constellation rearrangement technique cannot be applied

and therefore only frequency diversity can be achieved through subcarrier rearrangement. Performance of these enhanced hybrid ARQ schemes will be presented in the following section.

3.8.3 Performance Evaluation for Enhanced Hybrid ARQ Schemes

Firstly, the performance of enhanced Hybrid ARQ schemes for Chase Combining is investigated. As can be observed from Figure 3-18, the retransmission technique based on the combination of both subcarrier rearrangement and constellation rearrangement outperforms the conventional Chase Combining by approximately 5dB at PER of 10^{-2}. The scheme that utilizes subcarrier rearrangement performs slightly better than the scheme that utilizes constellation rearrangement and both schemes outperform the conventional Chase Combining by approximately 2-3 dB. The similar throughput performance can also be observed in Figure 3-19. From Figure 3-19, it can be seen that all schemes obtain significant throughput gains in low channel SNR and the performance gain diminishes when the channel SNR improves. The combined diversity scheme can therefore provide a significant throughput enhancement over the conventional scheme, especially at low SNR scenario.

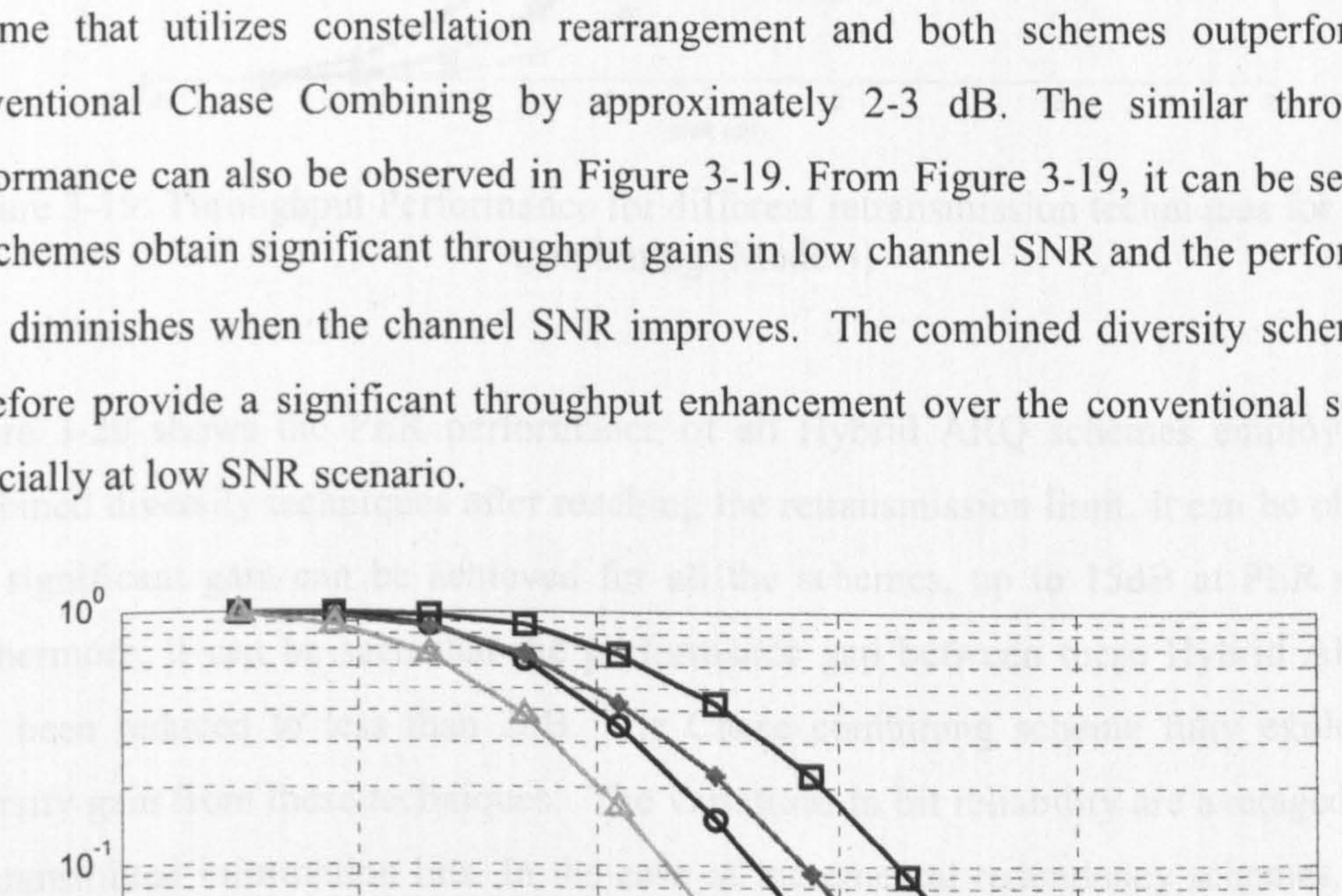

Figure 3-18: PER Performance for different retransmission techniques for Chase Combining. (Mode 4)

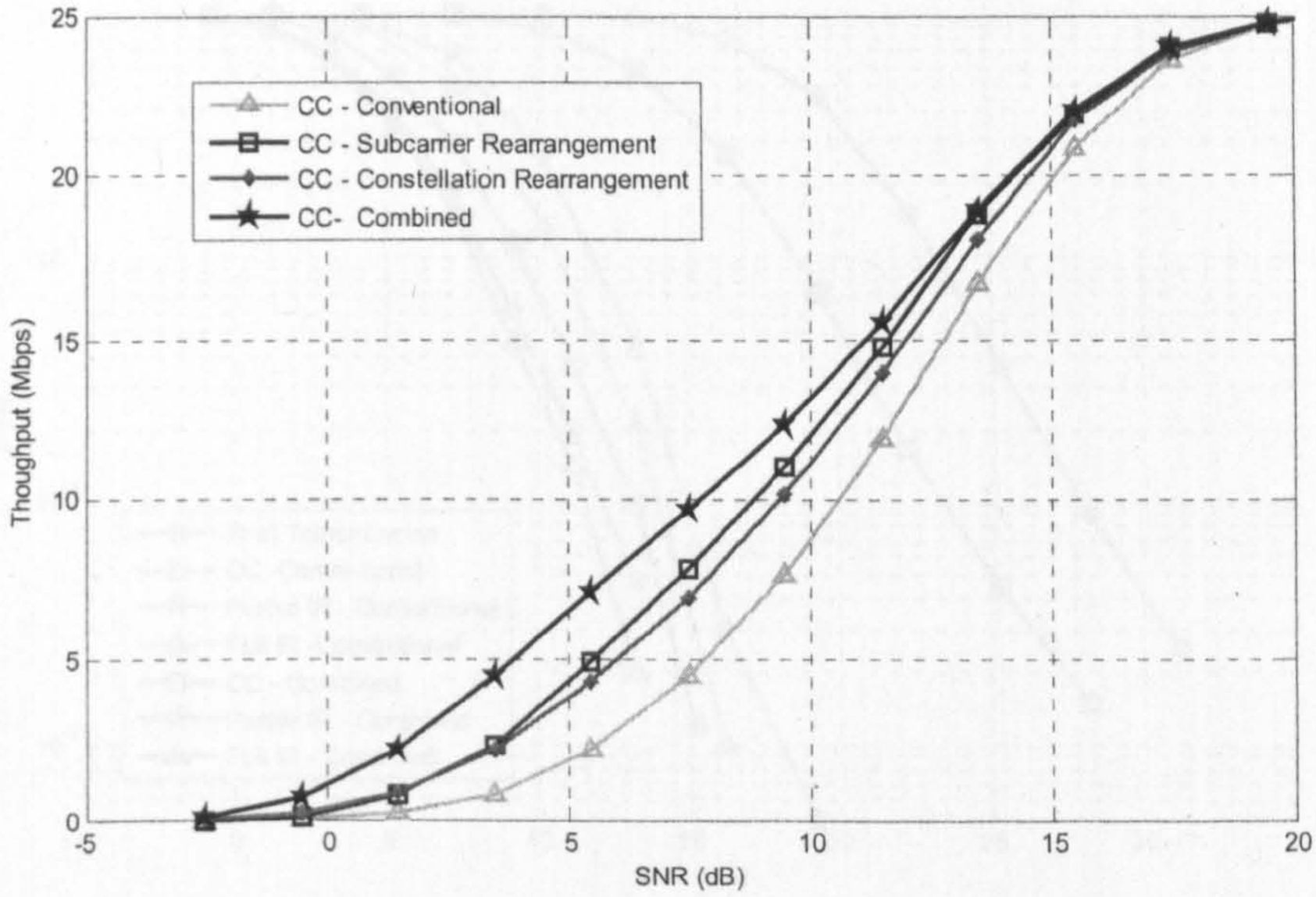

Figure 3-19: Throughput Performance for different retransmission techniques for Chase Combining (Mode 4)

Figure 3-20 shows the PER performance of all Hybrid ARQ schemes employing the combined diversity techniques after reaching the retransmission limit. It can be observed that significant gain can be achieved for all the schemes, up to 15dB at PER of 10^{-2}. Furthermore, it can be seen that the performance gap between these Hybrid ARQ has now been reduced to less than 2dB. The Chase combining scheme fully exploits the diversity gain from these techniques. The variations in bit reliability are averaged for all the transmitted information bits. In the case of incremental redundancy schemes, not all the information bits are repeated in each transmission and thus less diversity can be exploited.

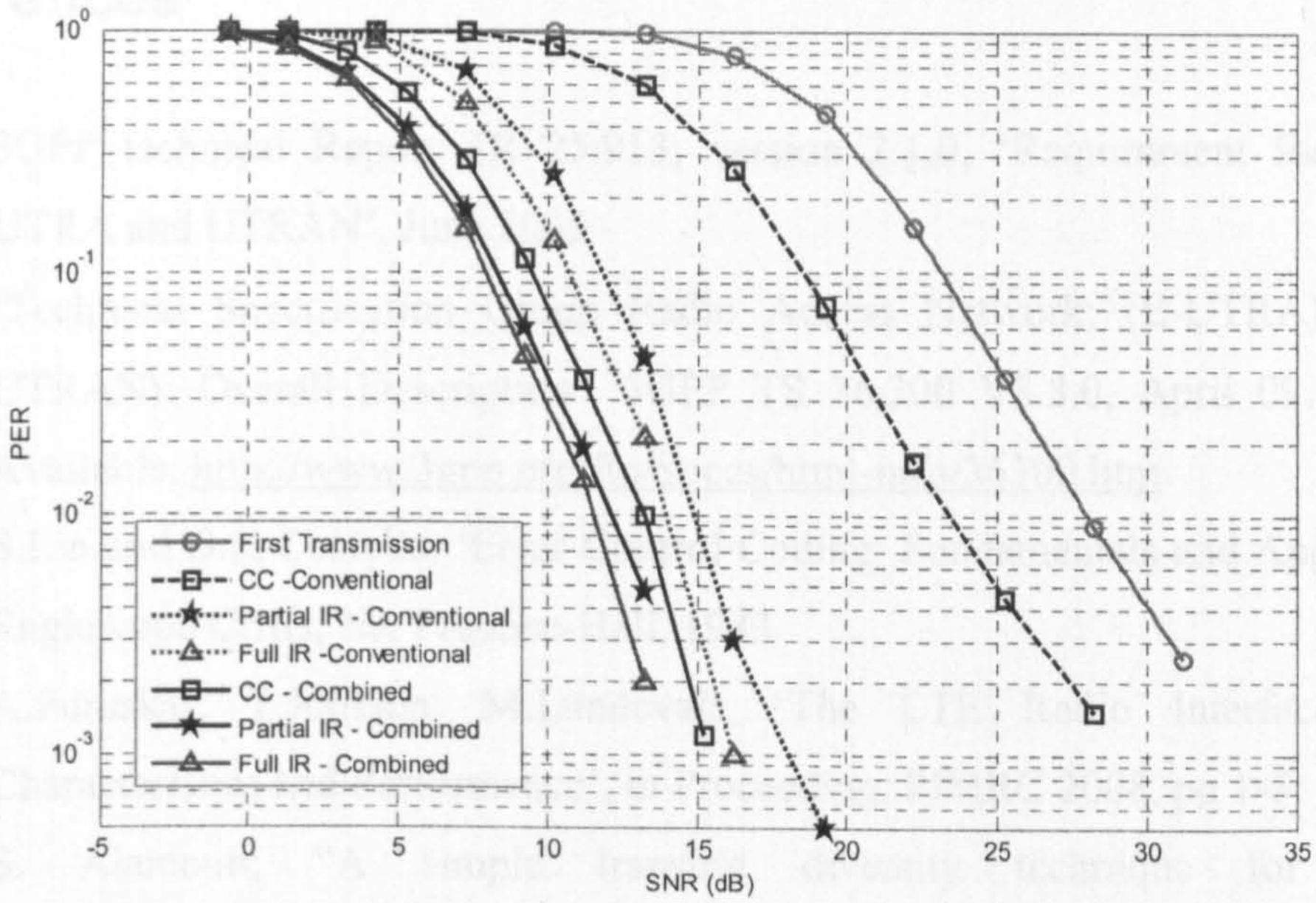

Figure 3-20: PER Performance comparison for Mode 6 for enhanced Hybrid ARQ schemes

3.9 Conclusion

In this chapter, the overview description of LTE is given. The new evolution, together with an optimized architecture, ensures a lower cost per bit for a competitive service offering in future wireless communications. Then, the downlink performance of a LTE OFDM system is presented. LTE offers a promising result of achieving spectral efficiency of nearly 4 bits/s/Hz at high SNRs.

Also in this chapter, the performance of different Hybrid ARQ techniques has been evaluated for the LTE downlink. Simulation results have shown that Full IR offers the best throughput performance for high modulation schemes but at the cost of higher memory requirement. If the cost of the system in term of memory requirement is considered, Chase Combining is favoured instead as it provides comparable performance at lower cost especially for lower modulation schemes. Partial IR provides a good trade off between these two techniques. Retransmission techniques which adopt frequency diversity and constellation diversity provide an enhancement to existing Hybrid ARQ schemes and offer better throughput performance for various modulations and coding rates. Chase combining scheme exploits most diversity gain from these techniques and the performance gap between these schemes is narrowed to less than 2dB in high MCS.

References

[1] 3GPP technical Report TR 25.913, version 2.1.0, 'Requirement for Evolved UTRA and UTRAN', June 2005

[2] 'Technical Specification Group Radio Access Network; (E-UTRA) and (E-UTRAN): Overall Description', 3GPP TS 36.300 V8.8.0, April 09. [Online]. Available: http://www.3gpp.org/ftp/Specs/html-info/36300.htm

[3] S.Lin and D.K Costello, 'Error Control Coding: Fundamentals and Applications' Englewood Cliffs, NJ: Prentice-Hall, 1983

[4] A.Furuskar, T.Jonsson, M.Lundevall, 'The LTE Radio Interface - Key Characteristics and Performance', in Proceeding, PIMRC 2008, pp 1-5

[5] S. Alamouti, "A simple transmit diversity technique for wireless communications", IEEE JSAC, Vol. 16, No. 8, pp. 1451-1458, 1998

[6] Gerard J. Foschini, Glen D. Golden, Reinaldo A. Valenzuela, and Peter W. Wolniansky, "Simplified Processing for High Spectral Efficiency Wireless Communication Employing Multi-Element Arrays", IEEE Transactions on Selected Areas in Communications, Vol. 17, No. 11, Nov 1999

[7] W. W. Peterson, D. T. Brown. 'Cyclic Codes for Error Detection',in Proceeding in IRE, vol.49,pp.228-235,Jan. 1961

[8] Cooley, James W., and John W. Tukey, 1965, "An algorithm for the machine calculation of complex Fourier series," *Math. Comput.* 19: 297–301.

[9] 'C. Berrou, A. Glavieux, and P. Thitimajshima, "Near Shannon limit error-correcting coding and decoding: Turbo codes," in Proc. IEEE Int. Conf. on Communications, Geneva, Switzerland, May 1993.

[10] 3GPP Technical Specification, 'Physical Layer Procedures (Release 8)', 3GPP TS 36.213 V8.7.0, June. 09. [Online]. Available: http://www.3gpp.org/ftp/Specs/html-info/36213.htm

[11] B.Sklar, 'A Primer on Turbo Code Concepts', IEEE Communication Magazine, pp 94-102, December 1997

[12] Richard van Nee and Ramjee Prasad, 'OFDM for Wireless Multimedia Communications', Artech House, Boston and London, 2000.

[13] Technical Specification Group Radio Access Network; (E-UTRA) and (E-UTRAN): Physical Channels and Modulation', 3GPP TS 36.211 V8.4.0, Sept 08. [Online]. Available: http://www.3gpp.org/ftp/Specs/html-info/36211.htm

[14] 'Physical Layer Aspects of UTRA High Speed Downlink Packet Access', 3GPP TR 25.848 V4.0.0, March 01 [Online]. Available: http://www.3gpp.org/ftp/Specs/html-info/25848.htm

[15] David Chase, 'Code Combining – A Maximum-Likelihood Decoding Approach for Combining an Arbitrary Number of Noisy Packets' IEEE Transaction on Communications, Vol.Com 33, No.5, May 1985

[16] S. Le Goff, A. Glavieux, C. Berrou, "Turbo-codes and high spectral efficiency modulation," IEEE SUPERCOMM/ICC '94, vol.2, pp.645-649, 1994

[17] S.Bliudze, N.Billy, D.Krob, "On Optimal Hybrid ARQ control schemes for HSDPA with 16QAM", IEEE Conference on Wireless And Mobile Computing, Networking And Communications, 2005, pp 121-127

[18] C.Xiu, Y.Li, Y.Fan, 'A Hybrid ARQ Scheme Using RCPT Codes and Its Performances over Rayleigh Fading Channel', IEEE Conference on Global Telecommunications Conference, 2002, pp 1517-1521

[19] "Performance comparison for bit level and symbol level Chase combining", Texas Instruments, 3GPP R1-01-0472, May 21-25, Busan, Korea.

[20] J. Haugenauer, "Rate-compatible Punctured Convolutional Codes (RCPC codes) and their applications", IEEE Trans. On Communications, Vol.4, April 1988 , Page 389-400

[21] D.N.Rowitch, L.B.Milstein, "On the Performance of Hybrid FEC/ARQ Systems using RCPT Codes", IEEE Trans. On Comm., Vol 48,, No.6, June 2000

[22] T.Kumagai, M.Mizoguchi, T.onizawa, H.Takanashi and M.Morikura " A Maximal Ratio Combining Frequency DiversityARQ Scheme for OFDM Signals", Proc. PIMRC 1998, Lissaboa, Portugal 1998

[23] C.Wengerter, A.G.E.V.Elbwart, E.Seidel. 'Constellation Rearrangement: Enhancement for Multilevel Modulation Formats and Transmit Diversity', Wireless Personal Communications, Vol 29, pp 35-45, 2004

[24] K.Beh, A.Doufexi, S.Armour, 'Performance Evaluation of Hybrid ARQ Schemes of 3GPP LTE ODFMA System', PIMRC 2007, pp 1-5

[25] F.Xiong, 'Digital Modulation Techniques', Norwood, MA: Artech House, 2000

[26] "Tech. Spec. Group RAN; Multiplexing and channel coding (FDD)" 3GPP TR 25.212 V7.10, June '06. [Online] Available: http://www.3gpp.org/ftp/Specs/html-info/25212.htm

Chapter 4

Joint Time and Frequency Scheduling

4.1 Introduction to Scheduling

Future wireless communication systems are expected to offer users a wide range of rich multimedia services. These multimedia services often have different QoS requirements in term of service parameters such as delay, jitter, packet loss rate and throughput. Therefore, downlink scheduling algorithms at the base station (BS) play a central role in determining the overall performance of the system.

In the past, several scheduling techniques have been proposed in order to maximize the throughput based on the priorities of the users in the network [1][2]. These scheduling techniques could be well-suited for wired networks, as it can be safely assumed that the physical link is reliable and time invariant. However, these assumptions do not apply to wireless networks as the network topology is dynamic and the link characteristics are highly variable as well as location/time dependent. This will lead to a very inefficient resource usage, e.g. a high priority service would be scheduled even if the channel condition is very poor. A good overview of conventional wireless scheduling algorithms is given in [3]. Some desired characteristics for an ideal wireless scheduler were also discussed, which include efficient link utilization, delay bound, fairness, throughput, implementation complexity, energy consumption and scalability.

Several scheduling algorithms [3-10] for wireless networks that aim to maximize the throughput performance have been proposed. These algorithms attempt to exploit the multiuser diversity that is present in the fading environment. In a system with multiple users fading independently, there is likely to be a user with a very good channel at any time. Hence, total throughput of the system can be maximized by serving the user with the strongest channel, and thus exploiting multiuser diversity.

However, a more demanding challenge is to exploit the multiuser diversity while maintaining fairness among all the users. Two representative types of fairness are Proportionally Fairness and Max-Min Fairness, to optimize efficiency and to optimize fairness, respectively. A proportionally fair scheduler gives approximately the same number of resources to all users, but tries to transmit to each user when the channel condition is at its best [10]. This is achieved by transmitting to user with a maximum priority, which is calculated based on a ratio of instantaneous rate and average throughput. Max-min fairness imposes a strict fairness criterion where the lower rates will be given absolute priority. This fairness is achieved if the following criterion holds. A feasible allocation of rates r is max-min fair if and only if an increase of any rate within the domain of feasible allocations is at the cost of decreasing of some others with smaller rate.

Nevertheless, a conventional proportionally fair or max-min scheduler does not consider some wireless link characteristics in the behaviour of the scheduling algorithms. For example, these algorithms do not include the fact that packet transmission in the wireless link is error prone and some error correction mechanisms such as HARQ may be required in order to recover erroneous packets. In the previous chapter, it has been shown that the use of HARQ can results in significantly throughput performance [11]. As a matter of fact, in beyond 3G systems, such as HSDPA and LTE, HARQ will be employed to provide high-speed packet data services, together with AMC and scheduling. Therefore, the system performance can be further improved through a HARQ aware scheduler design. By incorporating HARQ information into scheduling, throughput improvement could be expected [4] [5].

In particular, the authors in [4] proposed a scheduling algorithm which takes account of retransmission information. The paper proposes an optimized mapping between SINR and MCS to maximize the throughput, given that an ARQ scheme is used. The author also incorporates frame error rate (FER) and retransmission information as part of the scheduling decision.

4.2 Modified Proportionally Fair Scheduler with HARQ Optimisation

The conventional proportionally fair (PF) scheduler does not consider any retransmission information into the scheduling decision, which is not optimal because it does not exploit any benefit from a wireless system employing HARQ. In this chapter, two approaches to

exploit the retransmission information in the scheduling process are considered. Firstly, the selection of the modulation and coding schemes (MCS) based on the channel quality of the link in terms of the SNR is considered. A systematic approach to optimise the mapping between the MCS and SNR to maximize the throughput by taking into account the underlying HARQ scheme is proposed. This piece of work is related to [4] but it is specific to an LTE system. Additionally, two advanced hybrid ARQ schemes, e.g. Partial and Full incremental redundancy are also considered.

Secondly, a modified proportionally fair scheduler which is based on an effective rate rather than conventional instantaneous data is investigated. Two heuristic methods are proposed and these methods significantly outperform the conventional scheme.

4.2.1 Introduction to the Proportionally Fair Scheduler

A proportionally fair scheduler aims to transmit to a user when its channel is relatively good and at the same time the scheduler also ensures fairness to all the users in the long term. Figure 4-1 shows the achievable data rate for two users. Due the temporal fast fading, users will experience peaks and fades. Therefore in order to exploit this, a priority ranking for all the users is calculated for each scheduling instance, where the user with the highest priority will be selected to transmit.

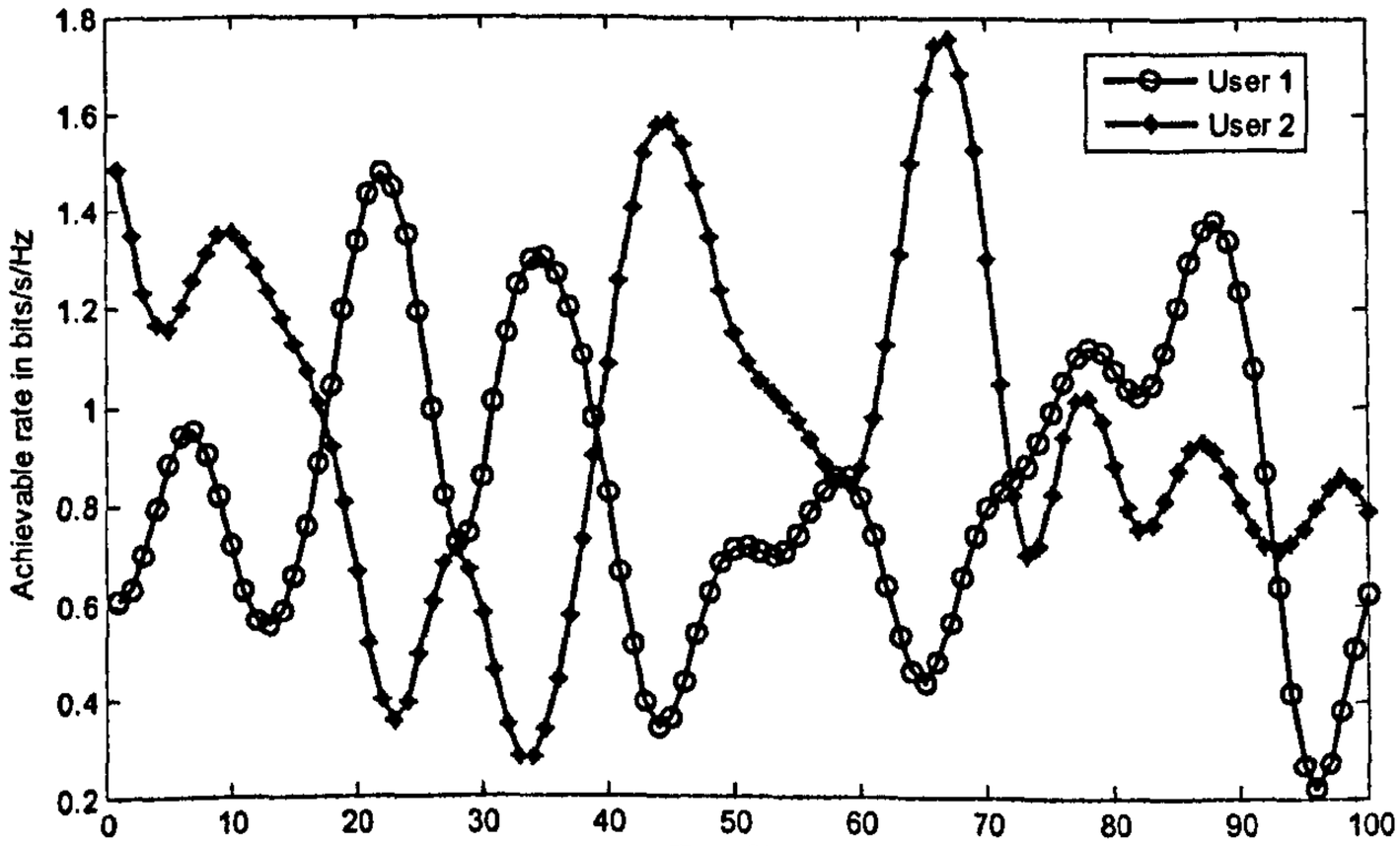

Figure 4-1: Achievable data rate for two users

The selection is based on the following selection rule:

$$\arg\max \quad \frac{R_{MCS(k)}(t)}{T_k(t)} \quad k \in K \tag{4-1}$$

where $R_{MCS(k)}(t)$ represents the current requested transmission rate of user k which is normally chosen from a set of available MCS schemes based on the SNR feedback from user k. K is the set of all the considered users. $T_k(t)$ represents user k's average throughput over a window in the past. The user's average throughput at time t is calculated by:

$$T_k(t) = \begin{cases} (1-\frac{1}{t_c})T_k(t-1) + \frac{1}{t_c}R_k(t) & \text{if } k \text{ is served at time } t \\ (1-\frac{1}{t_c})T_k(t-1) & \text{otherwise} \end{cases} \quad (4\text{-}2)$$

where t_c is the window size of the average throughput. When user k is scheduled, the average throughput of user k will be reduced as shown in Equation 4-2, however the average throughputs for other users remain unchanged. This is meant to reduce the priority of the selected user in the next scheduling since this user has been selected to transmit. Therefore by updating the average throughput after each transmission, the long term fairness among all the users can be maintained, while maintaining high throughput by transmitting to the user who has the highest priority.

4.2.2 Mapping Optimisation between SNR and MCS

Link adaptation allows a suitable modulation and coding scheme (MCS) to be selected depending on the signal quality to maximize the instantaneous usage of the wireless channel [12]. The transmitter will select the appropriate MCS level (based on the user's feedback) for the user that is to be served in the current time slot. For instance, a high spectrally efficient MCS is used when the channel conditions are good but a more robust MCS with a lower transmission rate will be employed when the channel condition worsens. The selection of MCS based on the channel condition (SNR) is often known as mapping. Mapping can be adapted for different objectives, such as to maximise the throughput or to minimise the delay or power. A good mapping strategy would aim to maximise the throughput given a delay constraint.

Traditionally, the mapping between an instantaneous SNR and MCS is selected to achieve a target PER of 1% [13] for voice transmission and whereas for data transmission, a more aggressive target PER of 10-20% is selected to maximise the short term throughput of a non-HARQ system. However, these mapping thresholds are not optimum for a wireless system which employs HARQ, e.g. LTE. Therefore, these mapping should be optimised based on the underlying HARQ operation.

Several conventional mapping strategies are considered. PER01, PER10, PER50 and PER90 represent the mapping strategies that ensure a maximum of 1%, 10%, 50% and 90% of packet errors in the first transmission, respectively. The SNR threshold for each mode is determined by interpolation from the link level PER performance as shown in Figure 4-2.

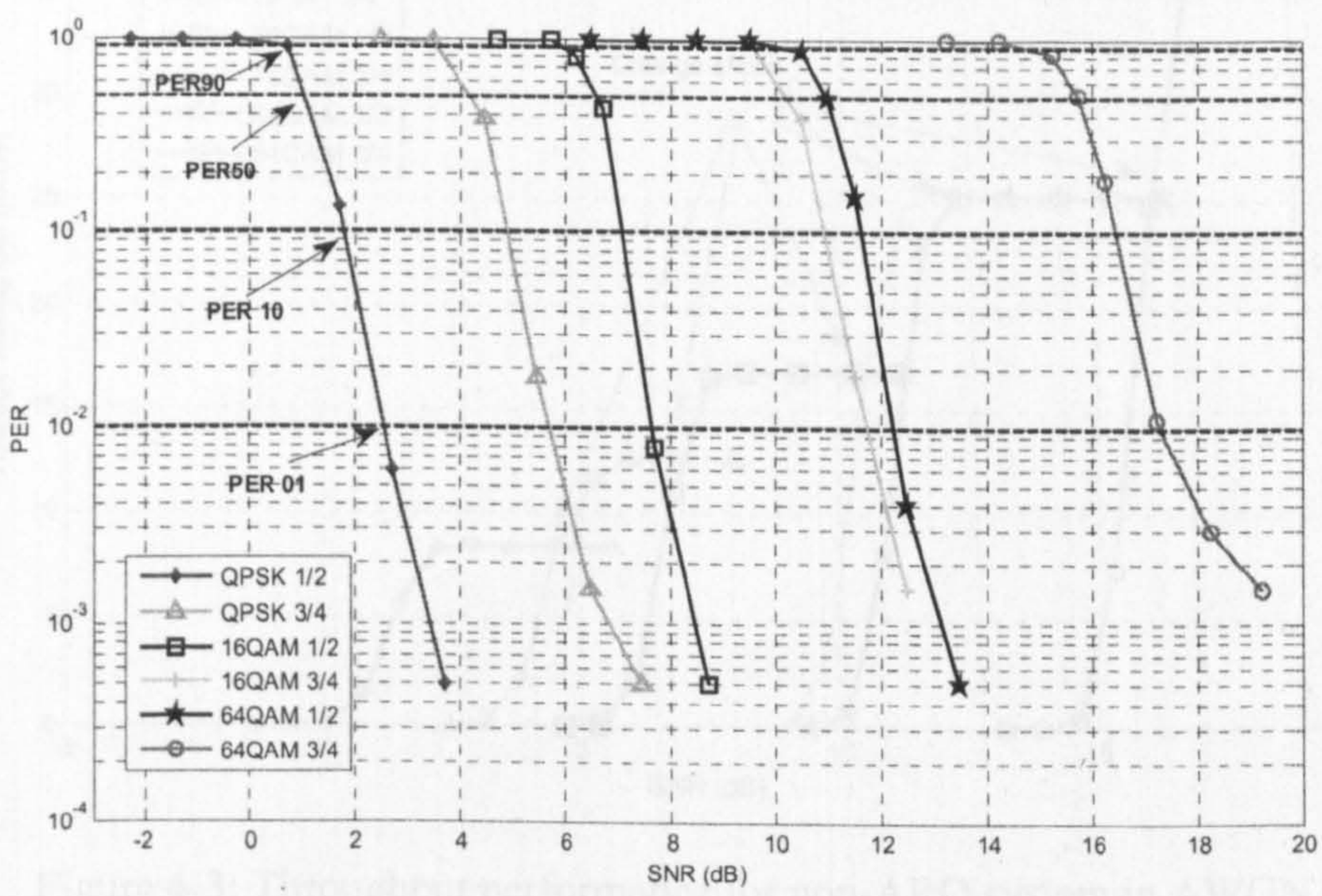

Figure 4-2: Link Level PER Performance for all MCSs in AWGN (no HARQ)

In the case of a non-HARQ system, the throughput performance is shown in Figure 4-3. The mapping of SNR and MCS is obtained via ideal link adaptation which is based on the (throughput) optimum switching point as shown in the figure. However this mapping is only throughput optimal for a non-HARQ system.

As described in Chapter 3, several hybrid ARQ schemes were considered. From the previous analysis, it can be observed that a significant decoding and combining gain can be achieved in the retransmissions, especially for incremental redundancy schemes. Thus the achievable throughput performance for these schemes was also significant improved, especially for low SNRs. Therefore in order to best exploit the advantage of Hybrid ARQ, the mapping should be optimised so that it can maximise the throughput after the HARQ operation. The mapping for systems employing Chase Combining (*Chase_thrpt)*, Partial IR (*PIR_ thrpt)* and Full IR (*FIR_ thrpt)* are calculated based on the throughput performance. An example of the mapping for Chase Combining is shown in Figure 4-4. For Full IR and Partial IR schemes, the figures are shown in Appendix A3. To recap, the

maximum number of transmission for a packet is limited to 4 and the achievable throughput is calculated based on Equation 3-6. Table 4-1 shows the different mapping thresholds in dB for all the mapping strategies.

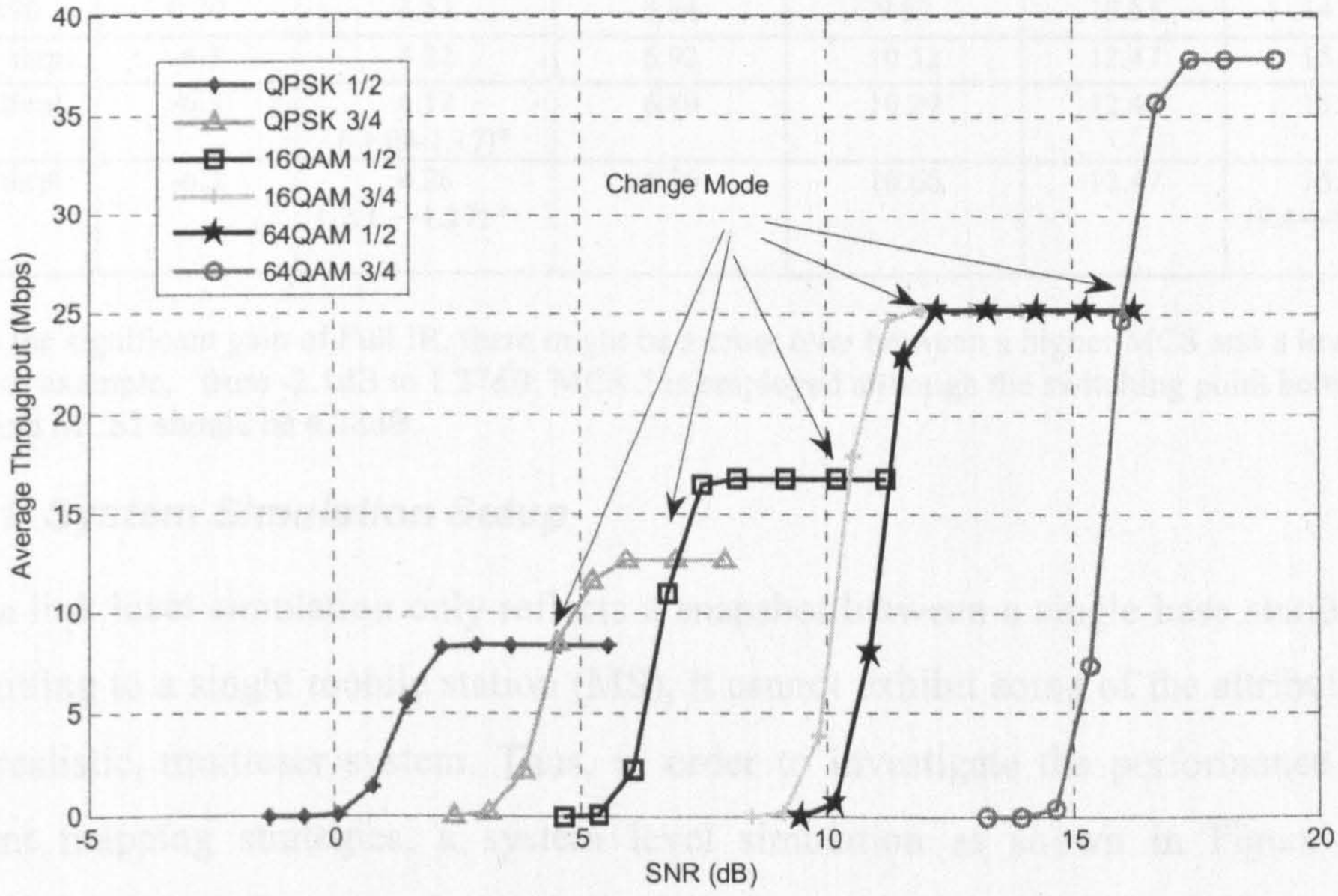

Figure 4-3: Throughput performance for non-ARQ system in AWGN

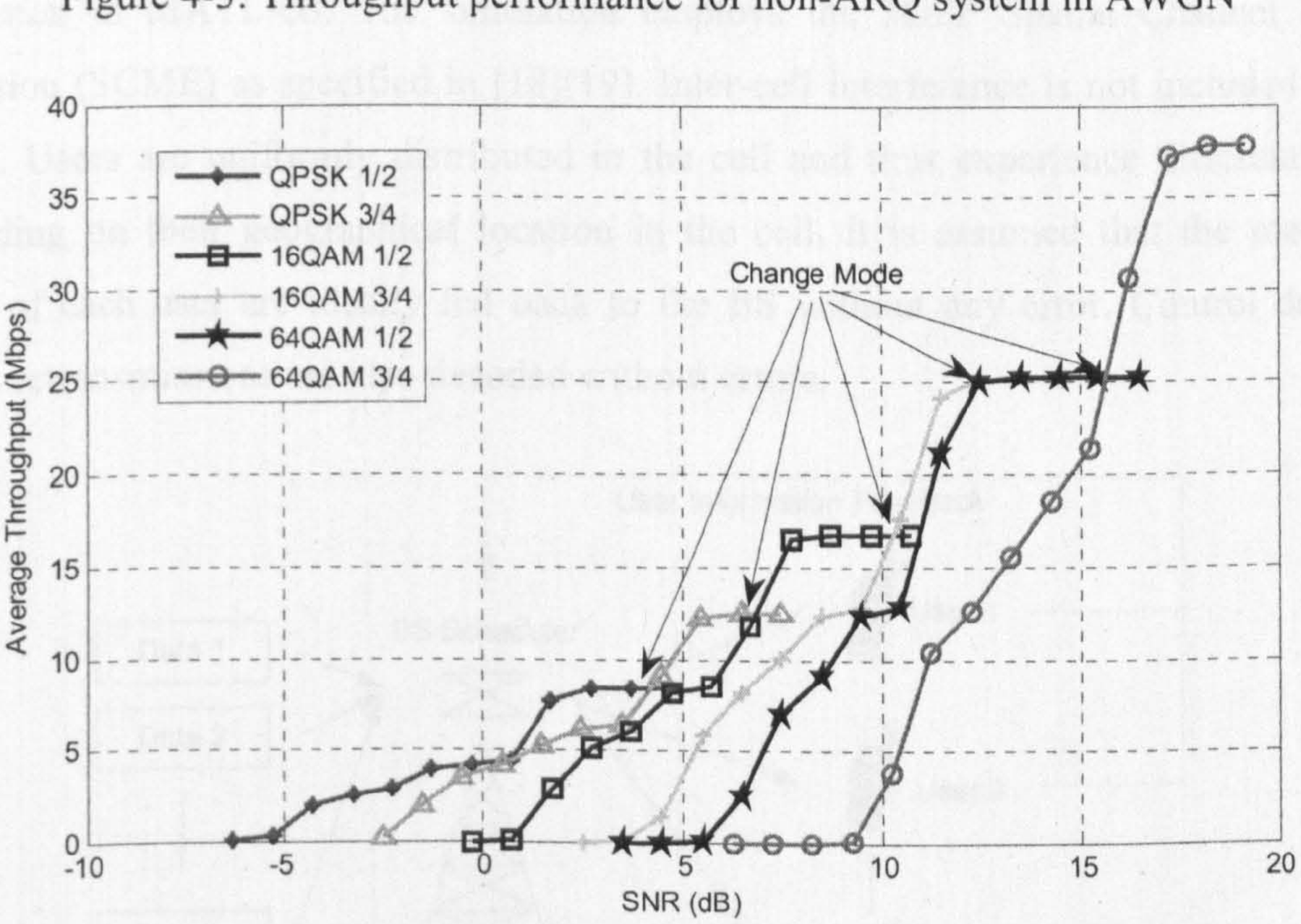

Figure 4-4: Throughput performance for Chase Combining in AWGN

Table 4-1: SNR(dB) Mapping Table

Mode (MCS)	1 QPSK 1/2	2 QPSK 3/4	3 16 QAM 1/2	4 16 QAM 3/4	5 64 QAM1/2	6 64 QAM3/4
PER01	2.45	5.70	7.66	11.72	12.22	17.31
PER10	1.80	4.89	7.08	10.92	11.59	16.45
PER50	1.01	4.17	6.67	10.31	10.95	15.59
PER90	0.70	3.53	5.84	9.57	10.51	14.70
Chase_thrpt	-6.3	4.22	6.92	10.32	12.47	15.66
PIR_ thrpt	-6.3	4.17 (-1.08-1.17)*	6.89	10.29	12.42	15.66
FIR_ thrpt	-6.3	4.28 (-2.1 →1.27) *	6.76	10.66	12.47	15.66 (9.4→10.66)*

*Due to the significant gain of Full IR, there might be a cross over between a higher MCS and a lower MCS. For example, from -2.1dB to 1.27dB, MCS 2 is employed although the switching point between MCS1 and MCS2 should be 4.28dB.

4.2.2.1 System Simulation Setup

Since a link level simulation only reflects a snapshot between a single base station (BS) transmitting to a single mobile station (MS), it cannot exhibit some of the attributes of a more realistic, multiuser system. Thus, in order to investigate the performance of the different mapping strategies, a system level simulation as shown in Figure 4-5 is performed. The performance analysis is done in a single cell scenario by software simulation in MATLAB. The simulation employs the 3GPP Spatial Channel Model Extension (SCME) as specified in [18][19]. Inter-cell interference is not included in the model. Users are uniformly distributed in the cell and thus experience different SNR, depending on their geographical location in the cell. It is assumed that the measured SNRs of each user are ideally fed back to the BS without any error. Control data for packet retransmissions are also decoded without errors.

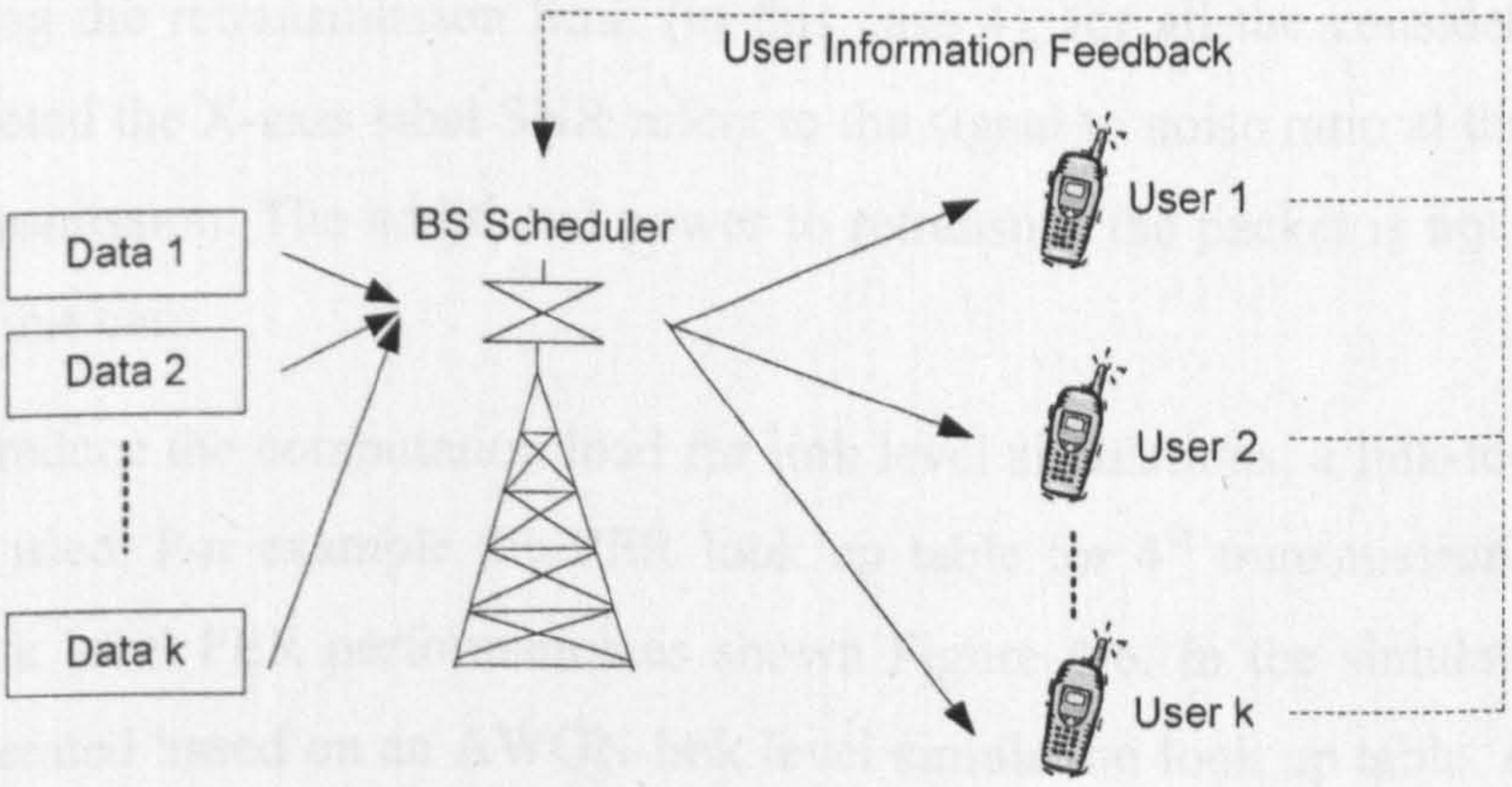

Figure 4-5: System level simulation setup

SCME defines three environments (Suburban Macro, Urban Macro, and Urban Micro) where the default scenario is Urban Macro unless stated otherwise. Path loss, large scale shadowing fading and temporal fast fading are included in the simulation. In the case of urban macro scenario, the path loss model is given by:

$$PL = 34.5 + 35\log_{10}(d) \qquad (4\text{-}3)$$

where d is the distance between a mobile station(MS) and base station (BS). The large scale shadowing fading is log-normal distributed with 0 mean and 8dB standard deviation. A new channel impulse response is used at each new packet transmission and remains the same during the transmission of that packet. The channel is also assumed to be constant during retransmissions as it is likely that retransmissions will occur soon after the initial transmission, especially for slowly varying channels. The maximum number of retransmissions is limited to 4.

A proportionally fair scheduling algorithm is considered unless otherwise stated. Throughout the simulation, the window size or the filter length, t_c is set to 500 unless otherwise stated. The initial average throughput value of each user defaults to the first reported channel quality indicator (CQI) and is based on the MCS selected for the user via link adaptation.

The performance of several Hybrid ARQ schemes in the LTE downlink has been investigated in Chapter 3. Therefore in this performance analysis, hybrid ARQ schemes including Chase Combining (CC), Partial Incremental Redundancy (PIR) and Full Incremental Redundancy (FIR) are considered. Figure 4-6 shows the PER performance of different hybrid ARQ schemes in additive white Gaussian noise (AWGN) channels after reaching the retransmission limit (in this case 4), for all the considered MCSs. It should be noted the X-axis label SNR refers to the signal to noise ratio at the receiver for the first transmission. The additional power to retransmit the packet is not accounted to the SNR in this case.

In order to reduce the computation load for link level simulations, a link-to-system level mapping is used. For example the PER look up table for 4^{th} transmission is generated from the link level PER performance as shown Figure 4-6. In the simulation, a packet error is generated based on an AWGN link level simulation look up table. As a result of temporal fast fading, the perceived SNR at the receiver is fluctuating. The effect of fading is considered in the simulation by generating random packet errors based on the instantaneous SNR. In our simulation, the instantaneous SNR is calculated by the

average of the frequency responses of the subchannels [20]. A more advanced method, called Exponential Effective SNR Mapping (EESM) can be found in [21]. The system simulation parameters and assumptions are summarised in Table 4-2.

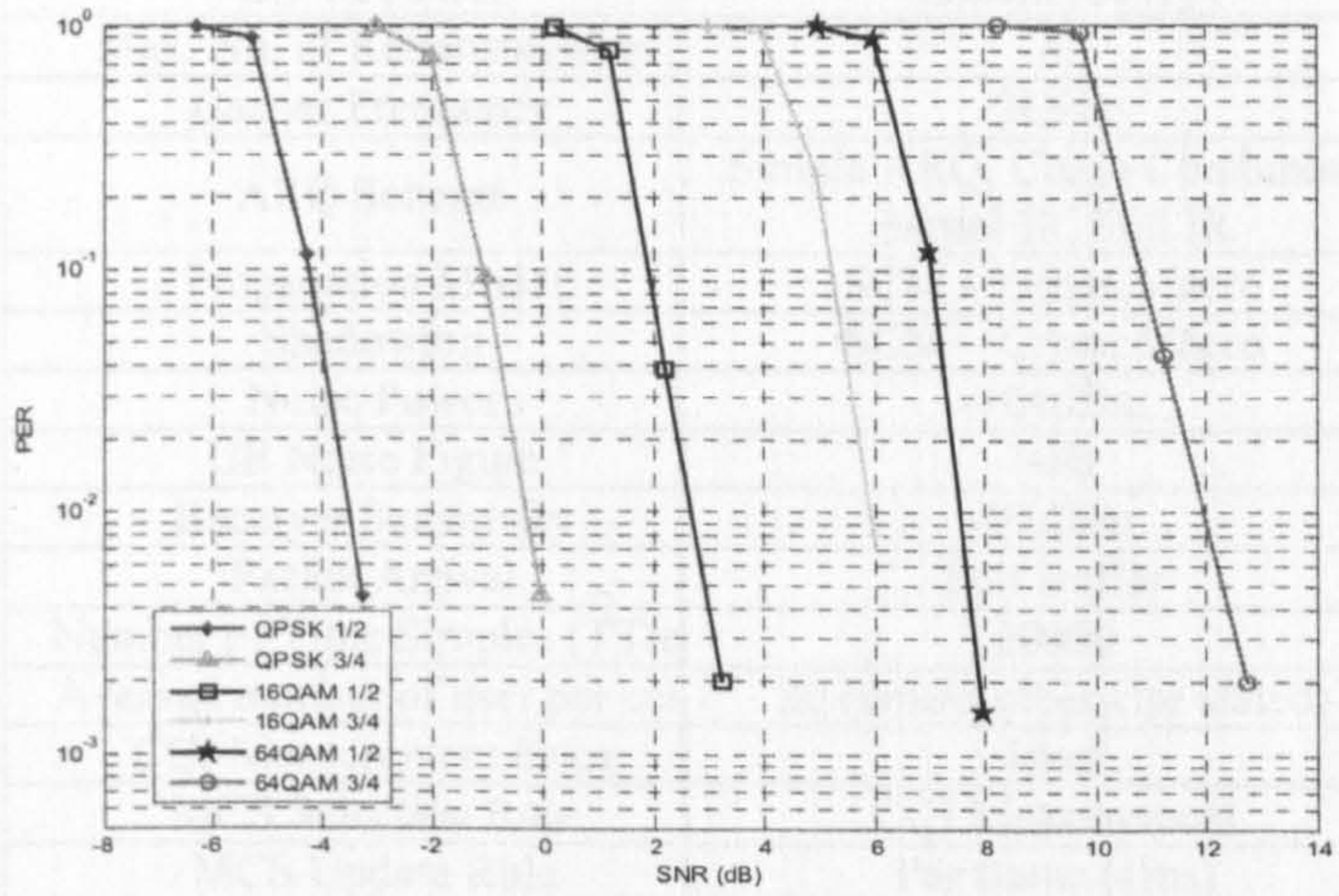

(a)

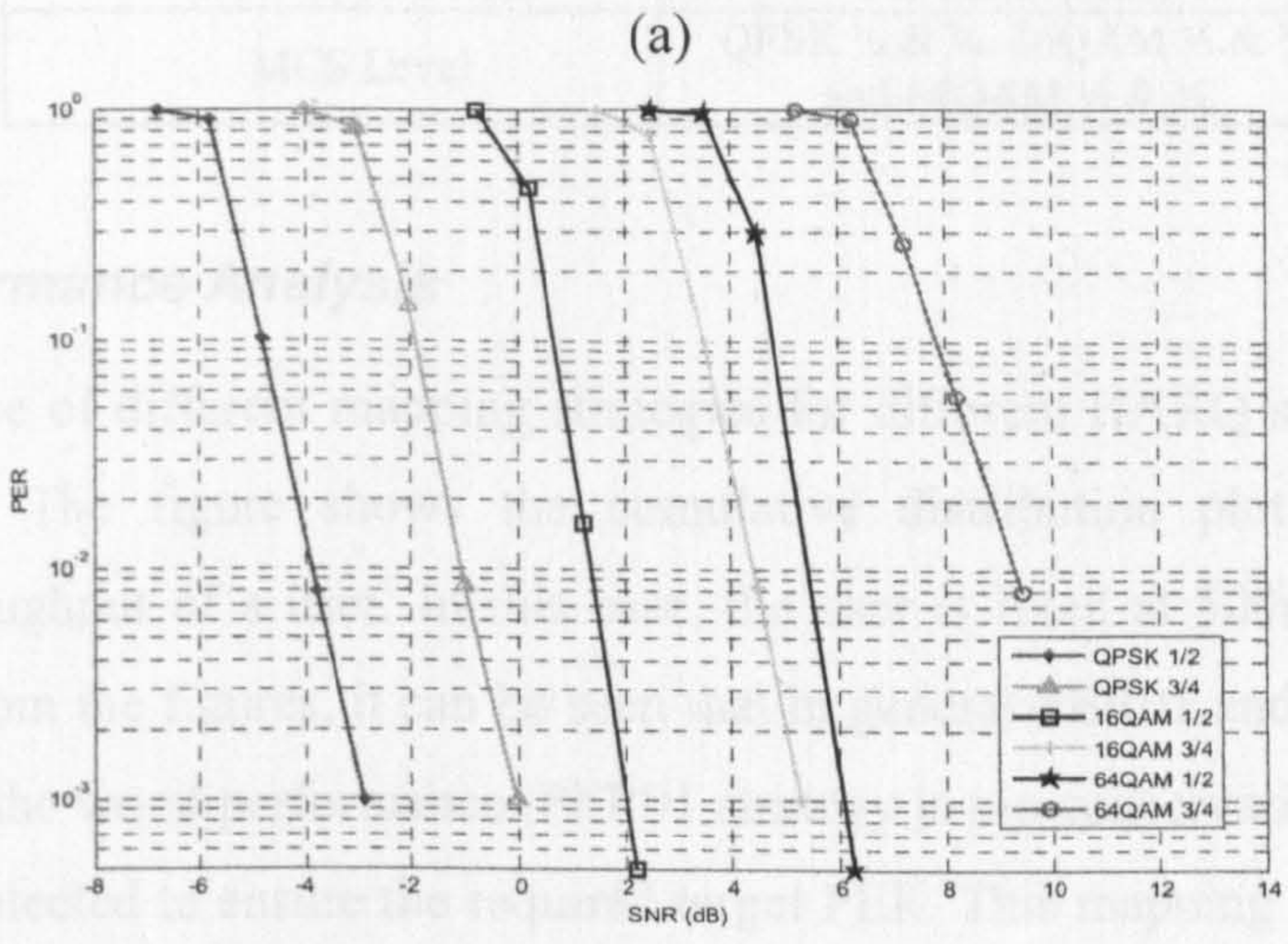

(b)

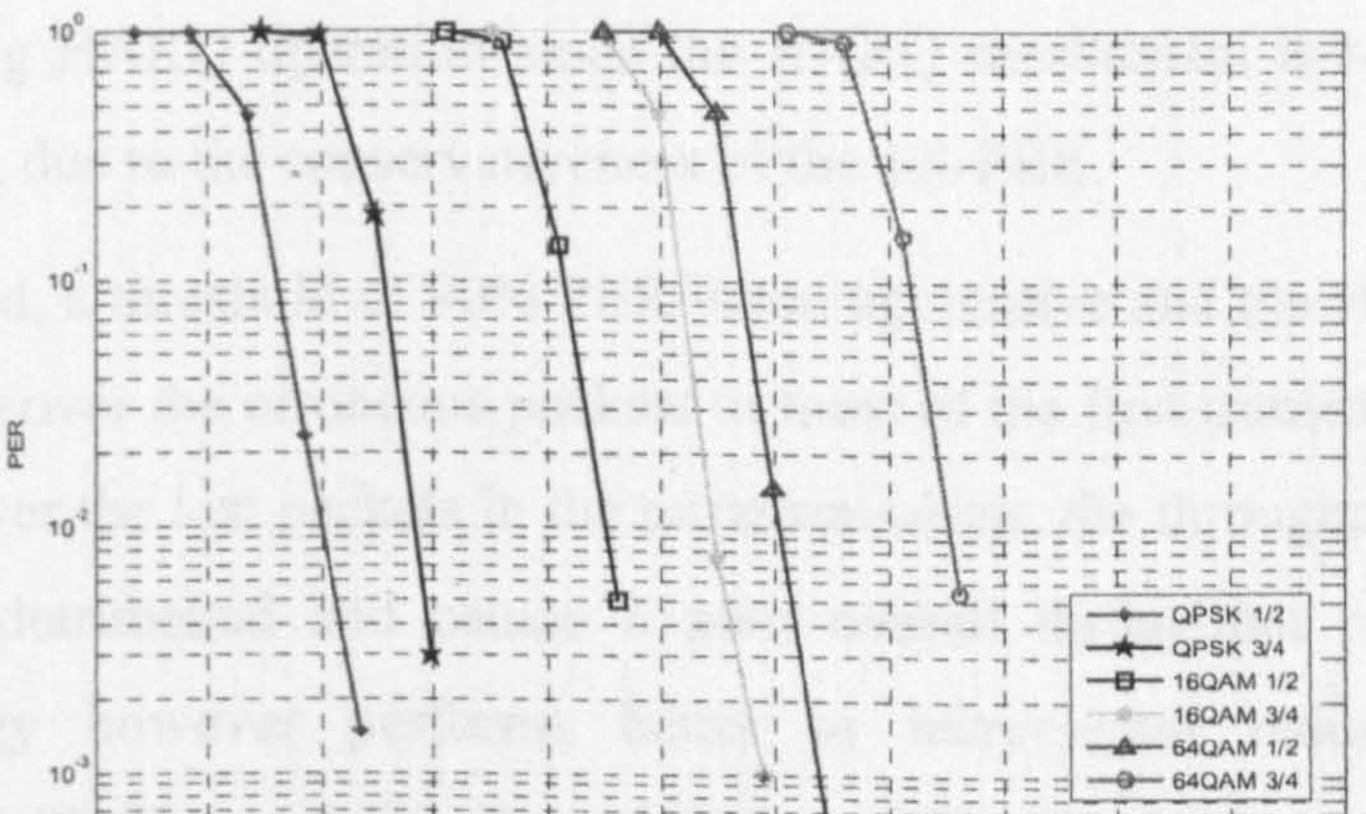

(c)

Figure 4-6: Link Level PER Performance for a) Chase Combining b) Partial IR and c) Full IR for all MCSs in AWGN

Table 4-2: Default System Simulation Parameters and assumptions

Cell Layout	Single Cell
Radius of Cell	500m (min 35 meter)
BS Tx Power	43dBm (20W)
Max. No. of Retransmission	4
Carrier Frequency	2GHz
ARQ Scheme	Simple ARQ, Chase Combining Partial IR, Full IR
Propagation Model	SCM – Urban Macro
Shadowing	SCM – Urban Macro
Noise Power	-104dBm
UE Noise Figure	9dB
Receiver Sensitivity	-95dBm
Packet Arrival	Full Buffer
Number of Time Simples (TTIs	20000
Average number of user per cel	20 (unless otherwise stated)
CQI Measurement Error	Ideal
MCS Selection Rule	CQI Measurement
MCS Update Rule	Per frame (1ms)
MCS Level	QPSK ½ & ¾, 16QAM ½ & ¾ and 64QAM ½ & ¾

4.2.2.2 Performance Analysis

The performance of different mapping strategies for different HARQ schemes is shown in Figure 4-7. The figure shows the cumulative distribution plot of the average achievable throughput of a user. In this case, the user is fixed at 500m away from the base station. From the figures, it can be seen that in general PER01 and PER90 mapping strategies have the worst performance. PER01 strategy is too conservative. Thus, a lower MCS is often selected to ensure the required target PER. This mapping strategy is unable to exploit much gain from the underlying HARQ operation. It is also not affected much by the underlying HARQ operation since the HARQ mechanism is rarely triggered to recover the error, due to the conservativeness of the 1% PER.

On the other hand, a threshold of 90% PER is too aggressive and the HARQ mechanism is triggered to recover the erroneous packets in most of the first transmissions. Although HARQ can recover the lost packets in the retransmissions, the throughput lost in the first transmission is detrimental and causes a poor overall throughput performance. This mapping strategy however performs better in incremental redundancy schemes, especially in Full IR (Figure 4-7c). Due to the large decoding and combining gain of the Full IR scheme, most of the retransmissions can be transmitted successfully.

Both PER10 and PER50 strategies perform relatively well. Similarly to PER01 strategy, PER10 strategy does not seem to be able to exploit much gain even in the Full IR scheme.

Whereas the PER50 strategy performs considerably better due to it's more aggressive target PER in the first transmission and ability to recover the erroneous packets in the retransmissions.

The performance of throughput optimised mapping strategies performed best in terms of average achievable throughput. This is due the fact a MCS is selected based on thresholds where each MCS has the highest throughput in a HARQ system. *Chase_thrpt* performs better than the other mapping strategies that are based on a target PER, but inferior to both *PIR_thrpt* and *FIR_thrpt*. *FIR_thrpt* outperforms all other strategies due to its highest gain from the decoding and combining gain.

Thus, in order to increase the throughput performance of a system, the mapping between SNR and MCS needs to be optimised based on the underlying HARQ operation. However, these throughput optimised mapping strategies are not suitable for delay sensitive services e.g. voice transmission, as these mapping strategies do not guarantee a target PER which might lead to a possible high delay.

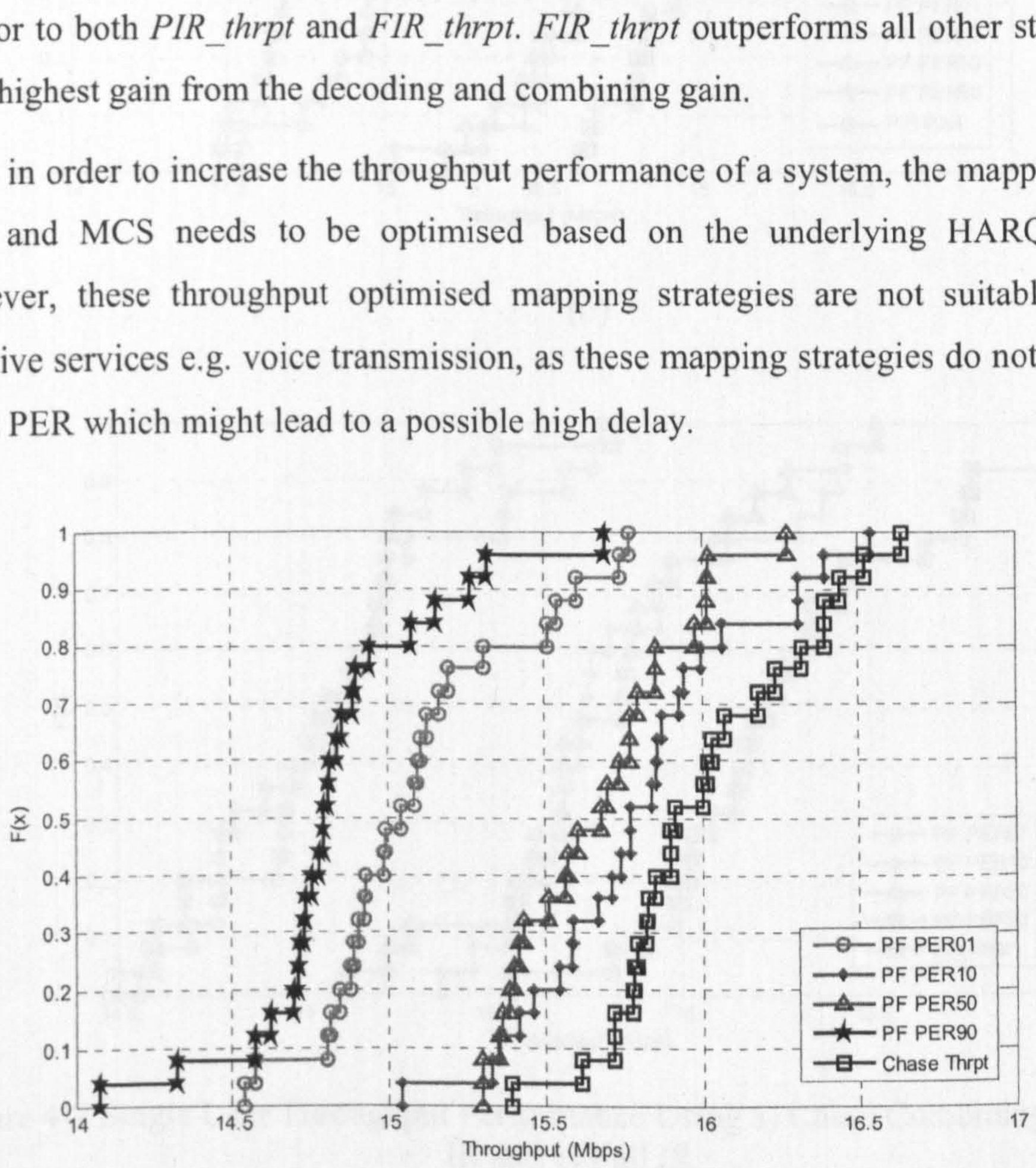

(a)

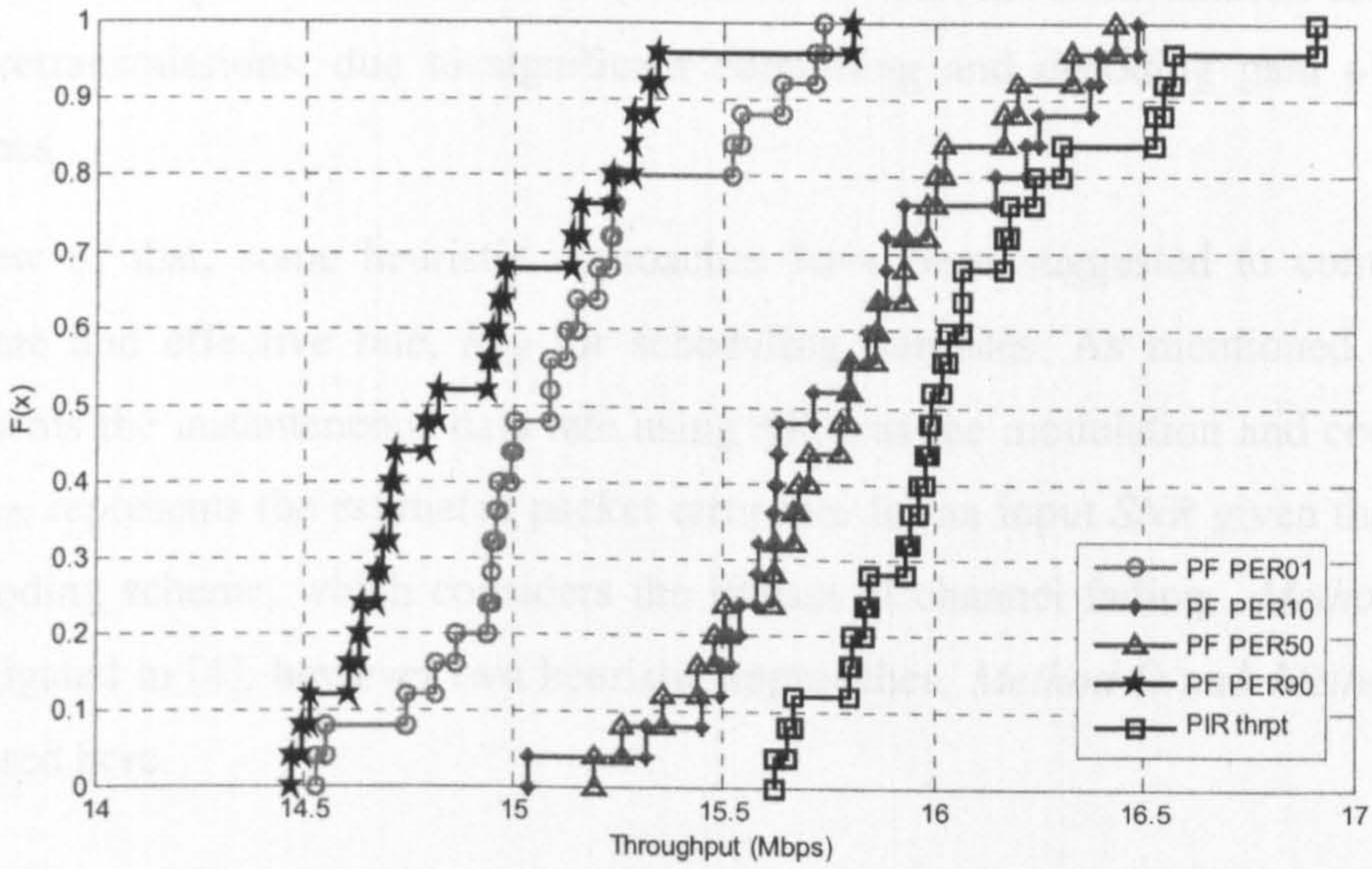

(b)

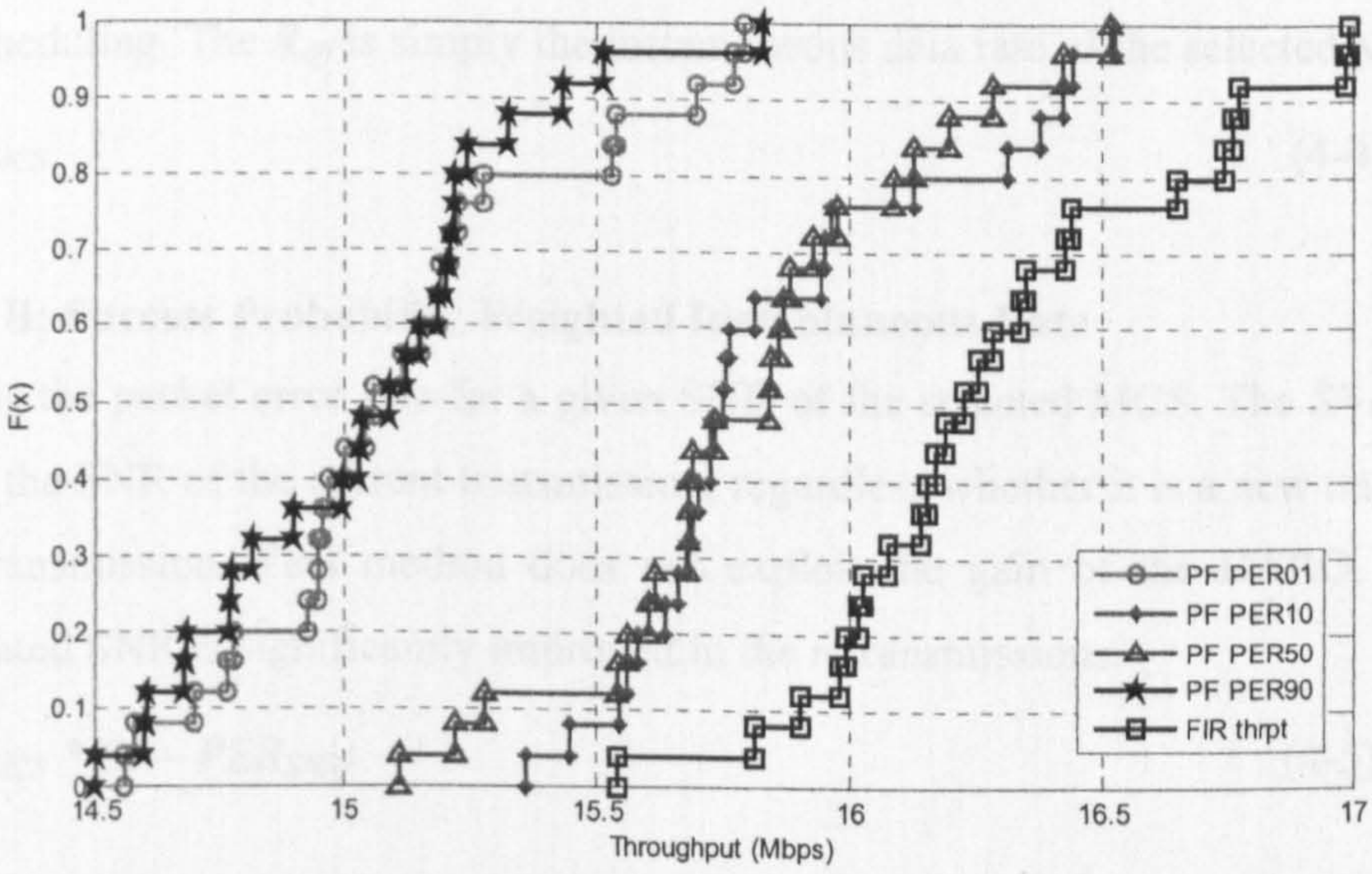

Figure 4-7 Single User Throughput Performance Using a) Chase Combining, b) Partial IR and c) Full IR

4.2.3 Effective Rate for the Proportionally Fair Scheduler

In a conventional proportionally fair scheduler, the requested transmission rate of a user is based on the instantaneous SNR feedback from the user. However the instantaneous rate does not reflect the actual achievable transmission rate as it does not take into account the fact that the wireless media is error prone and retransmission is possible via HARQ mechanism. Therefore, the actual achievable transmission may well be higher

than the requested transmission rate (based on the current instantaneous feedback SNR) with retransmissions, due to significant combining and decoding gain of the HARQ schemes.

In view of that, some heuristic approaches have been suggested to compute a more accurate and effective rate, R_{Eff} for scheduling purposes. As mentioned earlier, R_{MCS} represents the instantaneous data rate using MCS as the modulation and coding scheme. PER_{SNR} represents the estimated packet error rate for an input *SNR* given the modulation and coding scheme, which considers the impact of channel fading. *Methods A-C* were investigated in [4], however two heuristic approaches, *Method D* and *Method E* are also proposed here.

Method A: Instantaneous Rate

This is the conventional approach that does not consider any retransmission information in the scheduling. The R_{eff} is simply the instantaneous data rate of the selected MCS.

$$R_{Eff} = R_{MCS} \tag{4-4}$$

Method B: Success Probability Weighted Instantaneous Rate

PER_{SNR} is the packet error rate for a given SNR of the selected MCS. The *SNR* notation refers to the SNR of the current transmission, regardless whether it is a new transmission or a retransmission. This method does not exploit the gain of the HARQ, since the accumulated SNR is significantly improved in the retransmissions.

$$R_{Eff} = R_{MCS} * (1 - PER_{SNR}) \tag{4-5}$$

Method C: HARQ Success Probability Weighted Instantaneous Rate

PER_{SNR_HARQ} is the packet error rate given that *SNR_HARQ* is the accumulated SNR over the retransmissions. Since the packet combining of multiple transmissions gives a higher SNR, it gives a better packet error rate performance. Thus the R_{Eff} gives a more accurate estimation of the achievable data rate for each instance.

$$R_{Eff} = R_{MCS} * (1 - PER_{SNR\_HARQ}) \tag{4-6}$$

Method D: Instantaneous Rate based on Accumulated SNR

$R_{MCS}(SNR\_HARQ)$ is the instantaneous rate of the given *SNR_HARQ* where *SNR_HARQ* is the accumulated SNR over the retransmissions. Since the packet combining of multiple

transmissions give a higher SNR, the instantaneous data rate based on accumulated SNR gives a more realistic reflection of the actual achievable data rate.

$$R_{Eff} = R_{MCS}(SNR\_HARQ) \quad (4\text{-}7)$$

Method E: HARQ Success Probability Weighted Instantaneous Rate based on Accumulated SNR

This method is similar to the Method D but weighted by the success probability, $1 - PER_{SNR\_HARQ}$. It can be observed that this method has less priority compared to Method D, as the R_{Eff} is weighted by the success probability, which decreases the achievable instantaneous data rate.

$$R_{Eff} = R_{MCS}(SNR\_HARQ) * (1 - PER_{SNR\_HARQ}) \quad (4\text{-}8)$$

4.2.3.1 Performance Analysis

In this performance analysis, we assume the same simulation parameters as the previous section, and the number of users K =10. A mapping strategy using *Chase_thrpt* is employed. Instead of evaluating the performance in terms of throughput, a fairness metric is considered. It is well known that a proportionally fair scheduler should maximize the logarithmic sum of all users' rates [14]. In order to evaluate the performance of different methods, a slightly modified fairness metric is employed based on [14][4]:

$$Fairness\_Metric(t) = \left(\prod_{k=1}^{K} R_{ave(k)}(t) \right)^{\frac{1}{K}} \quad (4\text{-}9)$$

$R_{ave(k)}$ is the average achievable throughput of user k, which is constantly sampled throughout the simulation. The equation in [4] is used to evaluate the performance of internet browsing using HTTP traffic model. This is not applicable and thus it is modified to employ average data rate in order to better compare the performance. Figure 4-8 shows the cumulative distribution plot of the fairness metric for all the methods. It shows that both Methods A and B do not perform well due the fact that these approaches neglect the retransmission information in the scheduling. Particularly in Method B, the inaccurate success probability weight decreases the effective data rate and consequently reduces the priority of the user. This causes undesired consequences as priority should be given to the retransmission, since retransmission has higher chance of successful

transmission than other new transmissions. Thus, the failure to include this crucial information into scheduling results in a non-optimum user being selected for transmission. Methods C, D and E achieved similar but far more superior performances than Method A and B. Method C estimates a precise PER based on the accumulated SNR and therefore gives a more accurate weight to the instantaneous data rate. Both Method D and E estimate a more precise instantaneous rate for priority ranking based on the accumulated SNR.

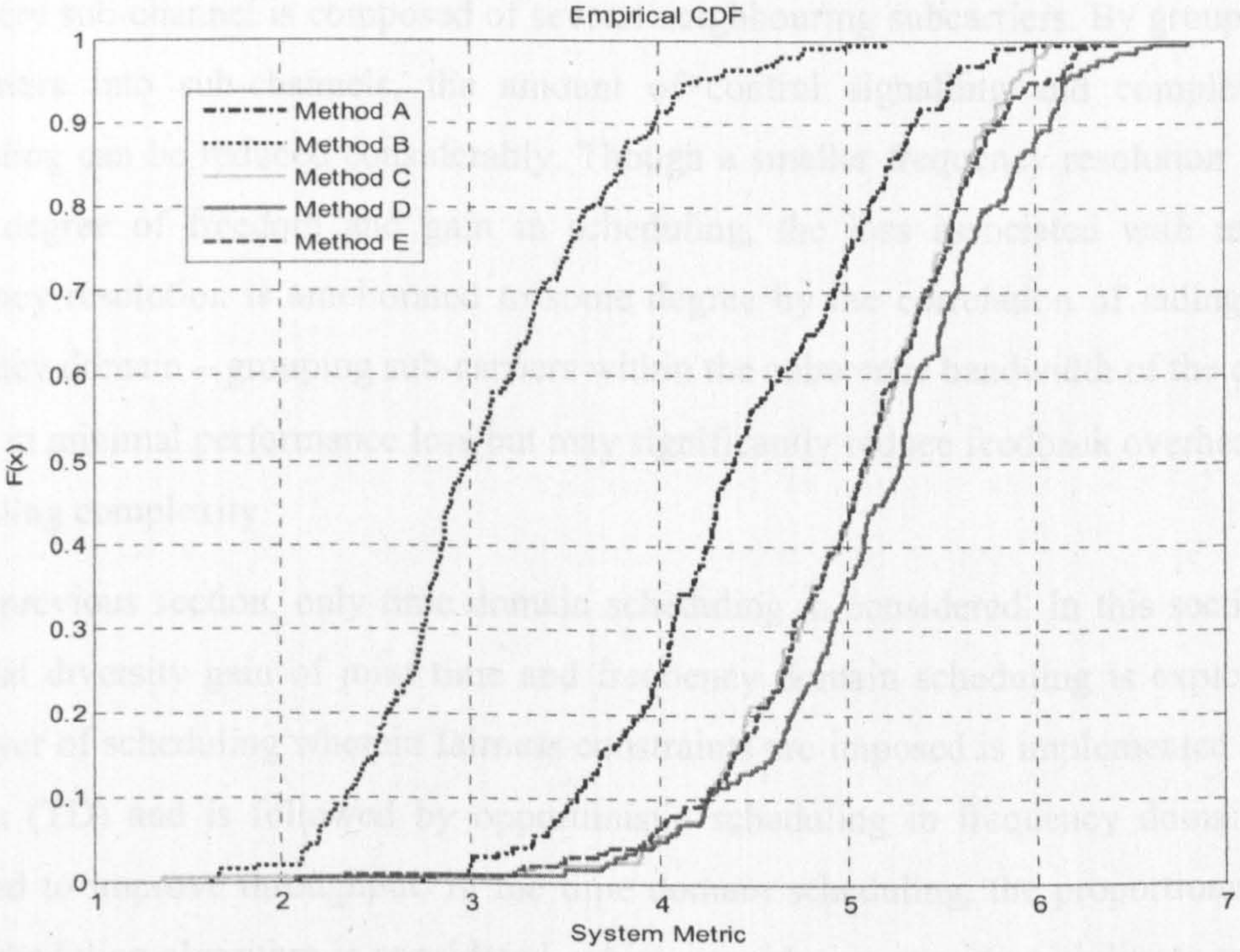

Figure 4-8: Multiuser fairness performance of various calculation methods of effective rate for PF Scheduler

Due to the fact that a high decoding gain and combining gain can be achieved with retransmissions, the higher priority given to the retransmission in a proportional fair scheduler will increase the overall performance. Therefore, Method D in this case performs best among all. In the Method E, the success probability weight reduces the instantaneous rate and also the priority. While this work wells for Method C, it does not give the best performance when the instantaneous rate is based on the accumulated SNR. From the analysis of the simulation results, it can therefore be concluded that by giving higher priority to the retransmissions based on the accumulated SNR (due to HARQ mechanism), better performance can be achieved.

4.3 Joint Time and Frequency Scheduling

Orthogonal Frequency Division Multiple Access (OFDMA) has been selected as the downlink access technology for the 3GPP LTE system as it is suitable for high data rate transmission in wideband wireless systems due to its spectral efficiency and good immunity to multipath fading. Moreover, this access technology also provides a possible further enhancement to the system by enabling opportunistic scheduling in the frequency domain. To frequency multiplex users in LTE, subcarriers are divided into sub-channels, and every sub-channel is composed of several neighbouring subcarriers. By grouping the subcarriers into sub-channels, the amount of control signalling and complexity of scheduling can be reduced considerably. Though a smaller frequency resolution gives a larger degree of freedom and gain in scheduling, the loss associated with reducing frequency resolution is ameliorated to some degree by the correlation of fading in the frequency domain – grouping sub-carriers within the coherence bandwidth of the channel results in minimal performance loss but may significantly reduce feedback overheads and scheduling complexity.

In the previous section, only time domain scheduling in considered. In this section, the potential diversity gain of joint time and frequency domain scheduling is exploited. A first layer of scheduling wherein fairness constraints are imposed is implemented in time domain (TD) and is followed by opportunistic scheduling in frequency domain (FD) intended to improve throughput. In the time domain scheduling, the proportionally fair (PF) scheduling algorithm is considered, which provides an attractive ability to trade off between throughput and fairness. This algorithm is used to schedule a sub-set of users for the transmission interval under consideration. In the frequency domain, the scheduler aims to optimize the gain of multi-user frequency diversity, within the constraints of the prior TD scheduling of selected users. Figure 4-9 shows how information is fed into schedulers and interactions between time and frequency domain schedulers.

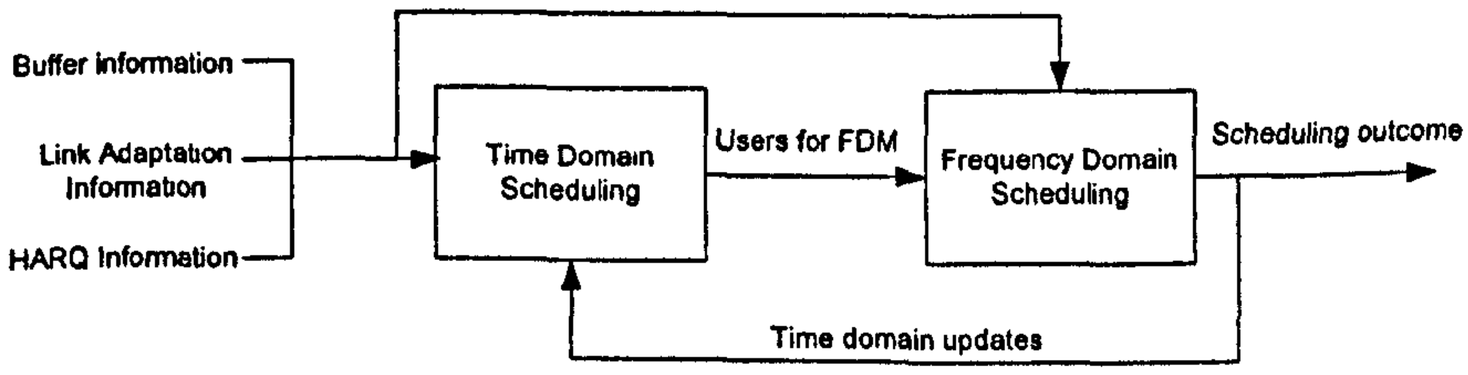

Figure 4-9: Illustration of the Joint Time-Frequency scheduler

Many algorithms for a joint time frequency scheduler in OFDMA systems have been proposed to improve the system performance [15][16]. However, many of them do not jointly consider design issues of a practical system such as retransmission mechanisms, overhead of control signalling, number of multiplexing users and overall system fairness. In this work, also publish in [17], these crucial design issues will be taken into consideration. Several joint time frequency schedulers are investigated, as well as a low complexity dynamic allocation scheme in the frequency domain, which attempts to exploit multiuser diversity and fairness is proposed in the joint time and frequency scheduler.

4.3.1 Time Domain Scheduler

In the time domain, a PF scheduler which is well known to provide an attractive ability to trade off between maximum average throughput and user fairness is considered. The essence of this algorithm is to allocate approximately the same number of resources to all users (averaged over a period of time) and to try to allocate resource in any given scheduling interval to a user whose channel condition is near its peak.

In the context of OFDMA, a subset of users, the number of which is termed 'multiplexing users' and denoted k, with the highest priorities will be selected for subsequent FD scheduling. The effect of different number of multiplexing users in each time slot or sub frame will be investigated. All users within the cell will be considered, including users with new data as well as users with pending retransmission. Users with retransmission will be prioritized with the fact that their retransmissions will have higher chance of successful transmission due to the gain of Hybrid ARQ. The effective rate for user with pending retransmission is calculated based on Equation 4-7, which was shown to give promising results in the previous section.

4.3.2 Frequency Domain Scheduler

To frequency multiplex users in the LTE system, the total bandwidth is divided into sub-channels, denoted as physical resource blocks (PRBs). A PRB is the minimum resolution for scheduling in the frequency domain. There are 50 PRBs in a 10MHz system, each consisting of a 12 neighbouring sub-carriers. The sub-carrier bandwidth is 15 kHz and the PRB bandwidth is 180 kHz. A single Channel quality indicator (CQI) (calculated from the average quality of the 12 sub-carriers) can be fed back for each PRB as shown

in Figure 4-10. An example of how subcarriers are grouped and allocated is shown in Figure 4-11.

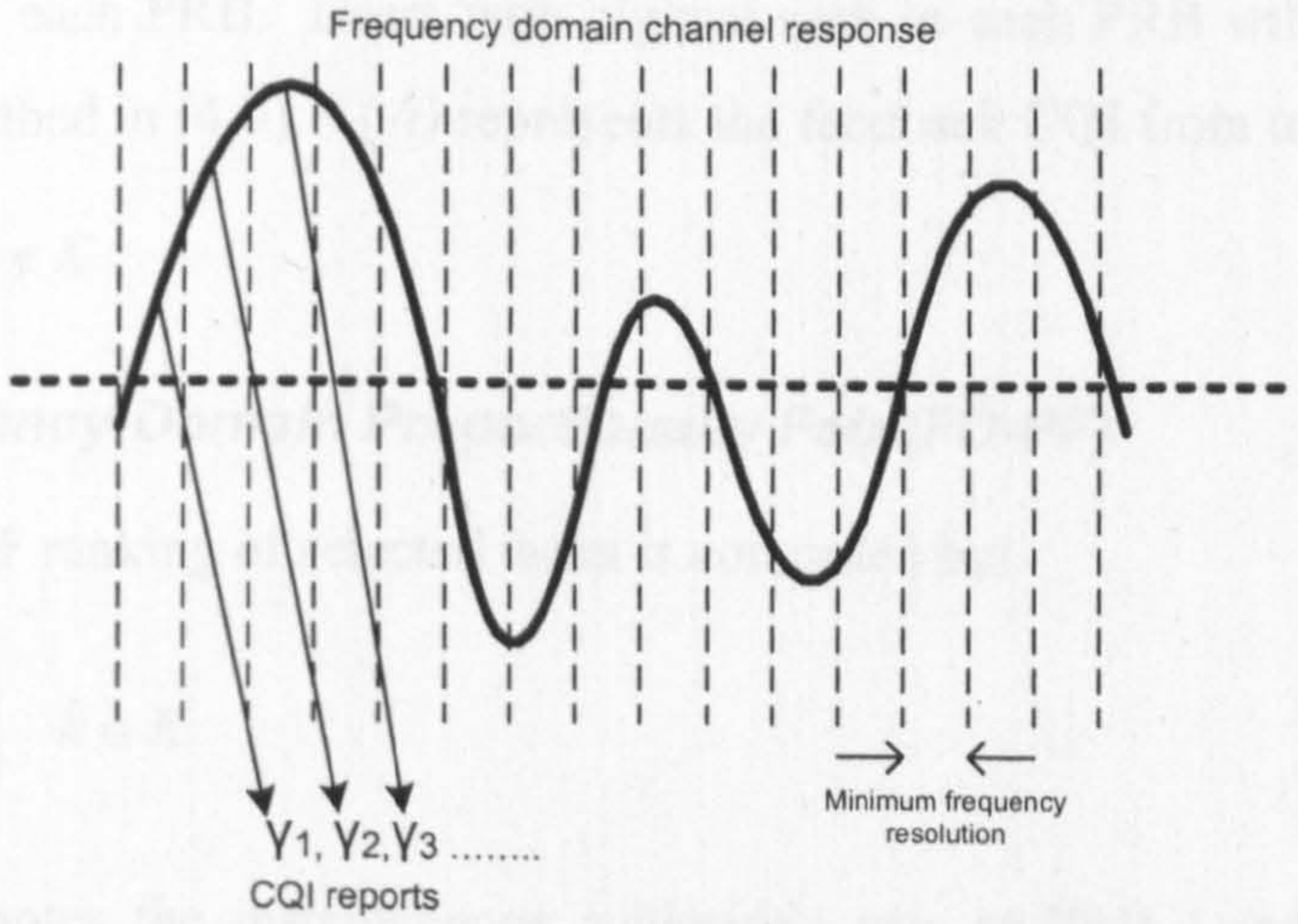

Figure 4-10: Illustration of CQI Feedback

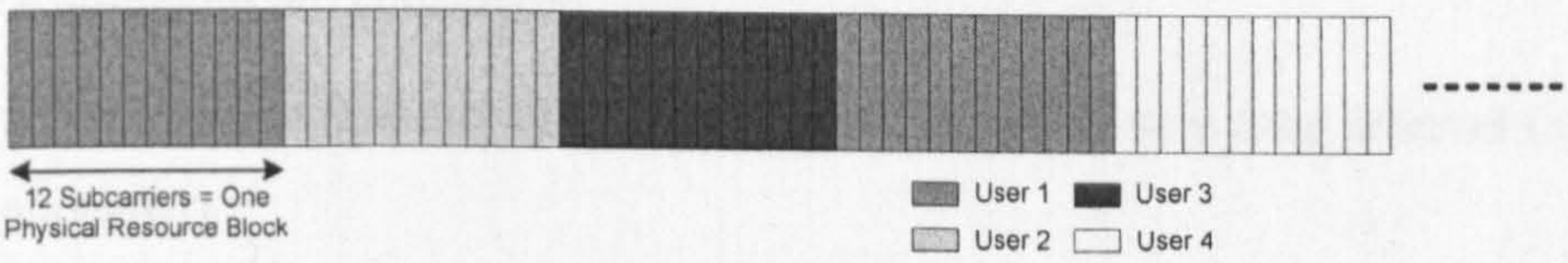

Figure 4-11: Illustrations of PRBs groupings

In order to allocate the resources in the frequency domain to the selected users, several well-known scheduling techniques will be investigated. Additionally a novel sub-optimal but low complexity dynamic allocation strategy is considered.

4.3.2.1 No Frequency Domain Scheduling (TD-PF)

Scheduling is only performed in the time domain using the PF algorithm described above. There is no opportunistic scheduling operation in the frequency domain.

4.3.2.2 Frequency-Domain Round Robin (FD-RR)

All PRBs are scheduled with a straightforward method where selected users are serviced in a round-robin fashion. All users must be allocated a PRB before re-allocating to the same user since it is assumed that all users require the same QoS.

4.3.2.3 Frequency-Domain Max C/I (FD-MAX)

All PRBs are scheduled with a straightforward method where all users are ranked by the order of SNR in each PRB. Users with highest rank in each PRB will be scheduled to transmit as described in (4-9). $\gamma_{(k)}(t)$ represents the feedback CQI from user k.

$$\arg\max(\gamma_k(t)) \quad k \in K \tag{4-10}$$

4.3.2.4 Frequency-Domain Proportionally Fair (FD-PF)

For each PRB, PF ranking of selected users is computed by:

$$\arg\max\left(\frac{R_{k,j}(t)}{T_k(t)}\right) \quad k \in K \tag{4-11}$$

where $R_{k,j}(t)$ denotes the instantaneous achievable rate at PRB j and $T_k(t)$ represents user's average throughput. The highest ranked user k will be scheduled to transmit at that PRB j.

Two FD-PF strategies are considered:

Strategy I: The average throughput $T_k(t)$ is updated for each new time interval (after all PRBs are allocated).

Strategy II: The average throughput $T_k(t)$ is updated after each PRB is allocated. This strategy ensures a more proportionally fair environment due to the frequent updates to the average throughput, but is undoubtedly more computational demanding.

4.3.2.5 Frequency domain Dynamic Allocation (FD-DA)

A joint time frequency scheduler based on dynamic subcarrier allocation (DSA) [22] is proposed. The DSA algorithm ensures an equal share of resources among selected users, but not a fair fraction of capacity. However this sub-optimal but low complexity algorithm approximately maximises capacity given the equal resource constraint. In the pseudo code, P_k represents the average received power for user k. M represents all the usable subcarriers from 1 to N. $h_{k,n}$ is the channel gain (CSI) for subcarrier n and user k. The pseudo code of the algorithm is given below:

1. Initialization
Set $P_k = 0$ for all users k = 1 to K, n={ 123,...N}
2. First time
For every user k = 1 to K
{
(a) Find subcarrier n satisfying $|h_{k,n}| > |h_{k,j}|$ for all $j \in N$
(b) Update P_k and M with the n from (a) according to:
$P_k = |h_{k,m}|^2$, $M = M - \{n\}$ -remove this subcarrier from the available subcarriers
}
3. While M not equal to 0 (until all subcarriers are allocated)
{
(a) Sort users according to the user that has less power.
This means find user k satisfying $P_k < P_i$ for all i, $1 \leq i \leq K$
(b) For the found user k, find subcarrier n satisfying
$|h_{k,n}| > |h_{k,j}|$ for all $j \in N$
(c) Update P_k and M with the k and n according to:
$P_k = |h_{k,n}|^2$, $M = M - \{n\}$
(d) Go to the next user in the short list, until all users are allocated another subcarrier
}

4.3.3 Performance Analysis

4.3.3.1 Throughput Analysis

In order to obtain diversity gain in the time and frequency domain, sufficient numbers of users must be present. The capacity performance of various schedulers with the increasing number of users in a cell is first investigated. The FD-MAX and FD-RR schedulers mainly serve as reference schedulers. However, in order to quantify the performance gain of additional opportunistic scheduling in the frequency domain, the TD PF scheduler is also considered. From Figure 4-12, it can be seen that the joint time-frequency PF schedulers, FD-PF-I and FD-PF-II achieve near identical performance which is significantly superior to TD-PF. With increasing number of users, more diversity gain can be exploited and thus the performance gain increases. In the case of equal resource allocation, the proposed scheduler significantly outperforms FD-RR. The FD-DA scheduler also achieves higher throughput than TD-PF when there are a sufficient number of users in the cell, e.g. more than 17 users. The slight oscillatory nature of this performance curve can be attributed to the ability to allocate extra resource to strong users when the number of PRBs slightly exceeds an integer multiple of the

number of users. The FD-MAX scheduler clearly offers the best performance in terms of capacity but is not expected to achieve good performance in terms of fairness.

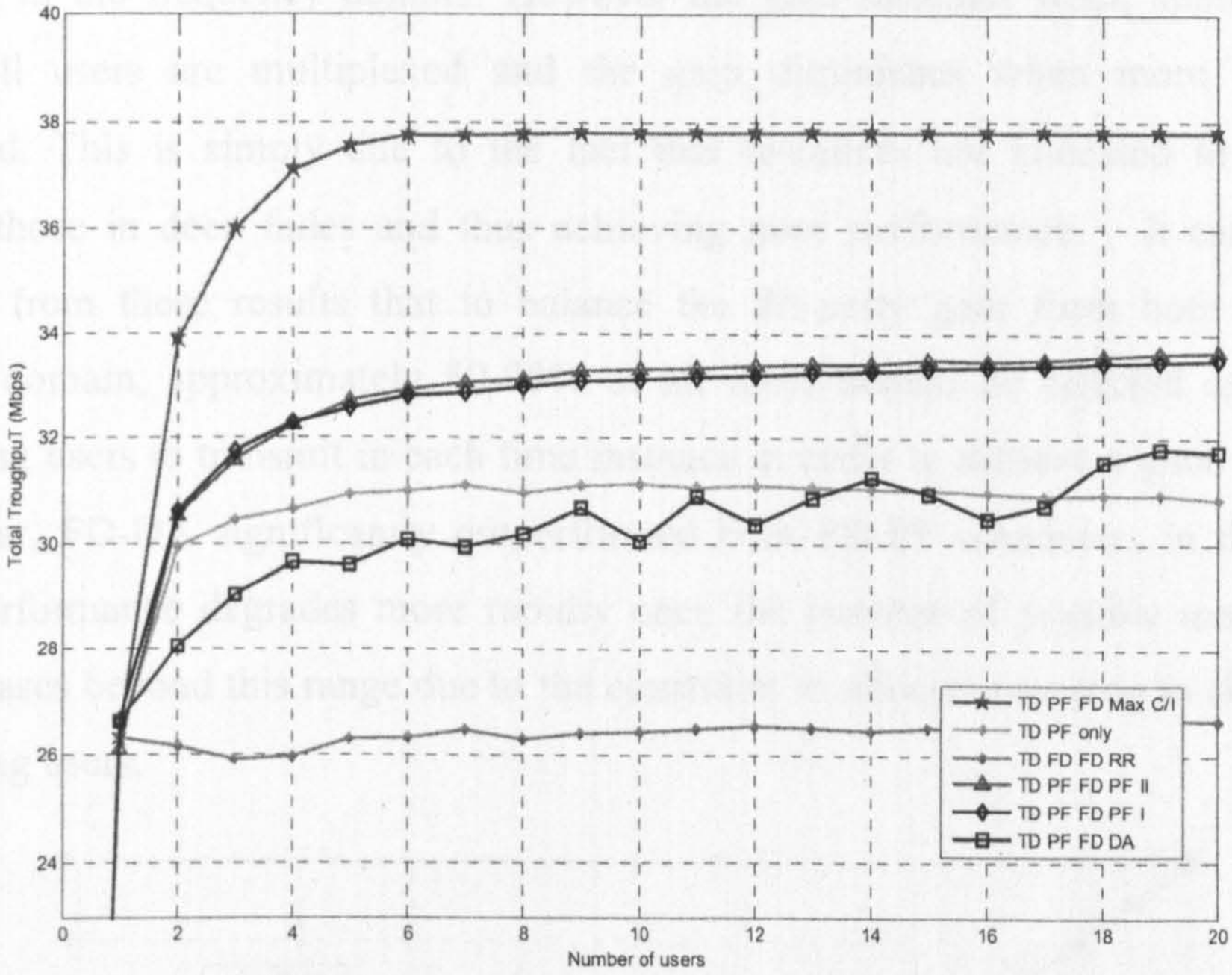

Figure 4-12: Throughput performance with increasing number of users in a cell

4.3.3.2 Effect of Number of Multiplexing Users

For the results in Figure 4-12, the number of possible multiplexing users per time slot is fixed and equal to the number of users in the cell. However, not all users are actually scheduled per time slot due to the nature of some schedulers. Figure 4-13 shows the number of users actually scheduled. For round robin and dynamic allocation methods, the number of scheduled users always equals the number of multiplexing users as these algorithms ensure an equal share of resource among all users. The Max C/I algorithm favours only users with high SNR, which is location dependent. In the case of FD-PF, the average number of scheduled users for strategy II is much higher than strategy I. This is due to the fact that in strategy I, there is no instantaneous update to the average throughput after each PRB and thus users with lower PF ranking priorities will not be selected.

If all the multiplexing users are scheduled in the frequency domain, multi-user diversity might well be maximized but the inherent multi-user diversity in the time domain is not being utilized, especially in the case of the equal resource allocation algorithms. Figure 4-14 shows how the FD-PF-I, FD-PF-II and FD-DA schedulers perform with increasing

number of possible multiplexing users in each time slot. These schedulers all benefit from increasing number of multiplexing users in each time slot due to opportunistic scheduling in the frequency domain. However the gain saturates when approximately 70% of all users are multiplexed and the gain diminishes when more users are multiplexed. This is simply due to the fact that resources are allocated to all users including those in deep fades and thus achieving poor performance. It can then be concluded from these results that to balance the diversity gain from both time and frequency domain, approximately 50-70% of all users should be selected as possible multiplexing users to transmit in each time instance in order to achieve a good trade-off. In particular, FD-DA significantly outperformed both FD-PF schedulers in this range. FD-DA performance degrades more rapidly once the number of possible multiplexing users increases beyond this range due to the constraint to allocate resource to all possible multiplexing users.

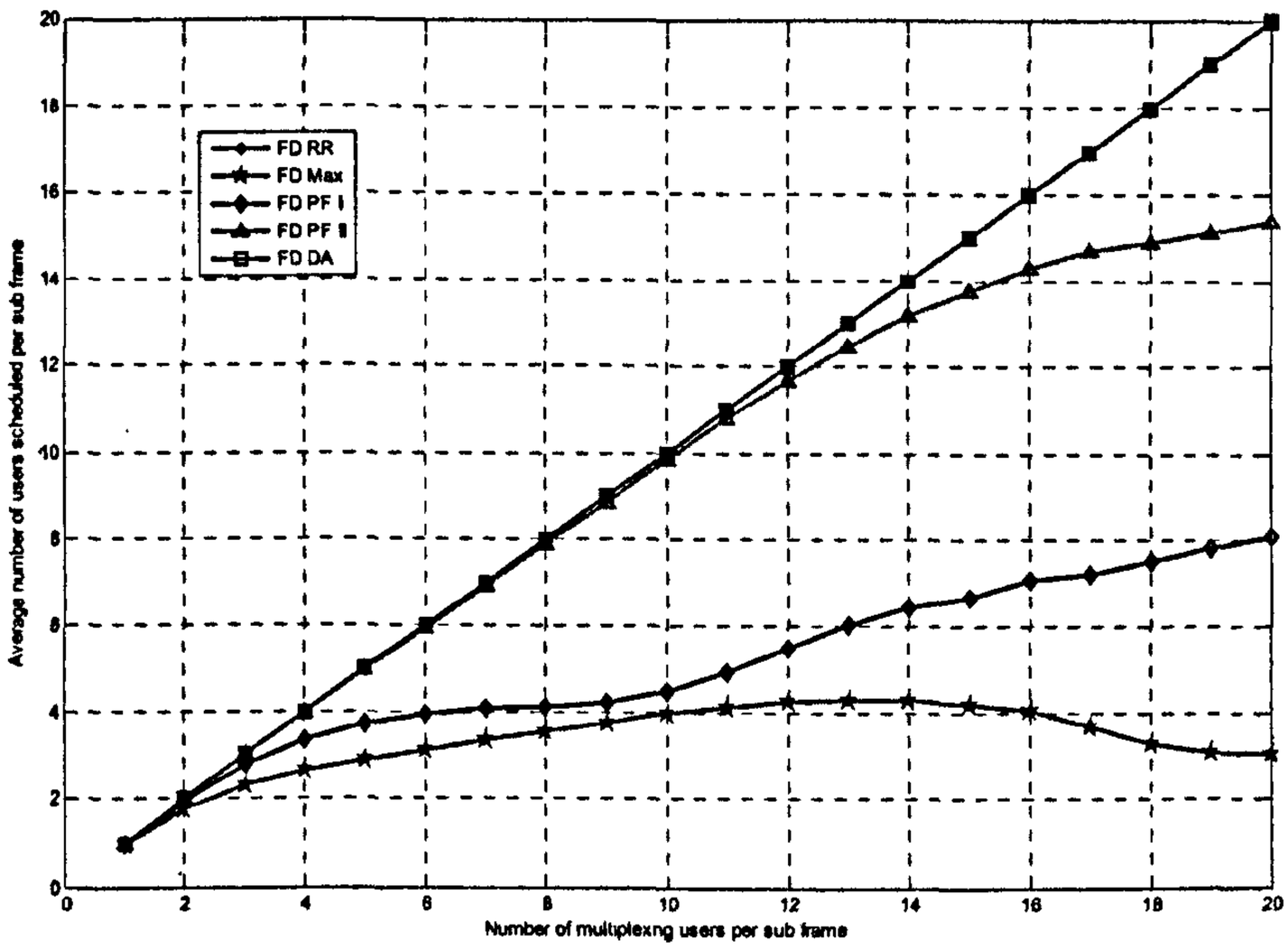

Figure 4-13: Number of multiplexing users vs. scheduled users

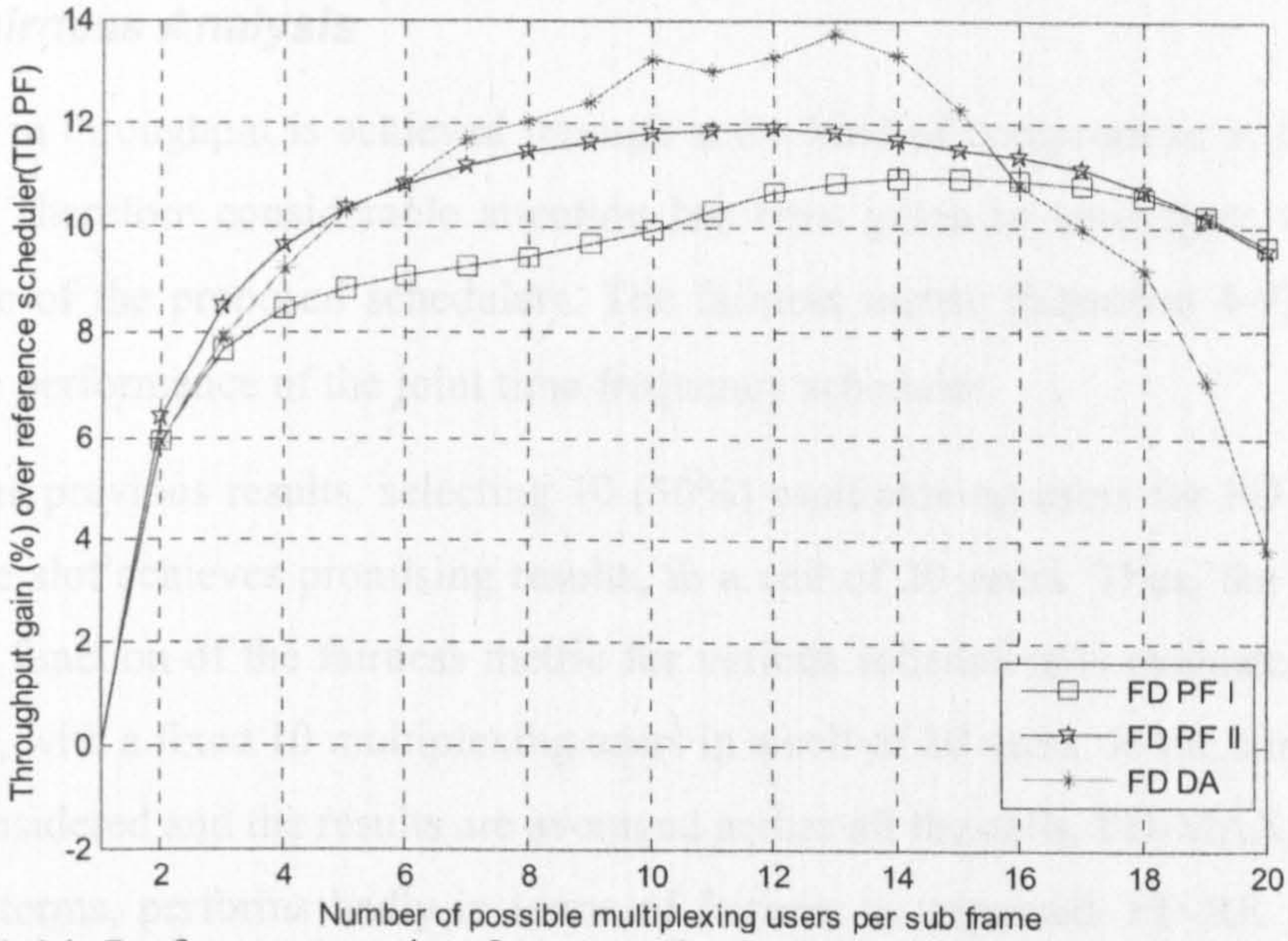

Figure 4-14: Performance gain of proposed schedulers with increasing number of possible multiplexing users in a sub frame

Throughput performance with the number of possible multiplexing users equal to 50% of all users is then considered in Figure 4-15 (with performance also shown for the 100% case as a reference). It can be seen that FD-DA outperforms all other schemes except TD-MAX when there are a sufficient number of users in a cell, e.g. 6 or more. This is clearly a likely scenario. It can also be seen that the FD-PF strategies are much less sensitive than FD-DA to the number of multiplexing users.

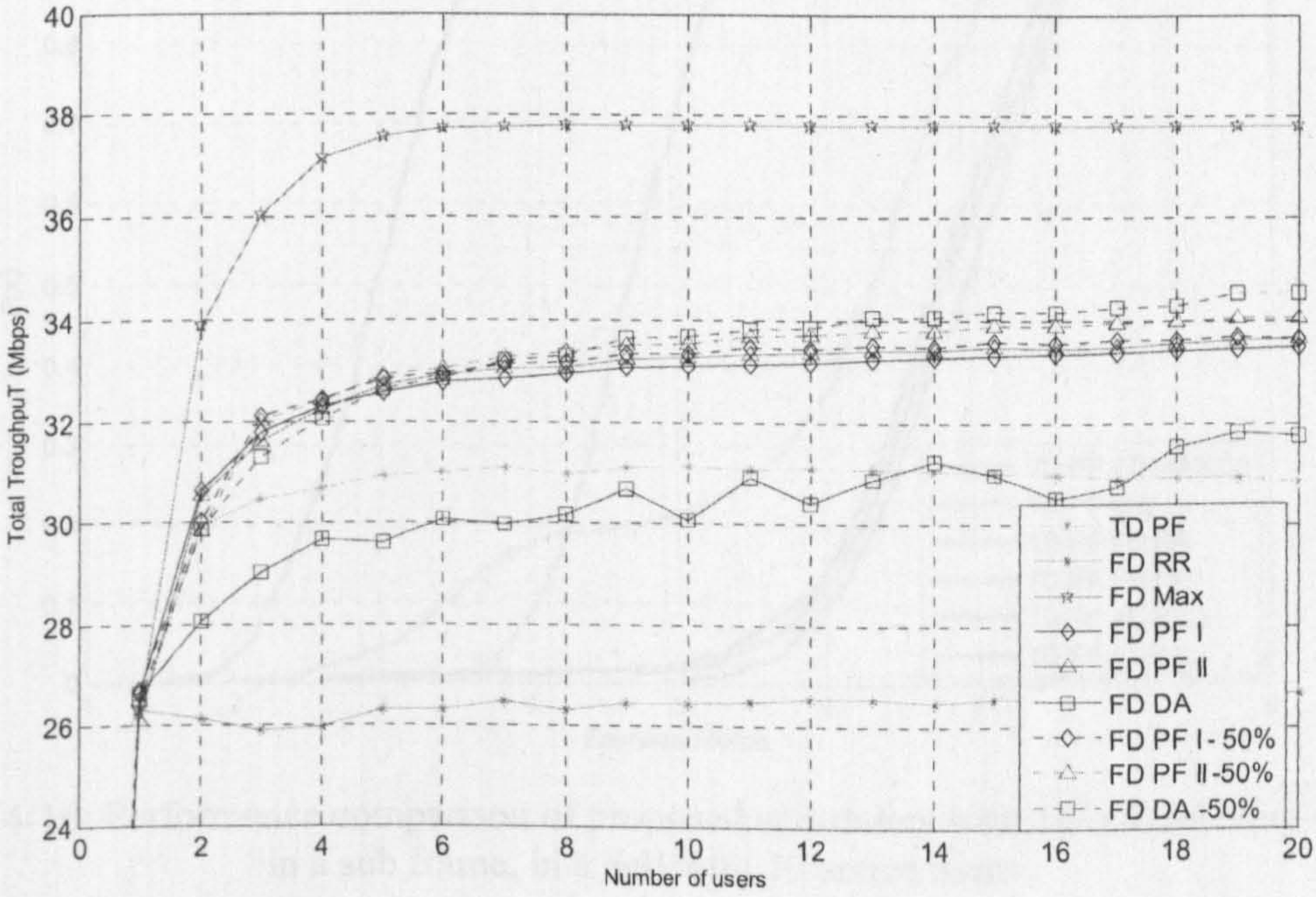

Figure 4-15: Throughput performance with 50% users selected of all multiplexing users

4.3.3.3 Fairness Analysis

Often, gain in throughput is achieved through some kind of compromise in fairness and vice versa. Therefore considerable attention has been given to investigate the fairness performance of the proposed schedulers. The fairness metric (Equation 4-9) is used to evaluate the performance of the joint time frequency scheduler.

Based on the previous results, selecting 10 (50%) multiplexing users for FD scheduling in each time slot achieves promising results, in a cell of 20 users. Thus, the cumulative distribution function of the fairness metric for various schedulers is evaluated shown in Figure 4-16, with a fixed 10 multiplexing users in a cell of 20 users. In the simulation, 10 cells are considered and the results are averaged across all the cells. FD-MAX, optimal in throughput terms, performs badly in terms of fairness as expected. FD-RR and TD-PF achieve better fairness than FD-MAX. By exploiting the diversity in the time and frequency domain, it is possible to allocate resources more fairly to all users. Hence, both FD-PF strategies achieve better fairness than the TD-PF scheduler, with FD-PF-II being superior due to its more frequent update of $T_k(t)$. FD-DA, which attempts to maximise throughput in the frequency domain, but maintains an element of fairness by allocating equal resources, performs best, exceeding both the FD-PF-I and FD-PF-II.

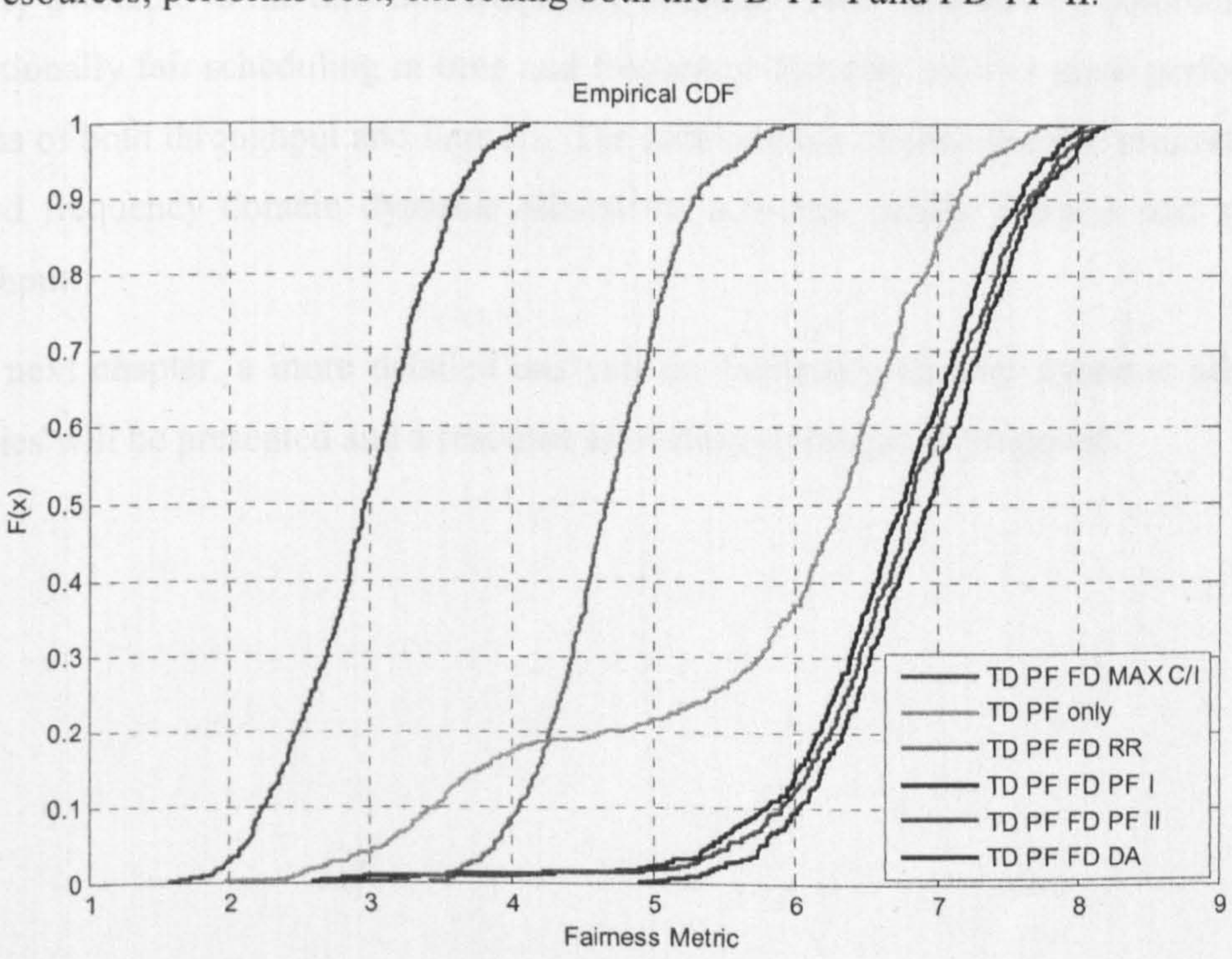

Figure 4-16: Performance comparison of proposed schedulers with 10 multiplexing users in a sub frame, in a cell with 20 active users

4.4 Conclusion

From the performance analysis, it can be concluded that it is important to consider the underlying HARQ operation in order to optimise the mapping between SNR and MCS. The proposed mapping has shown a significant improvement especially in the case of the full incremental redundancy (IR) scheme. In addition to that, simulation results have shown that a modified proportionally fair scheduler, which incorporates retransmission information to compute a more accurate effective data rate, outperforms the conventional proportionally fair scheduler.

In addition, in this chapter, the potential gain achievable through scheduling jointly in both frequency domain and time domain to exploit both domains of diversity has been investigated for an LTE OFDMA system employing HARQ. Simulation results have shown that joint time frequency proportionally fair schedulers achieve significant improvements in performance compared to a frequency-blind, time-domain-only proportionally fair scheduler. For the scenario considered, in order to balance the diversity gain from both time and frequency domain, approximately 50-70% of all multiplexing users should be selected to transmit in each time slot to best exploit the diversity available in the time and frequency domains. Two variants of a combination of proportionally fair scheduling in time and frequency domains achieve good performance in terms of both throughput and fairness. The combination of time domain proportionally fair and frequency domain dynamic allocation, achieves similar fairness and superior throughput.

In the next chapter, a more detailed analysis on frequency domain dynamic allocation strategies will be presented and a resource allocation technique is proposed.

References

[1] Hui Zhang, "Service disciplines for guaranteed performance service in packet-switching networks," *Proceedings of the IEEE* , vol.83, no.10, pp.1374-1396, Oct 1995

[2] Andrew S.Tanenbaum, "Computer Networks", 4th Edition, Pearson Education, 2003

[3] H. Fattah, C.Leung "An Overview of Scheduling Algorithms in Wireless Multimedia Networks", IEEE Wireless Communications, vol 9, no.5, Page 76-83, Oct. 2002

[4] H. Zheng, H.Viswanathan, "Optimizing the ARQ Performance in Downlink Packet Data Systems with Scheduling ", IEEE Transactions on Wireless Communications, Vol. 4, No.2, March 2005

[5] J.Huang, R.A.Berry, M.L.HOnig, "Wireless Scheduling With Hybrid ARQ", IEEE Transactions on Wireless Communications, Vol.4, No.6, Nov. 2005

[6] G.Song, Y.Li "Cross-Layer Optimization for OFDM Wireless Networks- Part I: Theoretical Framework" IEEE Transactions on Wireless Communications, Vol. 4, No.2, March 2005

[7] P.Liu, R.Berry, M.L.Honig, " Delay-Sensitive Packet Scheduling in Wireless Networks" Proc. IEEE WCNC 2003, Vol. 3, March 2003 Page 1627 - 1632

[8] Q. Liu, S. Zhou, G.B.Giannakis "Cross Layer Scheduling with Prescribed QoS Guarantees in Adaptive Wireless Networks", Selected Areas in Communications, IEEE Journal, Vol.23, No.5, May 2005

[9] Aimin Sang, XiaoDong Wang, Mohammad Madihian and Richard D.Gitlin, " A flexible Downlink Scheduling Scheme in Cellular Packet Data Systems", IEEE Transactions on Wireless Communications, Vol. 5, No. 3, March 2006

[10] D.Tse, P.Viswanath, ' Fundamentals of Wireless Communication', ,Cambridge University Press,2005,pp258-262

[11] Samir Kaller, "Analysis of a Type II Hybrid ARQ Scheme with Code Combining" IEEE Transaction on Communications, Vol. 38, N0.8, August 1990, page 1133-1137

[12] A.J.Goldsmith , S.G.Chua," Adaptive Coded Modulation for Fading Channels" IEEE TRANSACTIONS ON COMMUNICATIONS, VOL. 46, NO. 5, MAY 1998

[13] Harri Holma, Antti Toskala, ' WCDMA for UMTS: HSPA Evolution and LTE', 4th Edition, John Wiley & Sons Ltd, 2007, pp175-221

[14] P.Viswanath, D.Tse, P.Laroia, "Opportunistic Beamforming using dumb antenna", IEEE Trans. on Info. Theory, Vol.48,No.6. June 2002

[15] A.Wang, L.Xiao, S.Zhou, X.Xu, Y.Yan, 'Dynamic resource management in the fourth generation wireless systems' , in Proceedings of International Conference on Communication Technology (ICCT), Beijing, April 2003, pp. 1095-1098.

[16] A.Pokhariyal, K.I. Pederson, G.Monghal, I.Z.Kovavs, C.Rosa, T.E. Kolding, P.E.Mogensen, 'HARQ Aware Frequency Domain Packet Scheduler with Different Degrees of Fairness for the UTRAN Long Term Evolution', in Proceedings of IEEE Vehicular Technology Conference (VTC) ,Dublin, April 2007, pp.2761-2765.

[17] K.C.Beh, S.Armour ,A.Doufexi, 'Joint Time-Frequency Domain Proportional Fair Scheduler with HARQ for 3GPP LTE Systems', in Proceedings of Vehicular Technology Conference, Calgary, October 2008.

[18] "Spatial channel model for multiple input multiple output (MIMO) simulations", 3GPP TR 25.996 V6.1.0, Sep'03. [Online]. Available: http://www.3gpp.org/ftp/Specs/html-info/25996.htm

[19] D. S. Baum, J. Hansen, and J. Salo, "An Interim Channel Model for Beyond-3G Systems: Extending the 3GPP Spatial Channel Model (SCM)," *VTC Spring 2005.*

[20] Raghavan, V.; Onggosanusi, E.N.; Dabak, A.G., "Single rate communication is advantageous over per-tone rate control in a multi-user OFDM system," *Vehicular Technology Conference, 2005. VTC-2005-Fall. 2005 IEEE 62nd* , vol.1, no., pp. 626-630, 28-25 Sept., 2005

[21] Blankenship, Y.W.; Sartori, P.J.; Classon, B.K.; Desai, V.; Baum, K.L., "Link error prediction methods for multicarrier systems," *Vehicular Technology Conference, 2004. VTC2004-Fall. 2004 IEEE 60th* , vol.6, no., pp. 4175-4179 Vol. 6, 26-29 Sept. 2004

[22] A.Doufexi, S. Armour 'Design Consideration and Physical Layer Performance Results for a 4G OFDMA System employing Dynamic Subcarrier Allocation', in Proceedings of Personal, Indoor and Mobile Radio Communications (PIMRC),Berlin, September 2005, pp. 351-361

Chapter 5

Dynamic Resource Allocation in OFDMA systems

In the previous chapter, a joint time and frequency domain scheduling was considered. In this chapter, the focus is on the resource allocation in the frequency domain. In particular, attention has been given on how to achieve near optimum resource allocation algorithms, given that the optimum resource allocation strategy is computationally expensive and not practical for actual implementation.

In a frequency selective channel, each OFDM subcarrier experiences distinct fading pattern and thus different received signal quality. Due to different locations of users in a cell, each user will undergo an independent fading pattern and the probability of all users suffering deep fades or peaks at the same subcarrier is very low. Therefore, by utilizing the channel state information, subcarriers experiencing good channels for different users can be loaded and multiuser diversity can be exploited [1]. However, an optimal allocation strategy is not trivial compared to the water filling principle as multiple users are involved. A multiuser water filling algorithm [2], which just gives each subcarrier to the user with the highest gain is easy to devise, but does not support minimum rate requirements for individual users or ensure fairness among the users. In the context of equal resource sharing, it is well known that the Hungarian method [3] can be extended to maximize the total channel gains of all users in a subcarrier allocation scenario. This exhaustive method represents the optimal performance [5] that can be obtained in an assignment problem and hence represents an upper bound of system performance. However, this method is not practical for use because of the high computational time and complexity which increases tremendously with higher number of resource units.

The infeasibility of the Hungarian method for practical use raises the need to consider a lower complexity but near optimal solution. Maximum Gain Sort-Swap (MGSS) is a technique published in the literature [4][5] which attempts to achieve a maximum perceived channel gain by sorting and swapping the subcarriers. This algorithm sorts subcarrier pairs by a metric of total perceived channel gain, which is the relative gain of

swapping two subcarriers between two users. Subcarriers are swapped between the users to achieve maximum gain. This algorithm is sub-optimal but of lower complexity compared to the Hungarian method. Nonetheless, the complexity of this algorithm remains high due to the fact that the iterations of the sort and swap operation increase almost quadratically with the number of users. Another sub-optimal low complexity algorithm, known as DSA [6] further reduces the complexity of the allocation process at the expense of a small decrease in the achieved gain. A detailed investigation of these dynamic resource allocation schemes was given in [7][8], and some extended work has been considered in this chapter. Some algorithms which consider both subcarrier and power allocation are given in [9][10]. However, due to insignificant gain of power allocation and the undesired increased computational complexity, only equal power allocation is considered further in this work.

Channel gains of the mobile users are somehow uncorrelated and follow certain fading profiles, e.g. Rayleigh distribution. Thus, it is difficult for a non-exhaustive search or iterative algorithm to decide which user has an edge over another user to transmit on a certain subcarrier by merely comparing the channel gain. Allocating a subcarrier to a user based solely on channel gain in this context does not usually result in an optimum overall outcome. Therefore, it would be beneficial to create a comparative relationship between the channel gains of all the users before allocating the resources. In this chapter, the optimal solution using the Hungarian method and sub-optimal solutions are presented. A low complexity but sub-optimal algorithm based on a maximal ratio weighted metric that is derived from the normalized channel gains of all users is proposed and evaluated in the downlink of LTE.

Feedback overhead increases rapidly with the number of sub-channels (PRBs). In order to efficiently feedback to the transmitter, the channel gains need to be quantized. While better quantization gives higher accuracy of the channel, the overhead caused by the feedback becomes prohibitive when the number of resource units is high. Therefore, a 1 bit feedback scheme [11][12] is employed in the performance analysis, where a mobile terminal will feedback a bit per resource unit to inform the transmitter whether or not the channel gain falls above a threshold. If the channel gain is above the threshold, the resource unit will be prioritised for selection. An analytical model is presented and compared with the simulation results.

5.1 Problem Formulation

In order to compare the performance of the proposed algorithms to the optimal solution, the classical assignment problem using channel gain as a metric is first described. The optimal solution based on the Hungarian method and suboptimal solutions proposed in the literature are presented and compared with the proposed algorithm. An analysis of the computational complexity of all the solutions is also presented. These algorithms should work perfectly on a subchannel (PRB) or a subcarrier. Since some of these algorithms were originally intended for subcarrier allocation, subcarrier terminology is used in the descriptions.

The goal of resource allocation algorithms that aim to maximise throughput is to maximise the channel gain of all the users while satisfying the requirement that any resource is unique to only one user. Assuming a generic OFDMA system, the channel gain matrix is given by $H = \{|h_{k,n}|^2\}$ where $k = 1,2, \ldots,K$ and $n=1,2,\ldots.N$ (K is the number of all users and N is the number of data subcarriers). P_{total} is the total perceived channel gain for all users. The optimization problem can be formulated by:

$$\text{Maximise } P_{total} = \sum_{k}^{K}\sum_{n}^{N} c_{k,n} \mid h_{k,n} \mid^2 \qquad (5\text{-}1)$$

The objective is to find the values of the assignment variable $c_{k,n}$ to maximize P_{total} while satisfying the following constraints:

$$c_{k,n}\begin{cases}1, & \textit{subcarrier n is assigned to user k}\\ 0, & \textit{otherwise}\end{cases} \qquad (5\text{-}2)$$

$$\sum_{n} c_{k,n} = S \qquad (5\text{-}3)$$

$$\sum_{k} c_{k,n} = 1 \qquad (5\text{-}4)$$

Constraint (5-3) specifies that the total number of subcarriers allocated to user K is S while constraint (5-4) restricts that each sub-carrier can only be allocated to one user. In this work, it is assumed that subcarriers are shared equally among all the users, thus $S= N/K$. In addition, due to the increased computational complexity and the insignificant gain of power control [14], equal power allocation is assumed throughout the chapter.

5.2 Optimal Solution

5.2.1 Hungarian Method

The Hungarian algorithm [3], also known as the Hungarian method, is a well-known combinatorial optimization algorithm, which minimises the cost of an assignment problem. However, this algorithm can also be modified to solve the assignment problem of profit maximization. Therefore, the Hungarian method can be extended to maximize the total channel gains of all users in a subcarrier allocation scenario. The Hungarian method represents the optimal performance that can be obtained in an assignment problem and is therefore used to determine an upper bound of system performance in this thesis. Further details on how the assignment problem can be reformulated to suit the Hungarian algorithm are given in [16]. Nonetheless, this method is not practical due to the high computational time and complexity which increase tremendously with larger channel gain matrices. The optimal assignment problem can be solved with a computational complexity order of $O(N^4)$*[15]*.

5.3 Suboptimal Solutions

5.3.1 Iterative Algorithms –MGSS

A near optimal solution, MGSS attempts to achieve a maximum perceived channel gain by sorting and swapping the subcarriers. This algorithm sorts subcarrier pairs by a metric of total perceived channel gain, which is the relative gain of swapping two subcarriers between two users. Subcarriers are swapped between the users to achieve maximum gain.

The average computational complexity of sorting is about *O(N log N)*, and that of searching is *O(log N)* [17]. The MGSS algorithm is divided into two parts, initial allocation and sort-swap operations. Initial allocation of the algorithm aims to generate a fast and rough version of the allocation matrix which will be refined in the iterative operations in the second phase. Initial allocation involves sorting all of the channel gains of each user and the computational complexity of the initial allocation is approximately *K*O(N log N)*. The sort and swap operation is performed for every two users. Each iteration incurs complexity of *3*O (S)* which involves calculating two reduction vectors and summing the reduction vectors. A complexity of *O(S log S)* is added for sorting the reduction vectors. The number of iterations in a sort and swap operation, *C*, depends on the number of subcarriers assigned and the accuracy of the initial allocation. The number of the sort and swap operations increases almost quadratically with the number of users.

Therefore, the computational complexity of this algorithm is further increased by approximately *(K-1) 2*C* (3*O (S) + O(S log S))* on top of the initial allocation.

5.3.2 Dynamic Subcarrier Allocation – DSA

DSA is a low complexity but sub-optimal algorithm which attempts to exploit and maximise multiuser diversity. This algorithm achieves substantial increases in perceived channel gain which are approximately equal for all users. Complexity is very low since this algorithm does not perform exhaustive searches nor iterations between users. Only simple sorting operations are needed.

The allocation algorithm will first loop through all the users and choose the highest channel gain among the available subcarriers. After the first loop, users are sorted according to the assigned channel gains. Subsequent loops start with the user with the least channel gain in order to achieve near equal channel gain among all the users. Loops are repeated until all subcarriers are allocated. The pseudo code of the algorithm was shown in Section 4.3.2.5. The average computational complexity of this algorithm is approximately *K*O (N log N) + (S-1)*O ((K log (K))*.

5.3.3 Proposed Low Complexity Algorithms Based on Maximal Ratio Weighted Metric

Maximal ratio combining [18] (MRC) is of vital importance in wireless diversity systems both fundamentally and practically. It is the optimum theoretical diversity combining method for branch signals having an arbitrary signal amplitude fading distribution. The method proposed here allocates resources based on a metric that is originated from the concept of maximal ratio combining where higher weight is given to a channel which has a better channel gain. The metric is derived from the normalized channel gains of all users. For each subcarrier of all the users, the metric is calculated based on the proportion of channel gain of one user over all the channel gains of all users. This maximum ratio weighted (MRW) metric [19] indicates the weight or the importance of one user's subcarrier, which can be calculated by:

$$h^{'}_{k,n} = \frac{|h_{k,n}|^2}{\sum_{k}^{K} |h_{k,n}|^2} \qquad (5\text{-}5)$$

Figure 5-1 compares the channel gain and the maximal ratio weighted metric of all the subcarriers for a user. The maximal ratio weighted metric amplifies the channel gain of

the user if it is relatively good compared to other users and vice versa. Since the relative gain of a user's subcarrier to other users' is implicitly embedded in the metric, this can virtually eliminate the need to perform sort and swap iterations between the users. Two simple yet efficient allocation algorithms are then used to make the most of the MRW metric. These algorithms ensure equal share of resources among the users, however this constraint can be relaxed easily. These simple algorithms use only simple searching and comparison operations. In the pseudo code, M represents all the usable subcarriers from 1 to N. $h'_{k,n}$ is the maximum ratio weighted metric for subcarrier n and user k. The pseudo codes of the algorithms are given below:

Algorithm 1

```
While the available subcarrier, M is not equal to 0
{
  Loop through all the users
  {
    User k selects highest h'k,n from the available subcarriers, M
    If two users x,y select the same subcarrier n
      Compare sum of highest gain of user x & second highest gain of user y and
      sum of highest gain of user y & second highest gain of user x
      M = M – {n}  -Remove that subcarrier from available subcarriers
      If sum of highest gain of user x and second highest gain of user y is higher
        User y reselects from the remaining available subcarriers
      Else
        User x reselects from the remaining available subcarriers
      End if
    End if
  }
  End user loop
  M = M – {ni} for all i ∈ K -Remove selected subcarriers from available subcarriers
}
End while loop
```

Algorithm 2

```
While the available subcarrier, M is not equal to 0
{
  Loop through all the users
  {
    User k selects highest h'k,n from the available subcarriers, M
    M = M – {n}  -Remove selected subcarrier from available subcarriers
  }
  End user loop
}
End while loop
```

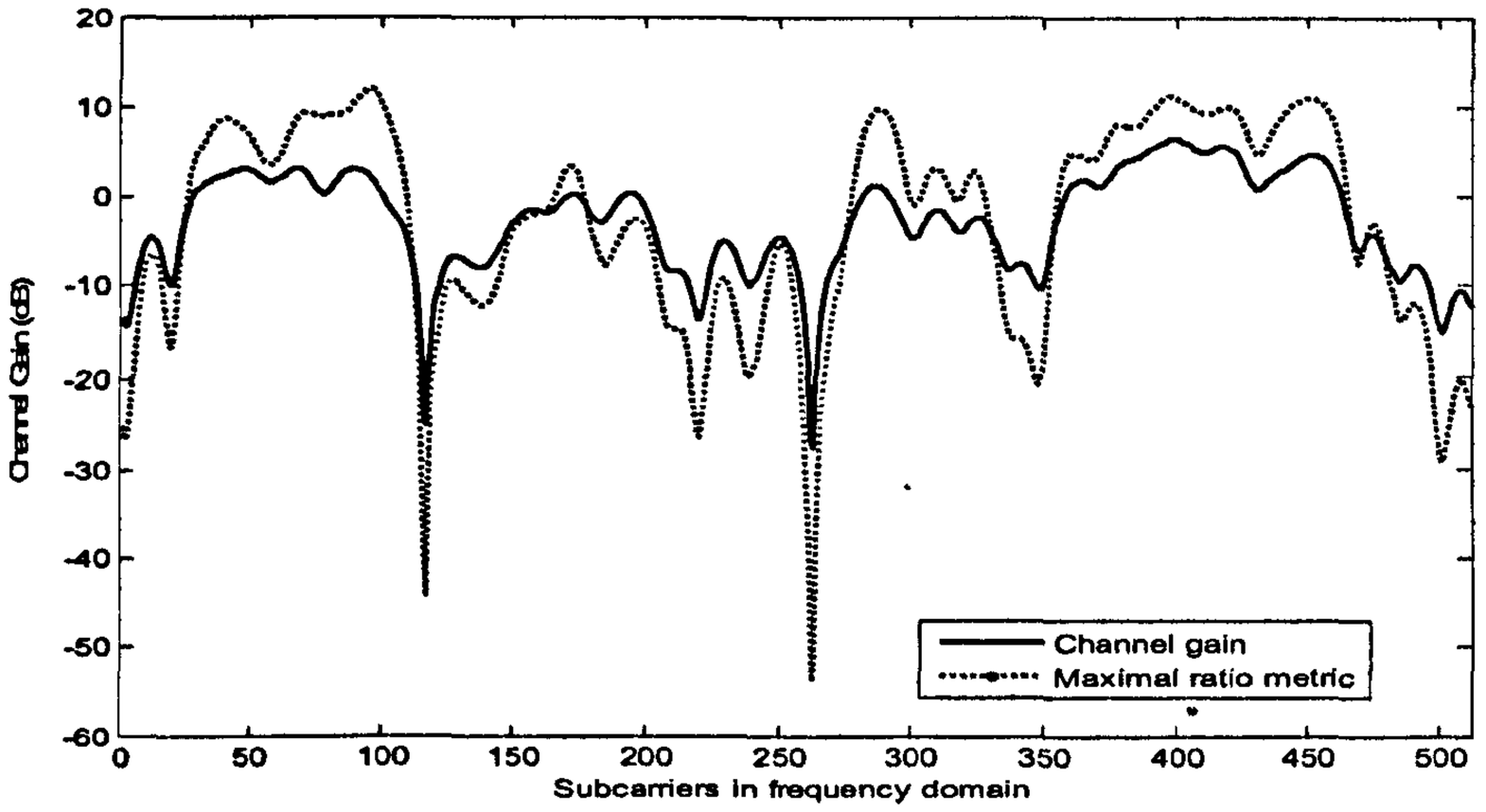

Figure 5-1: Maximal Ratio Weighted metric

An example of how an allocation based on the MRW metric outperforms the conventional allocation based on channel gain is shown in Figure 5-2 and Figure 5-3. For better illustration purposes, only a section of the subcarriers are shown. According to the conventional allocation strategies based on channel gain, a dynamic resource allocation algorithm will select the subcarriers as shown (by the arrow) in Figure 5-2. User 1 will always select its best channel, but will ignore the fact that other users might have better channel gain than user 1. Allocation based solely on channel gain would not maximise the overall gain of the system as the allocation does not take into the account other users into the selection process. Based on the maximal ratio weighted metric, user 2 will be given higher priority to select those subcarriers and thus achieving better performance overall (shown by the arrow in Figure 5-3).

Without the need for sort and swap iterations between the users, the complexity of the algorithm can be greatly reduced without affecting the performance. The computational complexity order of the algorithm is still $K+(S-1)^* O(N \log N)$ although slightly increased by trivial calculation of the metric. The calculation of the metric can be done with 2 nested *for* loops. Each $h'_{k,n}$ involves a division and a multiplication where $\sum_{k}^{K} | h_{k,n} |^2$ only need to be calculated once for each resource unit.

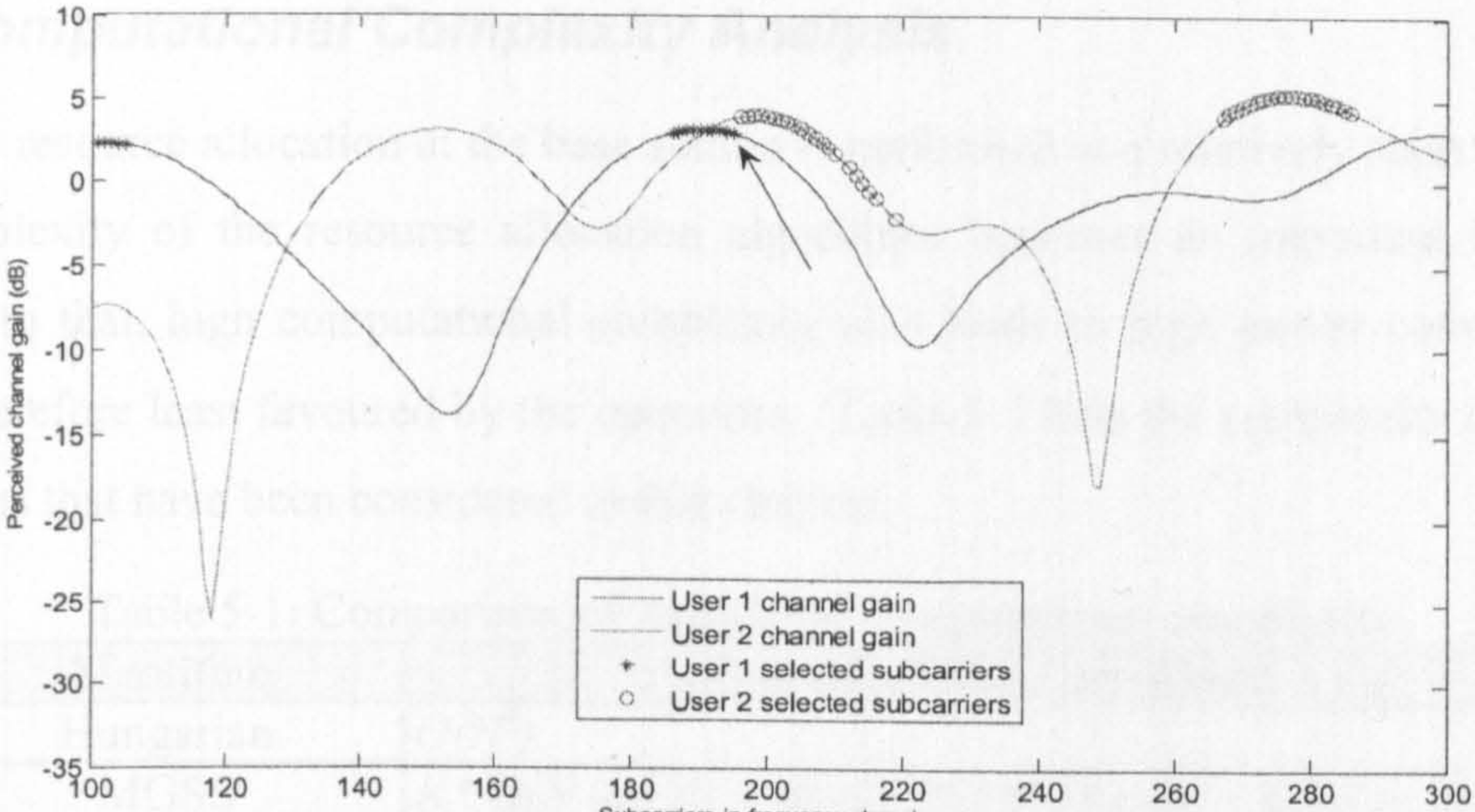

Figure 5-2: Subcarrier selection based on channel gain

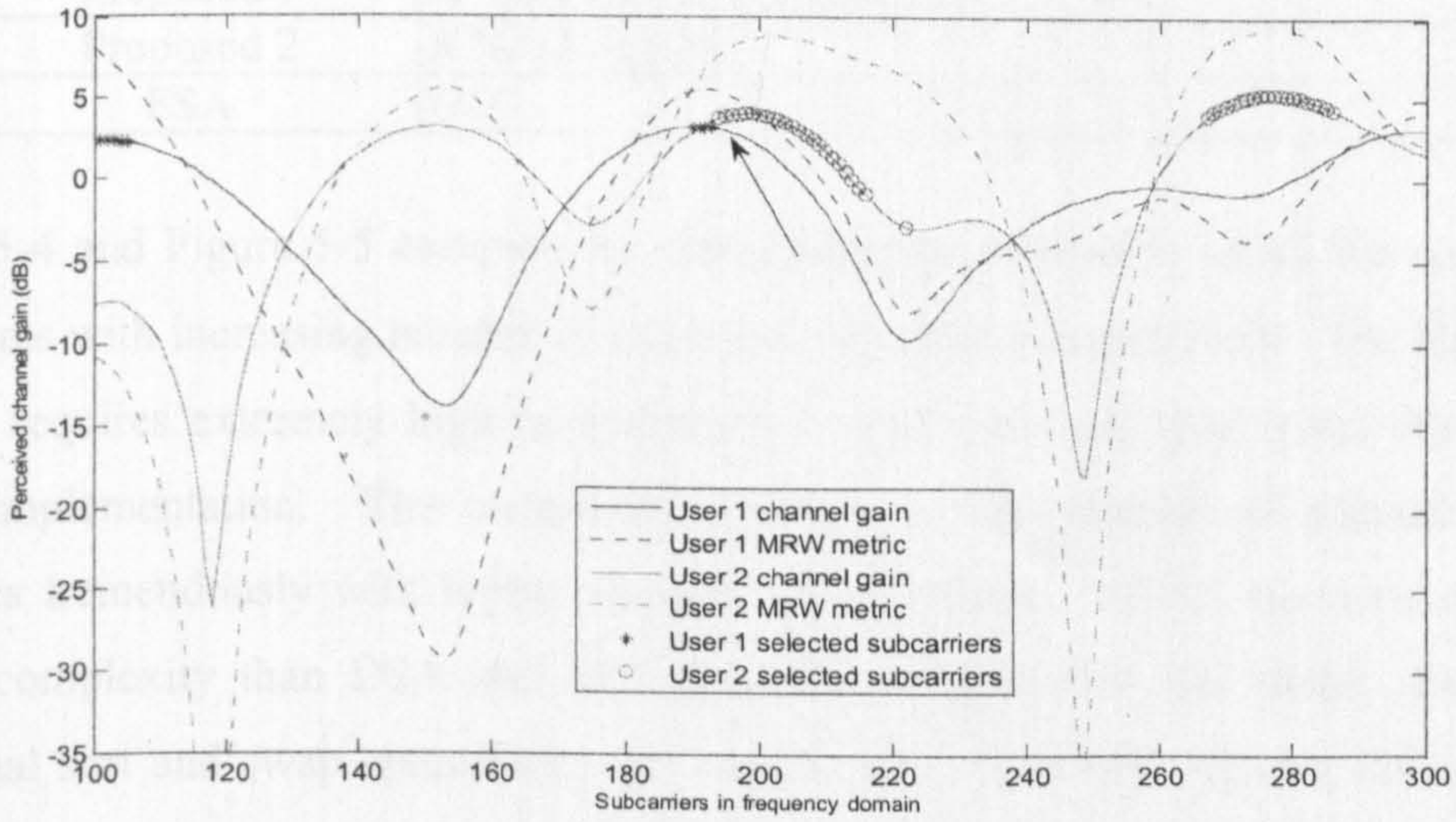

Figure 5-3: Subcarrier selection based on MRW metric

5.3.4 Fixed Subcarrier Allocation (FSA)

A fixed set of subcarriers is pre-determined for all users in FSA. FSA does not exploit the inherent diversity that exists in a multiuser OFDMA system since no dynamic allocation is performed. FSA does not increase the allocation complexity as no added computational power is needed at the base station to allocate the subcarriers. In addition, no extra signalling overhead is required. Here, it is assumed that subcarriers are distributed evenly across the frequency domain.

5.4 Computational Complexity Analysis

Since the resource allocation at the base station is performed at a relatively short interval, the complexity of the resource allocation algorithms becomes an important issue. In addition to that, high computational complexity also leads to high power consumption and is therefore least favoured by the operators. Table 5-1 lists the complexity of all the algorithms that have been considered in this chapter.

Table 5-1: Comparison of Algorithm computational complexity

Algorithm	Computational Complexity
Hungarian	$O(N^4)$
MGSS	$K^* O(N \log N) + (K-1)^2 * C^* (3*O(S) + O(S \log S))$
DSA	$K*O(N \log N) + (S-1)*O((K \log (K))$
Proposed 1	$K*O(N \log N) + 2*N*O(1)$
Proposed 2	$K*O(N \log N)$
FSA	$O(1)$

Figure 5-4 and Figure 5-5 compare the computational complexity of all the considered algorithms with increasing number of users and subcarriers respectively. The Hungarian method requires extremely high computational complexity and thus is not feasible for actual implementation. The complexity depends on the number of subcarriers and increases tremendously with higher number of subcarriers. MGSS has a considerably higher complexity than DSA and the algorithms proposed in this thesis, due to the additional sort and swap operations. As can be seen from both figures, DSA and the proposed algorithms maintain the lowest level of computational complexity with increasing number of users or subcarriers.

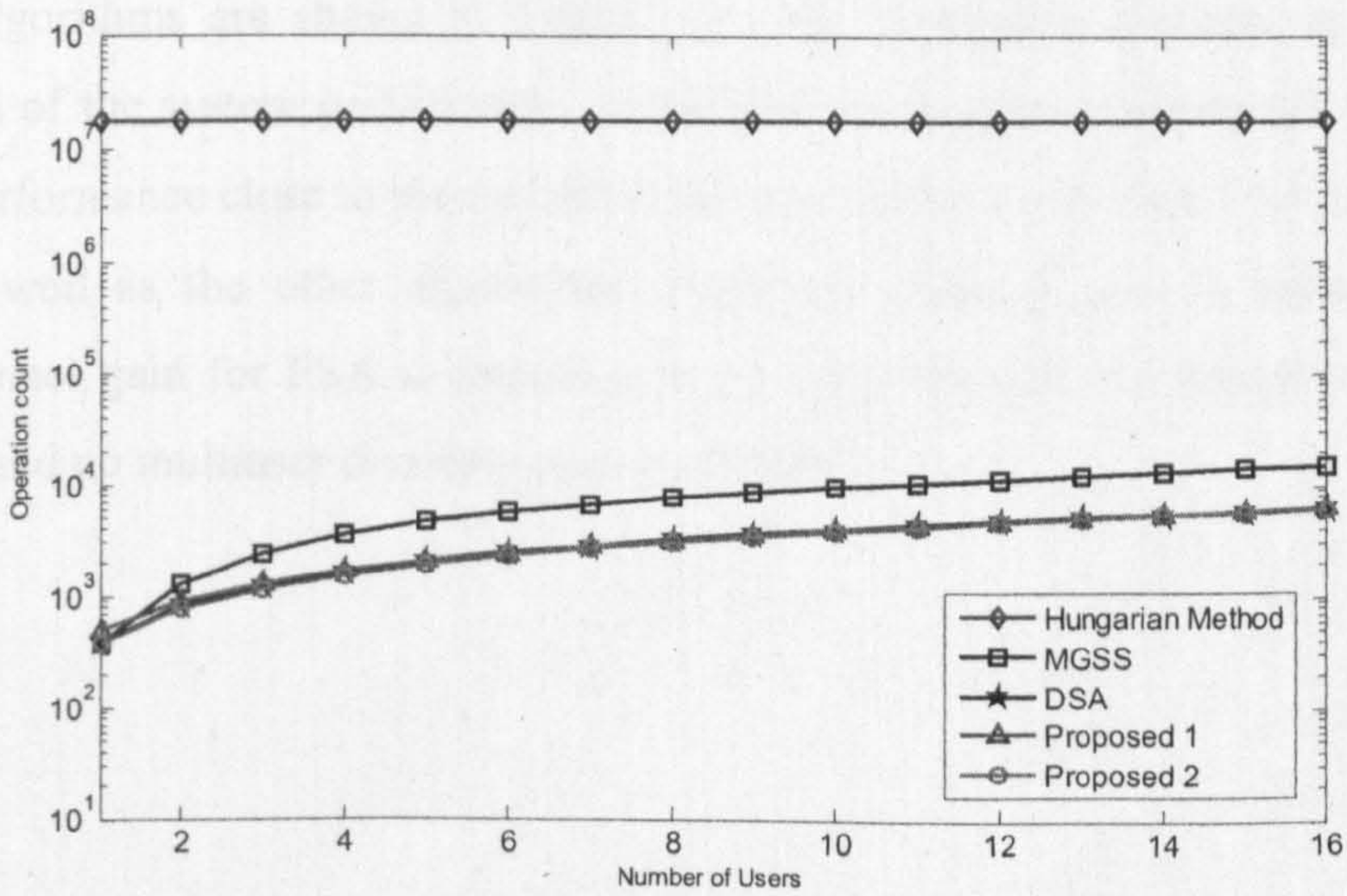

Figure 5-4: Computational complexity comparison for various algorithms with increasing number of users and a fixed number of subcarriers, $N = 64$

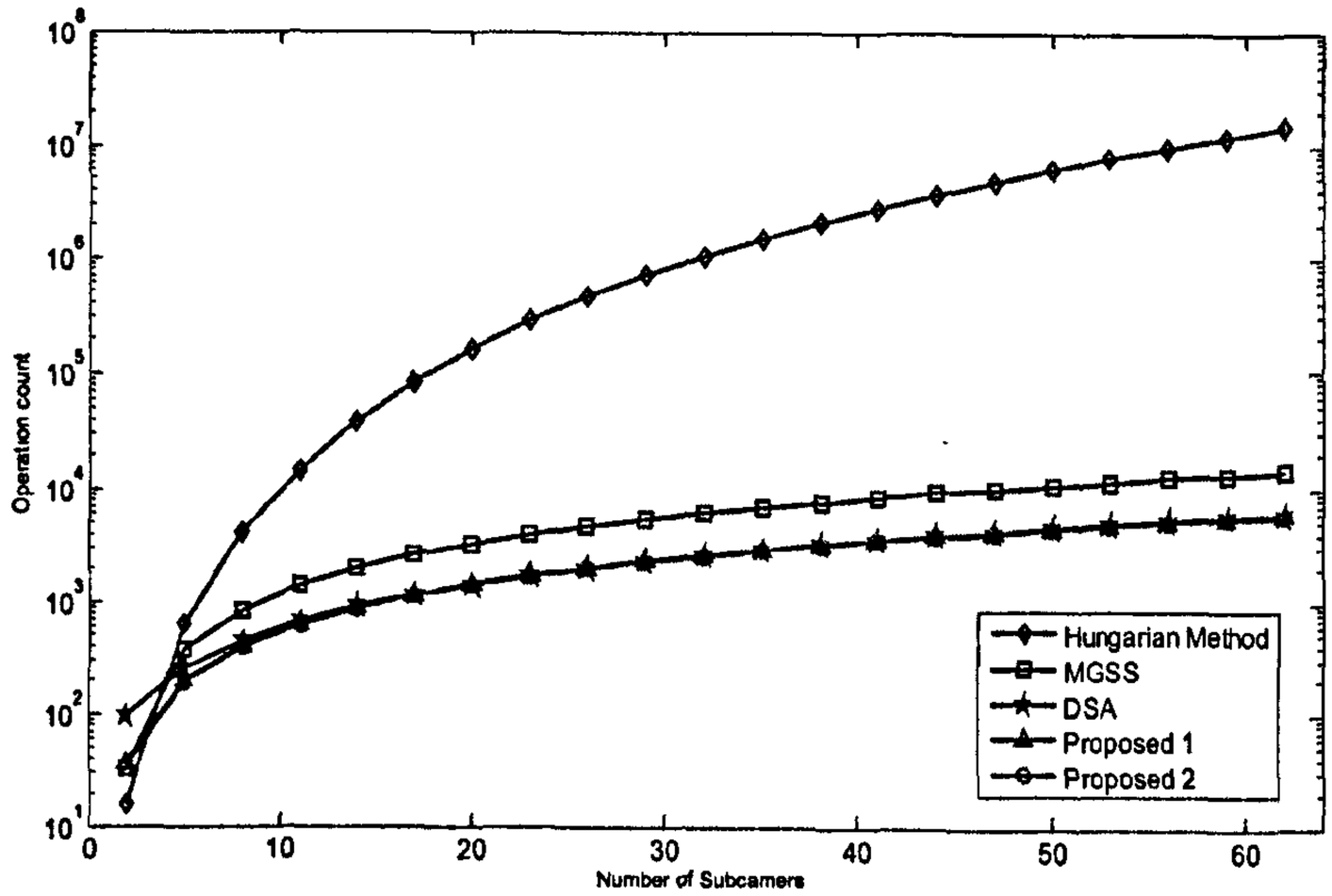

Figure 5-5: Computational complexity comparison for various algorithms with increasing number of subcarriers and a fixed number of users, K =16

5.5 Error Performance Analysis

In this section, a detailed analysis on the performance of frequency domain resource allocation algorithms is conducted in the downlink of LTE in urban macro scenario. The same simulation parameters from the previous chapters are assumed and the number of users, K=10 is assumed unless otherwise stated. As mentioned previously, allocation is based on a subchannel (PRB) basis in LTE.

First of all, the normalized average channel gains of the allocated subchannels for all the users are simulated. The average channel gains of all the users using different resource allocation algorithms are shown in Figure 5-6. The Hungarian method represents the upper bound of the system performance while both the proposed algorithms and MGSS achieve a performance close to the optimum. DSA performs better than FSA but does not perform as well as the other algorithms. Since the channel gain is normalized, the average channel gain for FSA is expected to be unity because the subcarriers are pre-determined and no multiuser diversity gain is obtained.

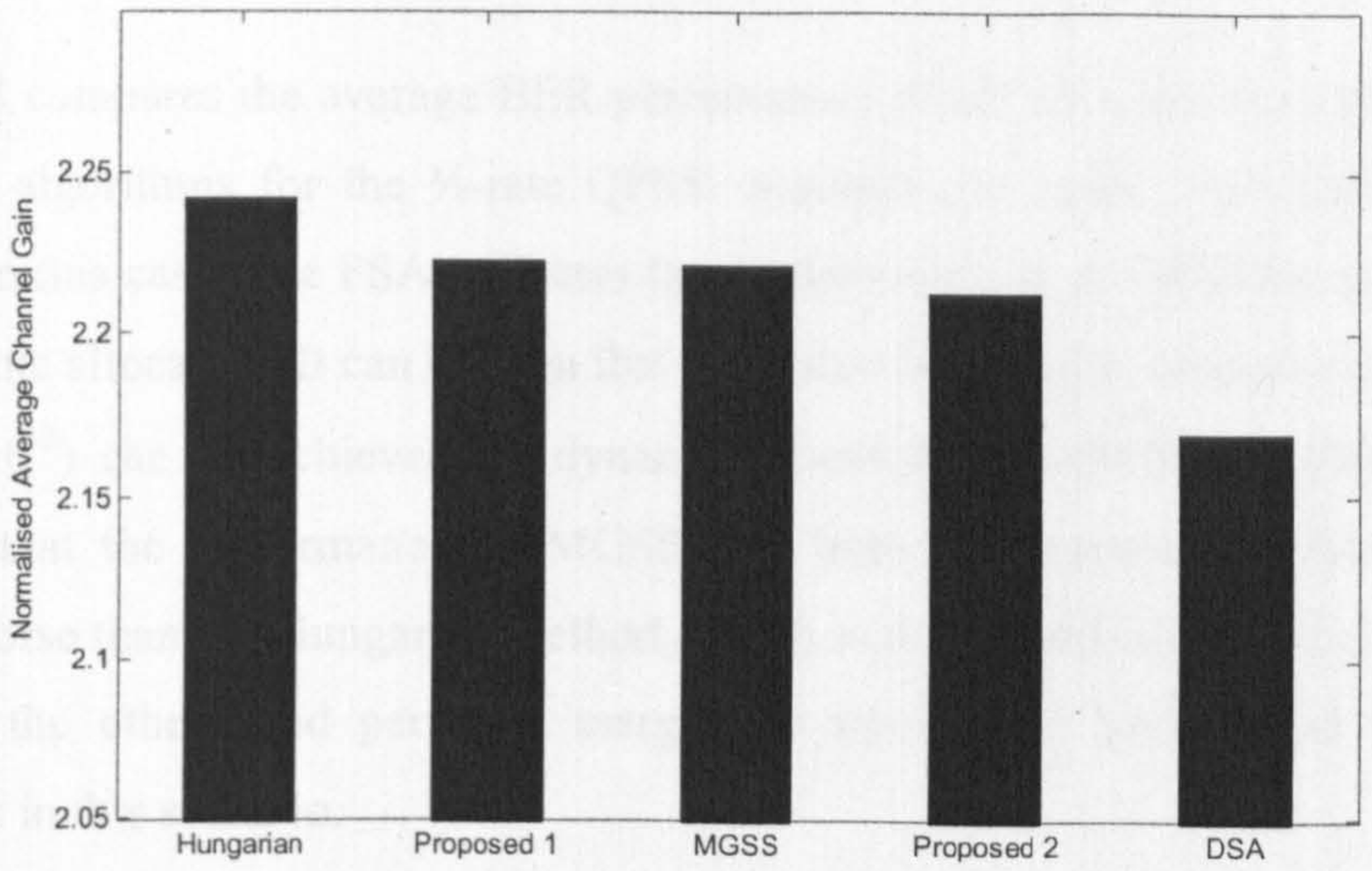

Figure 5-6: Normalized average channel gains for various resource allocation algorithms

Figure 5-7 shows the average channels gain of the allocated sub-channels as a function of increasing number of users. A 10 MHz system bandwidth is considered and 50 sub-channels are available for allocation at each allocation instance. The resource hungry Hungarian method once again shows the upper bound of the system. As the number of users increases, the proposed algorithm 1 outperforms all other sub-optimal algorithms. The proposed algorithm 2 performs better than the DSA algorithm, but is inferior to the MGSS algorithm. Thus it can be seen that, as the number of users in the system increases, the proposed algorithms which are based on the MRW metric can perform close to the optimum, especially the proposed algorithm 1.

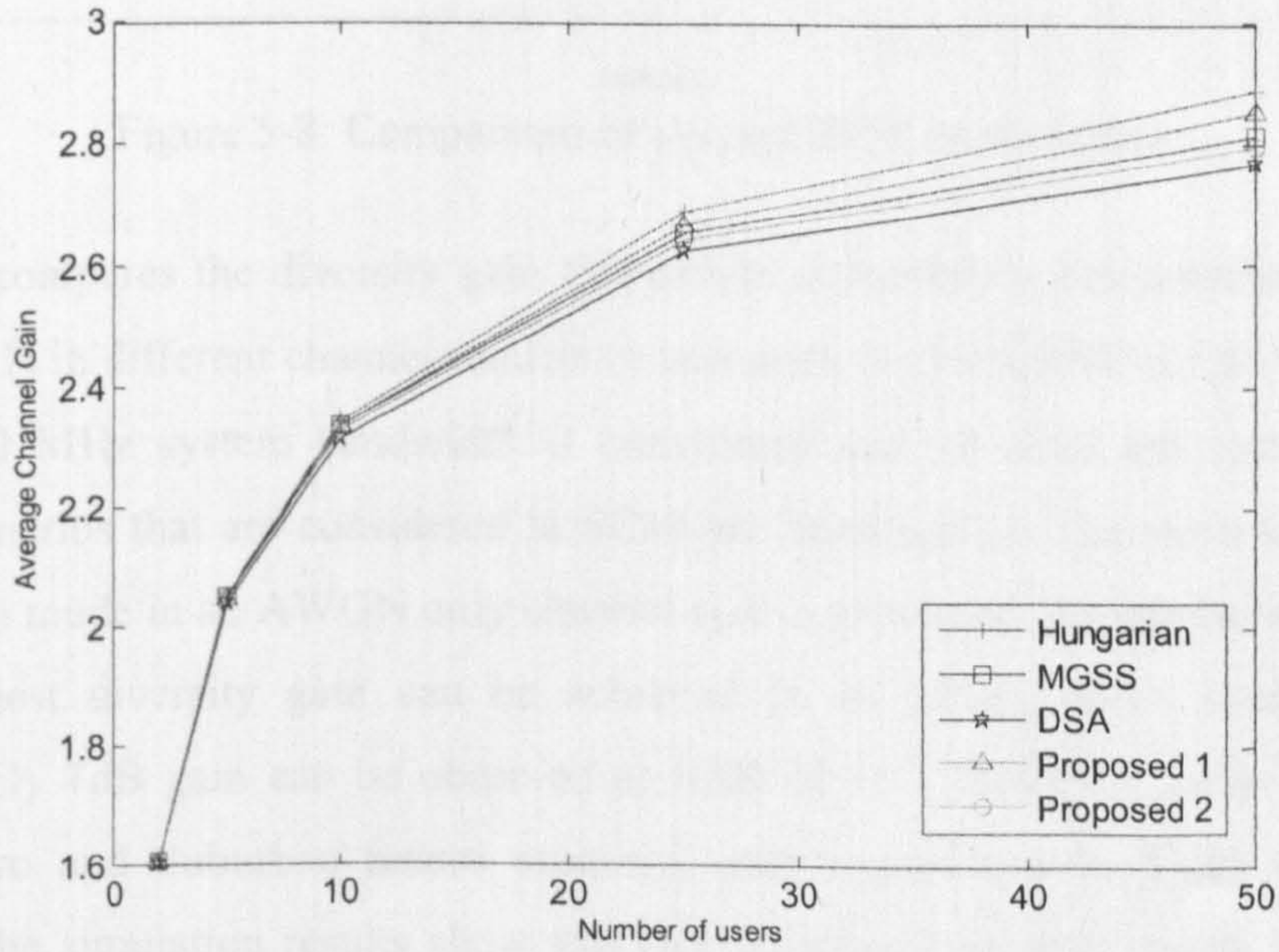

Figure 5-7: Normalized average channel gains for various resource allocation algorithms as a function of number of users

Figure 5-8 compares the average BER performance of all the users for various resource allocation algorithms for the ½-rate QPSK transmission mode. Full CQI feedback is assumed in this case. The FSA indicates the performance of an OFDMA system without any dynamic allocation. It can be seen that a substantial gain (up to approximately 6dB at BER of 10^{-3}) can be achieved by dynamic resource allocation algorithms. It can be observed that the performance of MGSS and both the proposed algorithms are just slightly worse than the Hungarian method, which is the upper bound of the performance. DSA, on the other hand performs marginally worse than MGSS and the proposed algorithms in this scenario.

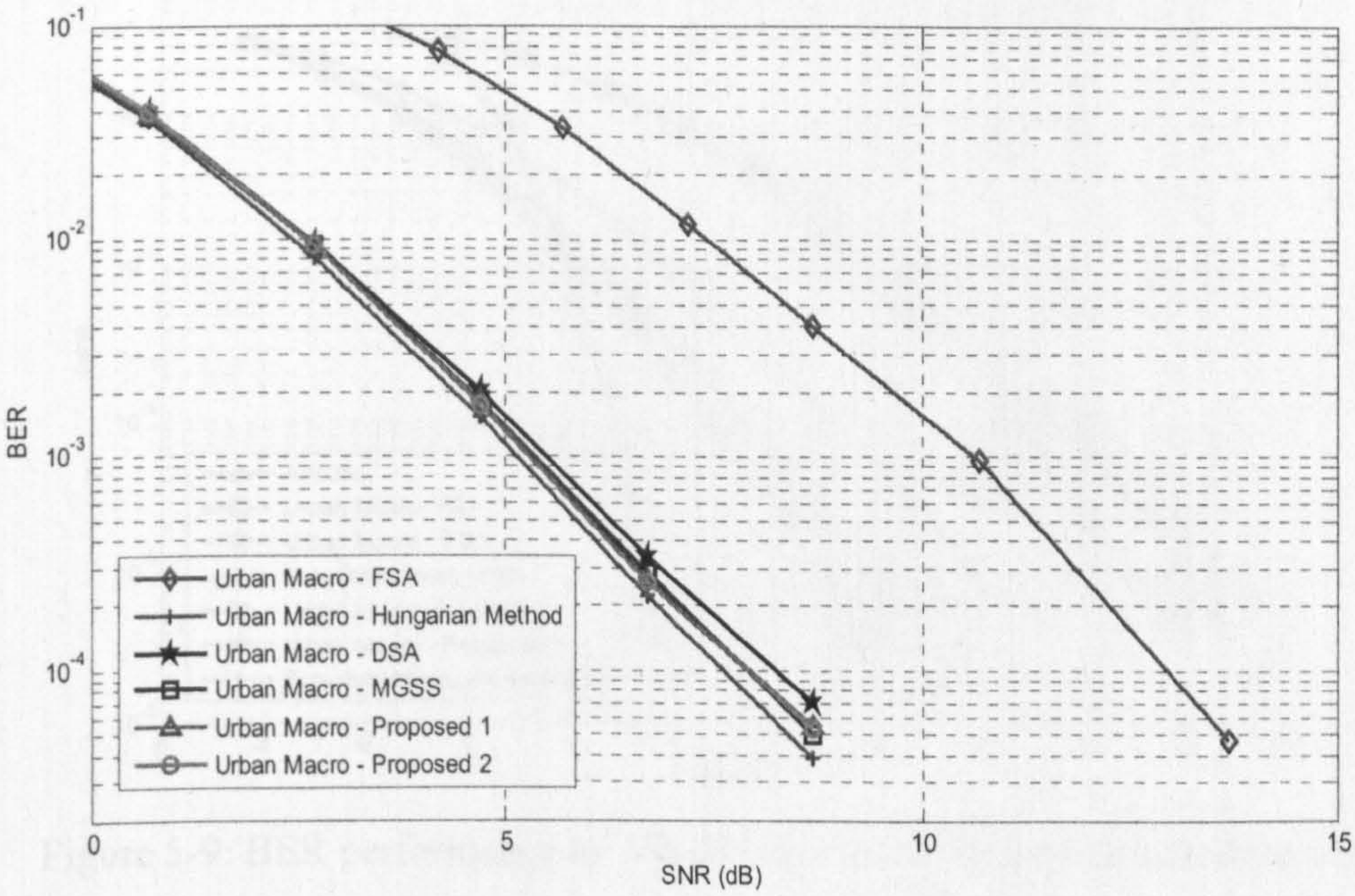

Figure 5-8: Comparison of average BER performance

Figure 5-9 compares the diversity gain that can be achieved by the proposed algorithm (Algorithm 1) in different channel models or scenarios for the QPSK ½ rate transmission mode. A 10 MHz system bandwidth is considered and 10 users are assumed. Three channel scenarios that are considered in SCM are investigated. The performance of the transmission mode in an AWGN only channel is also presented. As can be seen from the figure, highest diversity gain can be achieved in an Urban micro scenario, where approximately 7dB gain can be observed at BER of 10^{-4}. However, in the case of the Urban macro and Suburban macro scenario, only approximately 5 dB gain can be achieved. The simulation results show that rich frequency diversity exists in the Urban micro scenario and thus highest multiuser diversity can be achieved in this scenario.

It is also interesting to see that at low SNRs, the BER performance that can be achieved by the proposed algorithm in multipath fading channel can even exceed the performance in the AWGN. It thus shows the significance of resource allocation and how a system can actually exploit the fading to achieve a better performance than an AWGN only system. By dynamically selecting the best available subchannels, an increased average SNR relative to AWGN can be observed. However, it should be noted that the X-axis label SNR refers to the signal to noise ratio at the receiver for the case of an AWGN or FSA scenario. The increased average SNR that can be perceived by dynamic allocation is not reflected and thus it justifies the better than AWGN performance.

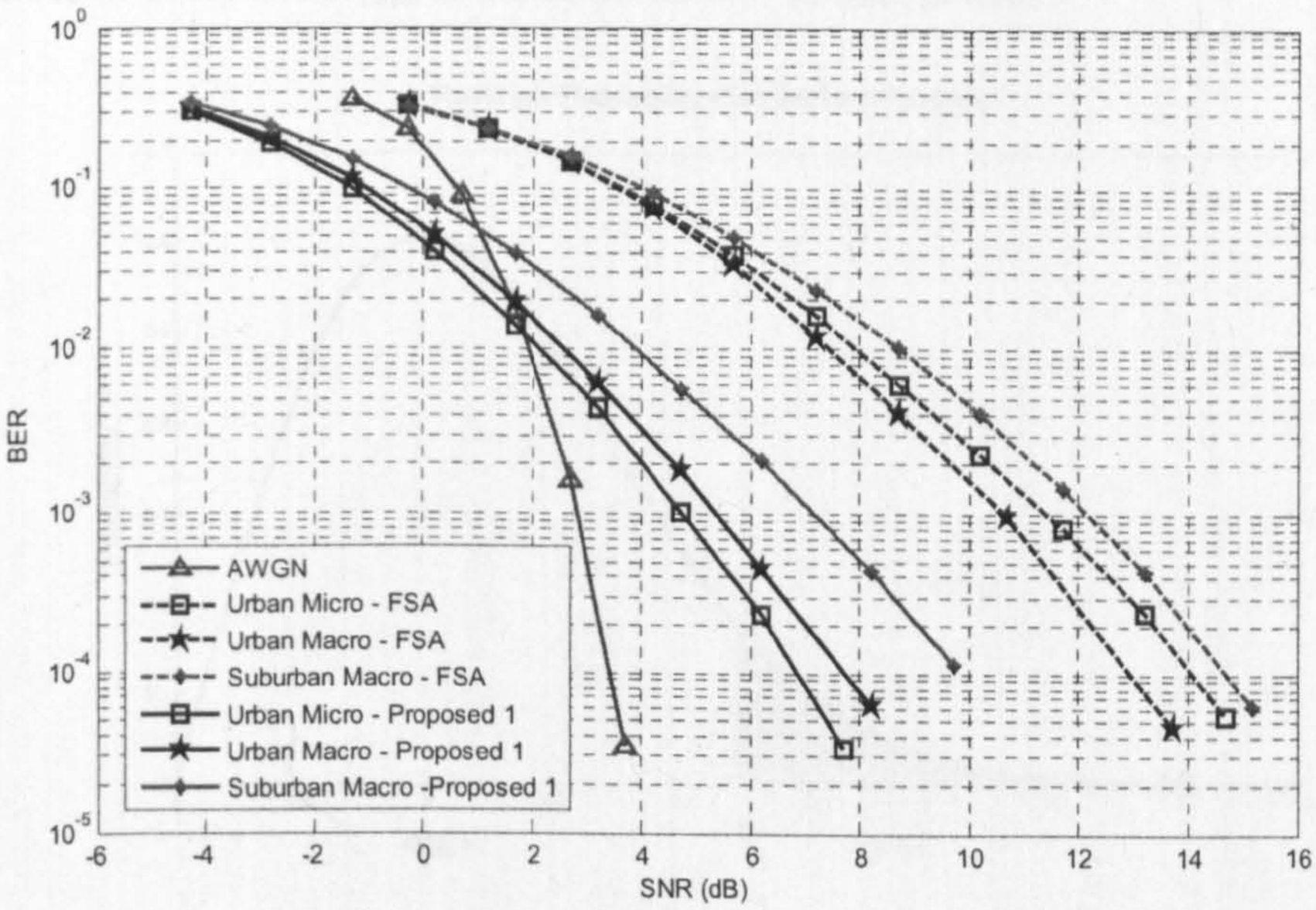

Figure 5-9: BER performance in AWGN and for different channel scenarios

5.6 Performance Analysis with limited feedback

Previous investigations were made with the assumption that the channel gains of the resource units were perfectly available at the transmitter. In order to efficiently feedback to the transmitter, the channel gains need to be quantised. While higher quantisation gives higher accuracy of the channel, the overhead caused by the feedback becomes prohibitive when the number of resource units is high. Therefore, a 1 bit feedback scheme is employed in the performance analysis, where a mobile terminal will feedback a bit per resource unit to inform the transmitter whether or not the channel gain falls above a threshold. If the channel gain is above the threshold, the resource unit will be prioritised for scheduling. When 1 bit feedback is used, determining the optimal

threshold becomes a challenging task. If the threshold is set too high, only a small number of subcarriers will fall above the threshold and thus insufficient subcarriers will be available for scheduling. On the other hand, if the threshold is too low, subcarriers with relatively weak performance will be scheduled for transmission.

In this section, it would be desirable to develop an analytical model to compute the optimal threshold in the 1 bit feedback scheme. The optimal threshold depends on the channel fading characteristic, number of users and the fairness constraint [11][13]. In this analytical model, it is assumed that the channels are Rayleigh distributed with standard deviation (σ) of 1 and the resource units are shared equally among all the users. K is the total number of users and N_{Total} is the total number of subcarriers.

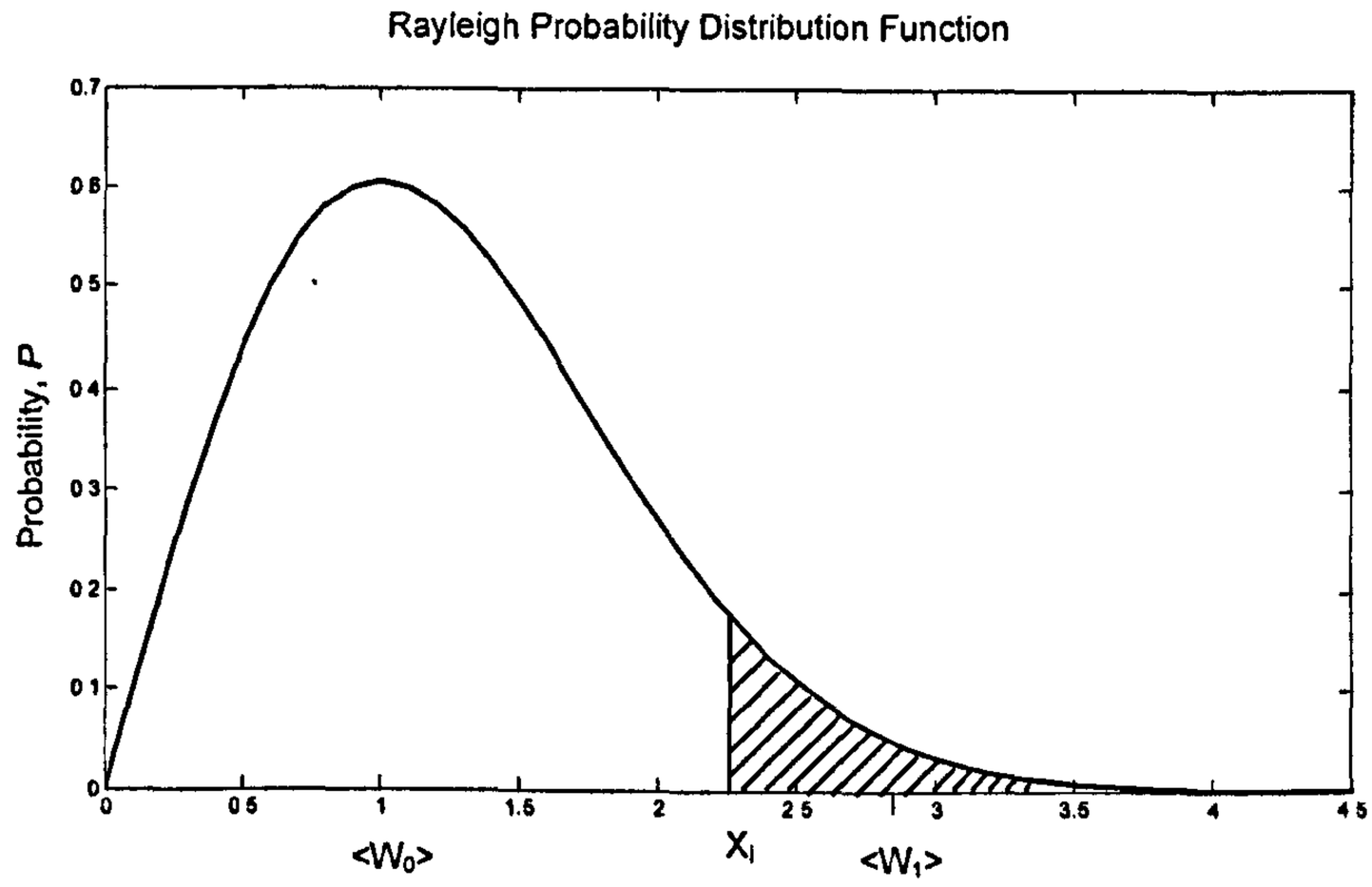

Figure 5-10: Rayleigh Probability Distribution Function

The Rayleigh probability density function is:

$$f(x) = \frac{x \exp(-\frac{x^2}{2\sigma^2})}{\sigma^2} \qquad (5\text{-}6)$$

for $x \in [0, \infty)$

Given a threshold X_i, the probability of a subcarrier that is above the threshold is given by:

$$P_a = \int_{X_i}^{\infty} \frac{x \exp(-\frac{x^2}{2\sigma^2})}{\sigma^2} dx$$

$$= \left[-\exp(-\frac{x^2}{2\sigma^2}) \right]_{X_i}^{\infty}$$

$$= \exp(-\frac{X_i^2}{2\sigma^2}) \tag{5-7}$$

Similarly, the probability of a subcarrier that is below the threshold X_i:

$$P_b = \left[-\exp(-\frac{x^2}{2\sigma^2}) \right]_{0}^{X_i}$$

$$= 1 - \exp(-\frac{X_i^2}{2\sigma^2}) \tag{5-8}$$

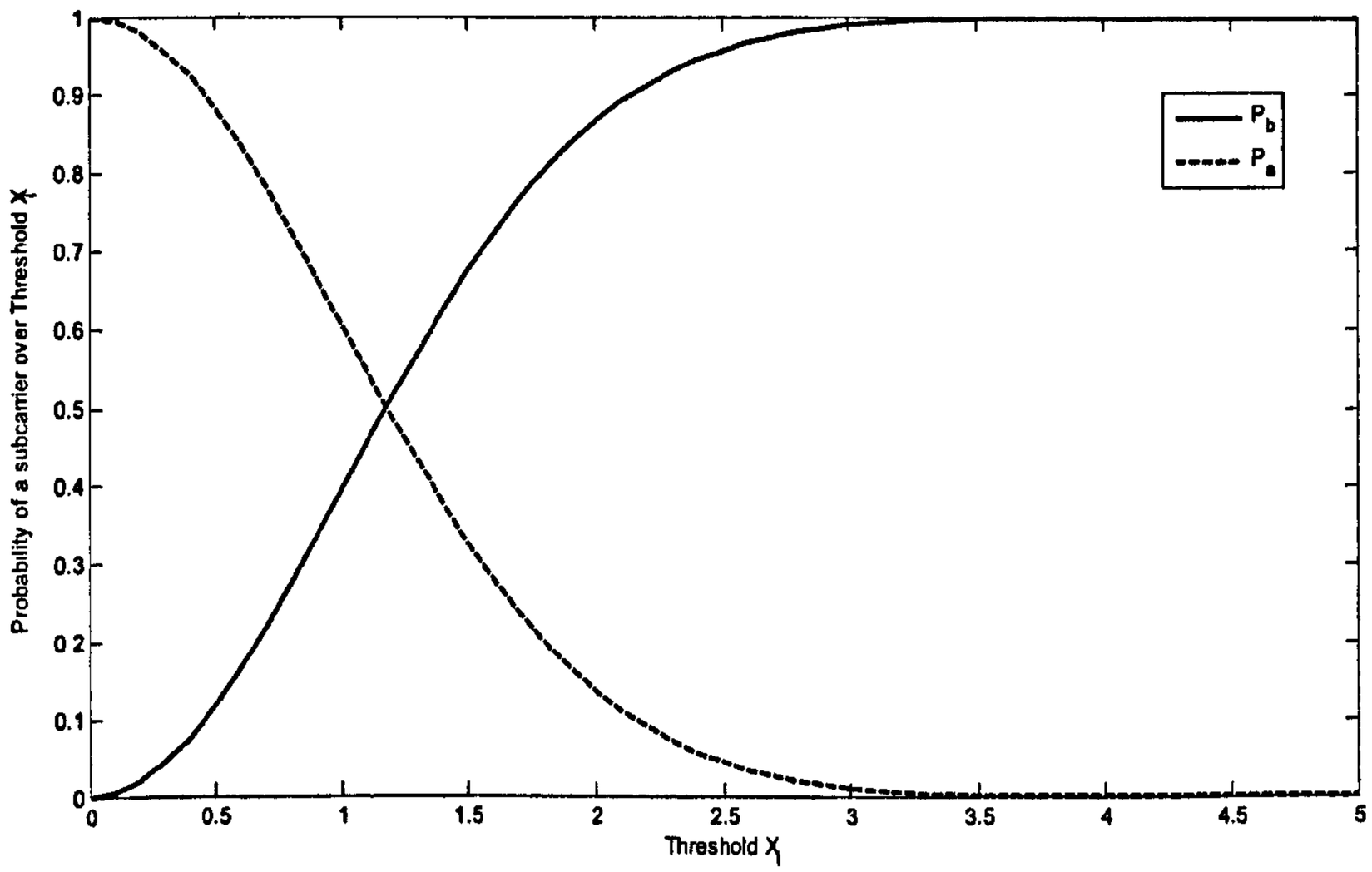

Figure 5-11: Probability of an arbitrary subcarrier that is above/below the threshold X_i

The expected value (or mean) of a continuous random variable X is the average value of all samples taken from X. To find the expected value, the infinitesimal probability of each real value in X's domain is multiplied by the value itself and summed. This can be easily represented by using an integral.

$$\langle X \rangle = \int_{-\infty}^{\infty} x f(x)\, dx \tag{5-9}$$

However, to find the expected value of a random variable X given that X is above the threshold X_i, the equation needs to be normalized by the its own probability density, which can be given as:

$$\langle X \rangle = \frac{\int_{X_i}^{\infty} x f(x)\, dx}{\int_{X_i}^{\infty} f(x)\, dx} \tag{5-10}$$

Thus, the expected channel gain of a subcarrier that is above the threshold is given by:

$$< X_a > = \frac{\int_{X_i}^{\infty} \frac{x^2 \exp(-\frac{x^2}{2\sigma^2})}{\sigma^2} dx}{P_1}$$

$$= \frac{\left[\sigma\sqrt{\frac{\pi}{2}} erf(\frac{x}{\sqrt{2}\sigma}) - e^{\frac{x^2}{2}} x\right]_{X_i}^{\infty}}{P_1}$$

$$= \frac{X_i \exp(-\frac{X_i^2}{2\sigma^2}) + \sqrt{\frac{\pi}{2}} - \sigma\sqrt{\frac{\pi}{2}} erf(\frac{X_i}{\sqrt{2}\sigma})}{P_1} \tag{5-11}$$

Similarly, the expected channel gain of a subcarrier that is below the threshold is given by:

$$< X_b >= \frac{\int_{0_i}^{X_i} \frac{x^2 \exp(-\frac{x^2}{2\sigma^2})}{\sigma^2} dx}{P_0}$$

$$= \frac{\left[\sigma\sqrt{\frac{\pi}{2}} erf(\frac{x}{\sqrt{2}\sigma}) - e^{\frac{x^2}{2\sigma^2}} x\right]_0^{X_i}}{P_0}$$

$$= \frac{\sigma\sqrt{\frac{\pi}{2}} erf(\frac{X_i}{\sqrt{2}\sigma}) - X_i \exp(-\frac{X_i^2}{2\sigma^2})}{P_0} \tag{5-12}$$

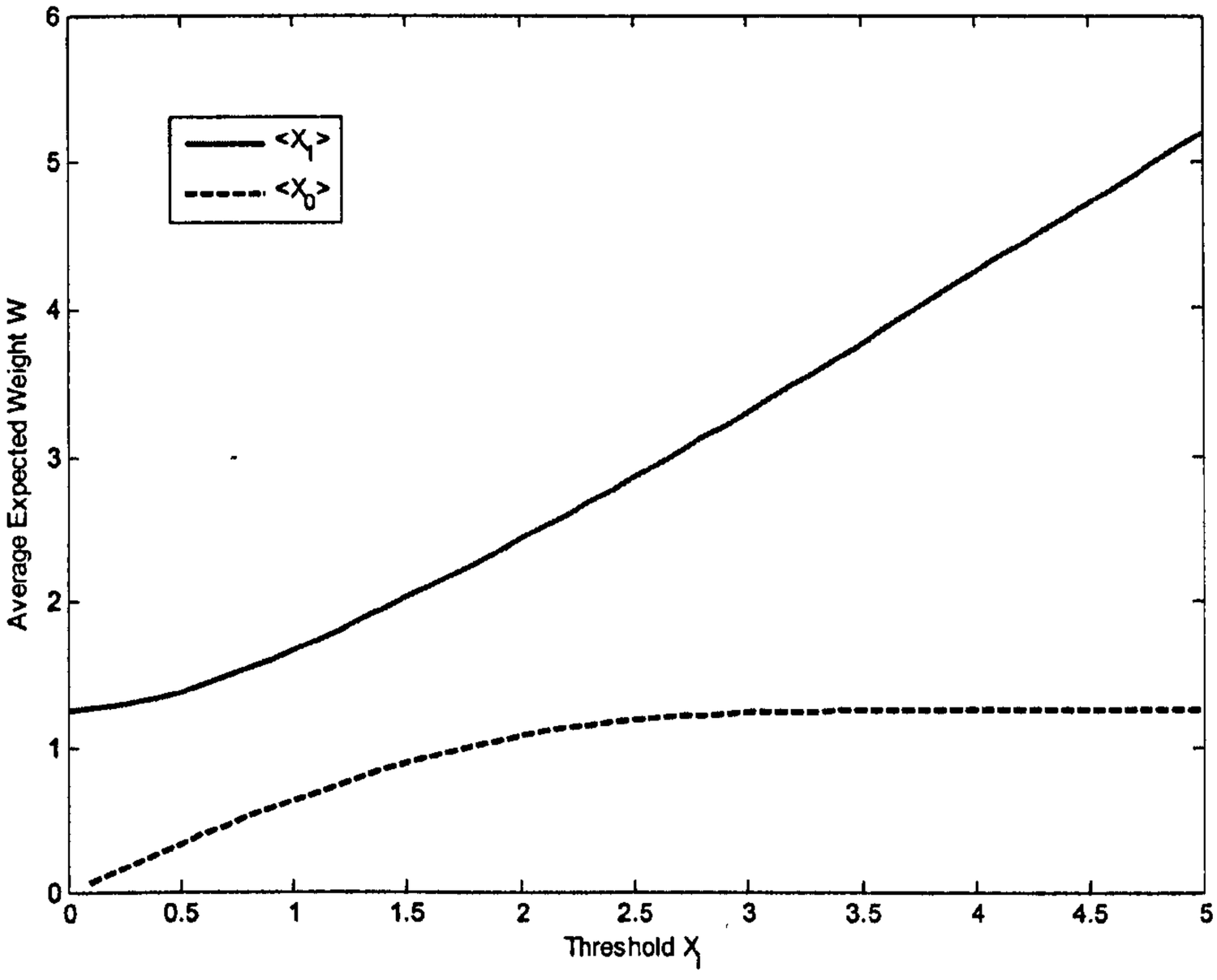

Figure 5-12: Expected channel gain for a subcarrier that is above/below the threshold X_i

Given the threshold X_i, the number of subcarrier that is above the threshold can be obtained by:

$$N_a = N_{Total} * P_a \tag{5-13}$$

The number of subcarrier that is below the threshold is simply:

$$N_b = N_{Total} - N_a \tag{5-14}$$

It is assumed that all the users are uniformly distributed across the cell and will experience different frequency selective fading patterns. Since the fading pattern is independent for each user, therefore the probability of a subcarrier falls above/below the threshold is independent from each other. Consequently, a product rule can be applied. Thus, the probability that no user has a subcarrier that is above the threshold can be calculated as:

$$P_{b'} = \prod_{k=1}^{K} \frac{N_{Total} - N_a}{N_{Total}} \tag{5-15}$$

For these subcarriers, it is assumed that the scheduler will pick the subcarrier randomly and these subcarriers will have an average weight of $\langle X_0 \rangle$. On the other hand, the

probability of at least one subcarrier being above the threshold for all the users K is given by:

$$P_{a'} = 1 - P_{b'} \tag{5-16}$$

For these subcarriers which are above the threshold, we assume the base station will optimally select these subcarriers and an average weight of $\langle X_1 \rangle$ is expected. Therefore, given the threshold X_i, the total average expected channel gain of the selected subcarriers is the summation of the expected channel gain of subcarriers below the threshold and above the threshold, which is given by:

$$< X_{Total} > = P_{a'} < X_a > + P_{b'} < X_b > \tag{5-17}$$

The achievable average gain can be illustrated in Figure 5-13. The red line indicates the average expected weight of subcarrier that is above the threshold, W_a and the blue line shows the average expected weight of subcarrier that is below the threshold, W_b. The black line shows the summation of both average weights and an optimum threshold can therefore be determined.

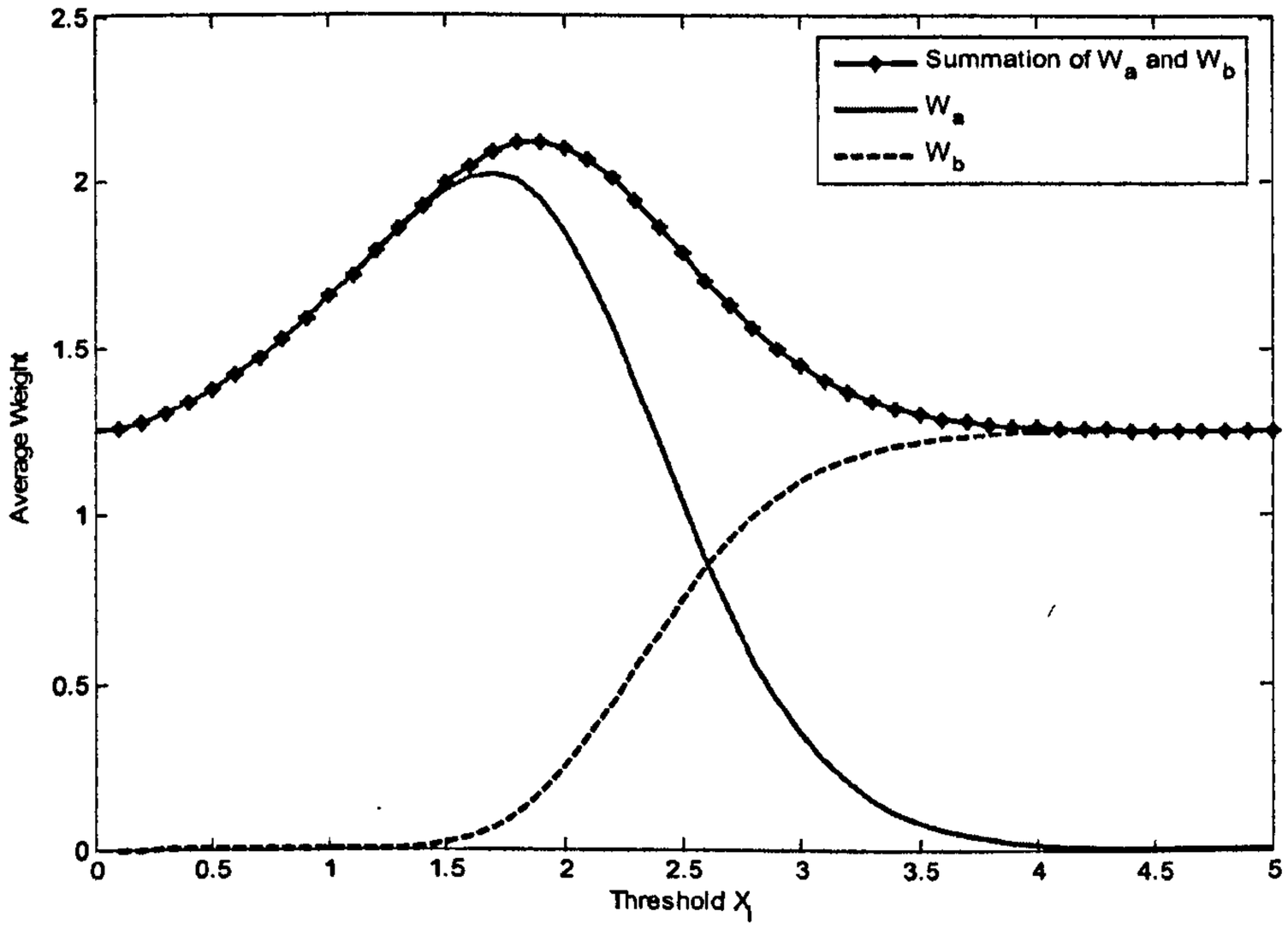

Figure 5-13: The analytical average channel gain

The average channel gain for different users in a system with different thresholds is computed analytically using equations 5-6 to 5-17 and compared with simulation results in Figure 5-14. In the simulation, the proposed algorithm 1 together with MRW metric is

employed. In the simulation, 50 i.i.d Rayleigh faded sub-channels are assumed. As it can been in Figure 5-14, the simulated results match very well with the analytical model, except when the number of users is large. This is due to the fact that in the analytical model, it is assumed that sub-channels tend to infinity. However in the simulation model, only 50 sub-channels are available and thus less diversity can be exploited. It is expected that when the number of sub-channels in the system is sufficiently large, the simulated results will match the analytical model. This is true for the case of 2 and 5 users, when the number of sub-channels is sufficiently larger than the number of users in the system.

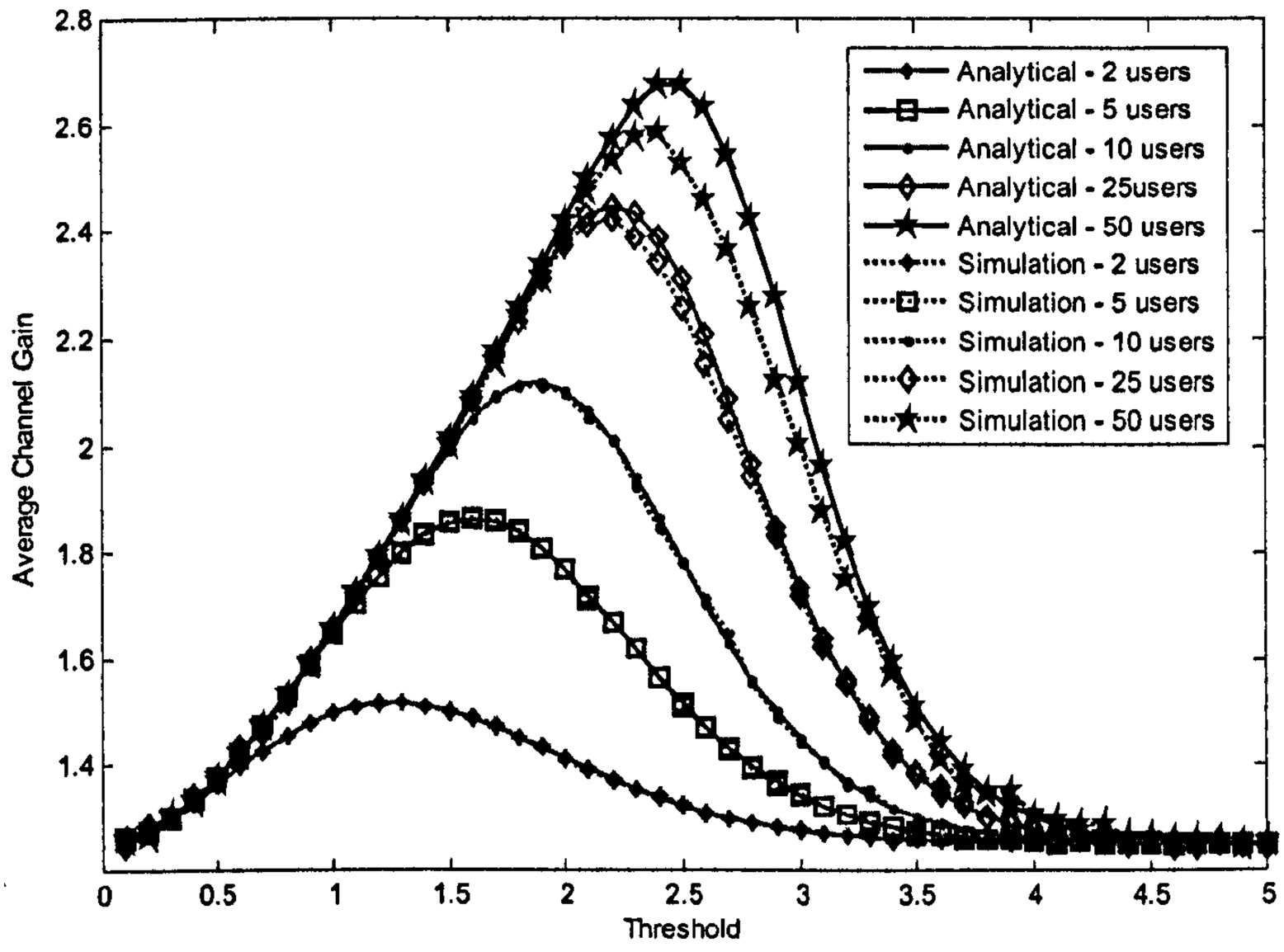

Figure 5-14: Optimal feedback threshold for different users

The optimal thresholds of 1 bit feedback scheme for the analytical model and the simulated results are shown in Figure 5-15. As it can be seen from the figure, when the number of users in a system increases, the optimal feedback threshold increases rapidly and it slowly saturates when the number of users gets large. Once again, the analytical model is verified by the simulations results. In particular, when the number of the sub-channels increases, e.g. from 50 to 100, the simulated results come close to the analytical results.

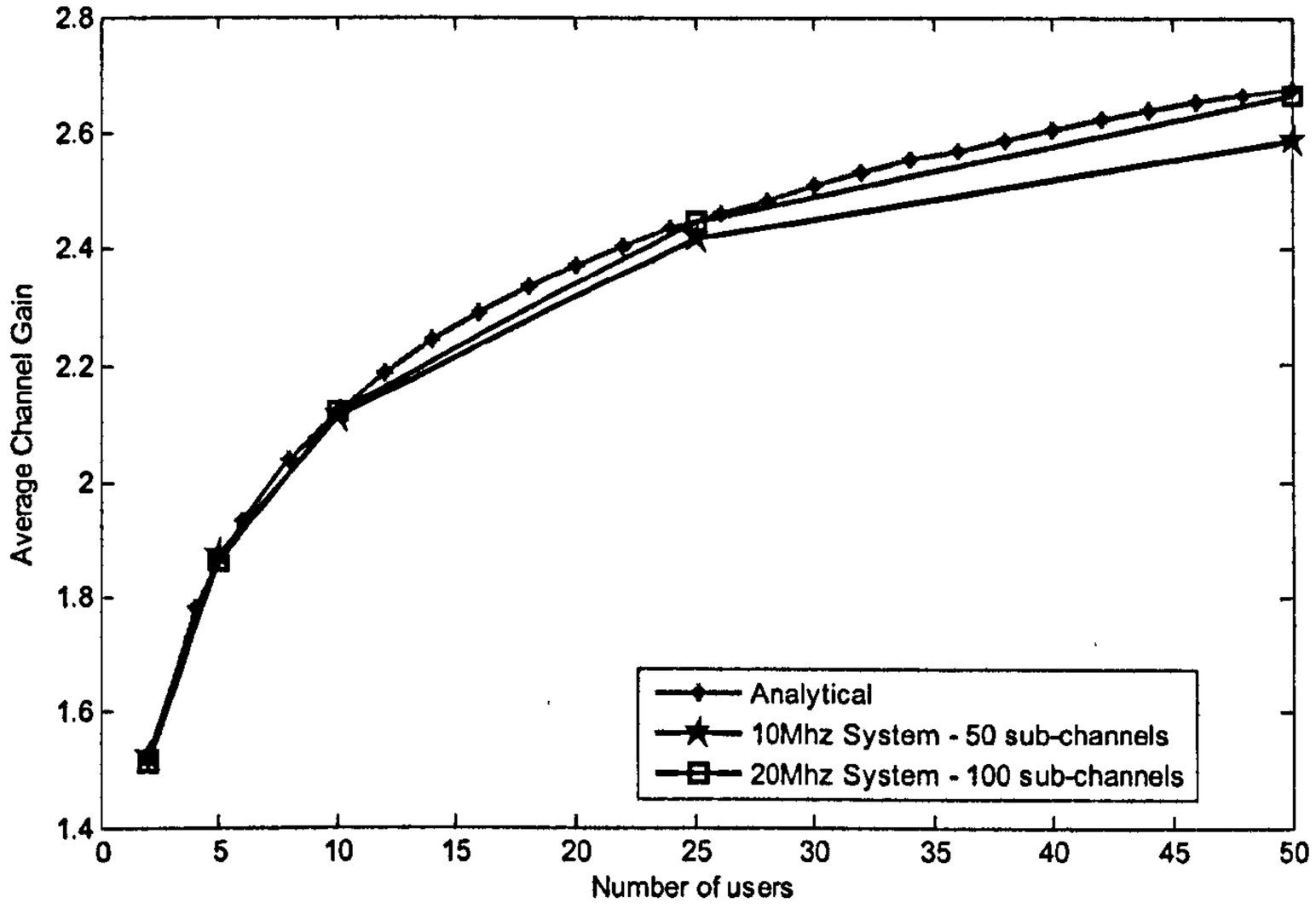

Figure 5-15: Optimal feedback threshold for increasing number of users

In addition to the i.i.d Rayleigh fading channels, some commonly deployed channel models, e.g. SCM channels models are investigated. Three scenarios are considered and the average channel gains using the proposed algorithm 1 are shown in Figure 5-16. As it can be observed from the figure, the Urban Micro scenario achieves the highest average channel gain compared to Urban Macro and Suburban Macro. These results tally with the results shown in Figure 5-9 as the Urban Micro achieved the highest multiuser gain compared to other two scenarios, due to the rich diversity in the frequency domain. Despite the difference in achievable channel gain, the optimal thresholds for all the channel models are approximately the same, which is about 1.8. Therefore, all the subchannels with normalised channel gain higher than 1.8 will be fedback as high priority. The same optimal threshold can be assumed for all the different scenarios.

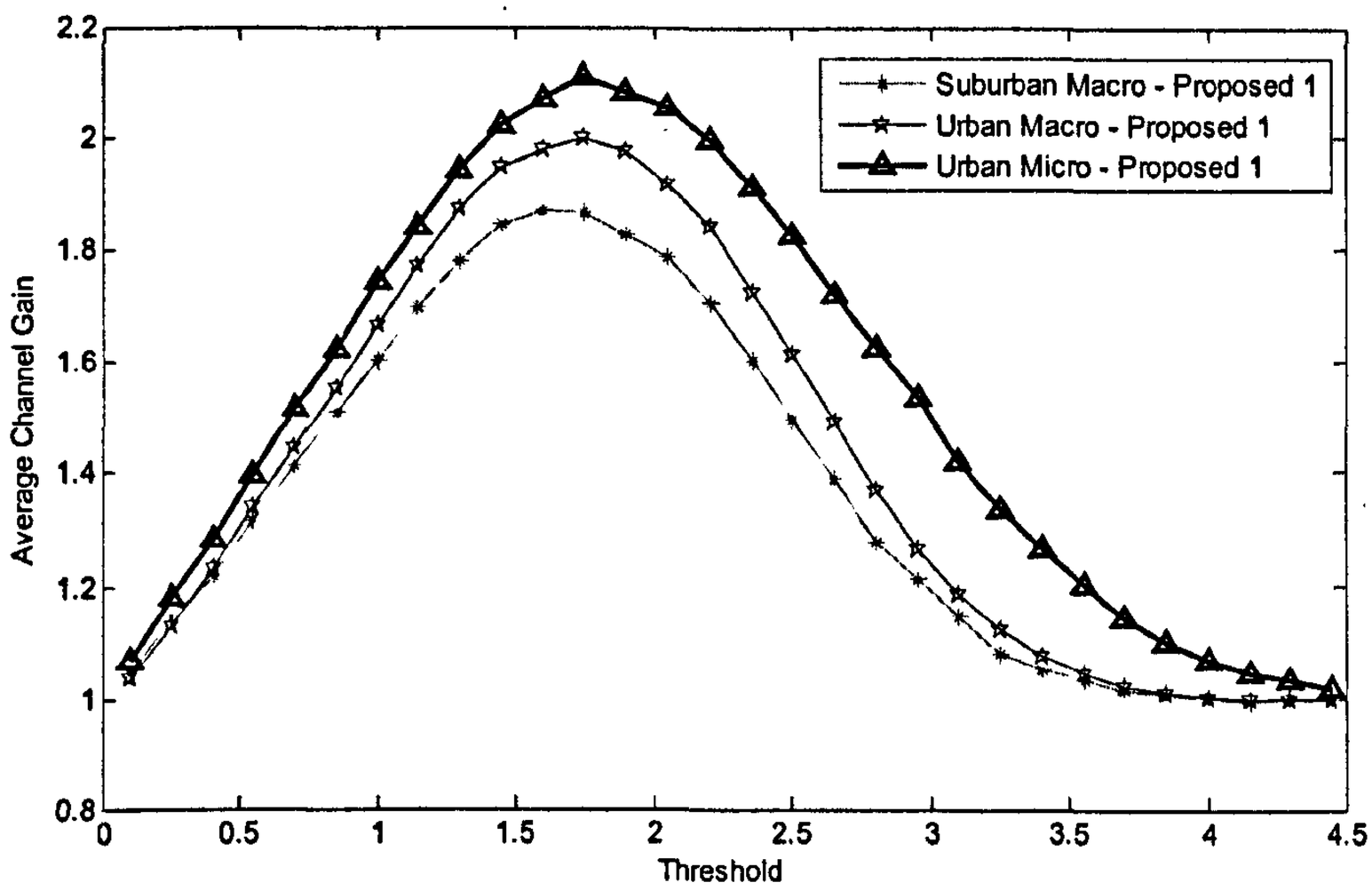

Figure 5-16: Optimal Threshold for Various Channels

In order to illustrate the MRW metric in the 1 bit feedback scenario, the metric is plotted in comparison to the conventional binary 1 bit feedback. As it can be seen in Figure 5-17, the MRW metric can create more level of priorities even with 1 bit feedback. By creating more priorities given the 1 bit quantization, a useful property can be observed. This is especially useful in dynamic allocation to assign resource more effectively. The MGSS scheme is unable to exploit full benefit from sort and swap iteration due to the 1 bit quantization. Swapping process is reduced significantly since if it only has binary information about channel quality. On the other hand, DSA algorithm is unable to maximize the throughput due to the limited information about the channel quality. In the contrary, the proposed algorithms work the MRW metric, which has more level of priorities. The performance comparison between different algorithms using 1 bit feedback scheme will be shown in the following section.

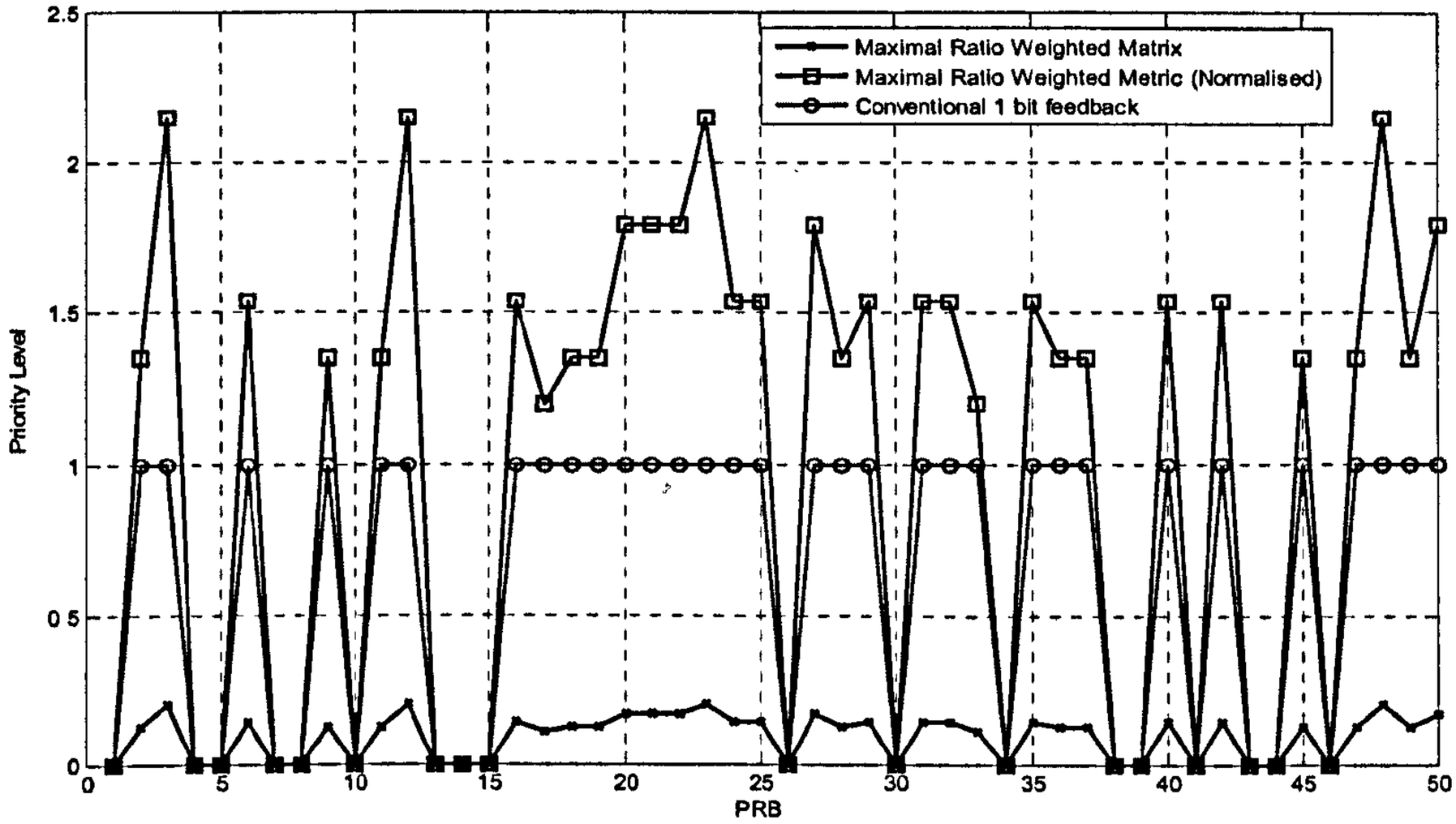

Figure 5-17: Maximal Ratio Weighted Metric for 1 bit feedback scheme

It is envisaged that some kind of performance trade off is expected due to the hugely reduced feedback overhead. Thus in this analysis, a comparison of the average channel gain between the 1 bit feedback scheme and the full CSI scheme for different resource allocation algorithms is shown in Figure 5-18. The Urban macro scenario is employed and 10 users are assumed in this case. To illustrate the optimal achievable channel gain, the Hungarian method with full CSI is presented. As can be seen from the figure, some significant loss in term of the average channel gain of the allocated sub-channels is shown. However, it is also shown that both the proposed algorithms outperform other sub-optimal algorithms, e.g. MGSS and DSA schemes.

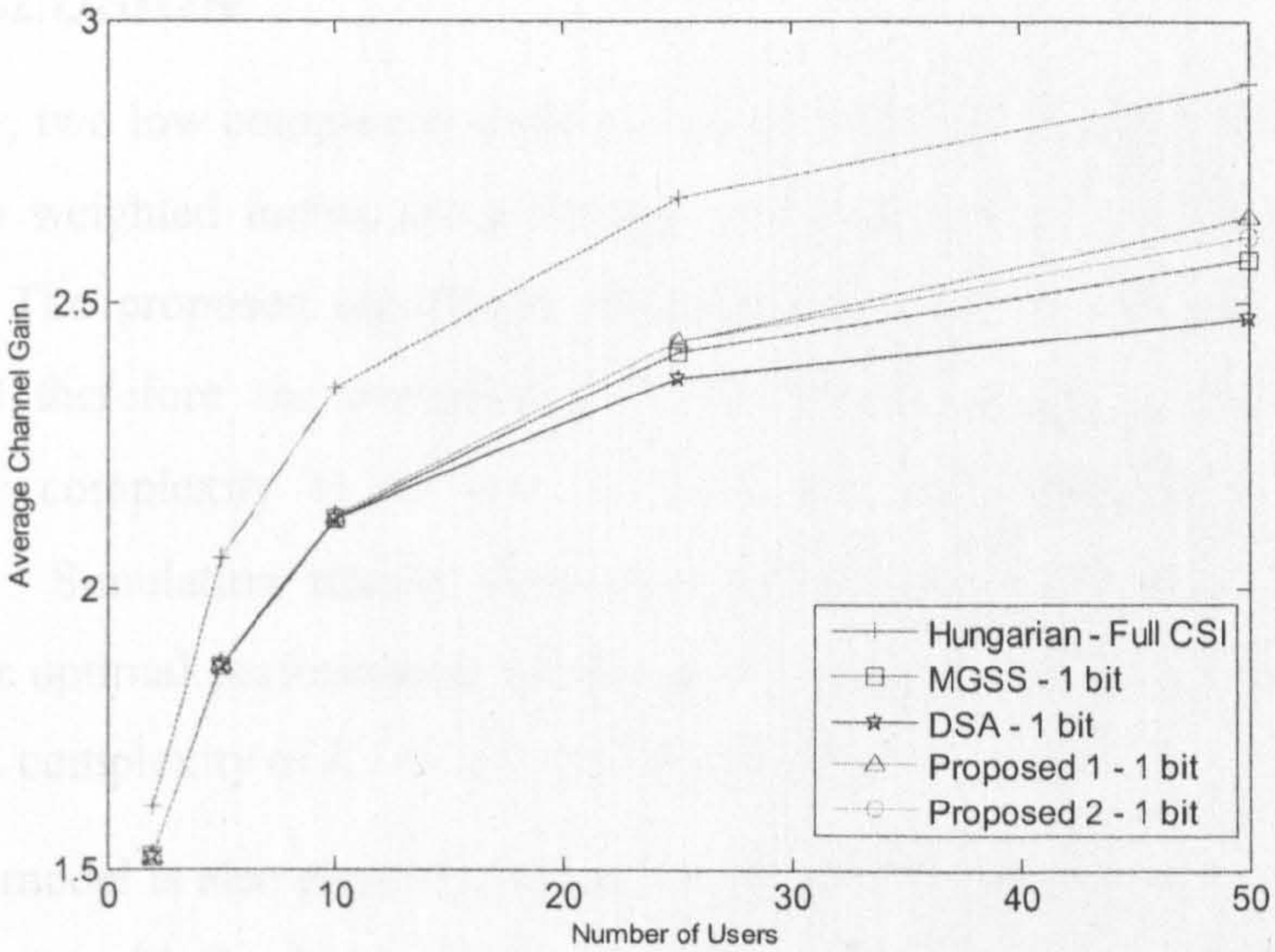

Figure 5-18: Average achievable channel gain using 1 bit feedback scheme and full CSI

Using the optimal threshold, The BER performance using 1 bit feedback for the ½-rate QPSK transmission mode is shown in Figure 5-19. To evaluate the performance loss of the limited feedback in terms of BER, the performance of FSA and the Hungarian method using full feedback is included for comparison. The figure shows that the performance of all the algorithms is decreased by approximately 1dB. In particular, the proposed algorithms are less susceptible to the inaccurate channel feedback and perform slightly better than MGSS and DSA.

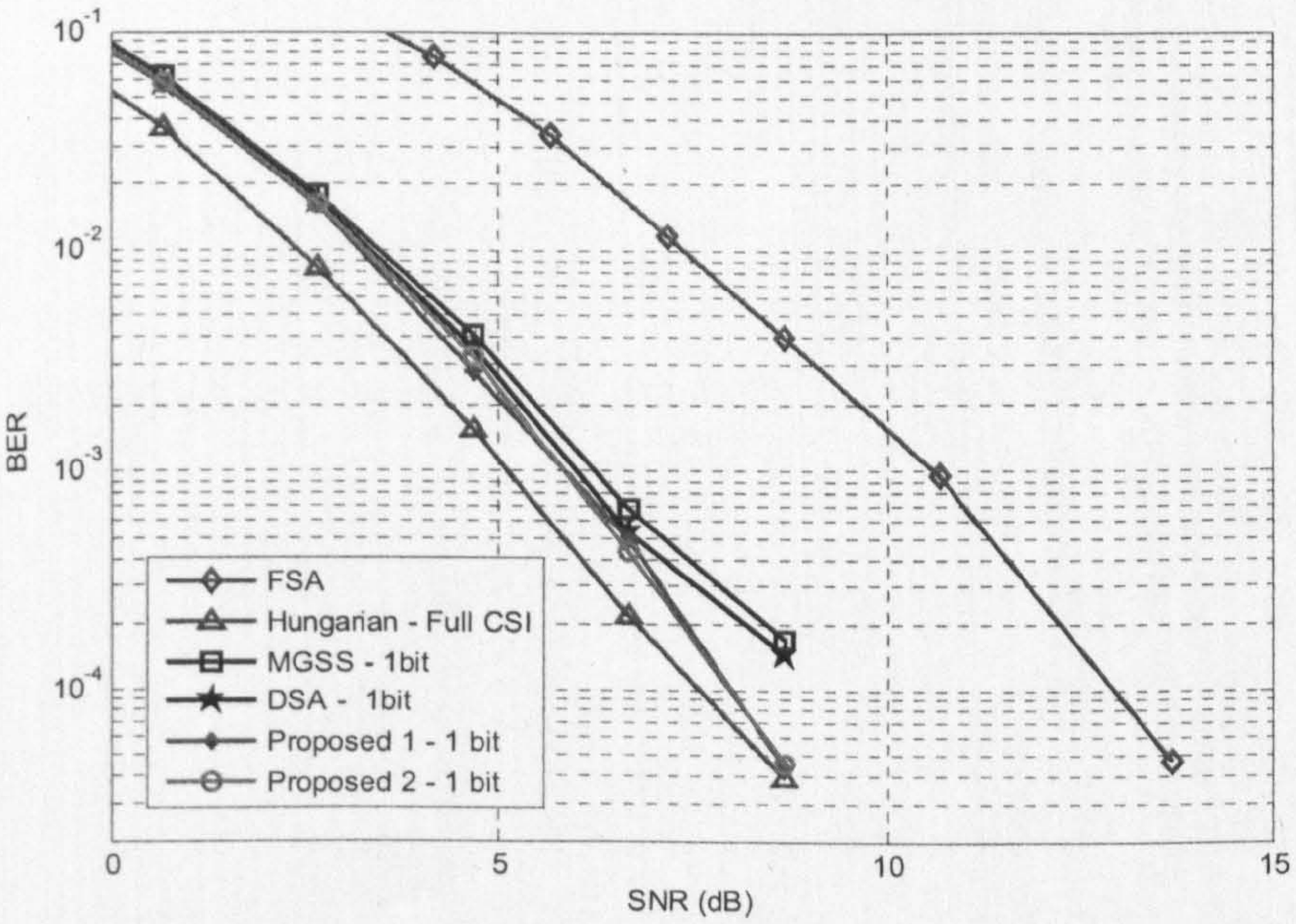

Figure 5-19: Average BER performance with 1 bit feedback

5.7 CONCLUSION

In this chapter, two low complexity dynamic resource allocation algorithms based on the maximal ratio weighted metric are presented and evaluated in the downlink of 3GPP LTE system. The proposed algorithms eliminate the need to perform sort and swap iterations and therefore the complexity of the algorithms are greatly reduced. The computational complexity is as low as DSA but with considerable performance enhancement. Simulation results show that the proposed allocation algorithms can achieve a near optimal performance, similar to the iterative algorithm (MGSS) but with computational complexity of $K+(S-1)* O(n \log n)$ only.

An analytical model is also presented to derive the optimal threshold for a 1 bit feedback scheme for users with Rayleigh distributed fading channels. This model can be easily extended to a more general class of fading distributions. From the simulation results, it can be observed that the proposed algorithms are also less susceptible to inaccurate channel feedback and perform better than other sub-optimal schemes e.g. MGSS when the 1 bit reduced feedback scheme is employed.

REFERENCES

[1] C.Y. Wong, R.S. Cheng and K.B. Letaief and R.D. Murch, 'Multiuser OFDM with adaptive subcarrier, bit and power allocation,' *IEEE J. Sel. Areas Commun.*, vol. 17, no. 10, pp 17478- 1758, Oct 1999

[2] R.S.Cheng and S. Verdu, ' Gaussian multi-access channels with ISI: Capacity region and multiuser water-filling', *IEEE Trans. Information Theory*, vol. 39, pp 773-785, May 1993

[3] H. W. Khun, 'The Hungarian method for the assignment problem', *Naval Research Logistics Quarterly*, Q.2: 473-489, Aug. 1955

[4] S. Pietrzyk and G. J. M. Janseen, 'Multiuser Sub-carrier Allocation for QoS Provision in the OFDMA Systems', *in Proceedings of Vehicular Technology Conference*, Sept. 2002,page 1077- 1081

[5] C.Y Wong, C.Y Tsui, R.S Cheng, K.B. Letaif, '*A Real-time Sub-carrier Allocation Scheme for Multiple Access Downlink OFDM Transmission*', IEEE Vehicular Technology Conference, Sept. 1999, page 1124-1128

[6] A.Doufexi, S. Armour 'Design Consideration and Physical Layer Performance Results for a 4G OFDMA System employing Dynamic Subcarrier Allocation', *in Proceedings of Personal, Indoor and Mobile Radio Communications Symposium (PIMRC)*, Berlin, Sept. 2005, pp. 351-361

[7] Rhee, W. Cioffi, J.M. , 'Increase in capacity of multiuser OFDM system using dynamic subchannel allocation', *in Proceedings of Vehicular Technology Conference (VTC)*, Tokyo, May 2000, pp 1085-1089

[8] Y. Peng, S. Armour, J. McGeehan, "An Investigation of Dynamic Sub-carrier Allocation in MIMO-OFDMA Systems," *IEEE Transactions on Vehicular Technology*, vol 56, no. 5, pp 2990- 3005, Sept. 2007.

[9] D. Kivanc, G.Liu and H. Liu, 'Computationally efficient bandwidth allocation and power control for OFDMA,' *IEEE Transaction on Wireless Communications*, vol 2, no.6, pp 1150-1158, Nov. 2003

[10] C.Woo, E.Oh, D.Hong, 'Simple Dynamic Allocation with CQI' Feedback Reduction for OFDMA Systems,' *IEEE Transactions on Vehicular Technology*, vol. 57, no. 5, Sept. 2008

[11] C.Jieying, R.A. Berry, and M.L. Honig, 'Large System Performance of downlink OFDMA with limited feedback', *in Proceedings of IEEE Int. Symp. Information Theory (ISIT)*, Seattle, Washington, July 9-14 2006, pp.1399-1403

[12] J.Leinonen, J. Hamalainen, M.Juntti, ' Performance Analysis of Downlink OFDMA Frequency Scheduling with Limited Feedback', *in Proceedings of International Conference on Communications (ICC)* , May 2008 ,pp 3318-3322

[13] S.Sanayei and A.Nosratinia, ' Opportunistic downlink transmission with limited feedback', *IEEE Transaction in Information Theory*, vol. 53, pp 4363-4372, Nov. 2007

[14] J. Jang, K. Bok Lee, 'Transmit Power Adaptation for Multiuser OFDM Systems', *IEEE J. Sel. Areas Commun.*, Vol. 21, No.2, Feb 2003, pp 171-178

[15] Zhu Han; Zhu Ji; Liu, K.J.R., "Low-complexity OFDMA channel allocation with Nash bargaining solution fairness," *Global Telecommunications Conference, 2004. GLOBECOM '04. IEEE* , vol.6, no., pp. 3726-3731 Vol.6, 29 Nov.-3 Dec. 2004

[16] T.Issariyakul and E.Hossain, 'Optimal radio channel allocation for fair queuing in wireless data networks', *in Proceedings of IEEE Int. Conf. on Comm.* May 2003, vol.1, pp. 142-146

[17] R.L Kruse and A.J. Ryba, '*Data Structures and Program Design*', 3rd Edition, Englewood Cliffs, NJ: Prentice-Hall, 1994

[18] D. G. Brennan, "Linear diversity combing techniques", *in Proceedings of IRE*, vol. 47, pp. 1075–1101, June 1959.

[19] K.C.Beh, A.Doufexi, S.Armour, 'A Low Complexity Dynamic Resource Allocation Algorithm for 3GPP LTE Based on a Maximal Ratio Weighted Metric with Limited Feedback', *in Proceedings of NEWCOM++/COST2100 Workshop on Radio Resource Assignment for LTE'*, Vienna, September 2009

Chapter 6

MIMO-OFDM

6.1 Introduction on MIMO

The use of multiple antenna systems as means to improve wireless communications was recognised in the very early ages of wireless transmission. However, most of the scientific progress has only occurred in the past decade or so, which is mainly driven by breakthroughs in signal processing and information theory. Key milestones were achieved with the invention of the so-called Multiple-Input Multiple Output (MIMO) systems in the mid 90s. Driven by the ever increasing multimedia services and personal mobile internet, the demand for a truly high speed cellular network is growing tremendously. Thus, LTE is the first global mobile cellular system to be designed with MIMO as a key component from the start [1][2][3]. MIMO is one of the crucial enabling technologies in the LTE system, particularly in the downlink, to achieve the required peak data rate.

A MIMO system can take advantage of the spatial diversity obtained by spatially separated antennas in an environment with rich multipath scatterings. MIMO systems can be implemented in a number of ways, mainly to obtain diversity gain to combat the signal fading or to obtain capacity gain. In general, there are three categories of MIMO techniques. The first category is trying to improve the power efficiency of the system by maximizing the spatial diversity. Such techniques include Space Time Block Bodes [6][7] (STBC) and Space Time Trellis Codes [10] (STTC). The second category uses a layered approach to increase the capacity of the system. The most popular example of this category is the Vertical Bell Labs Layered Space-Time [5] (V-BLAST), where independent data signals are transmitted over different antennas to increase the data rate, without fully exploiting the spatial diversity. The third category exploits the knowledge of the channel at the transmitter. This method decomposes the channel matrix using singular value decomposition [16] (SVD) and uses these optimized decomposed unitary

matrices as pre and post filters at the transmitter and receiver respectively to achieve the capacity gain.

LTE adopted all three categories of MMO techniques in some form or another. In this chapter we would like to discuss the MIMO architecture that is adopted in LTE. In addition to that, a detailed link level analysis of the MIMO schemes including Hybrid ARQ will be presented.

6.2 MIMO-OFDM

OFDM has become a popular choice for the transmission of signals over wireless channels. This technique converts a frequency selective wideband channels into multiple frequency flat channel, which simplifies the equalization process in the receiver. Besides low receiver complexity, OFDM is suitable for high data rate transmission over multiple fading channels and it is also relatively simple to implement via FFT. MIMO was also initially adopted for narrowband systems since in wideband systems it involves a computationally complex channel equalisation. To make matters worse, as the number of antennas increases, complexity becomes a more severe issue. Therefore, MIMO and OFDM could make up a good combination and this combination allows MIMO techniques to be easily implemented over wideband channels. OFDM can be easily combined with a MIMO technique [13] to increase the spectral efficiency and/or reliability by exploiting the spatial diversity gain through spatially separated antennas in rich multipath scattering environments.

To evaluate the performance of MIMO techniques that have been specified in LTE, the SISO simulator used in the Chapter 3 is extended with MIMO capability. The MIMO-OFDM configuration that is used in the simulator is shown in Figure 6-1. Basically, the physical layer processing such as interleaving etc. remains the same as the SISO simulator. The extension has been made to include the Spatial Multiplexing (SM) and Space Frequency Block Code (SFBC).

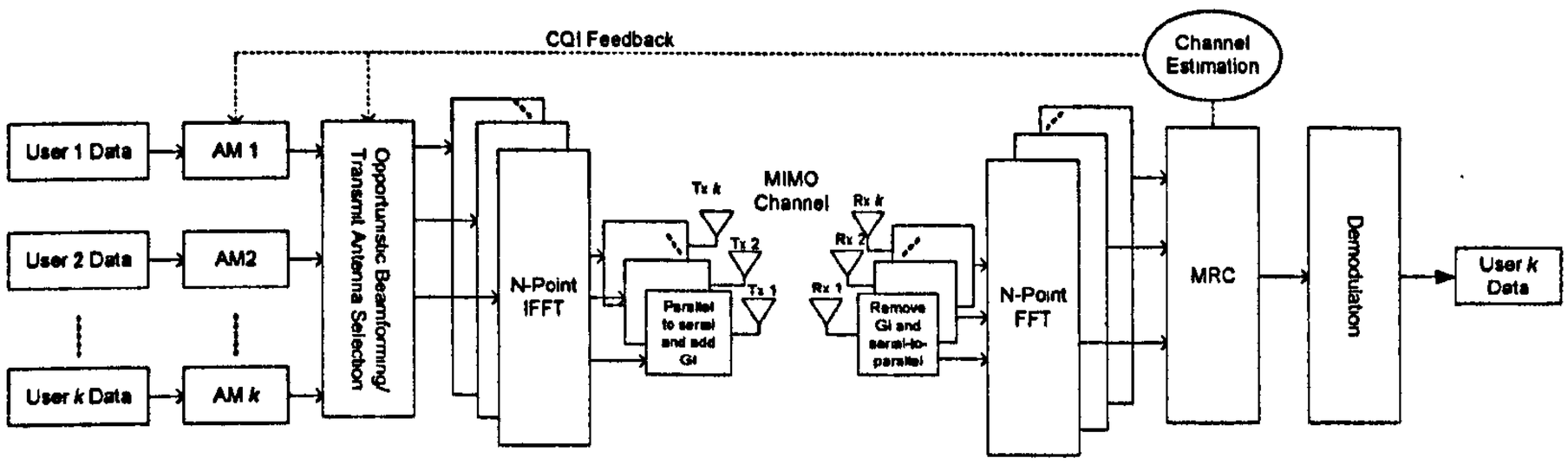

Figure 6-1: MIMO-OFDM Configuration

In the MIMO simulator, a MIMO system with N_t transmit antennas and N_r receiver antennas is considered. The complex channel between the transmitter and receiver antennas is:

$$\mathbf{H} = \begin{bmatrix} h_{11} & \cdots & h_{1N_t} \\ \vdots & \ddots & \vdots \\ h_{N_r1} & \cdots & h_{N_rN_t} \end{bmatrix}. \tag{6-1}$$

Assuming perfect timing and synchronization, the received signal at the UE for the kth PRB can be represented by:

$$Y = HX + N \tag{6-2}$$

where X is the transmit vector and N is the additive white Gaussian noise which can be modelled as complex normal and independent distributed according to $CN(0,N_0)$. N_o is the noise power density. In MIMO detection, a linear receiver is designed to detect the transmitted data. Linear receivers apply an N_t x N_r matrix G, chosen according to some criterion, to produce a detected symbol vector $\hat{S}$. G matrixes for Zero Forcing (ZF) or Minimum Mean Squared Error (MMSE) detection criterions are given as:

$$G_{ZF} = (H^H H)^{-1} H^H \tag{6-3}$$

$$G_{MMSE} = \left(H^H H + \frac{N_t}{SNR} I \right)^{-1} H^H \tag{6-4}$$

The received signal Y is then multiplied by G to obtain the detected data stream, $\hat{S}$ for the kth PRB.

$$\begin{aligned} \hat{S} &= GY \\ &= \hat{X} + \hat{N} \end{aligned} \tag{6-5}$$

The ZF receiver is simple to implement. By applying a pseudo-inverse of a channel matrix H to a received signal, the ZF linear receiver can eliminate the inter-stream interference and performs well at high SNRs, especially when the inter-stream interference is dominant over additive Gaussian noise. However, at low SNR, the noise enhancement will become an issue and the performance of the ZF system will be affected [14]. On the other hand, a MMSE linear receiver is more complex than a ZF receiver and needs some knowledge of the channel statistics, such as the noise variance. For this reason, MMSE is in general more complex due to the additional burden of estimating the channel statistic, and computing the filter coefficients. However, in comparison, MMSE receivers can performance significantly better but with tolerably increased complexity. Thus, the MMSE linear receiver is commonly used in the industry and is used at the receiver in the MIMO simulator throughout the chapter. Some advanced but nonlinear detectors can be exploited to provide a better error rate performance at a chosen SNR operating point, but at a cost of extra complexity. Such detection methods include the Successive Interference Cancellation (SIC) detector and the Maximum Likelihood Detector (MLD). Authors in [14][15] presented results on ML receiver and SIC-MMSE receiver, where significant improvement can be observed but at a cost of higher complexity. These detections method are beyond the scope of this thesis; the reader is referred to [16][17][18] for more information.

Two linear channel estimation techniques are considered for evaluation in this work, which are least square (LS) and minimum mean-square error (MMSE). The receiver uses the estimated channel information to decode the received data until next pilot symbol arrives. The LS channel estimates can be given by:

$$\hat{H}_{LS} = X^{-1}Y \tag{6-6}$$

where X is the known pilot signals and Y is the received signals. LS is very simple to implement as it involves an inversion process only. The MMSE channel estimation is more complex and is given by:

$$\hat{H}_{MMSE} = R_{HH}\left[R_{HH} + \sigma_N^2 (XX^H)^{-1}\right]^{-1}\hat{H}_{LS} \tag{6-7}$$

where R_{HH} is the autocovariance matrix of H and σ_N^2 is the noise variance. The MMSE estimator yields much better performance than LS estimators [28]. However the major drawback of the MMSE estimator is its high computational complexity, especially the

matrix inversion processes. The performance comparison between these two estimation techniques will be shown in a latter section.

According to the latest LTE specification [2], multi-antenna transmission with 2 and 4 transmit antennas are supported. The most common configuration in the industry is expected to be 2x2 at the moment and thus only this configuration is presented in detail and simulated in this chapter. Spatial multiplexing of multiple modulation symbol streams to a single user equipment (UE) using the same time-frequency resource is referred to as Single-User MIMO (SU-MIMO). However, additional diversity can be exploited in the space domain besides the diversity in time and frequency domain. Scheduling different UEs on different spatial streams over the same time frequency resource is referred to as MU-MIMO and can give more flexibility to the scheduler. MU-MIMO can also be known as Spatial Division Multiple Access (SDMA) and is expected to achieve the best overall system performance gain. These schemes will be described in detail in the next chapter.

6.2.1 Spatial Multiplexing (SM)

Spatial multiplexing (SM) is a transmission technique in MIMO wireless communications which transmits independent and uncoded/encoded data signals over different antennas that are multiplexed in space. Back in the mid 90s, Bell Labs first proposed an architecture and a reconstruction algorithm to exploit MIMO channels. The architecture was named Bell Labs Layered Space Time or BLAST. Two variations of BLAST were proposed, namely Diagonal BLAST (D-BLAST) and Vertical BLAST (V-BLAST). Both schemes have the same general system architecture but the demultiplexing and signal separation operations are different.

In D-BLAST each data stream is encoded individually and then cyclically assigned to different antennas for each symbol period. Therefore, the transmission of each coded stream is distributed in both space and time. In an independent Rayleigh scattering environment, this structure leads to a theoretical data rate which grows linearly with the number of antennas. However, this approach is not very practical to implement and has some drawbacks. One of the drawbacks is that some space-time is wasted at the start and at the end of a transmission with diagonal layering. The fundamental difference between Vertical BLAST (V-BLAST) and D-BLAST is the vector encoding process. For V-BLAST, each data stream is always assigned to the same transmit antenna. It does not wastes space-time resources as the D-BLAST architecture, where each data stream is

cyclically assigned to a different antenna in each symbol period. The major disadvantage of V-BLAST is a lack of transmit diversity, where the diversity gain comes entirely from the receive antennas. This technique is limited by the transmission environment and highly dependent on the channel characteristics, which are determined by antenna configuration and richness of scattering. The performance degrades severely when the spatial channel correlation is high, e.g. in a line of sight (LOS) scenario [23][24].

For both of these schemes to function, one of the requirement is that there must be at least as many received antenna elements as the transmit antennas although any further increase in the number of receiver elements can be used to help improve the detection performance. Secondly, both detection schemes also require accurate knowledge of the MIMO channel response matrix at the receiver. Therefore the implementation and the performance also very much depends on the accuracy of channel estimation [11]. Between these two schemes, V-BLAST is the most promising scheme due to its implementation simplicity [12]. Thus in this chapter, only V-BLAST will be implemented and will be known by the more generic term Spatial Multiplexing (SM) throughput the chapter.

6.2.2 Space Time/Frequency Block Code (STBC/SFBC)

Space-time trellis coding (STTC) is a combination of coding and modulation for multiple transmit antennas that achieves both a diversity and coding gain. These codes can be designed according to the criteria derived by Tarokh et.al in [10], in order to trade off the diversity and coding gains against each other. These space-time trellis codes can offer significant coding gains. However, higher gains come at the expense of a large number of states and hence higher complexity, which also increases exponentially with the number of antenna elements. Therefore space time block codes (STBC) are attractive since some schemes have been proposed, especially in [6], which allow the use of linear processing at the receiver. STBC are able to achieve the full diversity for a given number of antennas, without bandwidth expansion, although they do not offer the possible coding gains which can be obtained by the STTC.

In many scenarios, it may not be practical or necessary to exploit the very high spectral properties of the MIMO channel. Rather than using the parallel channels for increased spectral efficiency, the space time coding method is employed in such a way that it can increase the diversity order. In this way, a reduction in the number of parallel channels will only decrease the diversity order. This transmit diversity based method does not

provide a linearly increasing channel capacity as the number of transmit and receive element grows simultaneously. Only one data stream (or layer) is transmitted for 2 or even 4 antennas.

The STBC was proposed as a possible option in UMTS [8]. However a Space-Frequency Block Coding (SFBC) is proposed in LTE instead. This is due to the fact that in LTE the number of available OFDM symbols in a subframe is often odd while STBC operates in a pair of adjacent symbols in the time domain. While the implementation of STBC is not straightforward for LTE, the multiple subcarriers of OFDM lead themselves to the application of SFBC [9]. In LTE, an Alamouti based SFBC technique is proposed in the standard. For SFBC transmission, the symbols transmitted from the two antennas on each pair of adjacent subcarriers are defined as follows:

$$\begin{bmatrix} y^{(0)}(1) & y^{(0)}(2) \\ y^{(1)}(1) & y^{(1)}(2) \end{bmatrix} = \begin{bmatrix} x_1 & x_2 \\ -x_2^* & x_1^* \end{bmatrix} \tag{6-8}$$

where $y_{(k)}^{(p)}$ denotes the symbols transmitted from antenna port p on the k^{th} subcarrier. Since SFBC is not considered in combination with multi-user diversity, no channel feedback is required for resource allocation purposes.

6.2.3 LTE Pilot Structure

In the downlink of LTE, the OFDM downlink transmission can be described by a two dimensional lattice in both time and frequency domains. Thus, in order to estimate the channel as accurately as possible, the correlation between channel coefficients in time, frequency and space should be taken into consideration. Since reference signals are not available for all the subcarriers, the channel estimates for those subcarriers need to be computed via interpolation. A two-dimensional Wiener filter interpolation [19] is an optimal interpolation channel estimator in terms of mean squared error. However, due to the high complexity of such a filter, a trade-off between complexity and accuracy is often considered by using a one-dimensional filter.

The reference signal or the pilot pattern for 2x2 MIMO is shown in Figure 6-2. As shown in the figure, the pilot pattern is similar to the SISO configuration for antenna port 1. For each antenna port, a different pilot pattern is designed. For antenna port two, the location of reference signals are swapped. The location of reference signals in antenna port 1 are left empty at antenna port 2 to avoid interference and vice versa. Thus, the amount of overhead has increased in the case of 2x2 MIMO configuration. The amount of overhead

due to reference signals in the 4x4 MIMO configuration is even higher [4]. In the MATLAB simulator, it is assumed that a channel remains the same during the transmission of a packet. Thus, a linear interpolation strategy is used in the frequency domain. To evaluate the performance of the LTE pilot structure, a preamble strategy is also considered. The reference signal for the preamble strategy is shown in Figure 6-3.

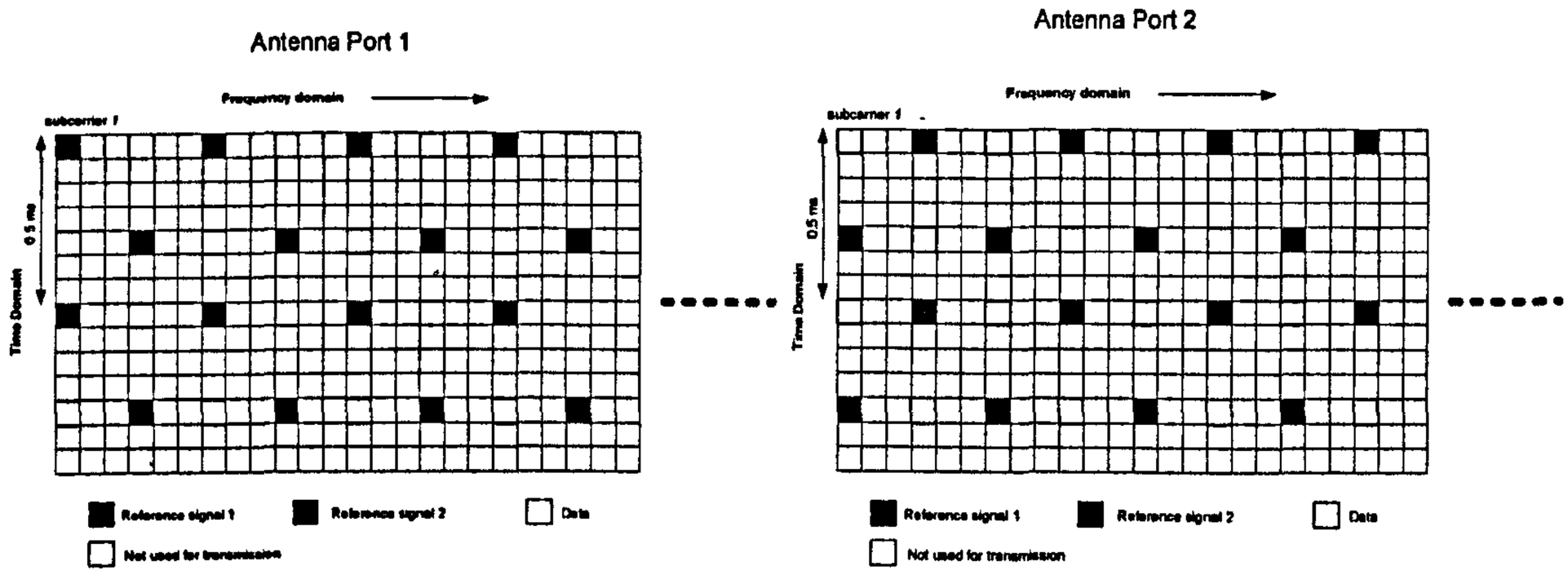

Figure 6-2: LTE pilot structure for 2x2 MIMO

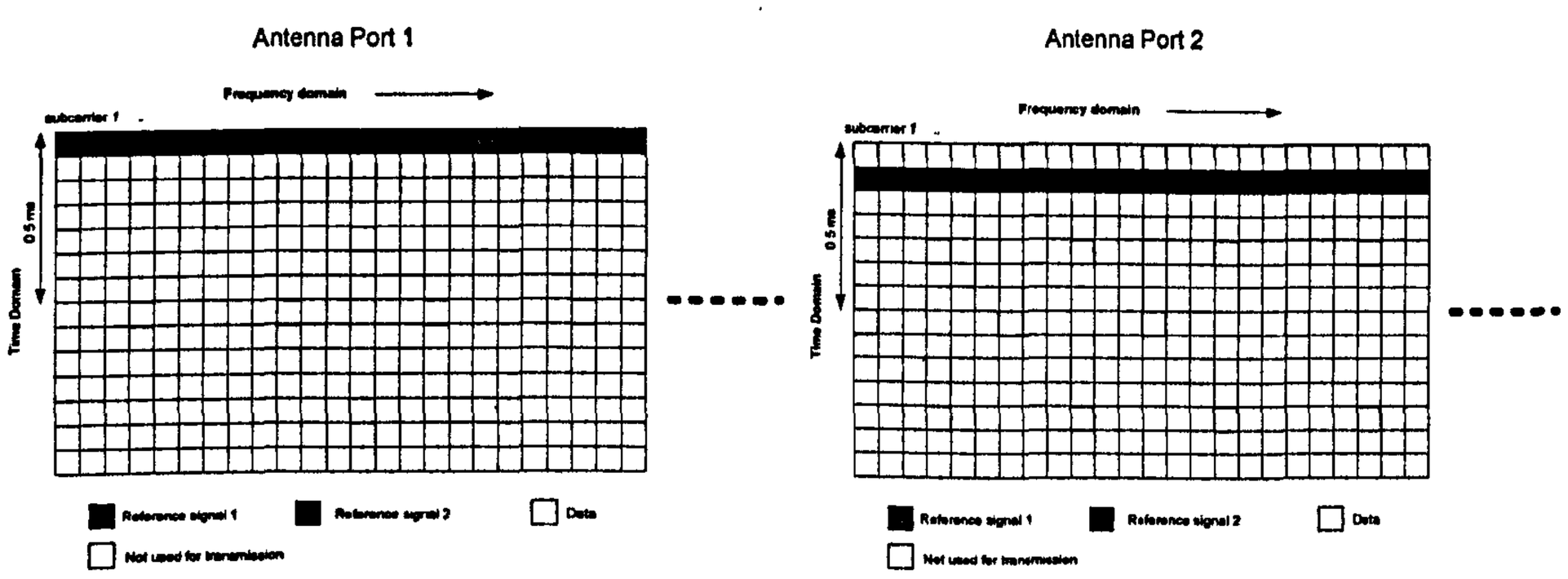

Figure 6-3: Channel estimation using preamble strategy

To compare the performance of different channel estimation strategies, the error performance will be evaluated in a MIMO 2x2 spatial multiplexing (SM) scheme for QPSK ½ rate. The channel model used in the simulation is the Spatial Channel Model Extension (SCME) [20][21]Urban Macro scenario which is specified in 3GPP [22]. Figure 6-4 and Figure 6-5 show the PER and BER performance of the different channel estimation strategies. As can be seen from the figure, the performance of LS estimates for both the preamble and the LTE pilot strategies dropped quite significantly, approximately 6dB throughout the whole SNR range, compared to an ideal channel estimation scenario. The difference between the preamble and LTE pilot structure is minimal in the case of

LS estimates. The performance of MMSE channel estimation technique is much better as expected. In the case of preamble strategy, the performance is very close to the perfect channel estimation. However, the performance is slighted degraded by 2dB in the case of pilot strategy. This is mainly due to a lesser amount of pilots and the imperfection due to the interpolation. Nevertheless, LTE specifications do not mandate any specific channel estimation technique and therefore there is complete freedom for the manufacturers to decide which channel estimation technique to employ and hence what trade off between performance and complexity to adopt.

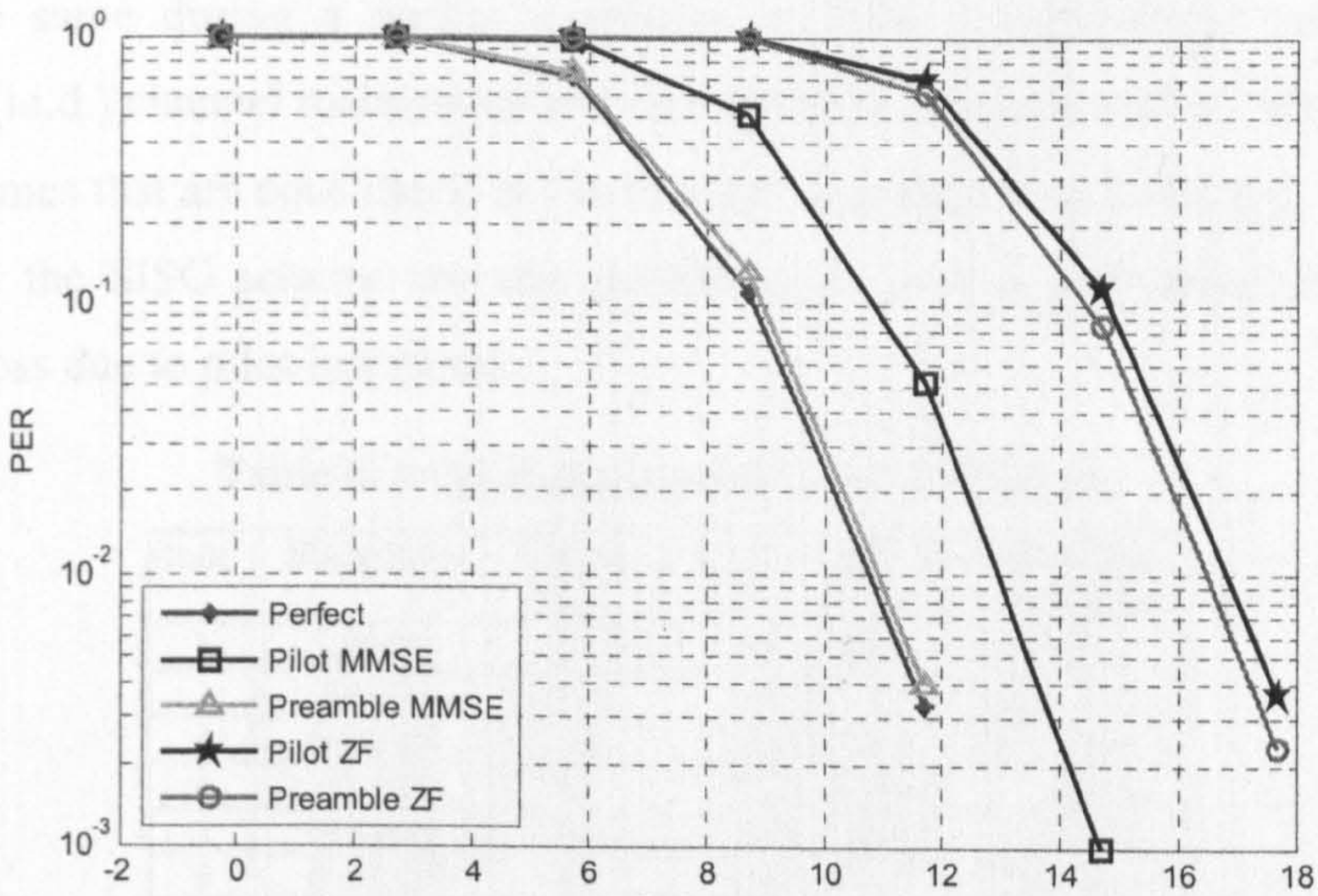

Figure 6-4: PER performance of different channel estimation schemes in QPSK 1/2 rate for 2x2 SM

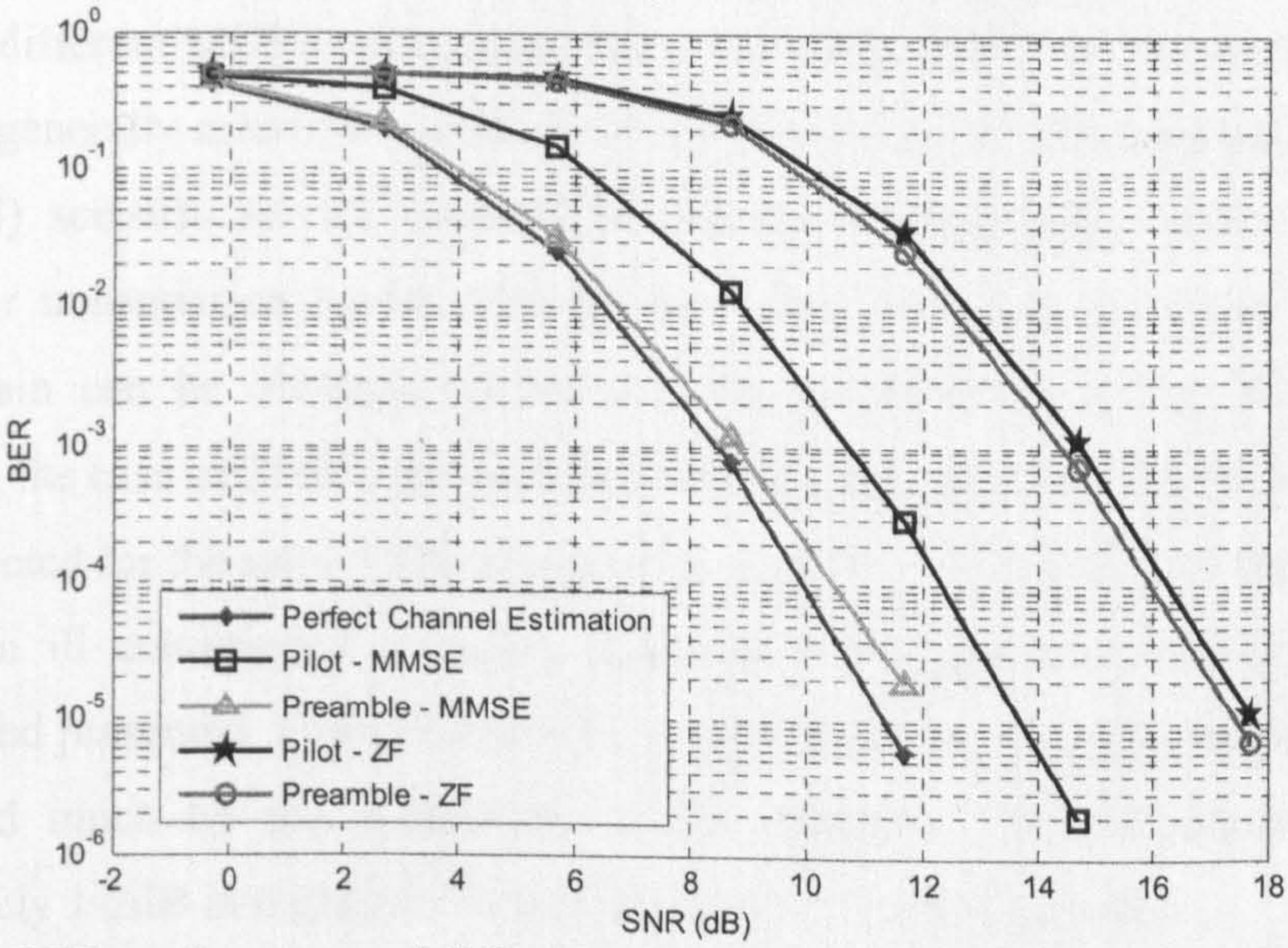

Figure 6-5: BER performance of different channel estimation schemes in QPSK 1/2 rate for 2x2 SM

6.3 MIMO Physical Layer Performance for LTE

This section gives a detailed physical layer performance of the downlink of a 3GPP LTE OFDMA system with a 2x2 MIMO configuration. Similarly, the SCME urban macro scenario is assumed and will be used throughout this section unless otherwise stated. To further evaluate the performance of MIMO schemes in LTE, different scenarios have been considered. Antenna spacing at the BS with 0.5λ-spacing, 4λ-spacing and 10λ-spacing are considered. Users with 0.5λ, 4λ and 10λ spacing have an average correlations of 0.9 (very high) 0.5 (low) and 0.1 (very low) respectively. In the simulation, a channel remains the same during a packet transmission. 2000 independently and identically distributed (i.i.d.) channel realisations are considered in each simulation. Modulation and coding schemes that are considered in the simulation are given in Table 6-1. The nominal bit rates for the SISO scheme are also presented, to give an indication of the spectral efficiency loss due to pilot insertions.

Table 6-1: Modulation and Coding Schemes

Mode	Modulation	Coding Rate	Data bits per time slot (1x1), (2x2)	Bit Rate (Mbps)
1	QPSK	1/2	4000/7600	8/15.2
2	QPSK	3/4	6000/11400	12/22.8
3	16 QAM	1/2	8000/15200	16/30.4
4	16 QAM	3/4	12000/22800	24/45.6
5	64 QAM	1/2	12000/22800	24/45.6
6	64 QAM	3/4	18000/34200	36/68.4

Figure 6-6 shows the PER performances of the MIMO 2x2 SFBC for the LTE OFDMA system for different MCS in the urban macro scenario. From the figure, it can be seen that SFBC generally achieved a clear diversity gain of up to 7dB compared to the SISO (Figure 3-4) scenario for all transmission modes. In particular, higher gain can be obtained for transmission modes with higher coding rate, e.g. ¾ coding rate as more diversity gain can be obtained to improve the performance of the channel coding. However in the case of SFBC, the peak data rate remains the same but higher throughput can be expected for the same SNR compared to the SISO. To investigate the performance of SFBC in ill conditioned channels, scenarios with various correlation factors are simulated and presented. From Figure 6-7 it can be seen that the performance of SFBC is not affected much by the correlation of the channels. The performance drops by approximately 1-2dB in highly correlated channels even for high MCS.

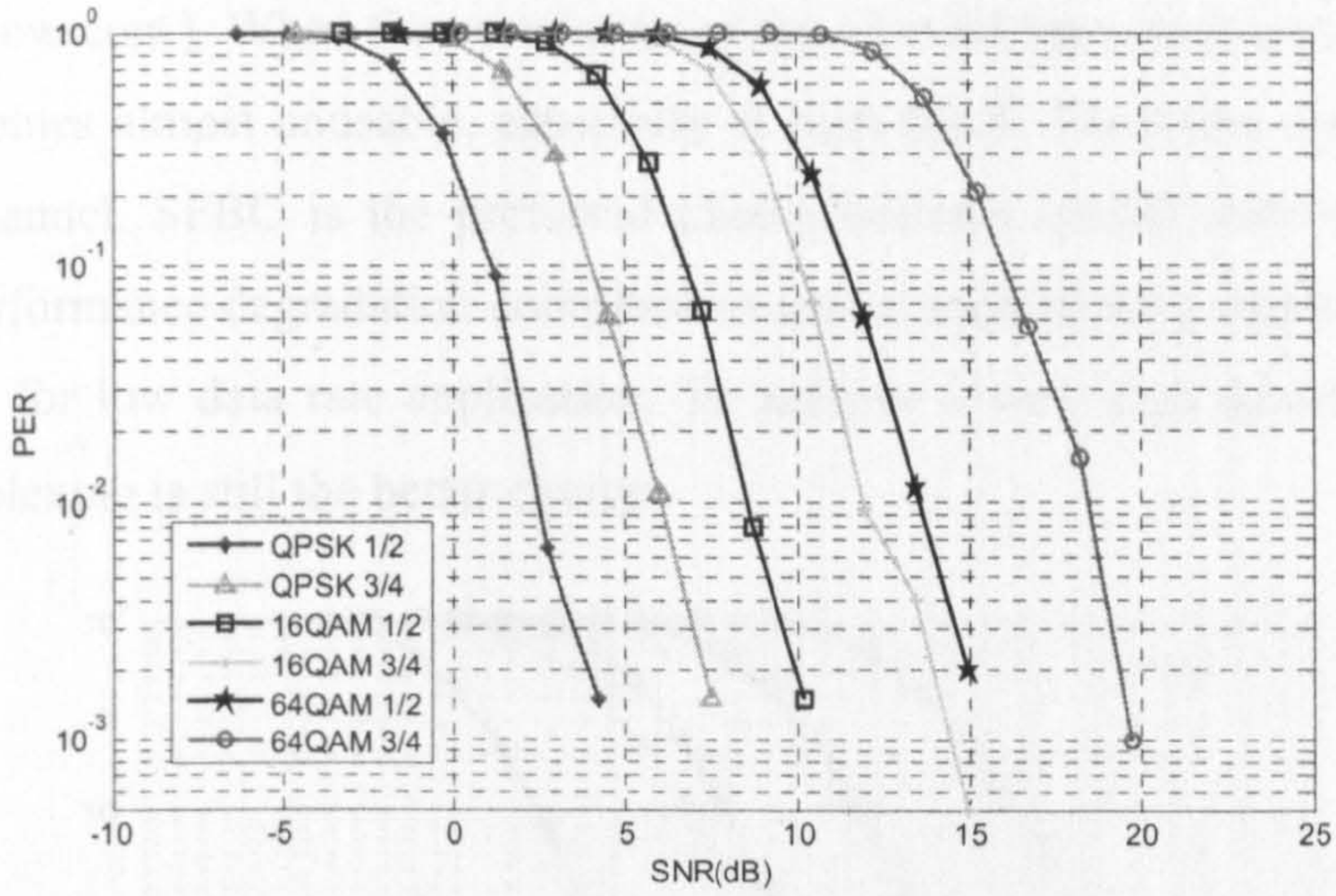

Figure 6-6: MIMO 2x2 SFBC PER Performance for Urban Macro channel with very low correlation (0.1)

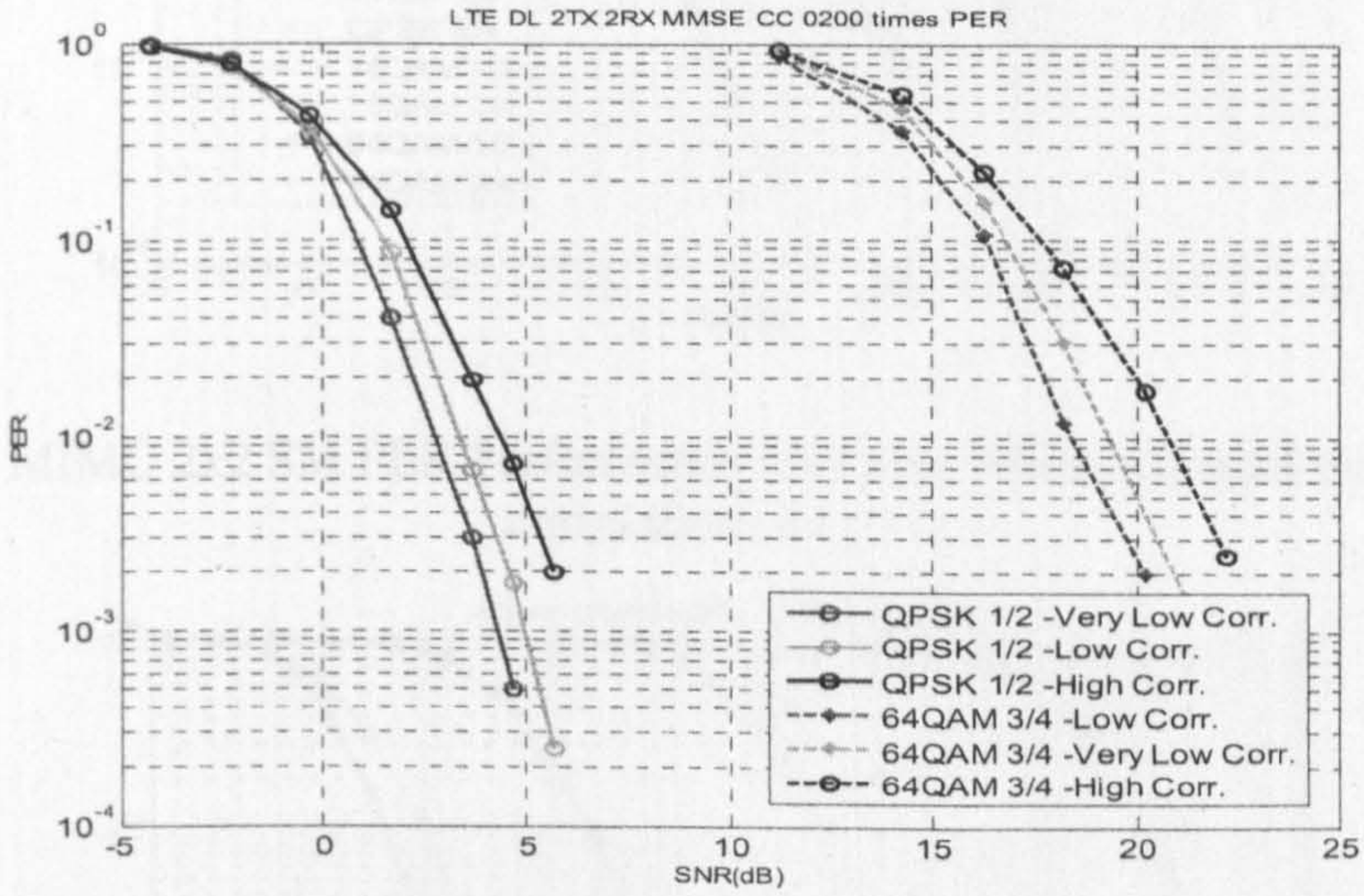

Figure 6-7: MIMO 2x2 SFBC PER Performance for QPSK ½ rate and 64QAM ¾ rate with different correlation modes

Figure 6-8 shows the PER performances of the MIMO 2x2 SM LTE OFDMA system for various modulation and coding schemes in the urban macro scenario. Figure 6-8 shows that to achieve the same level of PER performance as the SISO, the SM generally requires slightly higher SNR for all the MCS. Nevertheless, in the case of 2x2 SM, data rate can be almost doubled due to the simultaneous transmission of multiple parallel data streams. Performance of spatial multiplexing is highly dependent on the channel characteristics, which is determined by antenna configuration and richness of scattering. Therefore, from Figure 6-9 it can be seen that the SM performance is reduced by approximately 3 dB when the correlation of the channel increases from 0.1(very low

corr.) to 0.5(low corr.). When the correlation of the channel becomes very high, e.g. 0.9, 2x2 SM becomes almost unusable, especially at high MCS. Therefore, over a spatially correlated channel, SFBC is the preferred choice because spatial correlation leads to much less performance degradation compared to spatial multiplexing. However, SFBC is only suitable for low data rate application. To achieve a very high spectral efficiency, spatial multiplexing is still the better choice.

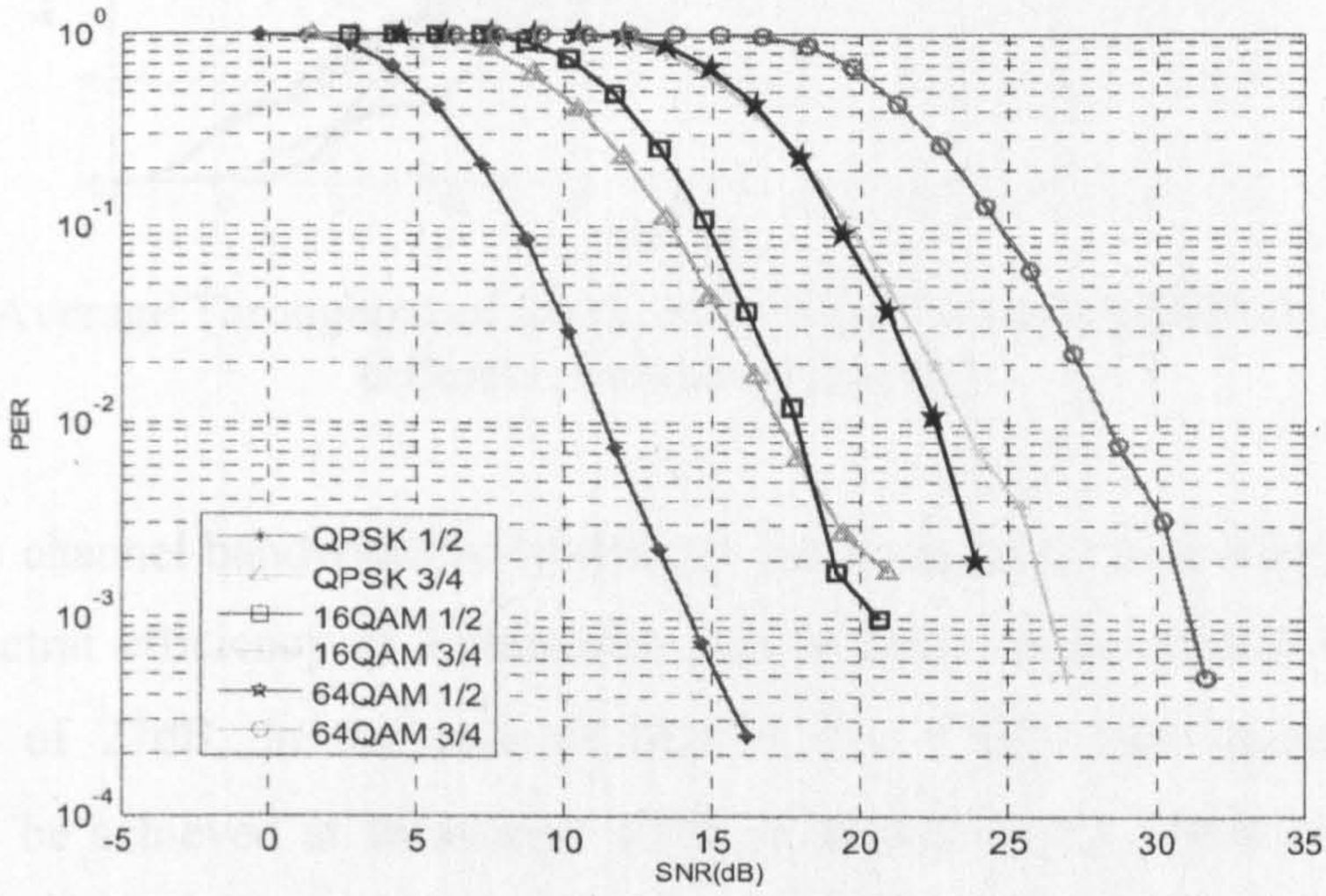

Figure 6-8: MIMO 2x2 SM PER Performance for Urban Macro channel with very low correlation (0.1)

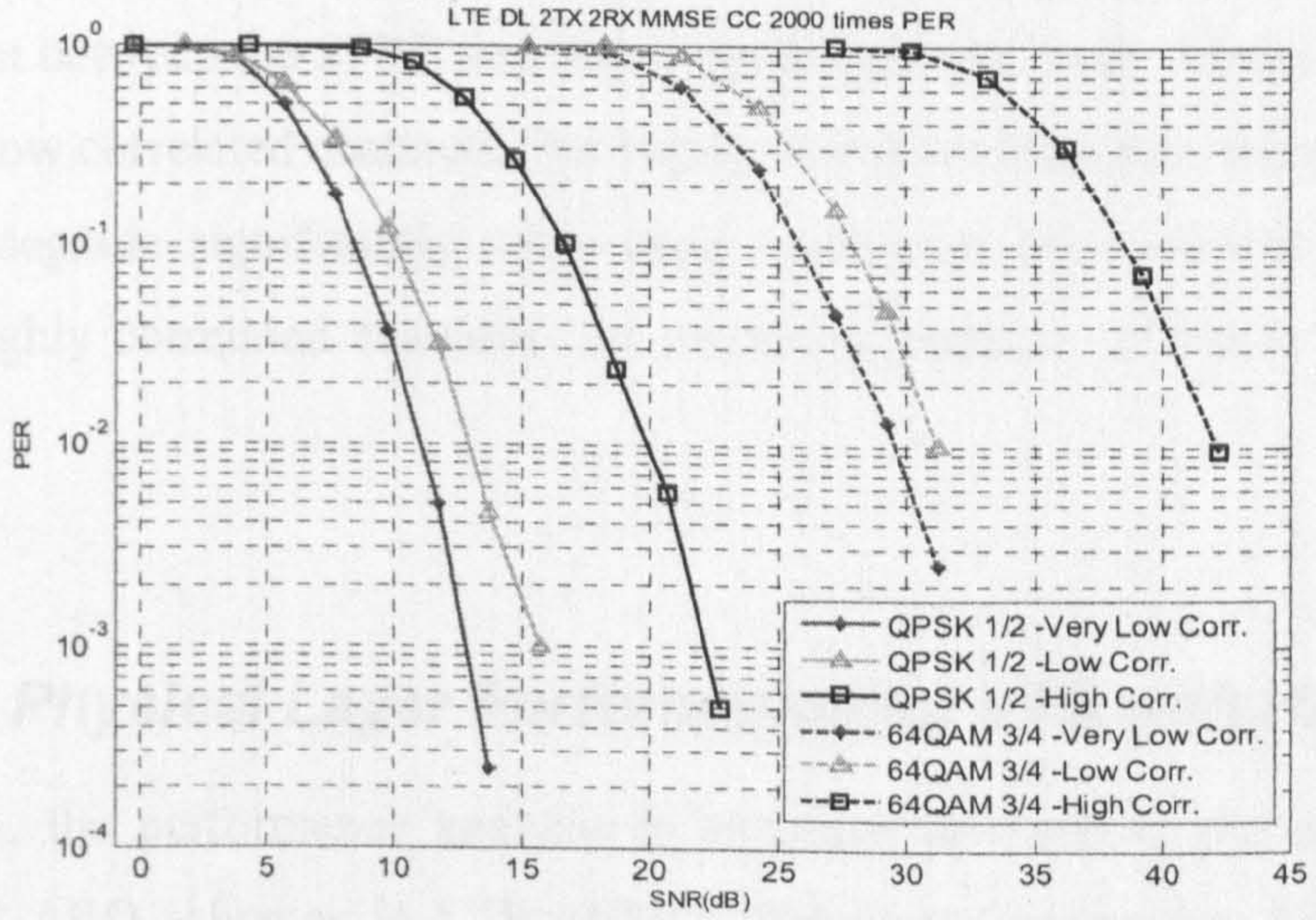

Figure 6-9: MIMO 2x2 SM PER Performance for QPSK ½ rate with different correlation factors

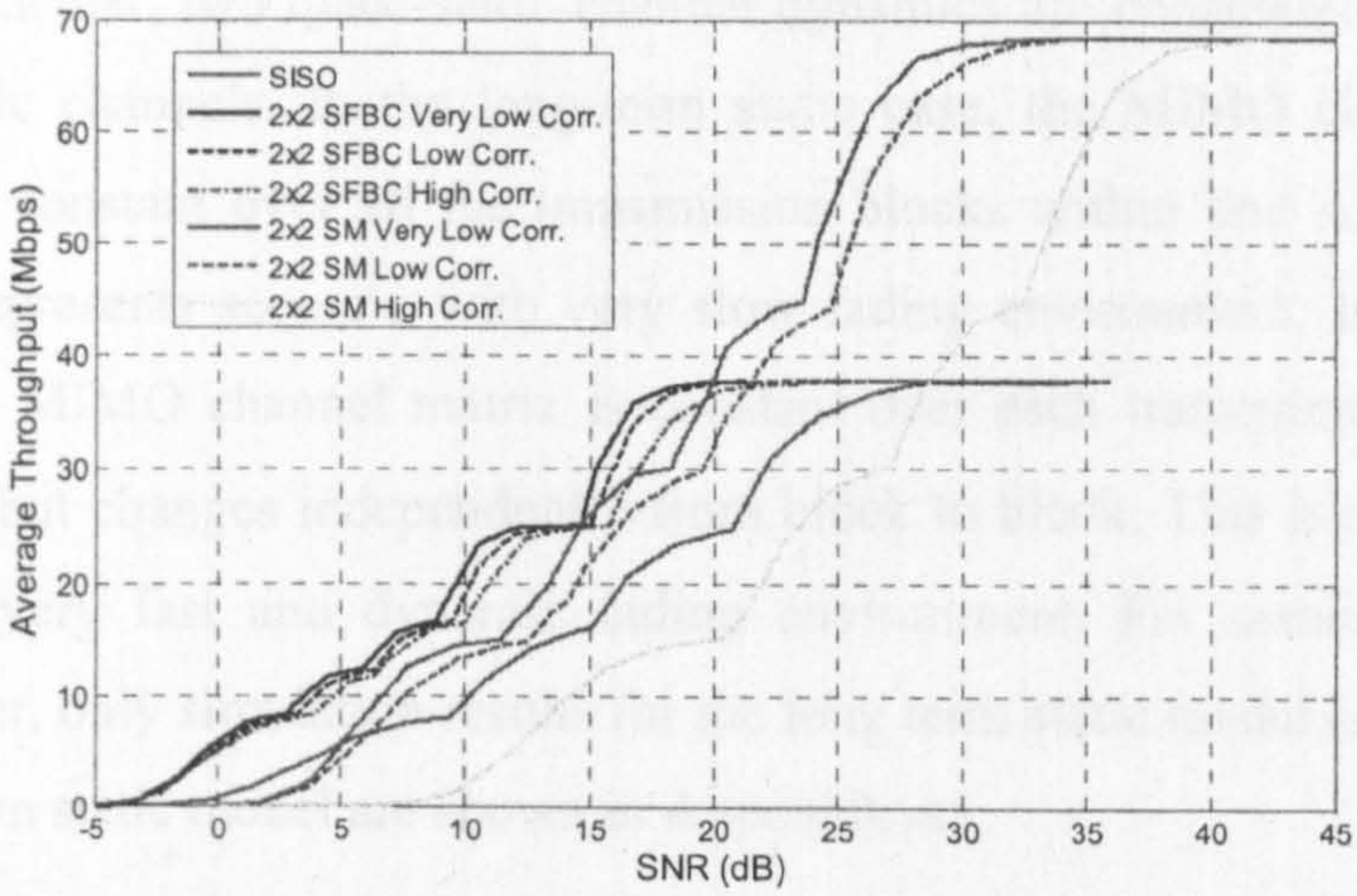

Figure 6-10: Average Throughput of SISO, MIMO 2x2 SM and MIMO 2x2 SFBC with different correlation factors

Given that the channel bandwidth is 10MHz, it can be deduced from Figure 6-10 that a maximum spectral efficiency of 3.6bits/s/Hz can be achieved in a SISO scenario at an average SNR of 27dB. In the case of MIMO 2x2 SFBC, this maximum spectral efficiency can be achieved at an average SNR of approximately 19dB, an 8dB gain in comparison to the SISO scenario. SISO is completely outperformed by SFBC across the whole SNR range. For the case of MIMO 2x2 SM, a spectral efficiency up to 6.84bits/Hz/s can be achieved at an average SNR of 30dB. It can be seen that the switching point between the SFBC and SM is approximately 20dB. However, this is only applicable to low correlated channels. For highly correlated channels, the performance of the SM will degrade significantly while high correlation only has minimal effect on SFBC. For highly correlated channels, the switching point is shifted to approximately 28dB [27].

6.4 MIMO Physical Layer Performance for LTE with HARQ

In the section, the performance analysis is extended to consider the performance of several hybrid ARQ schemes in LTE MIMO. Simulation parameters from section 3.7 have been assumed. Similarly to Chapter 3, four HARQ schemes are considered and investigated, namely Simple ARQ, Chase Combining, Partial Incremental Redundancy and Full Incremental Redundancy.

In the analysis, a quasi-static fading channel is assumed where the channel gain is constant during one transmission block and changes independently from one block to

another. In particular, two quasi-static channel dynamics are considered: long-term and short-term static channels. In the long-term static case, the MIMO channel matrix is assumed to be constant over all the transmission blocks within one ARQ mechanism. This usually represents scenario with very slow fading environment. In the short-term static case, the MIMO channel matrix is constant over each transmission block of the ARQ protocol but changes independently from block to block. This is representative of scenario with very fast and dynamic fading environment. For consistency with the previous chapter, only simulation results for the long term static model is shown. Results on the short term static model are shown in Appendix A1.

6.4.1 Hybrid ARQ Error Performance on SM

Figure 6-11 a-d presents the PER performance of various Hybrid ARQ schemes for different MCS levels, with a packet size of 54 bytes. As can be seen from Figure 6-11a, the gain from the Simple ARQ method is insignificant. The results is expected, as a long term static model is assumed, thus no time diversity can be exploited in the retransmission. In the case of a short term static model, the gain in the retransmission is considerably improved. The results are presented in Appendix A2. In the case of Chase Combining, gain in the retransmission is considerable improved compared to the Simple ARQ. The highest combining gain is achieved in the first retransmission (2nd Transmission); this is consistent with the SISO behaviour studied in Chapter 3. In the subsequent retransmission, the combining gain is decreasing [25][26]. For the case of Partial IR, more gain can be achieved compared to Simple ARQ and CC. In Partial IR, the coding rate is gradually decreased in the retransmissions while maintaining self-decodability (including systematic bits). Thus, combining and coding gains can both be achieved in the retransmissions. Therefore, considerable gain can still be observed in the 3^{rd} or 4^{th} transmissions. From Figure 6-11d, it can be observed that the Full IR scheme achieves the best performance with the highest gain achieved in the first retransmission. A large coding gain is obtained since the coding rate is significantly reduced, due to the fact that only redundancy bits are transmitted in the retransmission. When the coding rate is reduced to the mother code rate, a repetition code is used and more gain can also be obtained from the combining process.

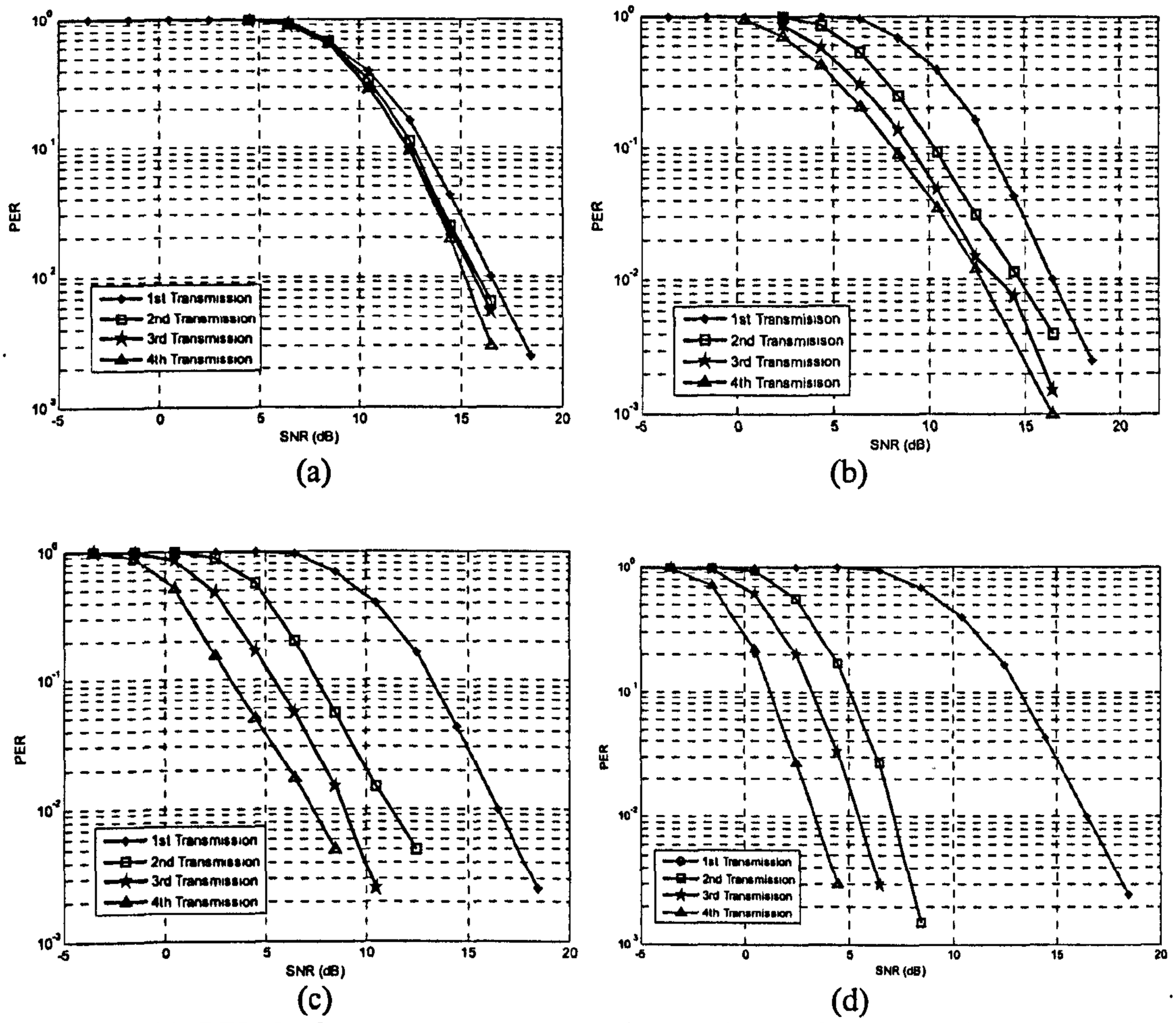

Figure 6-11: PER Performance over retransmissions in SM for a) Simple ARQ and b) Chase Combining c) Partial Incremental Redundancy and d) Full Incremental Redundancy

Figure 6-12a-d shows the comparison of PER performance after 4 transmissions for various HARQ schemes in for Mode 1, 2, 4 and 6. Compared to SISO (Figure 3-13), Hybrid ARQ schemes offer similar performance in SM. Simple ARQ and Chase Combining achieve consistent performance gain of approximately 1dB and 6dB at PER = 10^{-1} respectively, regardless of modulation and coding schemes. Both incremental redundancy schemes can achieve higher performance gain in high modulation and coding schemes, such as Mode 6. For example in Mode 6, up to 13 dB gain can be obtained at PER = 10^{-1} by the Full IR scheme. However in Mode 1, only up to 8 dB gain can be achieved by the Full IR scheme.

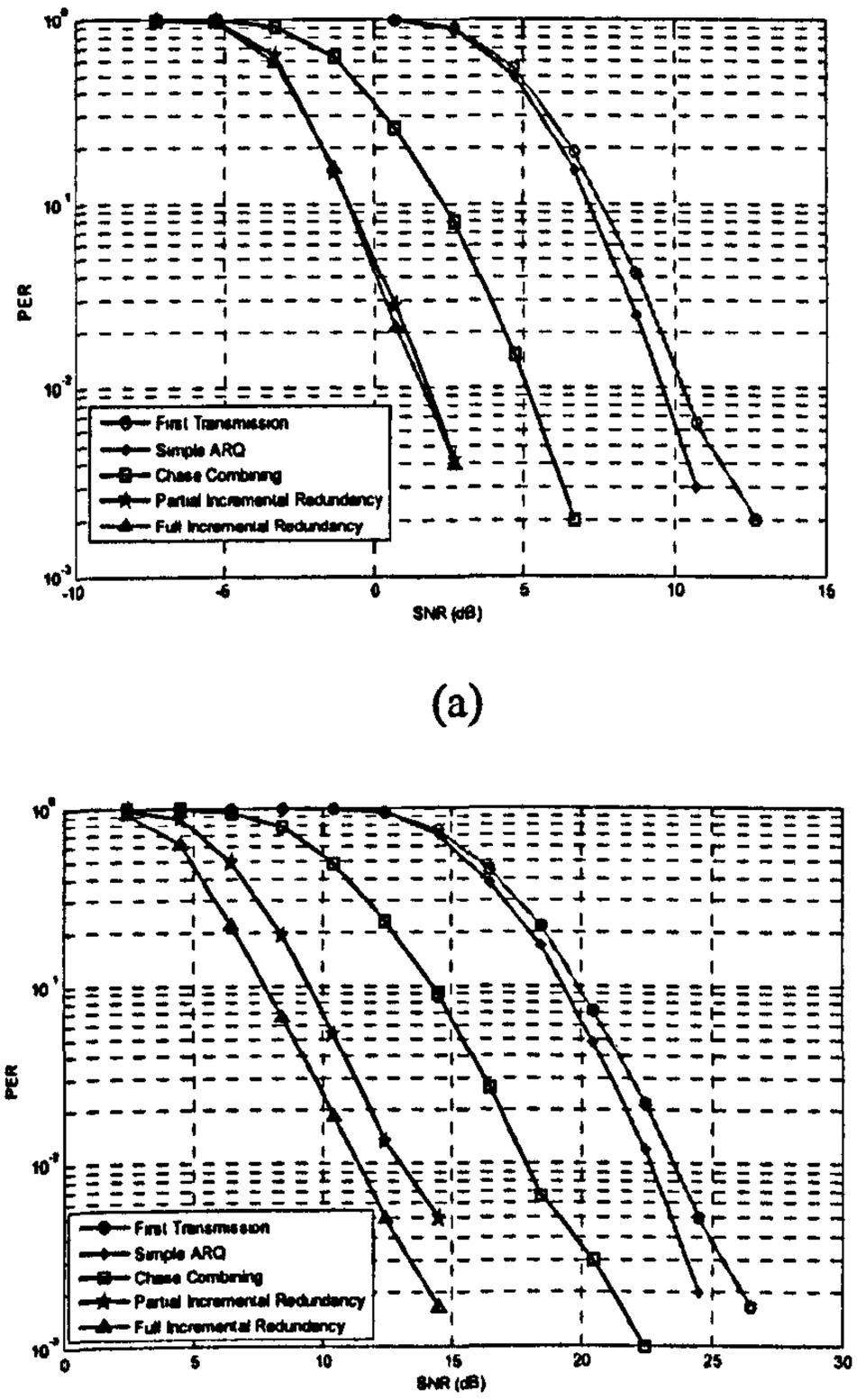

(a)

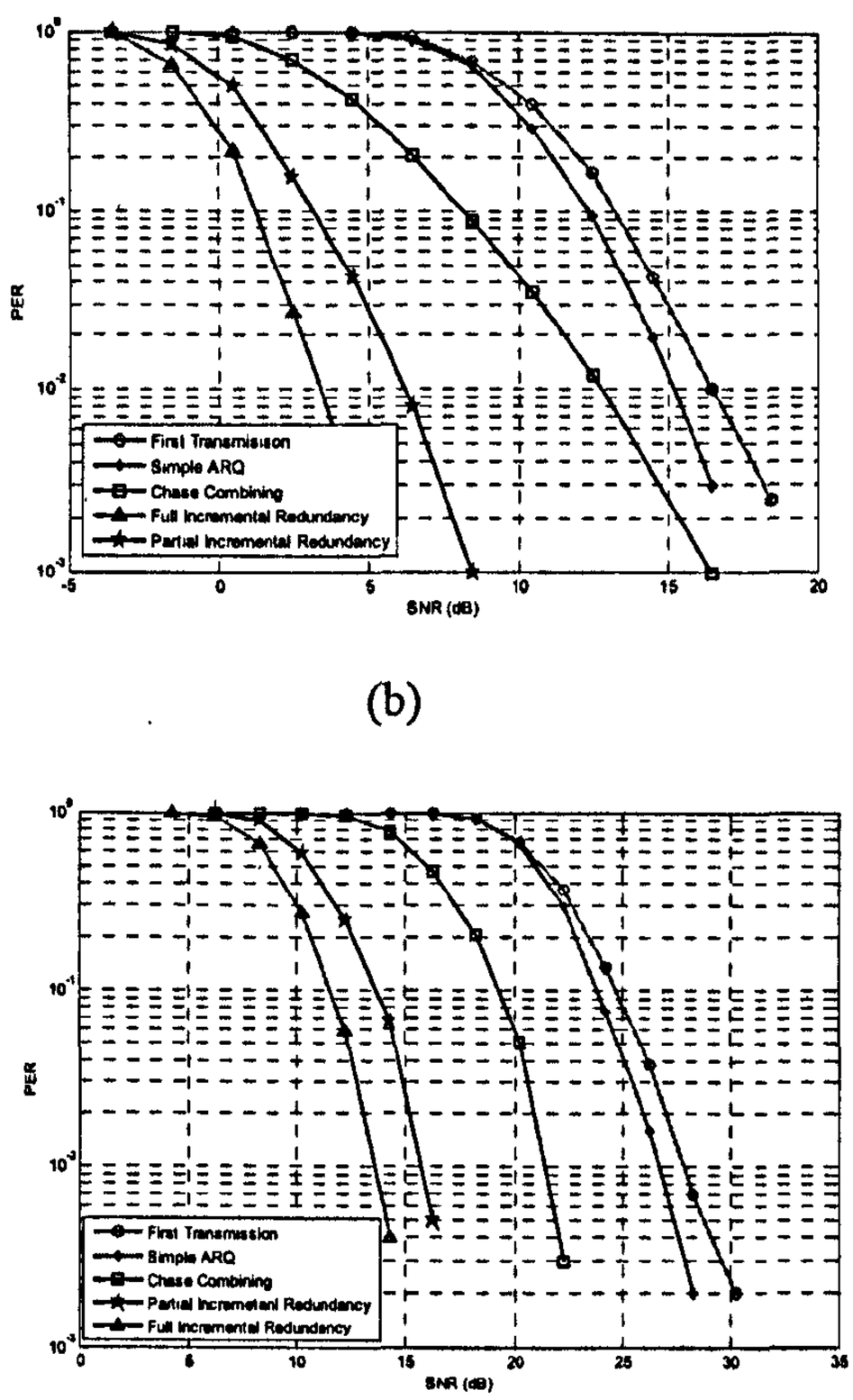

(b)

(c)

(d)

Figure 6-12: PER Performance of different HARQ schemes for a) Mode 1 b)Mode2 and c)Mode 4 and d) Mode 6 in SM

6.4.2 Hybrid ARQ Error Performance on SFBC

Figure 6-13a-d shows the PER of different hybrid ARQ schemes over the retransmission for SFBC in QPSK ¾ transmission mode. Similarly to SISO and SM, the simple ARQ scheme does not offer a good performance in SFBC, as this scheme does not exploit any combining gain or decoding gain from the previous erroneous packets. The gain from the Chase Combining scheme is similar to SISO and SM, which is approximately 6dB at the fourth transmission. The highest gain is obtained in the second transmission, where 3dB can be observed. The gains in the subsequent transmissions are reduced gradually.

In SFBC, both the incremental redundancy schemes achieve better performance than the Chase Combining method, which is consistent to both the SISO and SM. However, compared to SM and SISO, less gain can be achieved in the incremental redundancy schemes. Only 7.5dB of gain can be achieved in SFBC, in contrast to 11dB gain in the Partial IR schemes. Likewise Full IR in SFBC can only gain 8dB after 4 transmissions, contrary to SM where 12dB can be achieved.

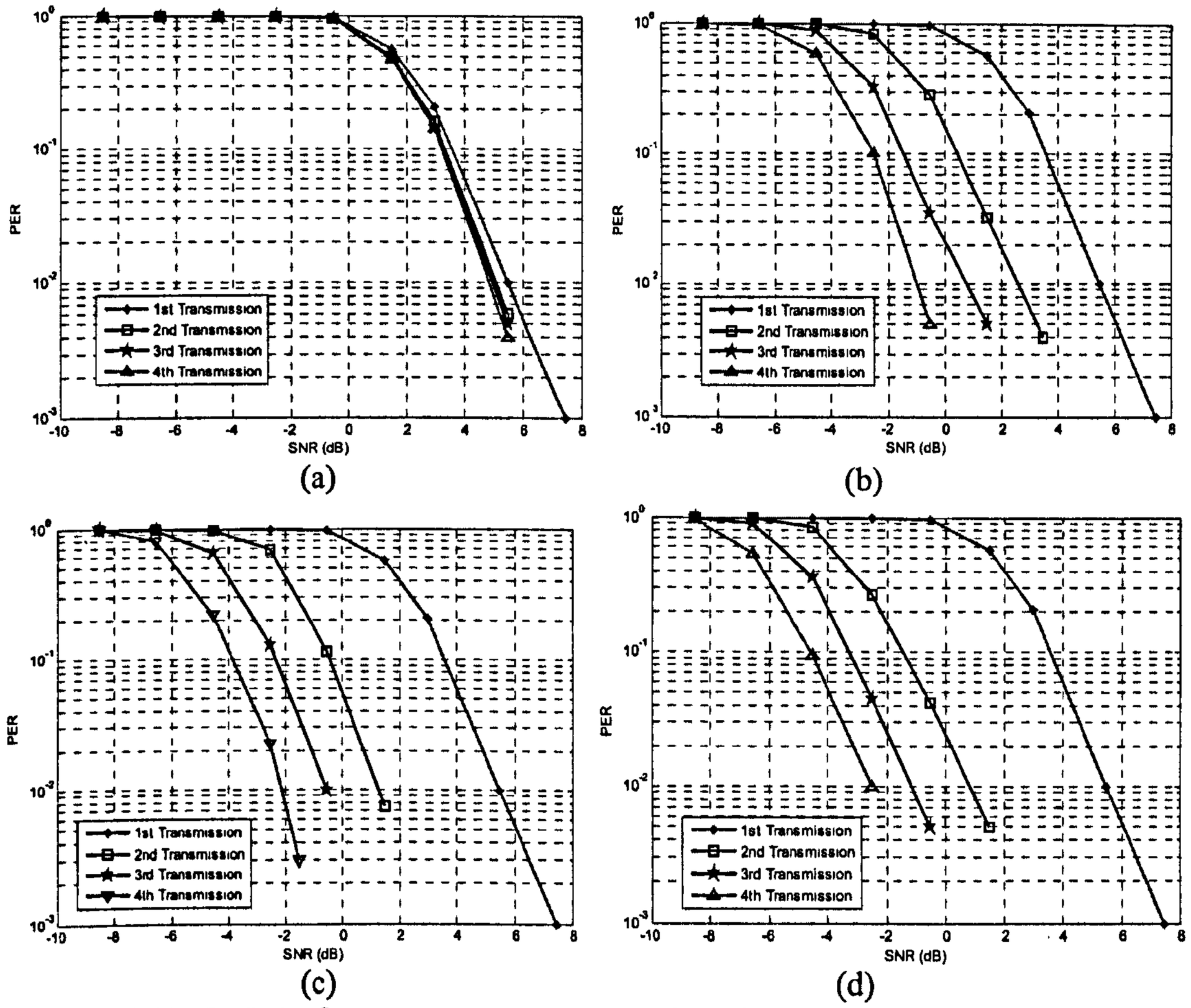

Figure 6-13: PER Performance over retransmissions for a) Simple ARQ and b) Chase Combining c) Partial Incremental Redundancy and d) Full Incremental Redundancy in SFBC

Figure 6-14a-d show the PER performance of different hybrid ARQ schemes for various transmission modes. Similarly to SISO and SM, Simple ARQ and Chase Combining achieve gains of approximately 1dB and 6dB respectively, for different modulation and coding schemes. Similarly to SM, more gain can be achieved at higher modulation and coding schemes by both the incremental redundancy schemes. However compared to SM, less gain can be obtained. Since SFBC is a diversity exploiting MIMO scheme, diversity order of up to 4 [16] can be achieved for the case of 2x2. Diversity gain that is achieved can significantly improve the performance of channel coding. As a result of that, the reduction of coding rate in the retransmission does not bring as much benefit as in the case of SM and thus lesser gain in SFBC.

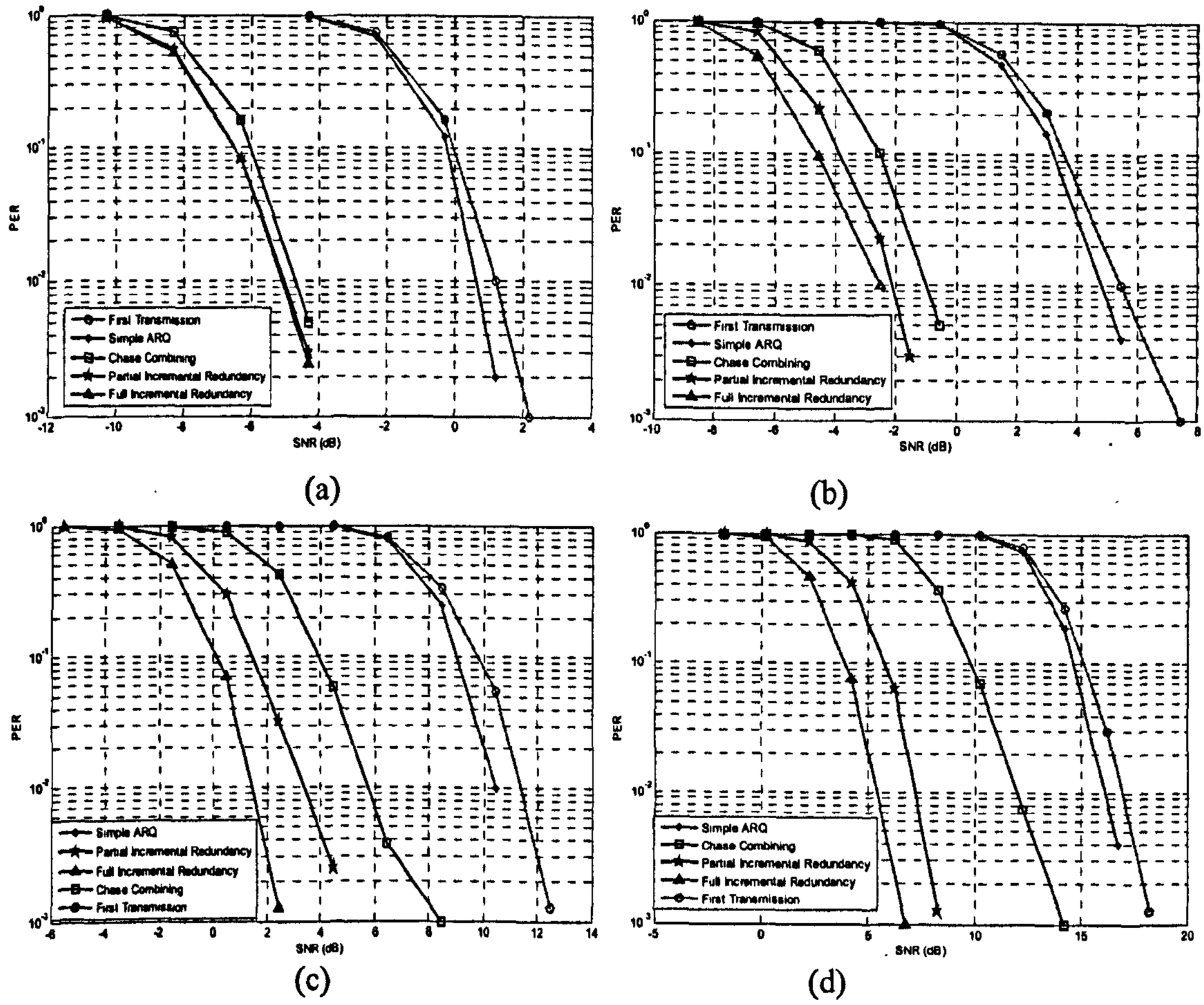

Figure 6-14: PER Performance for different HARQ schemes in SFBC for a) Mode 1, b) Mode 2, c) Mode 4 and Mode 6

6.5 Conclusion

In this chapter, a detailed link level simulation for two MIMO techniques, SFBC and SM, have been presented. SFBC is a transmit diversity technique which aims to increase the reliability and robustness of a transmission. SM on the other hand aims to increase the spectral efficiency by transmitting independent data streams over the spatial layers. From the simulations results, SFBC performs best at low SNRs in terms of spectral efficiency. At approximately 20dB, SM outperforms the SFBC and achieves better throughput performance. However, for highly correlated spatial channels, the switching point is increased to 28dB in 3GPP urban macro scenario.

In addition to that, the performance of several hybrid ARQ schemes is also presented in a MIMO scenario. Incremental redundancy schemes remain the best option for LTE, due to the significant gain achieved that can be achieved, especially at high modulation and

coding schemes. SFBC achieves less performance gain than SM due to the diversity exploiting nature of the scheme.

In the next chapter, several beamforming techniques which exploit channel quality information at the transmitter will be analysed and presented. In addition to that, the performance gain of resource allocation in MIMO-OFDMA will also be investigated.

References

[1] "3GPP; Technical Specification Group Radio Access Network; Requirements for E-UTRA and E-UTRAN (R7)", 3GPP TR 25.913 V7.3.0, March. 2006. [Online] Available:http://www.3gpp.org/ftp/Specs/html-info/25913.htm

[2] 'Technical Specification Group Radio Access Network; Evolved Universal Terrestrial Radio Access (E-UTRA) and Evolved Universal Terrestrial Radio Access Network (E-UTRAN): Overall Description', 3GPP TS 36.300 V8.4.0, March 08. [Online]. Available: http://www.3gpp.org/ftp/Specs/html-info/36300.htm#

[3] E. Dahlman, H. Ekström, A. Furuskär, Y. Jading, J. Karlsson, M. Lundevall, and S. Parkvall, "The 3G Long-Term Evolution - Radio Interface Concepts and Performance Evaluation," *IEEE Vehicular Technology Conference (VTC) 2006 Spring*, Melbourne, Australia, May 2006

[4] 'Technical Specification Group Radio Access Network; Evolved Universal Terrestrial Radio Access (E-UTRA) and Evolved Universal Terrestrial Radio Access Network (E-UTRAN): Physical Channels and Modulation', 3GPP TS 36.211 V8.4.0, Sept 08. [Online]. Available: http://www.3gpp.org/ftp/Specs/html-info/36211.htm

[5] Gerard J. Foschini, Glen D. Golden, Reinaldo A. Valenzuela, and Peter W. Wolniansky, "Simplified Processing for High Spectral Efficiency Wireless Communication Employing Multi-Element Arrays", IEEE Transactions on Selected Areas in Communications, Vol. 17, No. 11, Nov 1999

[6] S. Alamouti, "A simple transmit diversity technique for wireless communications", IEEE JSAC, Vol. 16, No. 8, pp. 1451-1458, 1998

[7] V. Tarokh, H. Jafarkhani, A. R. Calderbank, "Space-time Block Coding for Wireless Communications: Performance Results", IEEE Journal on Selected Areas in Communications, Vol. 17 No. 3, March 1999, pp.451-460.

[8] E. Dahlman,S. Parkvall, J. Skold, P. Beming,' 3G Evolution: HSPA and LTE for Mobile Broadband', Academic Press, 2008

[9] S.Sesia, I.Toufik, M.Baker, ' LTE The Long Term Evolution: From Theory to Practice,' John Wiley & Sons Ltd., 2009, pp243-282

[10] V.Tarokh, N.Seshadri, and A.R. Calderbank, 'Space-Time Codes for High Data Rate Wireless Communications: Performance Criterion and Code Construction,' IEEE Trans. Info. Theory, vol. 44, no. 2, Mar 1998, pp 744-65

[11] T.L. Marzetta, "Blast Training: Estimating Channel Characteristics for High Capacity Space-Time Wireless", Proc. 37th Allerton Conf., Monticello, Sept. 22-24th, 1999.

[12] G. D. Golden *et al.*, "Detection Algorithm and Initial Laboratory Results Using V-BLAST Space-Time Communication Architecture," *Elect. Lett.*, vol. 35, no.1, Jan. 1999.

[13] H. Yang. A Road to Future Broadband Wireless Access: MIMO-OFDMBased Air Interface. *IEEE Comm. Magazine*, pp. 53–60, Jan. 2005.

[14] Zijian Bai, et al. ' ON MIMO with Successive Interference Cancellation Applied to UTRA LTE,' International Symposium on Communications, Control and Signal Processing (ISCCSP), March 2008, pp: 1009 – 1013

[15] C.Spiegel, J.Berkmann, Zijian Bai Scholand, T.Drewes, 'MIMO Schemes in UTRA LTE, A Comparison,' 11-14 May 2008 Page(s):2228 - 2232

[16] D. Tse, P. Viswanath, Fundamentals of Wireless Communication, Cambridge University Press, June 27, 2005.

[17] Michele Morelli , Umberto Mengali , 'A Comparison of Pilot-Aided Channel Estimation Methods for OFDM Systems,' IEEE Transactions On Signal Processing, Vol. 49, No. 12, December 2001

[18] L. Deneire, P. Vandenameele, L. van der Perre, B. Gyselinckx, and M. Engels, "A low-complexity ML channel estimator for OFDM," *IEEETrans. Commun.*, vol. 51, pp. 135–140, Feb. 2003.

[19] N.Wiener, *Extrapolation, Interpolation, and Smoothing of Stationary Time Series. New York*: John Wiley & Sons, Ltd/Inc., 1949

[20] D.S.Baum, J.Hansen, J.Salo, "An interim channel model for beyond-3G systems: extending the 3GPP spatial channel model (SCM)", VTC 2005 Spring, Volume 5, Page 3132 – 3136

[21] J. Salo, G. Del Galdo, J. Salmi, P. Kyösti, M. Milojevic, D. Laselva, and C. Schneider. (2005, Jan.) MATLAB implementation of the 3GPP Spatial Channel Model (3GPP TR 25.996) [Online]. Available: http://www.tkk.fi/Units/Radio/scm/

[22] "Spatial channel model for MIMO simulations", 3GPP TR 25.996 V6.1.0, Sep'03. [Online]: http://www.3gpp.org/ftp/Specs/html-info/25996.htm

[23] D.P. McNamara, M.A. Beach, P.N. Fletcher & P. Karlsson, "Initial Investigation of Multiple-Input Multiple-Output (MIMO) Channels in Indoor Environments", IEEE Benelux Chapter SH. On Veh. Tech. & Comms, Leuven, Oct. 2000

[24] M.A. Beach, D.P. McNamara, P.N. Fletcher, P. Karlsson, , 'MIMO-a solution for advanced wireless access' International Conference on Antennas and Propagation, 2001, vol.1, pp 231-235

[25] G. Benelli, "An ARQ scheme with memory and soft error detectors," *IEEE Trans. Commun.*, vol. COM-33, no. 3, pp. 285–288, Mar. 1985.

[26] D. Chase, "Code combining—A maximum likelihood decoding approach for combining an arbitrary number of noisy packets," *IEEE Trans. Commun.*, vol. 33, no. 5, pp. 385–393, May 1985.

[27] K.Beh, A.Doufexi, S.Armour, 'On the Performance of SU-MIMO and MU-MIMO in 3GPP LTE Downlink,' *To appear in Proceeding of PIMRC 2009*

[28] Biguesh, M.; Gershman, A.B., "Training-based MIMO channel estimation: a study of estimator tradeoffs and optimal training signals," *Signal Processing, IEEE Transactions on* , vol.54, no.3, pp. 884-893, March 2006

Chapter 7

Unitary Precoding in LTE

7.1 Introduction on precoding

In order to overcome the effect of multipath and achieve a high throughput, channel equalization or precoding techniques can be used. The original principle of precoding is that if channel information is known at the transmitter side, the transmit signal can be designed in such a way that the Inter Symbol Interference (ISI) in the receiver side is greatly mitigated. In the recent years, precoding technique has been extended to improve the performance of a MIMO system. In this work, precoding is considered as a generalized beamforming scheme where the multiple streams of the signals are emitted from the transmit antennas with independent and appropriate weighting so as to increase the link throughput at the receiver output. Precoding can also optimize transmissions to the characteristics of the radio channel so that when the signals are received, they can be more easily separated back into the original data streams. Given an arbitrary, unitary pre-coding matrix **E**, it is possible to pre-code the transmitted data with **E** as shown in Figure 7-1, such that the receivers will perceive a pre-coded MIMO channel as **HE**.

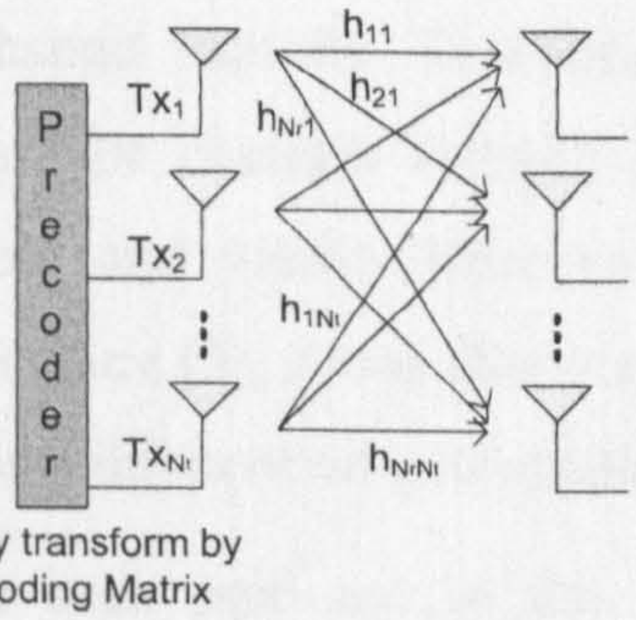

Figure 7-1 Pre-coding Concept

When used appropriately, precoding can achieve significant spectral efficiency improvement. Recently, precoding (or beamforming) has been officially adopted as an

optional feature for IEEE 802.11n [1], IEEE 802.16e (WIMAX) [2] as well as 3GPP LTE [3].

Recent breakthroughs in information theory and the growth of advanced signal processing are approaching the fundamental information limit on channel capacity. In a MIMO system, if channel information is known to the transmitter, precoding can be used to further improve the system performance based on various design criteria. However, in order to implement this feature, full channel information or partial channel information is required at the transmitter. For rapid time varying channels, full and accurate channel information may not be available in the transmitter.

For a time division duplexing (TDD) communication system, where uplink and downlink channels share the same frequency band at different times, the channel information can be estimated by the transmitter due to the channel reciprocity property. Channel reciprocity is a useful property but it should be noted it is susceptible to channel estimation error and RF circuit mismatches [4]. On the other hand, a frequency division duplexing (FDD) system uses different frequency bands for the downlink and uplink channel. The channel response in a different frequency spectrum can be quite different and thus it requires a feedback channel to deliver more accurate channel knowledge to the transmitter. For a time varying channel, the channel knowledge at the transmitter needs to be updated when the channel changes. For high mobility devices, the frequency of update is very high due to the fast changing environment. The feedback overhead could be very large due to frequent updates, especially for a high number of antennas or small normalised coherence bandwidth.

Consequently, the precoder design using full channel information is not practical for a system with a limited feedback channel capacity. Therefore, precoding schemes which require less feedback information, for example through quantized feedback bits or precoding sets are more desirable and viable. However, degradation in terms of performance is expected. In the literature [5], it was shown that satisfactory performance can still be achieved if partial channel information is available at the transmitter.

Several precoding methods have been proposed in the literature mainly due to a significant increase of interest in MIMO systems. Readers can refer to [5] for a detailed overview of precoding schemes with limited feedback. Non-linear methods such as Dirty paper coding (DPC) were proposed in [6]. When a transmitter has knowledge of the channel interference, it can employ the DPC method to design a code which can

compensate for the known interference. Although this method can achieve an optimal performance, deployment of DPC in real-time is infeasible due to high complexity.

Some linear precoding methods such as the channel inversion method [7], Block Diagonalization [8] (BD), Random Beamforming [16][17] and codebook based precoding have also been proposed in the literature. In particular, the codebook based precoding method has received considerable attention recently.

Some popular codebooks that have received considerable attention are the Grassmannian [15] and Discrete Fourier Transform [9][10][11][18] (DFT) based codebooks. The Grassmannian codebook is a near optimal codebook for a non-correlated environment. [15] showed that for a spatially uncorrelated Rayleigh Fading channel, the outage minimizing, SNR maximising and rate maximising design is to model a set $\mathcal{F}$ as a collection of lines in the Euclidean space $\mathbb{C}^M$ and also to maximise the angular separation between two closest lines. This problem can be modelled as a Grassmannian line packing problem. For further details of the Grassmannian codebook construction design and a full mathematical description, the reader is referred to [15].

In this chapter, the DFT based codebook will be described in detail as this linear precoding method has been included in the LTE specification due to its practicality and simplicity.

7.2 Unitary Precoding in LTE

One of the main challenges in the design of the beamforming vectors is the need for the transmitter to know the full channel information for all the users. This would require enormous amount of feedback to be signalled from the users to the base station. This is impractical in reality as doing so will reduce the spectral efficiency and thus defeat the purpose of beamforming.

A practical alternative to the full channel information is through a quantized feedback. Therefore a codebook method is proposed. A codebook consists of a finite number of possible beamforming matrices at both the transmitter and the receiver. By signalling the matrix best matched to the current channel, the amount of signalling can be greatly reduced. Usually at the receiver side, a user will apply a greedy approach to select one or more preferred beamforming matrices out of the codebook, by evaluating the Signal-to-Noise-Ratios (SINRs) of different beamforming combinations. Thus, each user has to signal one or several indices of the preferred vector or vectors, respectively. At the same

time, the user also will feedback one or more Channel-Quality-Indicator (CQI) values to indicate the corresponding SINRs for link adaptation purposes.

One of the key improvements of the LTE spectral efficiency is through the use of a code-book based unitary precoding, also known as per user unitary and rate control (PU2RC) [9][10][14]. In this code-book based scheme, a UE only needs to find out the most suitable matrix (usually capacity maximising) from the codebook and feed back the index to the BS. Thus, this scheme keeps the overhead and system complexity at a reasonable level but with considerable improvement in performance. One of the requirements for the pre-coder is that it must be unitary and orthogonal. The proposed unitary pre-coder for LTE is the Discrete Fourier Transform (DFT) precoder given in [9][10]:

$$e_{n_t}^{(l)} = \frac{1}{\sqrt{N_t}}\left[w_{0n_t}^{(l)} \cdots w_{(N_t-1)n_t}^{(l)}\right]^T \tag{7-1}$$

$$w_{n_r n_t}^{(l)} = \exp\left\{j\frac{2\pi n_t}{N_t}\left(n_t + \frac{l}{L}\right)\right\} \tag{7-2}$$

where N_t is the number of antenna, N_r is the number of receivers, $n_t = \{1,..., N_t\}$, $n_r = \{1,..., N_r\}$ and L is the codebook size. By using (7-2) and (7-3), the pre-coder matrices sets (also known as the codebooks) of size 2 and 4 are generated and are shown in Table 7-1. These codebooks are only used in the case of 2 antennas. For 4 antennas codebooks, the reader is referred to [13]. According to [3], only a codebook size, L= 2 is supported at the moment, a codebook size of 4 is simulated for comparison and evaluation purposes.

Table 7-1: Codebook for precoding

Codebook size, $L = 2$	Codebook size, $L = 4$
$E_0 = \frac{1}{\sqrt{2}}\begin{bmatrix}1 & 1\\ 1 & -1\end{bmatrix}$	$E_0 = \frac{1}{\sqrt{2}}\begin{bmatrix}1 & 1\\ 1 & -1\end{bmatrix}$
$E_1 = \frac{1}{\sqrt{2}}\begin{bmatrix}1 & 1\\ j & -j\end{bmatrix}$	$E_1 = \frac{1}{\sqrt{2}}\begin{bmatrix}1 & 1\\ \frac{1}{\sqrt{2}}(1+j) & \frac{1}{\sqrt{2}}(-1-j)\end{bmatrix}$
-	$E_2 = \frac{1}{\sqrt{2}}\begin{bmatrix}1 & 1\\ j & -j\end{bmatrix}$
-	$E_3 = \frac{1}{\sqrt{2}}\begin{bmatrix}1 & 1\\ \frac{1}{\sqrt{2}}(-1+j) & \frac{1}{\sqrt{2}}(1-j)\end{bmatrix}$

Some important properties of the LTE codebook [26] include:

Constant modulus property: The LTE precoders consist of pure phase correction, which involve no amplitude changes. This will ensure the power amplifier (PA) that is connected to each antenna is loaded equally.

Nested property: To fulfil the Nested property, the codebooks of different ranks are arranged in such a way that the lower rank codebook is a subset of the higher rank codebook vectors. In LTE, rank is used to denote the number of layers in transmission. This important property will simplify the CQI calculation across different ranks. This will further reduce the number of calculations required for the UE to generate the feedback.

Minimal complex multiplication: The 2-antenna codebook consists only of QPSK alphabets like ± 1 and $\pm j$ with magnitude of $1/\sqrt{2}$. This will eliminated the need for any complex multiplication.

The selection of the DFT based precoder is threefold:

- Simplicity in the CQI feedback calculation, where it can be done in some cases without complex multiplications.
- The characteristic of a highly correlation channel can be better captured by a DFT matrix [26]. [32] has shown that a DFT-based codebook can achieve a good performance especially in highly correlated channels.
- There is no need to store the codebook table as the codebook can be easily reconstructed.

In a MIMO-OFDM precoding system with full CSI available at the base station, the optimal linear precoding matrix can be obtained by using the singular value decomposition method (SVD). Therefore, this method is considered for comparison purposes and as a reference for optimal performance for the case of SU-MIMO. SVD converts MIMO channels into multiple parallel SISO eigen-channels with signal powers given by the eigenvalues. Capacity can be maximised by allocating power amongst the sub-streams according to the water filling principle. However, this method requires full channel estimation information at the transmitter, which is not spectrally efficient and not practical in a system design.

On top of the codebook based unitary precoding there is an additional option called cyclic delay diversity [13][27] (CDD). This technique adds antenna-specific cyclic time shifts to artificially create temporal dispersion of the received signal and prevents signal cancellation caused by the close spacing of the transmit antennas. This is not considered in this thesis but is discussed in future work (Section 8-3).

7.3 SU-MIMO and MU-MIMO in LTE

Spatial Multiplexing employs multiple antennas at the transmitter and the receiver to provide simultaneous transmission of multiple parallel data streams over a single radio link. Conventionally, the parallel data streams are intended for a single user only. This is often known as Single-User MIMO (SU-MIMO). However, this is not ideal to achieve the channel capacity when the channel is ill-conditioned, or highly correlated. SU-MIMO requires decorrelation between the spatial signatures of the antennas, which in turn requires a rich scattering multipath propagation environment. In a LOS situation, a strong correlation between spatial signatures is expected. This will limit the use of spatial multiplexing and degrade the overall system throughput.

By scheduling different UEs on different spatial streams over the same time frequency resource, additional diversity can be exploited in the spatial domain besides the diversity in the time and frequency domains. This is referred to as MU-MIMO and can give more flexibility to the scheduler. One of the advantages of the MU-MIMO is the decorrelation between the signatures of the different UEs, which occurs naturally due to the large separation (very large in terms of wavelength) between the UEs. MU-MIMO can also be referred to as Spatial Division Multiple Access (SDMA) and is expected to achieve the most overall system performance gain. MU-MIMO does not require much added complexity at the UEs and the burden of spatially separating the UES lies at the base station. Although the advantage of MU-MIMO over SU-MIMO is clear, the advantage comes at a price. One of the main challenges in making MU-MIMO feasible for real world application is devising a mechanism to allow for accurate channel state information to be delivered to the base station in a resource efficient manner. In LTE, this is possible through a codebook based unitary precoding. The configuration of the proposed MU-MIMO is shown in Figure 7-2. In the simulation setup, there are up to K number of users. Each user will feedback CQI information and a preferred precoding matrix index for each PRB to a controller in base station. The feedback information is used in user grouping, scheduling and modulation and coding selection. Users who select

the same precoding matrix will be grouped together. The scheduling process and feedback mechanism will be described in details in following section.

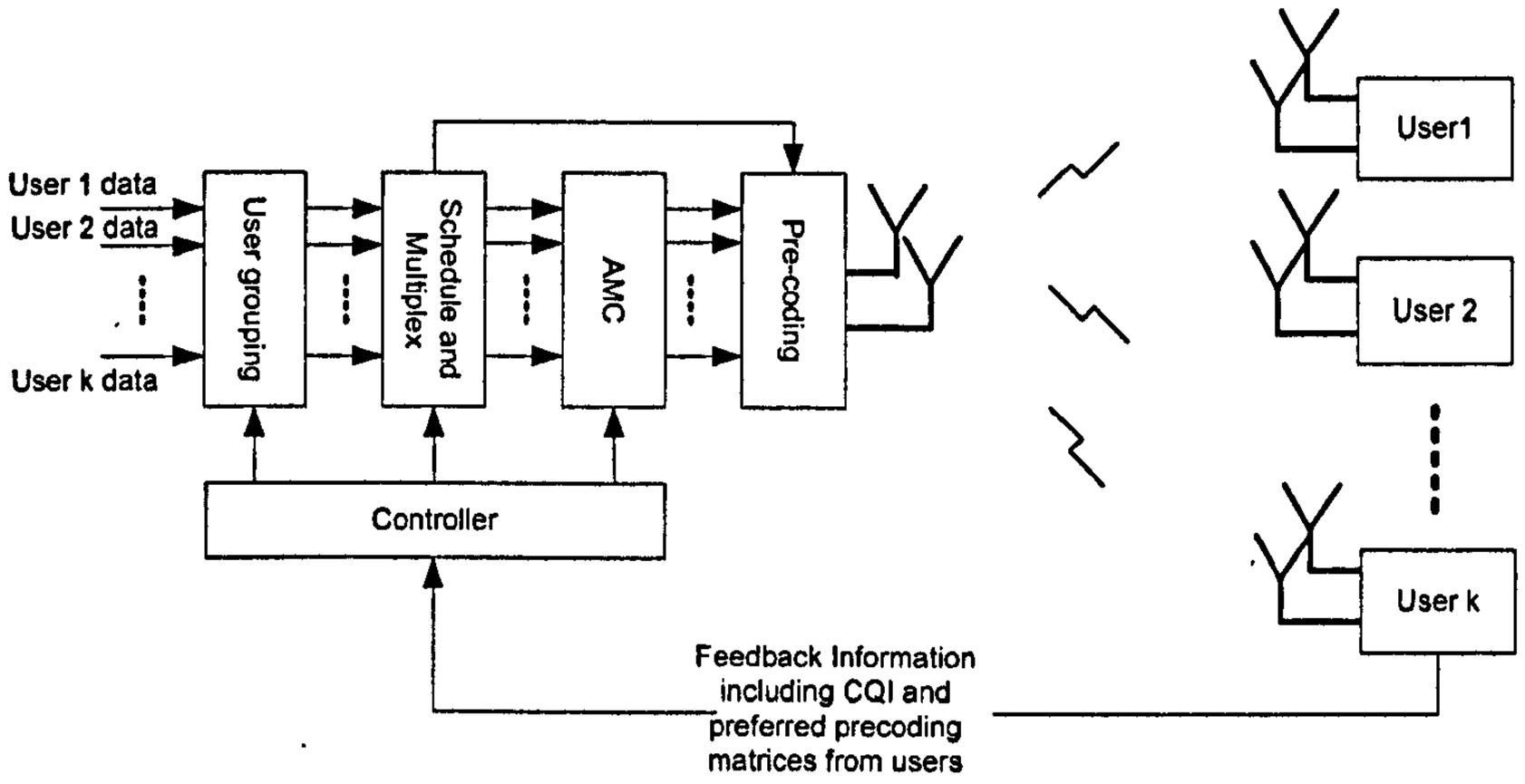

Figure 7-2: Configuration of MU-MIMO System

Assuming perfect timing and synchronization, the received signal at the UE for the *k*th PRB can be represented by:

$$Y(k) = H(k)E(k)X(k) + N(k) \tag{7-3}$$

where $H(k)$ is the complex channel between the transmitter and receiver antennas, $E(k)$ is the precoding matrix, $X(k)$ is the transmit vector and $N(k)$ is the additive white Gaussian noise which can be modelled as independent and distributed according to $CN(0,N_0)$. In MIMO detection, a linear receiver is designed to detect the transmitted data. Zero Forcing (ZF) or Minimum Mean Squared Error (MMSE) detection criteria are often used. The linear MMSE receivers can be obtained from [11]:

$$G_{(k)}^{MMSE} = [E(k)'H(k)'H(k)E(k) + (QN_0/\varepsilon_s)I_Q)]^{-1} E(k)'H(k)' \tag{7-4}$$

where Q is the number of data streams, ε_s is the total transmit energy. The received signal $Y(k)$ is then multiplied by $G(k)$ to obtain the detected data stream, $\hat{S}(k)$ for the *k*th PRB.

$$\begin{aligned} \hat{S}(k) &= G(k) * Y(k) \\ &= \hat{X}(k) + \hat{N}(k) \end{aligned} \tag{7-5}$$

For a MIMO system, the MIMO channels have subspaces that can transmit Q data streams through the parallel sub-channels. The number of data stream is limited by the number of transmit and receive antennas and thus Q is often $\leq N_r$ and N_t. In this work, N_t =2 and N_r =2 are assumed and the number of data stream that is supported, Q is 2. For

each data stream q at every RRB, the UE s computes the effective SINR. The SINR associated with each data stream is directly proportional to the eigenvalues of the channel matrix *H(k)*. The SINR for each data stream can be calculated from [11]:

$$SINR_q^{(ZF)} = \frac{\varepsilon_s}{QN_o[E(k)'H(k)'HE]^{-1}} \tag{7-6}$$

$$SINR_q^{(MMSE)} = \frac{\varepsilon_s}{QN_o[E(k)'H(k)'H(k)E(k)+(QN_O/\varepsilon_s)I_Q]^{-1}} - 1 \tag{7-7}$$

In order to obtain a good performance with reasonably complexity, a linear MMSE receiver is adopted at the UE in this work unless otherwise stated. In the case of SU-MIMO, both the spatial streams will go to the same UE. Thus in this work, the allocation is proposed to be based on the sum of achievable capacity of both spatial streams. The achievable data rate for PRB k is given by:

$$r_k = \sum_{q}^{\min(N_t,N_r)} \log_2(1+SINR_q) \tag{7-8}$$

The scheduler then uses this feedback information to allocate the PRB to the UE with the highest achievable data rate r_k. Compared to SU-MIMO, the scheduling is slightly complicated for the decision to choose the best precoding matrix in MU-MIMO. In order to maximize the system capacity of MU-MIMO, a most suitable precoding matrix needs to be selected from the codebook to transmit on each PRB. Based on the chosen precoding matrix, a simple greedy algorithm is employed to select the users with best channel. The selected users will then be precoded to share the same time and frequency resources to maximize the system capacity.

Since each of the spatial streams can be allocated and scheduled independently in MU-MIMO, the UE k calculates the data rate of each spatial layer and feeds it back to the BS. The data rate is calculated on a PRB basis by using:

$$r_k^q = \log_2(1+SINR_q) \tag{7-9}$$

Again, for every PRB, the scheduler allocates each spatial layer to a UE, which has the best channel conditions for the corresponding layer.

7.3.1 Feedback Schemes in MU-MIMO

Though MU-MIMO offers greater flexibility in the spatial domain, it requires additional signalling overhead for different spatial layers and for the preferred precoding matrix. The complexity of resource allocation at the base station is also inevitably increased.

In order to maximize the capacity of a precoded system, a suitable precoding matrix is chosen based on the feedback from the UEs. In the UE, the preferred precoding matrix for a PRB is chosen by selecting the highest sum of SINR that can be achieved by the UE. Two feedback strategies, namely a full feedback scheme and a partial feedback scheme are considered and compared.

In the full feedback scheme, an UE feedbacks a channel quality indicator (CQI) value for every matrix in the codebook, which gives more flexibility and accurate CQI information for scheduling. In the partial feedback scheme, the UE only feedbacks a CQI value for the preferred matrix. Based on the feedback, the BS then choose the precoding matrix which has the highest sum of average SINR of all the spatial layers. This process is repeated for each PRB.

However, when the preferred precoding matrix for a particular user is different from the chosen precoding matrix, the feedback SINR information is no longer accurate. In the full feedback scheme, the corresponding SINR is known to the scheduler since SINRs for all precoding matrices are fed back. This is not the case for the partial feedback scheme as only the SINR of the preferred precoding matrices is fed back. Only the users who declare the same preferred matrix are eligible for selection in the partial feedback scheme.

In the case of MU-MIMO, the amount of feedback increases by Q times compared to SU-MIMO, depending on the number of spatial layers. In the full feedback scheme, the amount of feedback is further increased L fold, where L depends on the size of the codebook. In practice, a partial feedback strategy will be used where only the CQI value of the best precoding matrix is fed back [26].

In the early stage of LTE standardization, it was proposed that 5 bits quantization be used to represent each CQI [16], with only very marginal performance degradation compared to perfect channel state information. However, it was later decided otherwise [25]. In LTE, the reported CQI is not a direct indication of received SINR of the UE. Instead a UE reports the highest MCS that it can decode with a packet (block) error rate of less than 10%. The feedback information received by the base station takes into account of

the receiver characteristics. UEs with advanced signal processing algorithms, e.g interference cancellation techniques or MMSE estimation can report a higher channel quality. Depending on the characteristics of the base station scheduler, a UE can receive a higher data rate and thus better performance.

Assuming 4 bits are used to represent the quantized MCS levels, feedback overhead for each physical resource block for various MIMO schemes are shown in Table 7-2. However it should be noted that in the link level simulation used in this chapter, a perfect SINR feedback is assumed.

Table 7-2: Feedback overhead for various MIMO schemes for L=2 and Q=2

	Preferred Layer 1 CQI	Preferred Layer 2 CQI	Alternative Layer 1 CQI	Alternative Layer 2 CQI	Preferred Matrix index	Total bits per PRB
MUMIMO Full Feedback Scheme	4 bits	4 bits	4 bits	4 bits	1 bits	17 bits
MUMIMO Partial Feedback Scheme	4 bits	4 bits	-	-	1 bits	9 bits
SUMIMO Feedback Scheme	4 bits		-		1 bits	7 bits

7.3.2 Theoretical Analysis

7.3.2.1 SU-MIMO and MU-MIMO System Capacity

As mentioned in the previous chapters, as the number of users in a system increases, the multiuser diversity gain will increase accordingly. If a scheduler selects the user with the maximum Shannon capacity among the users waiting to be scheduled, the overall system capacity can be increased. The capacity of a SU-MIMO system with equal power allocation can be given as:

$$C_{SU-MIMO} = \max_{k}\left[\sum_{i=1}^{\min(N_t,N_r)} \log_2(1+SINR_i)\right] \tag{7-10}$$

N_r and N_t are the number of receive antennas and transmit antenna where N_r =2 and N_t =2 are assumed. K is the number of users. The SINR for each stream is calculated from Equation 7-7. The theoretical capacity that can be achieved in SU-MIMO can be given by a SVD precoding matrix (Equation 2-19), which requires full channel information at the transmitter.

In this section, the possible capacity enhancement brought by MU-MIMO with unitary precoding is evaluated. The capacity of the MU-MIMO depends on the received SINR of the scheduled users. It can be given as:

$$C_{MU-MIMO} = \sum_{i=1}^{\min(N_t,N_r)} \underset{k}{Max} \left[\log_2(1+SINR_i)\right] \qquad (7\text{-}11)$$

Similarly, the received SINR for each stream is calculated from Equation 7-7. The capacity equation can be applied to both the full and partial feedback schemes. The difference between these two schemes depends on the scheduling process, which essentially depends on the feedback information from the users.

One of the potential issues with the partial feedback schemes is that, for a small number of users, a large codebook does not have any advantage over a smaller codebook. When the codebook gets larger, the number of users selecting a same codebook matrix will be less. Since only the users who select the same precoding matrix can be scheduled on the same time and frequency resource, the larger codebook will in fact achieve less multiuser diversity gain in the partial feedback scheme. For the full feedback scheme, a larger codebook does not have this limitation.

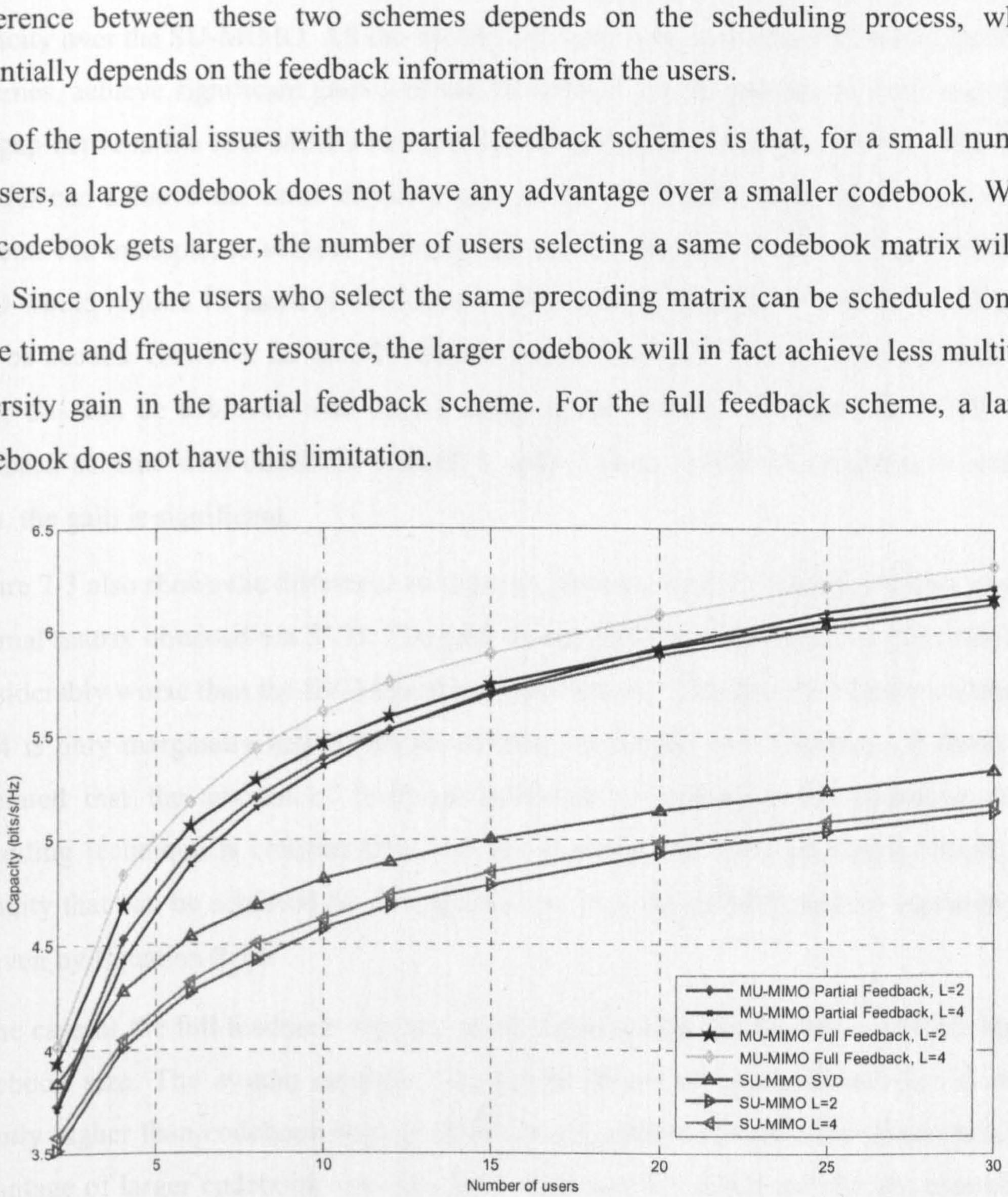

Figure 7-3: Average system capacity for SU-MIMO and MU-MIMO as a function of number of users

Figure 7-3 shows the average system capacity for SU-MIMO and MU-MIMO as a function of number of users. $N_t = 2$, $N_r = 2$, and a SNR of 5dB are assumed to plot the theoretical results. Similarly to previous chapters, a 10MHz system with 50 PRBs is assumed. All the users are assumed to have independent Rayleigh fading channels. A linear MMSE detector is assumed and no dynamic power allocation is employed. As described earlier, a greedy approach is employed for both the full and partial feedback schemes.

The main observation from the Figure 7-3 is the significant gain of MU- MIMO system capacity over the SU-MIMO. All the MU-MIMO schemes, including the partial feedback schemes, achieve significant gain over the SU-MIMO. As the number of users increases, the gap between the MU-MIMO and the SU-MIMO system capacity widens. The MU-MIMO can achieve the same capacity gain as the SU-MIMO with fewer users in the system. For example, to achieve a theoretical system capacity of 5bits/s/Hz, SU-MIMO SVD would require 15 users in the system. In the case of SU-MIMO with $L = 2$, 23 users will be needed. However for the MU-MIMO partial feedback scheme with codebook size of 2, this can be achieved with only 7 users in the system. For the MU-MIMO full feedback scheme with codebook size of 4, only 5 users would be required. As can be seen, the gain is significant.

Figure 7-3 also shows the difference in capacity between the DFT-based precoder and the optimal matrix obtained via SVD. The gain by the DFT-based precoder in SU-MIMO is considerably worse than the SVD based precoder matrix. The gain by a larger codebook, $L = 4$ is only marginally better than the smaller codebook, $L=2$. However, it should be reiterated that the amount of feedback information needed by the codebook based precoding technique is considerably less. By applying the SVD precoding matrix, the capacity that can be achieved by SU-MIMO can meet the MIMO capacity equation that is given by Equation 2-18.

In the case of the full feedback scheme, more capacity gain can be achieved for a higher codebook size. The system capacity that can be achieved by codebook size, $L = 4$ is slightly higher than codebook size, $L = 2$ for small number of users. For more users, the advantage of larger codebook size increases. However this holds true for the case of the full feedback scheme only.

For the partial feedback scheme, the capacity gain of a codebook size 2 outperforms the gain of codebook size 4. This is due to the lower multiuser diversity gain that can be

achieved by the larger codebook size, due to limited feedback information at the scheduler. However when the number of users is large enough, the capacity gain of the codebook size 4 will overtake the capacity gain of codebook size of 2. This occurs when the number of users is more than 15. The gain of codebook size of 4 (partial feedback) also outperforms the codebook size of 2 (with the full feedback scheme), when there is sufficient large number of users, approximately 20 in this case.

However, the full feedback scheme with codebook size of 4 significantly outperform the partial feedback scheme with codebook size of 4, due to the availability of full channel information of all the spatial layers for all codebook entries. It is envisaged that for a larger codebook, the performance of the full feedback scheme will increase further. However, the feedback information will also increase considerably. This is undesired as this will significantly reduce the spectral efficiency in the uplink. This justifies the selection of a small size codebook in LTE, as it trades off between performance gain and feedback overhead.

7.3.2.2 Power Reduction by MU-MIMO

Environmental issues and the need to reduce energy consumption for lowering operating costs have pushed power efficiency to become one of the major issues of current research in the field of wireless networks [19]. In this section, it will be shown how the exploitation of multiple antenna techniques and multiuser diversity in both the time, frequency as well as the space domain can bring a possible power reduction at the base station.

In order to better evaluate the performance gain of the MU-MIMO over a conventional SISO system, the performance gain of MU-MIMO over a single user SISO system is analysed and presented. Figure 7-4 shows the theoretical results of the performance gain of a multiuser SISO and MIMO schemes over the single user SISO system, as a function of the number of users at a fixed spectral efficiency of 3bps/Hz. The fixed spectral efficiency of 3bits/s/Hz is a fairly arbitrary but reasonable choice which can be achieved in LTE by higher order modulation schemes, e.g. 64QAM with coding. Thus this enables a comparison between theoretical and simulation results in later sections.

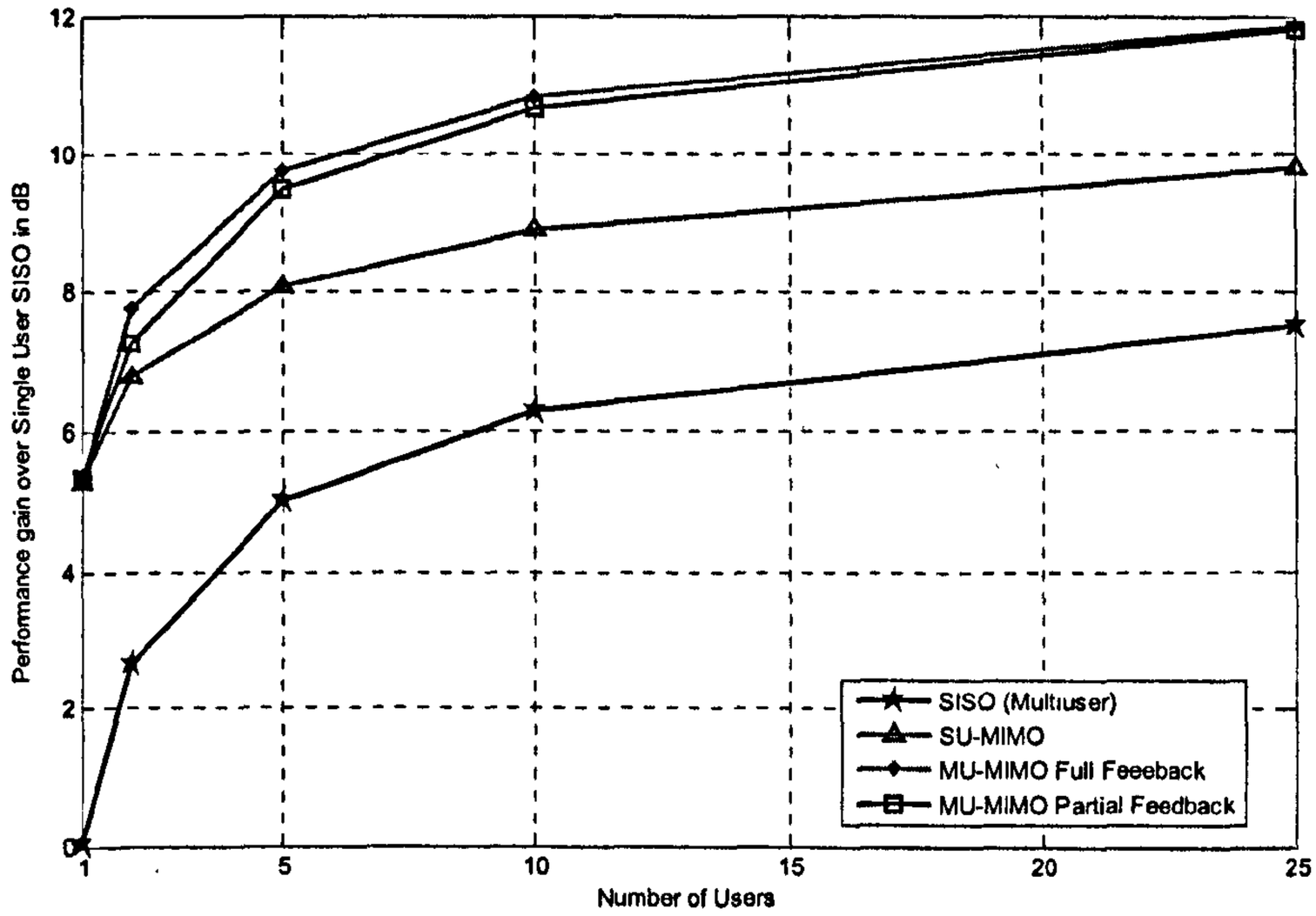

Figure 7-4: Performance gain of Multi-user SISO and MIMO schemes over the single user SISO at 3bps/Hz

First of all, it can be observed from Figure 7-4 that MIMO schemes have an advantage of more than 5 dB over a SISO scheme to achieve a spectral efficiency of 3bits/s/Hz in a single user scenario. To achieve higher values of spectral efficiency, MIMO schemes would have even higher advantages over SISO. This is due to the fact that MIMO techniques such as Spatial Multiplexing can increase the channel capacity by transmitting parallel signals through the MIMO channels. Thus the increase in channel capacity as a function of SNR for MIMO is higher than the SISO scheme, especially at high SNR. This can be also shown in Figure 2-10 and Figure 2-12.

The multiuser SISO and all the MIMO schemes benefit from multiuser diversity and show improved power efficiency as the number of users increases. In comparison to a single user scenario, the multiuser SISO achieves the highest multiuser diversity gain among all the considered schemes. Up to 7dB gain can be achieved in the case of 25 users. The SU-MIMO on the other hand achieves the least multiuser diversity gain. Despite that, up to approximately 4.5dB can be achieved for a 25 user scenario. MU-MIMO achieves more multiuser user diversity through the additional layer of spatial diversity. By exploiting the additional diversity at the space domain, up to approximately 6.5dB can be achieved..

Nevertheless, MU-MIMO remains the most power efficient scheme. Compared to the single user SISO, nearly 12dB gain can be achieved by employing MU-MIMO in the 25

users scenario. On the other hand SU-MIMO can achieve nearly 10dB gain. The performance gain over the single user SISO scenario can be translated into a power saving at the BS. Theoretical results [20][21] show that depending on the degree of multiuser diversity exploitation, transmit power from the BS could be significantly reduced, whilst attaining the same average service levels.

7.4 MIMO Physical Layer Performance Analysis for LTE with Precoding

This section presents a link level analysis on the performance of both Single User (SU) MIMO and Multi User (MU) MIMO with codebook based unitary precoding in the downlink of LTE. All the physical layer simulation parameters remain unchanged from Chapter 6. As shown in Figure 7-2, a 2x2 MIMO configuration is considered. A SCME urban macro scenario is assumed and will be used throughout this section unless otherwise state. In the simulation, a channel remains the same during a packet transmission. 2000 independently and identically distributed (i.i.d.) channel realisations are considered in each simulation. Perfect channel state information is assumed and the feedback channel is also assumed to be error free.

7.4.1 Comparison between precoding and SVD

First of all, the performance of the LTE defined unitary precoding is compared to the SVD based precoding in a single user scenario to investigate the gain that can be obtained by applying the precoding matrix. It should be noted that in the simulation, 12 adjacent subcarriers are grouped to form a subchannel (PRB) and the same precoding matrix is shared among all the subcarriers. Figure 7-5 shows the PER performance of SM with unitary precoding in comparison to the SVD and non-precoded system for the QPSK 1/3 rate transmission mode. From the figure it can be seen that unitary precoding of codebook size 2 outperforms the non-precoded system by less than a 1dB. Unitary precoding of codebook of size 4 performs slightly better than the codebook of size 2 due to richer selection of precoding matrices. SVD, on the other hand offers the best performance but full channel state information is required at the base station. As shown in Figure 7-6, the gain of the precoding and SVD decreases for QPSK 1/2 coding rate. The gain further diminishes for QPSK ¾ coding rate. It can be concluded that precoding performs well with a more robust channel coding especially for the case of SVD. Robust

channel coding can reduce the errors of the weak sublayer and the performance enhances with the presence of precoding. No multi-user diversity is considered in this scenario at this stage. That will be investigated in the following section.

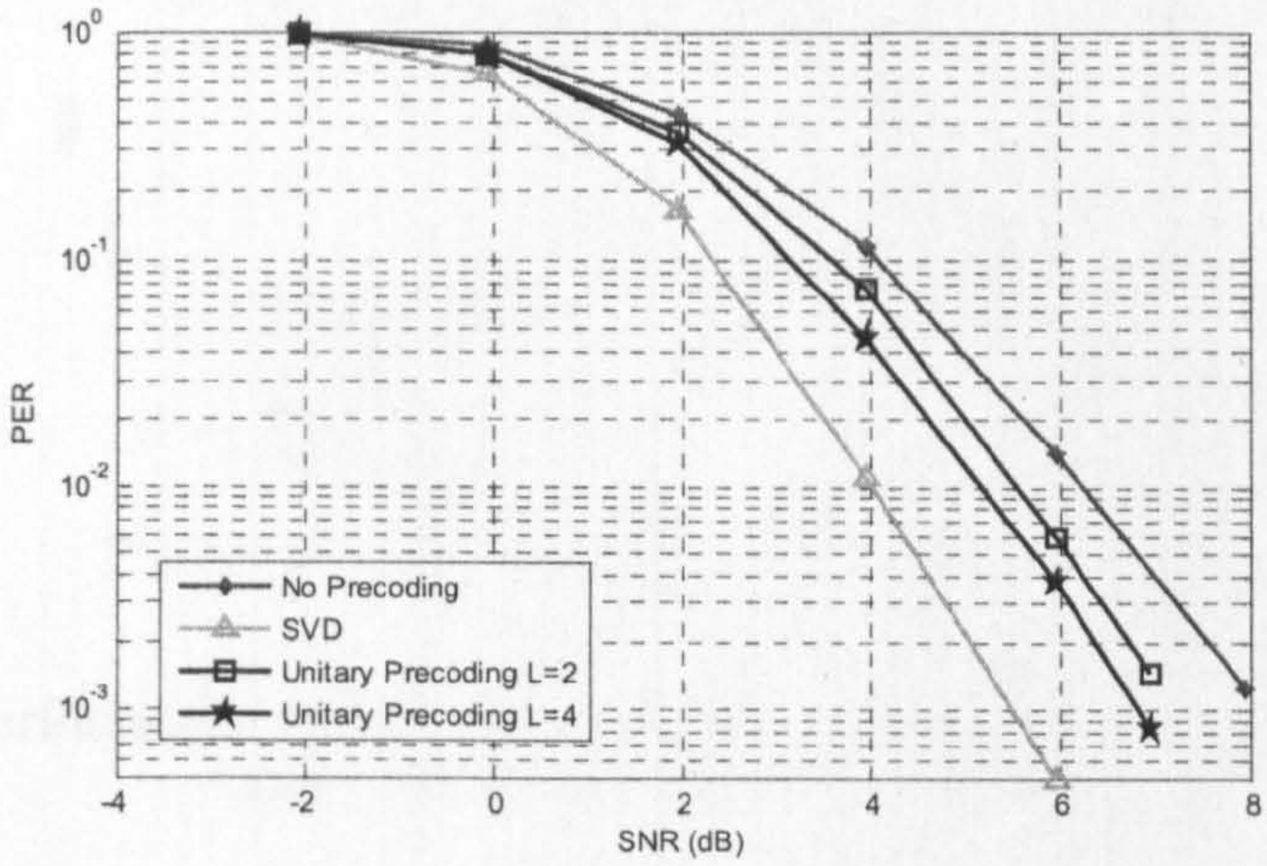

Figure 7-5: Performance comparison for LTE precoded system with SVD and non-precoded system for QPSK 1/3 rate

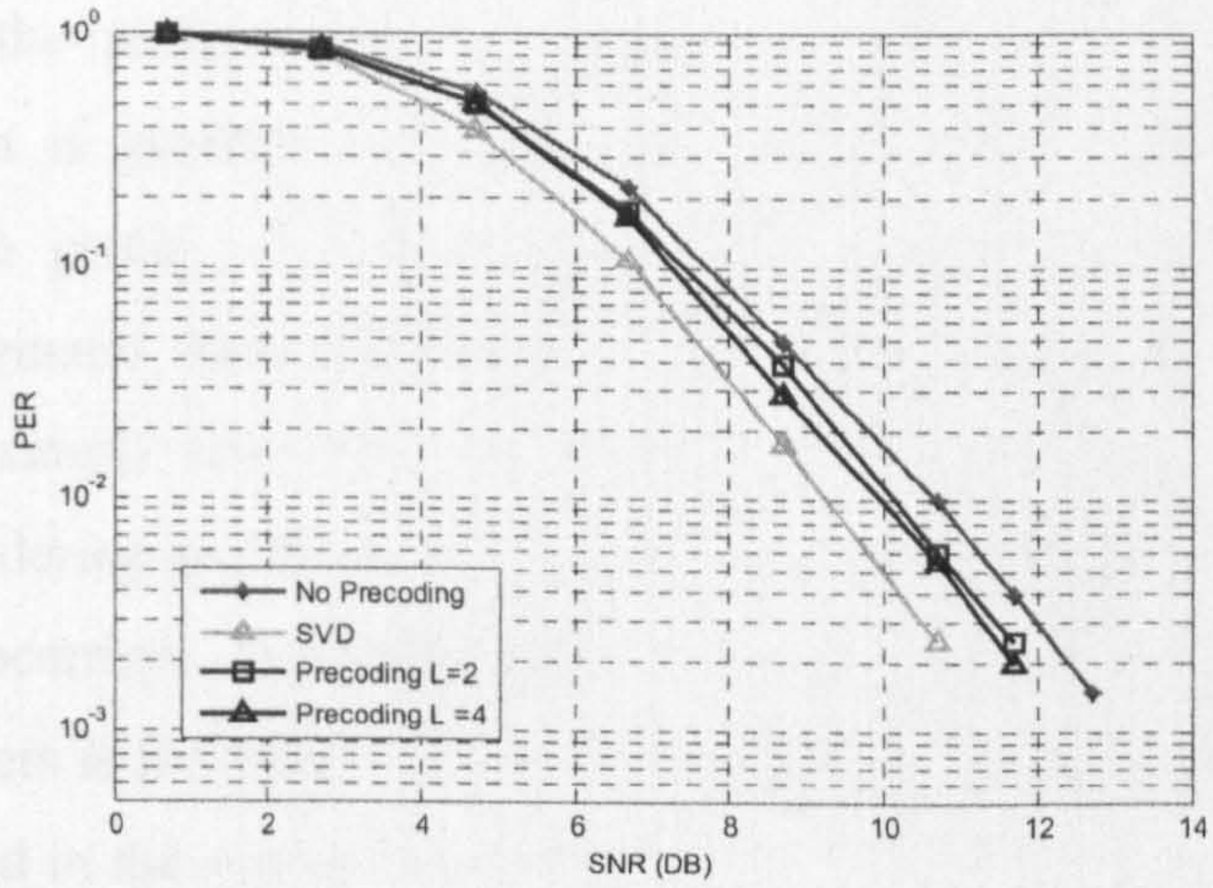

Figure 7-6: Performance comparison for LTE precoded system with SVD and non-precoded system for QPSK 1/2 rate

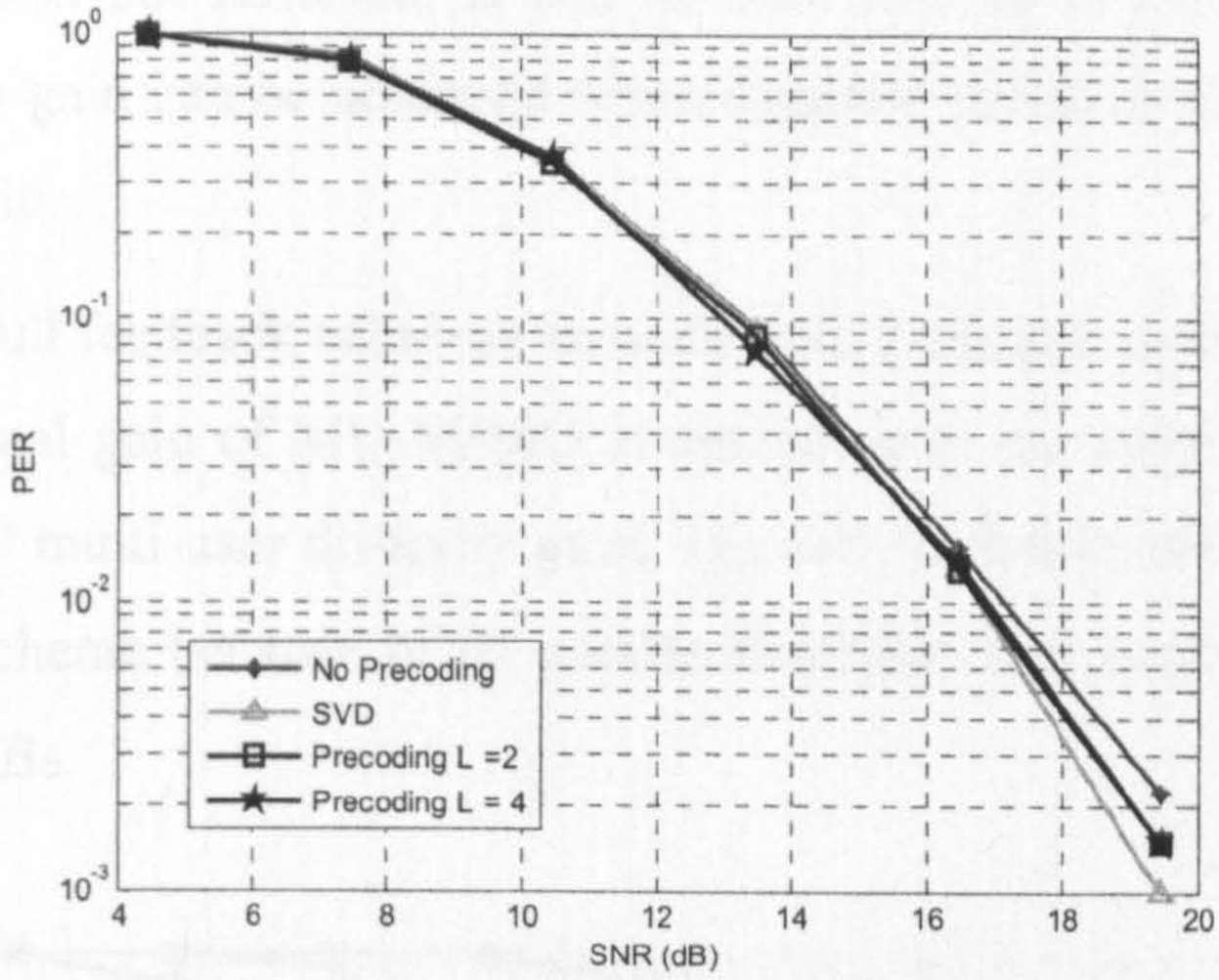

Figure 7-7: Performance comparison for LTE precoded system with SVD and non-precoded system for QPSK 3/4 rate

7.4.2 Performance of SU-MIMO and MU-MIMO

In this section, the performance of dynamic sub-channel (PRB) allocation in the frequency domain is presented for both SISO and MIMO schemes. To obtain the maximum gain, a greedy algorithm is employed to exploit the inherent multi-user diversity that originates from the frequency selectivity of the wideband channel. The greedy algorithm simply allocates a PRB to a user with the highest channel gain or data rate without considering any fairness constrain. As mentioned earlier, each PRB consists of 12 adjacent subcarriers. A single CQI which is based on the average quality of the 12 grouped sub-carriers is fed back for each PRB and is assumed to be perfectly known. 10 users are simulated in the system unless otherwise stated. Due to the high computational complexity and the insignificant gain of power control in the frequency domain dynamic allocation, equal power allocation is assumed throughout the simulation.

7.4.2.1 Error Performance Analysis

First of all, the multiuser gain that arises from the frequency domain dynamic allocation is evaluated for both the SU-MIMO and MU-MIMO schemes. Figure 7-8 shows the PER performance of SU-MIMO and MU-MIMO schemes employing frequency domain dynamic resource allocation for the QPSK ½ rate transmission mode. A single user SU-MIMO is simulated and shown as a reference. Similarly to previous sections, the X-axis label SNR refers to the signal to noise ratio at the receiver for the case of single user SU-MIMO scenario. The increased average SNR that can be achieved by exploiting

multiuser diversity is not reflected. It can be seen that up to (approximately) 5dB of multiuser diversity gain can be achieved when dynamic resource allocation is employed in a 10 user scenario.

MU-MIMO with full feedback achieves an additional 2 dB gain over the SU-MIMO. The significant additional gain of MU-MIMO is attributed to the ability to exploit both the spatial and spectral multi-user diversity gain. The full feedback scheme is superior to the partial feedback scheme because of its greater flexibility and accurate CQI information when selecting PRBs.

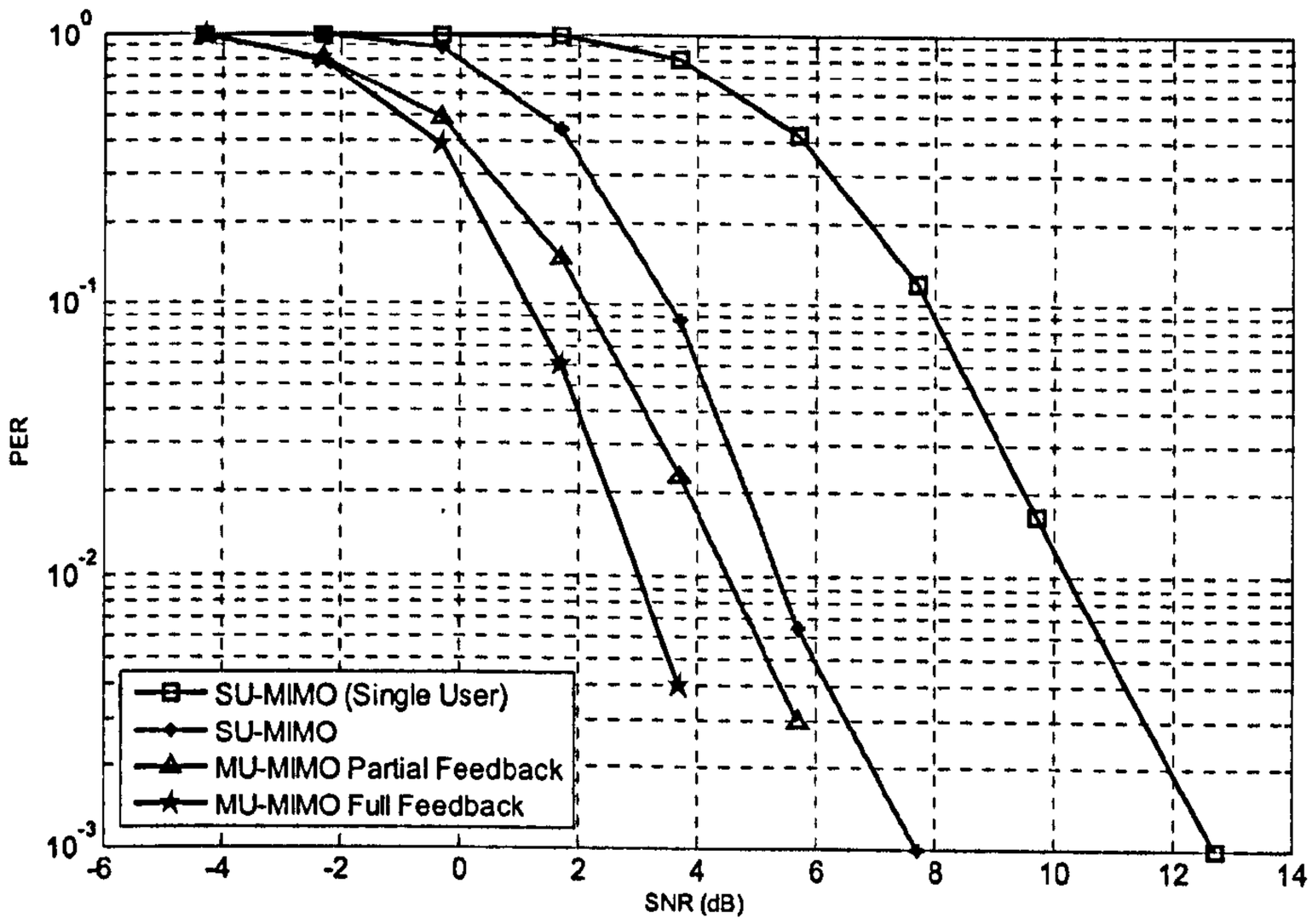

Figure 7-8: PER Performance of SU-MIMO and MU-MIMO

Figure 7-9 and Figure 7-10 show the PER performance of the SU-MIMO and MU-MIMO (with full feedback) with different number of users in the system respectively. As the number of users is increased from 1 to 25, the PER performances of both the SU-MIMO and MU-MIMO with unitary precoding improves as a result of richer spectral multi-user diversity gains. For both SU-MIMO and MU-MIMO schemes, the multiuser diversity gain increases rapidly when there is more than 1 user. However, when the number of users is getting much larger, e.g. from 10 to 25 users, the gain of multiuser diversity increases at a slower rate.

Nevertheless, in the case of MU-MIMO, more gain can be achieved through the additional dimension of diversity in the spatial domain. MU-MIMO can achieve similar

level of diversity gain even with fewer users in the system. In MU-MIMO, the multiuser diversity gain that can be achieved with 2 users is similar to the performance gain that can be achieved by 5 users in SU-MIMO. This result is consistent with the theoretical results that were presented in Section 7.3.2.1.

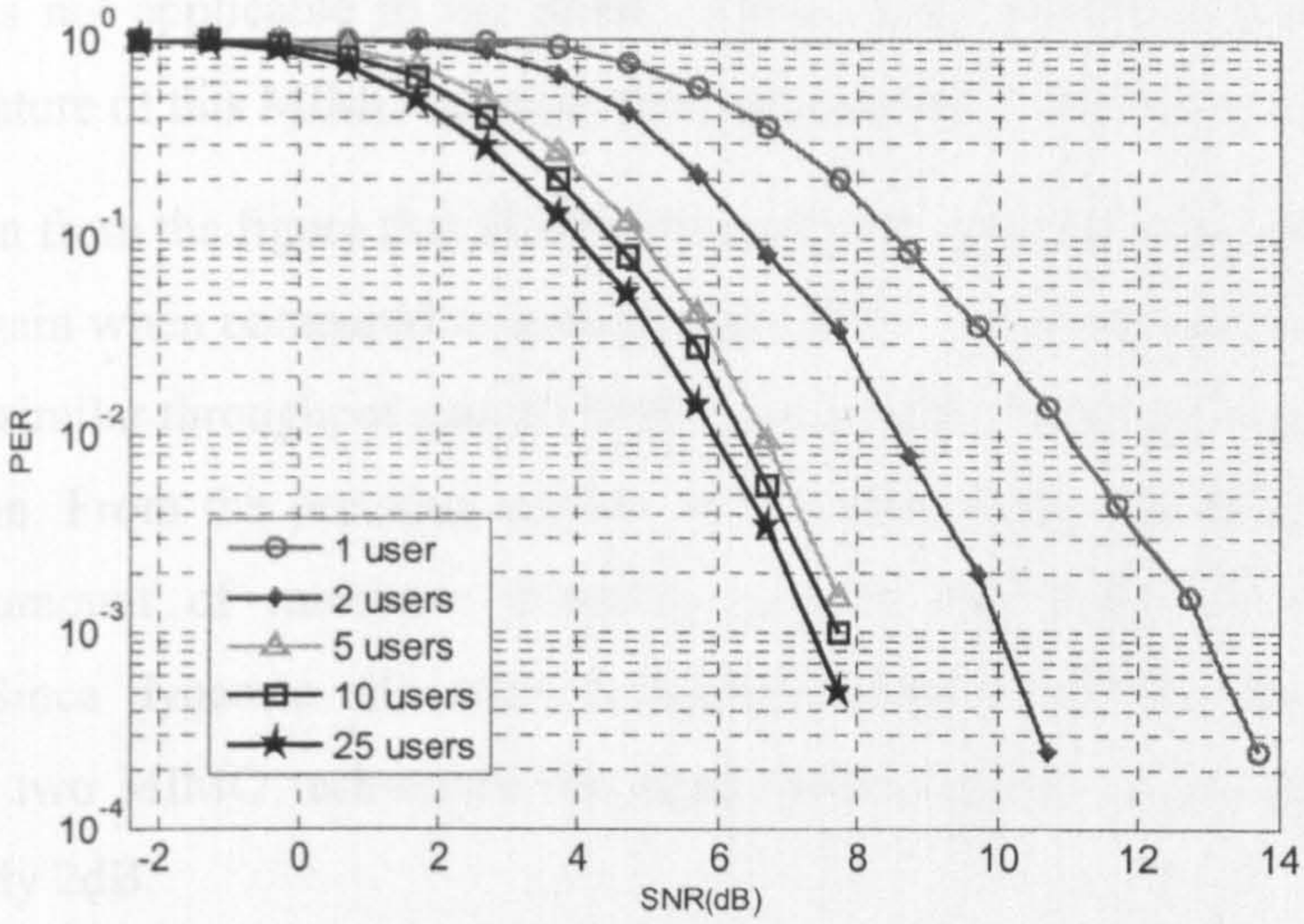

Figure 7-9: PER Performance of SU-MIMO with different number of users

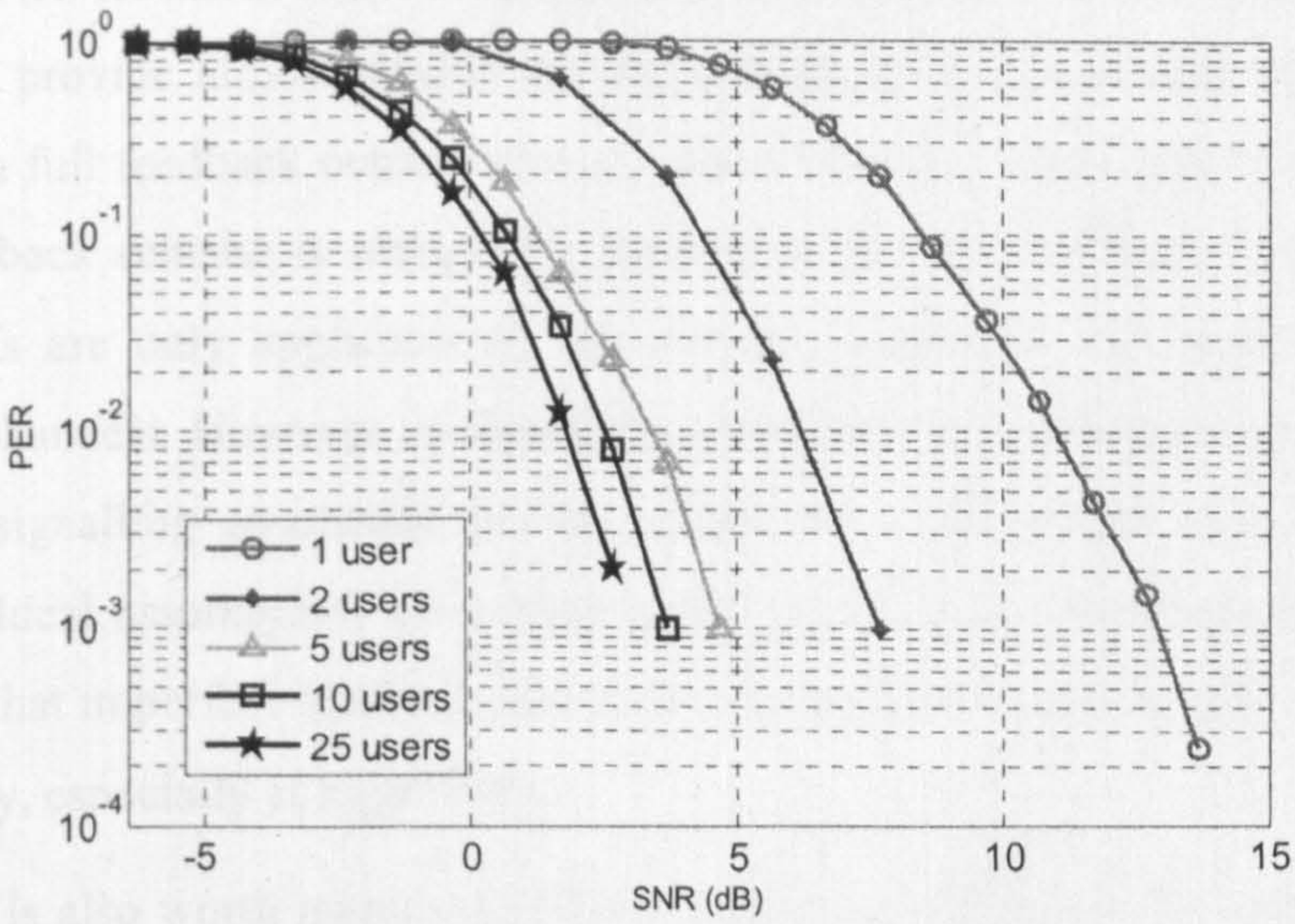

Figure 7-10: PER Performance of MU-MIMO with different number of users

7.4.2.2 Throughput Analysis

In this section, the average throughput performance of a LTE system employing frequency domain dynamic resource allocation is investigated. Figure 7-11 shows the average throughput performance of the LTE system where dynamic allocation in the

frequency domain is employed for a 10 user scenario. Similarly to previous chapters, a low correlated SCME urban macro channel model is assumed.

It is worth noting that resource allocation is not considered in the case of the SFBC scheme. This is consistent to the proposed LTE standard where channel dependent scheduling is not applicable to the SFBC scheme [30]. However, due to the diversity exploiting nature of this MIMO scheme, the performance is still very promising.

It can be seen from the figure that SISO with multiuser diversity gain achieves significant throughput gain when compared to a single user SISO scenario. In fact multiuser SISO can achieve similar throughput gain to SFBC, when SFBC does not exploit any multiuser diversity gain. From the previous section, it was shown that SU-MIMO can achieve a significant amount of multiuser diversity gain in the frequency domain dynamic allocation. Since dynamic allocation is not applicable to SFBC, the switching point between the two MIMO techniques has been shifted to a much smaller SNR value, to approximately 2dB.

The SU-MIMO allows for almost doubling the throughput of a multiuser SISO system at only high SNR. However when the additional spatial diversity can be exploited, the MU-MIMO can provide almost double the throughput across the whole SNR range. MU-MIMO with full feedback outperforms all other schemes except at very low SNRs. The partial feedback scheme is marginally inferior to the full feedback scheme. However, these results are only applicable to the scenario where all the users have very low correlated channels. However, it should be noted that MU-MIMO schemes also require additional signalling overheads in the uplink that will reduce the overall spectral efficiency. Ideal assumptions have been made regarding the feedback information. [31] has shown that imperfect feedback information deteriorate the throughput of MU-MIMO considerably, especially at high SNRs.

However it is also worth mentioning that the spectral efficiency that can be achieved in the LTE downlink is significantly less than the Shannon channel capacity. Granularities in the physical layer MCS mode selection and the different SNR ranges that arise from simulation result in different modes being selected, which is one of the reasons that explains the deviation of the performance gains from simulation results to theoretical capacity. The deviation is further caused by channel coding and coding block size [29]. Authors in [28] take into account the system bandwidth efficiency and the SNR efficiency of LTE and compare with the Shannon channel capacity.

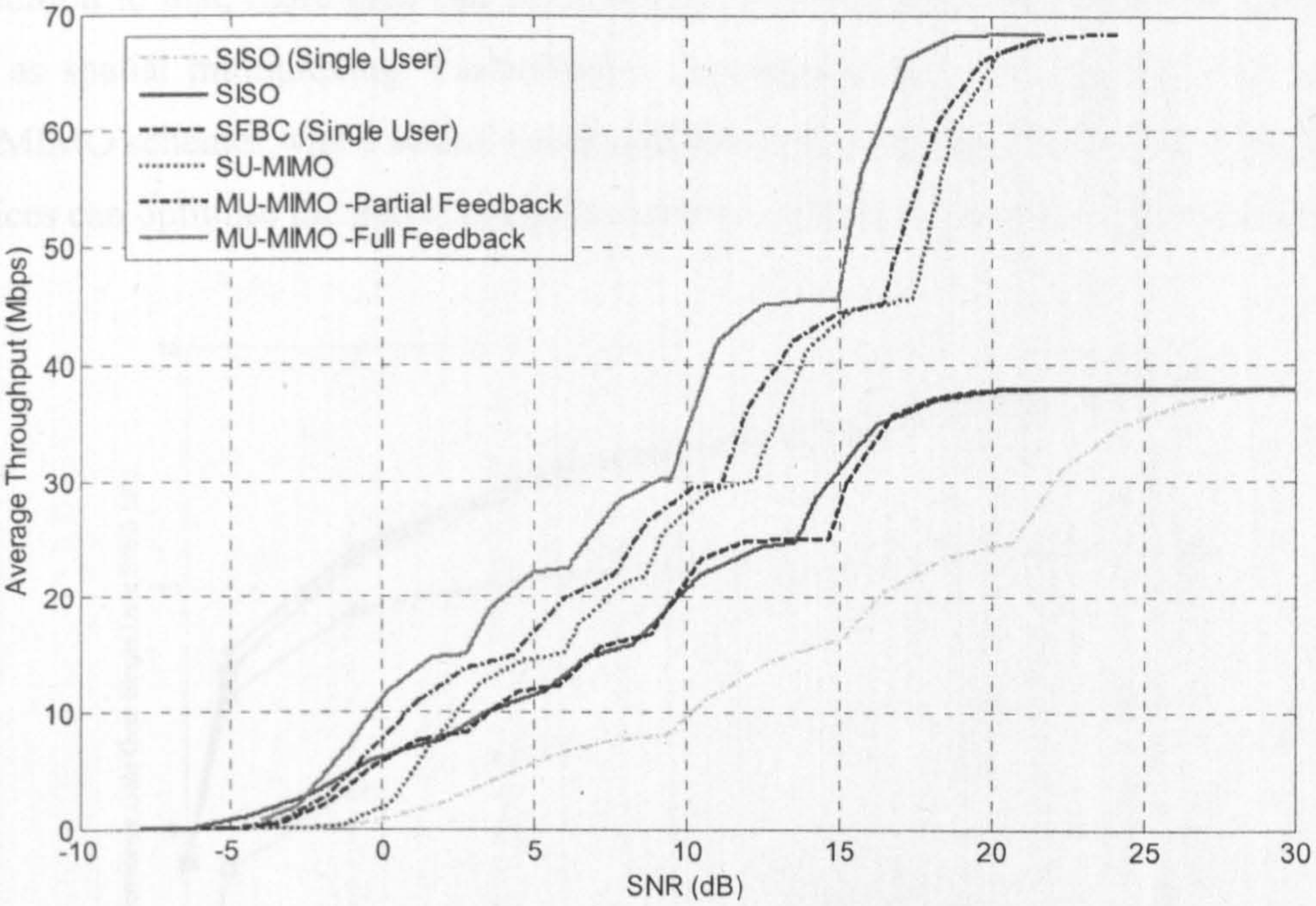

Figure 7-11: Average Throughput of SISO and MIMO schemes with frequency domain allocation at very low correlation channels

7.4.2.3 MU-MIMO Power Reduction Analysis

This section presents the simulation results of power reduction that can be achieved by MU-MIMO over a conventional single user SISO system. Theoretical analysis in Section 7.3.2.2 has shown that significant gain can be achieved by MU-MIMO schemes over the single user SISO system. It is intended in this section to compare the theoretical expectation with the simulation results in the LTE downlink. By comparing the performance gain relative to single user SISO, the performance gap between the LTE system and theoretical capacity can be essentially neglected. This enables a fair comparison of multiuser diversity gain that can be achieved in theory and by simulation.

Figure 7-12 shows the simulated results of the performance gain of multiuser SISO and other MIMO precoding schemes over a single user SISO scenario, as a function of the number of users at a fixed spectral efficiency of 3bps/Hz. The simulated results match very well with the theoretical results that were presented in Figure 7-4. Figure 7-12 shows that a significant gain is obtained by exploiting multiuser diversity, which accounts for 7-8dB of the power gain. This can be clearly observed in the SISO scenario,

where in this case, the performance gain comes solely from the multiuser diversity gain. In addition to that, more gain can be achieved by using MIMO transmission techniques such as spatial multiplexing. Furthermore, considerable gain can be achieved by both MU-MIMO schemes where additional spatial diversity is exploited. The use of precoding matrices can optimise the perceived gain in the receiver to achieve the additional gain.

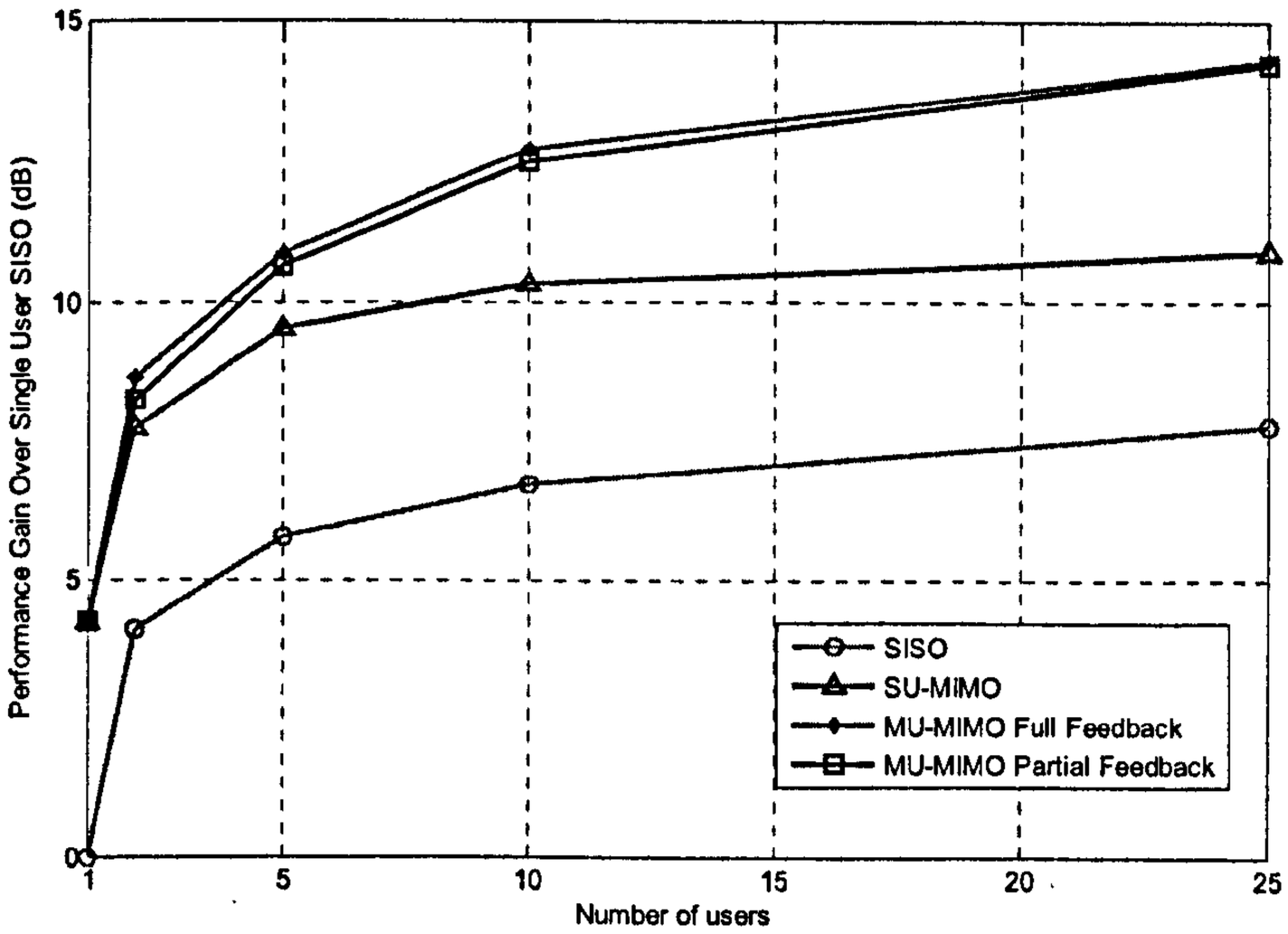

Figure 7-12: Simulated Performance Gain of Multiuser SISO and other MIMO Precoding Schemes over Single User SISO Scenario at 3bps/Hz

7.4.3 Modified Partial Feedback scheme

In the full feedback scheme, the corresponding SINR is known to the scheduler since SINR for all precoding matrices is fed back. However, this is not possible in the partial feedback scheme as only the SINR of the preferred precoding matrices is fed back. In [9], only the users who declare the same preferred matrix are eligible for selection in the partial feedback scheme. However, in order to achieve a larger multi-user diversity gain, [23] shows that a large number of users that compete in one PRB is more important than full frequency selectivity information. Thus, if those users who do not select the same precoding matrix are excluded from scheduling, then less multi-user diversity could be exploited. This is a huge concern especially when the number of users in the system is small. To address this issue, a modified partial feedback scheme is proposed and analysed in this section.

Employing a different precoding matrix at the BS will create a different perceived channel gain at the UE, which can be shown in Figure 7-13. The UE is assumed to have an average SNR of 5dB. As shown in the figure, different precoding matrices achieve peaks at different sub channels. The difference of the perceived SINR is substantial due to the fact that the data streams are transmitted with distinct phases and weightings. This observation could be potentially exploited in the partial feedback scheme.

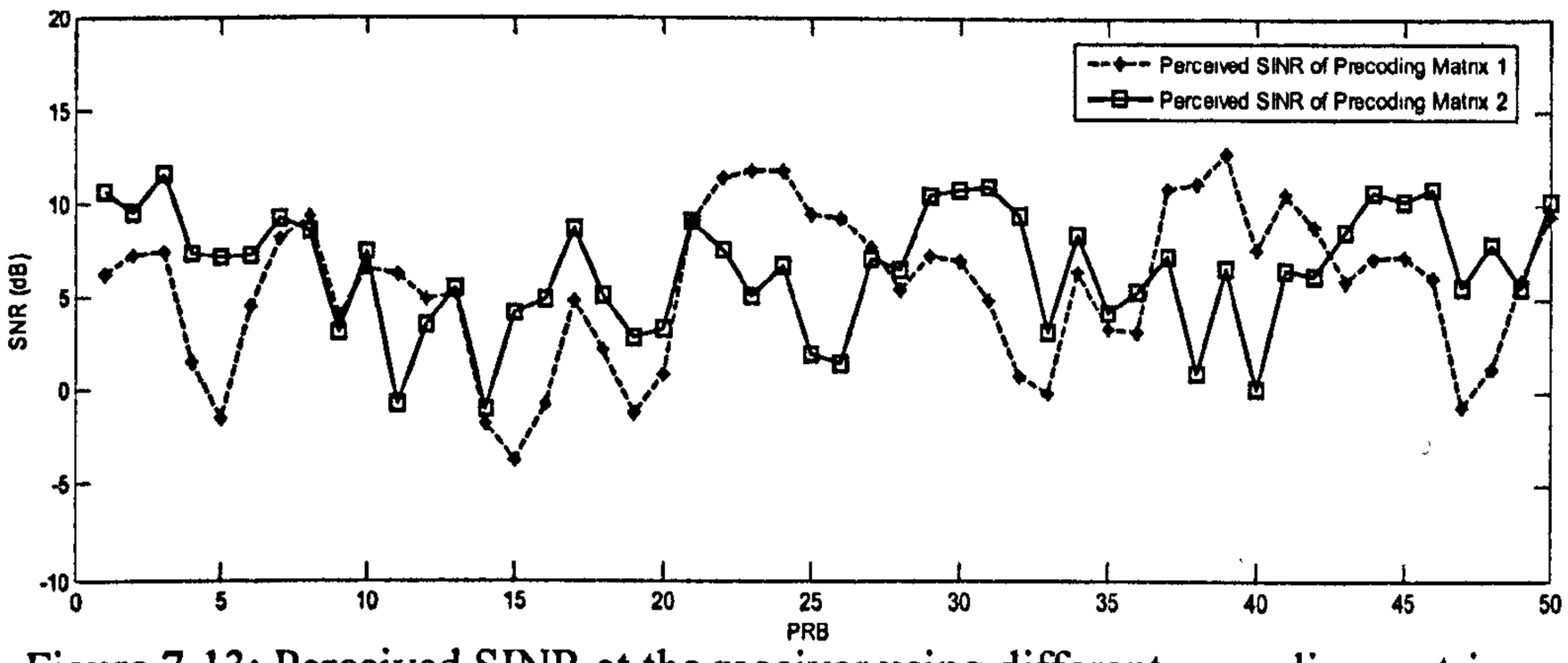

Figure 7-13: Perceived SINR at the receiver using different precoding matrices

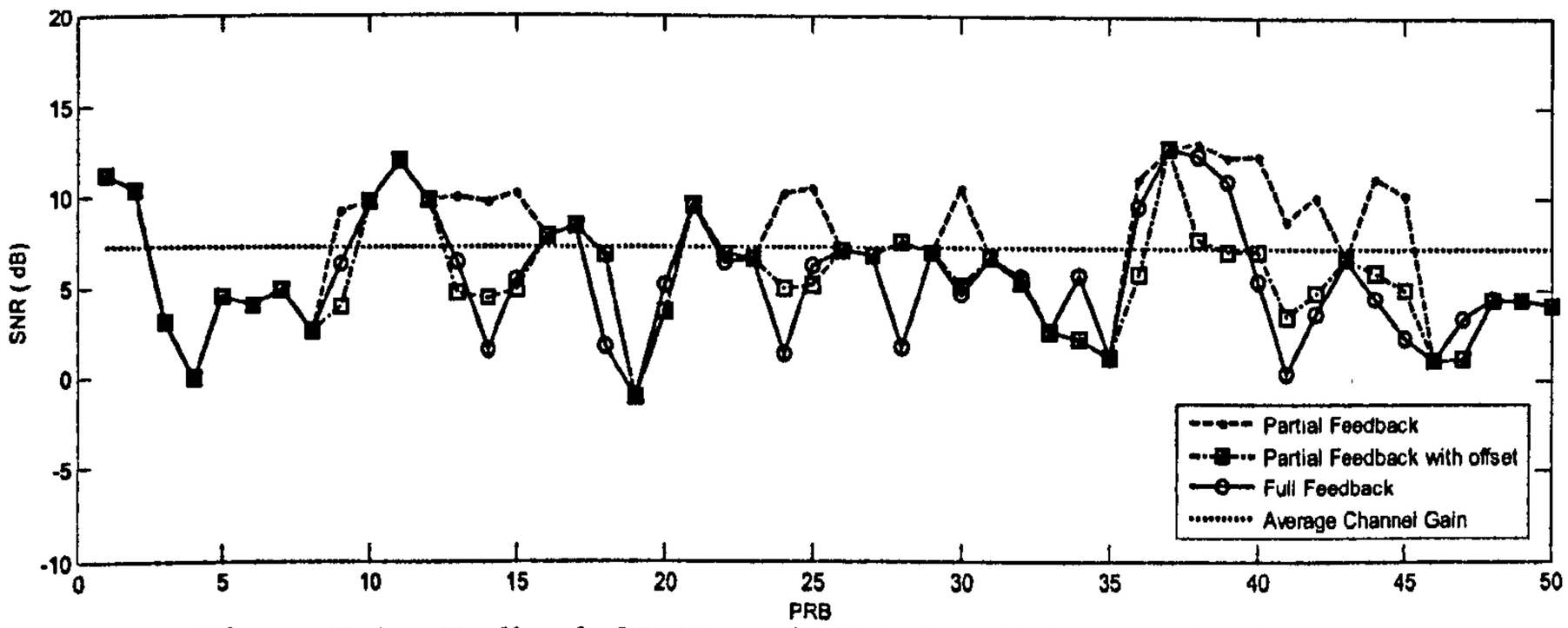

Figure 7-14: Fedback SINR at the BS for all feedback schemes

The fedback SINR of both the full feedback scheme and partial feedback scheme of a user are shown in Figure 7-14. From the figure, it can be seen that when the preferred matrix of the user matches the chosen precoding at the BS, the feedback SINR will be identical. However, when the preferred precoding matrix of the user is different, the SINR feedback will be inaccurate and usually overly high, especially for feedback which is higher than the average mean of the SINR. Thus a modified partial feedback scheme is proposed [22] at the BS where the fedback SINR is reduced by an offset value when the preferred precoding matrix of a user is different from the chosen precoding matrix and higher than the mean of the SINR:

$$SINR_{m'} = SINR_m - offset \qquad \forall SINR_m \geq \bar{x} \tag{7-12}$$

Several offset values are considered and simulated in the LTE downlink simulator. An example of the offset value of 3dB is shown in Figure 7-14. As can be seen from the figure the offset SINR matches quite well to the actual SINR.

7.4.4 Performance analysis of the modified Partial Feedback scheme

Ideally, in order to maximise the system capacity, users with the highest SINR for each stream will be selected. However, QoS and fairness constraint issues need to be taken into consideration. Therefore, a dynamic sub-carrier (sub-channel) allocation (DSA [12] [24]) algorithm is considered where this sub-optimal but low complexity algorithm approximately maximises the capacity given the equal resource constraint. Although the DSA algorithm achieves less throughput gain than a greedy algorithm, its equal resource constraint ensures short and long term fairness among all the users.

Figure 7-15 shows the PER performance of various MIMO schemes for the QPSK ½ rate transmission mode. From the figure, it can be seen that the performance of the DSA algorithm is slightly compromised compared to greedy algorithm that was shown in Figure 7-8. The slight degradation is expected as the DSA algorithm ensures fairness among all the users while maximising the throughput. The greedy algorithm, on the other hand does not take into account fairness or any QoS constrains.

From Figure 7-15, it can be seen that the PER performance of SU-MIMO with DSA is approximately 4dB better than the SU-MIMO with RSA, where no multiuser diversity can be exploited. MU-MIMO DSA with a full feedback scheme is approximately 2 to 3 dB better than the SU-MIMO DSA. The significant additional gain of the MU-MIMO is attributed to the ability to exploit both the spatial and spectral multi-user diversity gain. The full feedback scheme is superior to the partial feedback scheme due to the complete CQI information of all the streams at the scheduler. As the SNR increases, the effect of inaccurate CQI information of the partial feedback scheme becomes more obvious.

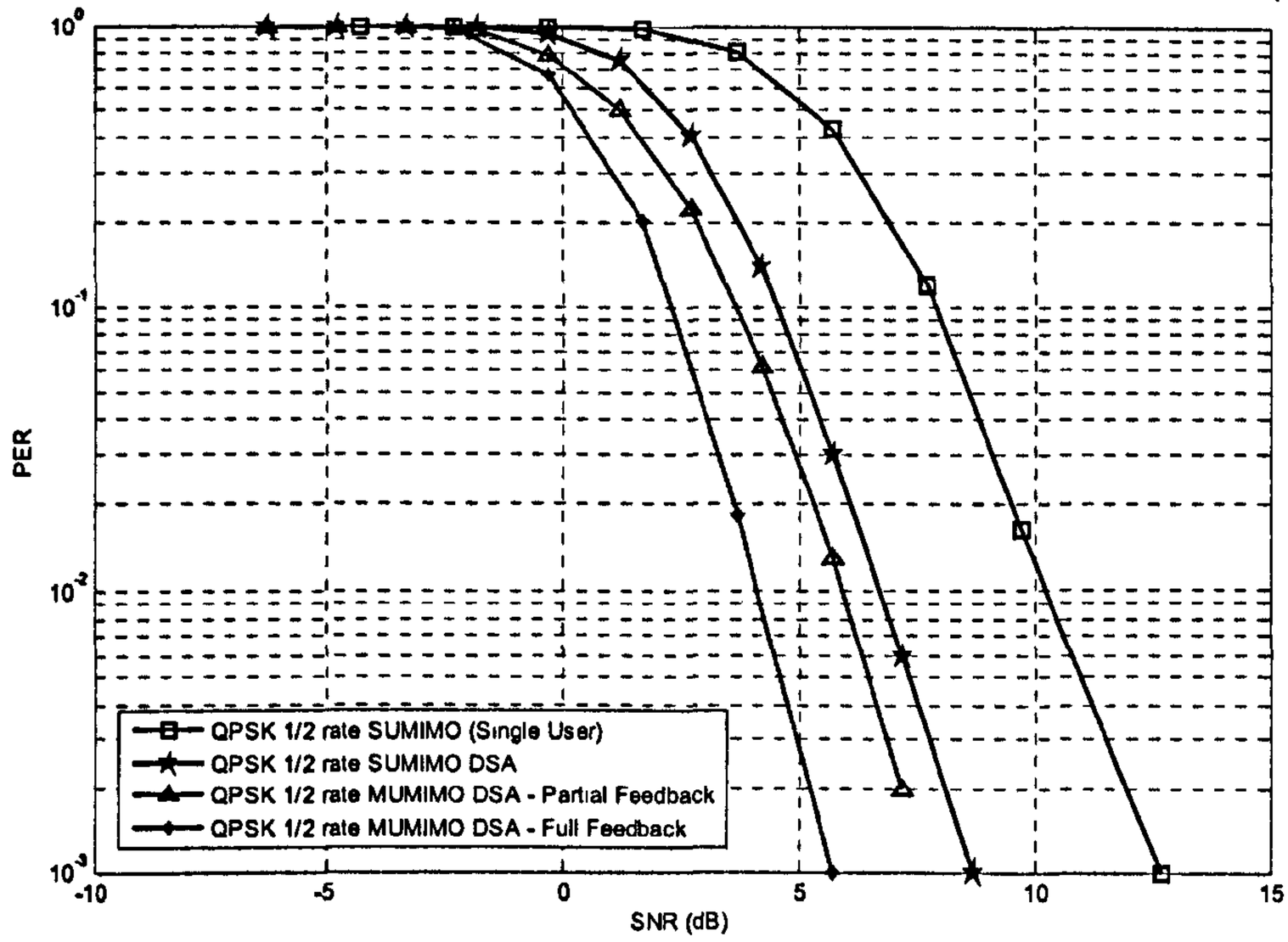

Figure 7-15: PER performance of MIMO schemes for SCM Urban Macro at QPSK ½ rate

Figure 7-16 shows the PER performance of the proposed modified partial feedback scheme in QPSK ½ rate transmission mode. Several offset values are simulated and shown in the figure. As seen from the figure, the performance of the offset value of 3dB achieves the best performance among all. The performance of the partial feedback scheme with offset value of 3dB is only 0.5dB worse than the full feedback scheme but is 1.5dB better than the conventional partial feedback scheme at PER of 10^{-2}. The gain is significant considering that no additional feedback is required compared to the conventional partial feedback scheme but the performance is close to the full feedback scheme.

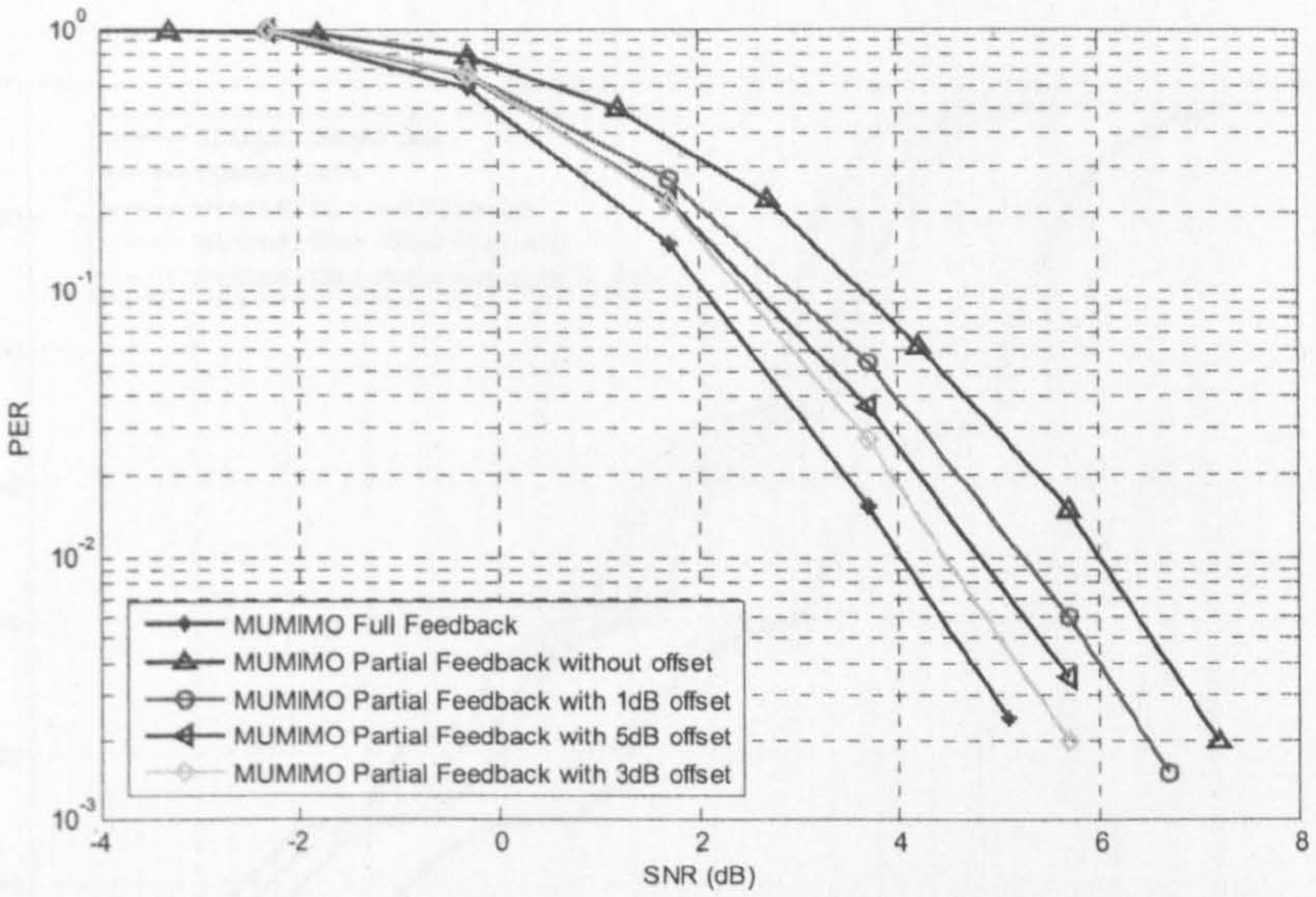

Figure 7-16: PER performance of Modified Partial Feedback Scheme

In addition, the throughput performance of various schemes is also investigated. The achievable throughput is given by: Throughput = R(1-PER), where R and PER are the bit rate and the packet error rate for a specific mode respectively. Similarly to the previous section, the throughput envelope is obtained by using ideal adaptive modulation and coding (AMC) based on the optimum switching point.

The average achievable throughput for various MIMO schemes in an urban macro scenario are presented and compared in Figure 7-17. From the figure, it can be seen that the SU-MIMO DSA scheme shows significant improvement over the SU-MIMO RSA scheme across the entire SNR range. In particular, more diversity gain can be obtained at the high SNRs. It can also be seen that the average throughput of the MU-MIMO with full feedback scheme is superior to all other schemes. MU-MIMO DSA with partial feedback is only marginally better than the SU-MIMO DSA. However when the modified partial feedback scheme is employed, the throughout performance comes close to the MU-MIMO full feedback scheme throughput the whole SNR range.

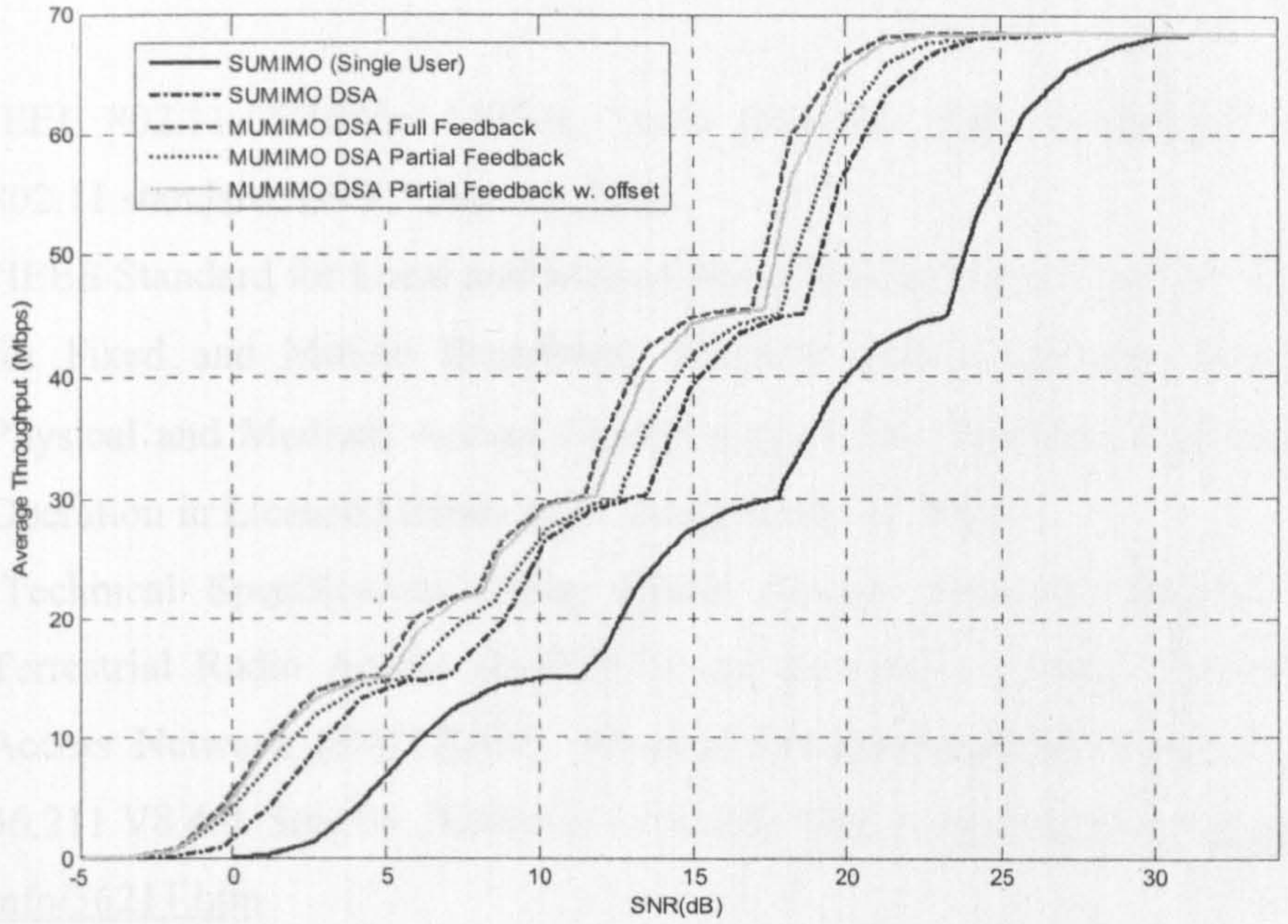

Figure 7-17: Average Throughput for different feedback schemes

7.5 Conclusion

In this chapter, a thorough analysis of LTE downlink including codebook based unitary precoding has been presented. Simulation results have shown that the performance gain of unitary precoding in a conventional single user MIMO scenario is limited. When spectral and multi-user diversity are exploited, significant gains can be achieved. Additional diversity in the spatial domain can be achieved when the same time-frequency resources are shared among different users. MU-MIMO SM with full feedback achieves superior performance to all other schemes but at the cost of higher signalling overhead and scheduling complexity. The MU-MIMO downlink transmission can achieve a significant gain due to the ability to exploit both the spectral and spatial diversity gain.

However in order to fully exploit both the diversity gains, intensive signalling overhead is needed. The MU-MIMO with partial feedback scheme is proposed in the literature due to the ability to trade-off between the performance and signalling overhead. However, the performance of the MU-MIMO partial feedback scheme is compromised. Thus in this chapter, a modified partial feedback scheme is proposed. By offsetting the received CQI, the proposed partial feedback scheme is able to achieve a good performance that is close to the performance of the full feedback scheme but without any additional signalling overhead.

References

[1] IEEE 802.11-05/1095r4,1102r4, "Joint proposal: High throughput extensionto 802.11 standard: PHY," Jan. 13, 2006.

[2] "IEEE Standard for Local and Metropolitan Area Networks, Part 16: Air Interface for Fixed and Mobile Broadband Wireless Access Systems, Amendment 2: Physical and Medium Access Control Layers for Combined Fixed and Mobile Operation in Licensed Bands and Corrigendum 1," 2005.

[3] 'Technical Specification Group Radio Access Network; Evolved Universal Terrestrial Radio Access (E-UTRA) and Evolved Universal Terrestrial Radio Access Network (E-UTRAN): Physical Channels and Modulation', 3GPP TS 36.211 V8.4.0, Sept 08. [Online]. Available: http://www.3gpp.org/ftp/Specs/html-info/36211.htm

[4] Jiann-Ching Guey; Larsson, L.D., "Modeling and evaluation of MIMO systems exploiting channel reciprocity in TDD mode," *Vehicular Technology Conference, 2004. VTC2004-Fall. 2004 IEEE 60th* , vol.6, no., pp. 4265-4269 Vol. 6, 26-29 Sept. 2004

[5] D.J. Live, et. al., 'An Overview of Limited Feedback in Wireless Communication Systems', *IEEE Journal on Selected Areas in Communications*, Vol. 26, No. 8, Oct. 2008, pp 1341-1365

[6] M.Costa, 'Writing on Dirty Paper', *IEEE Trans. Information Theory*, vol. 29, no. 3, May 1983, pp. 439 – 441

[7] T. Haustein, C.von Helmolt, E. Jorswieck, 'Performance of MIMO systems with channel inversion', *in Proceedings of Vehicular Technology Conference*, vol. 1, May 2002, pp. 35-39

[8] Q. H. Spencer, A. L. Swindlehurst, and M. Haardt, ' Zero-forcing methods for downlink spatial multiplexing in multiuser MIMO channels' *IEEE Trans. Signal Processing*, Vol. 52, no. 2, Feb. 2004, pp. 461-471

[9] R1-051353, Samsung, "Downlink MIMO for EUTRA," 3GPP RAN1 #43,. Seoul, Korea, November 2005.

[10] S. J. Kim, H. J. Kim, and K. B. Lee, "Multiuser MIMO Scheme for Enhanced 3GPP HSDPA," 11th European Wireless Conference 2005, Feb. 2005.

[11] David J.Love, Robert W. Health, ' Limited Feedback Unitary Precoding for Spatial Multiplexing Systems', *IEEE Transactions on Information Theory*, Vol. 51, No.8, August 2005

[12] Y. Peng , S. Armour , and J. McGeehan, 'An Investigation of Dynamic Subcarrier Allocation in MIMO–OFDMA Systems', *IEEE Transaction on Vehicular Technology*, Vol 56,pp. 2990-3005, 2007

[13] 'Technical Specification Group Radio Access Network; (E-UTRA) and (E-UTRAN): Physical Channels and Modulation', 3GPP TS 36.211 V8.4.0, Sept 08. [Online]. Available: http://www.3gpp.org/ftp/Specs/html-info/36211.htm

[14] S.Fang, L.Li, Q.Cui, P.Zhang, ' Non-Unitary Codebook Based Precoding Scheme for Multi-User MIMO with limited Feedback', *In proceedings of WCNC 2008*, pp 678-682

[15] David J.Love, Robert W. Health, Thomas Strohmer, ' Grassmannian beamforming for Multiple- Input Multiple-Output Wireless Systems,' *IEEE Transaction on Information Theory*, vol. 49, No. 10, Oct 2003, pp 2735-2747

[16] Eun Yong Kim, Joohwan Chun, ' Random beamforming in MIMO systems exploiting efficient multiuser diversity', *in Proceedings of Vehicular Technology Conference*, vol.1, 2005, pp 202-205

[17] C. Han, A. Doufexi, S. Armour, J. McGeehan, Y. Sun, "Random Beamforming OFDMA for Future Generation Cellular Communication Systems," *in Proc. IEEE 66th Vehicular Technology Conference*, Baltimore, USA, September 2007, pp. 516-520.

[18] D.J.Love, and R.W Heath,Jr., ' Equal gain transmission in multiple-input multiple-output wireless systems', *IEEE Trans. Commun.*, vol. 51, no.7, pp 1102-1110, July 2003

[19] S. Armour, et.al., 'Green Radio: Sustainable Wireless Networks: Addressing the Key Challenge of Designing Energy Efficient and Sustainable Wireless Networks for the Future', [Online]. Available: http://kn.theict.org/magazine/ratcit/communications/green-radio-article.cfm

[20] M. Nicolaou, C. Han, K. C. Beh, S. Armour, A. Doufexi, 'MIMO Techniques for Green Radio Guaranteeing QoS', *submitted to JCN Special Issue On Green Radio: Energy Efficiency In Wireless*

[21] K. C. Beh, C. Han, M. Nicolaou, S. Armour, A. Doufexi, "Power Efficient MIMO Techniques for 3GPP LTE and Beyond," *invited paper at special session on Green Radio at Vehicular Technology Conference*, Alaska, September 2009

[22] K.C.Beh, S.Armour ,A.Doufexi, 'A Modified Partial Feedback scheme for Multi-User MIMO' *submitted to VTC 2010 Spring*

[23] Myeon-gyun Cho, Shik Kim, ' An efficient CQI feedback schemes for Multi_user and Single-user MIMO/OFDMA systems', *IEEE International Conference on Wireless and Mobile Computing*, pp. 104-105, Oct. 2008

[24] A.Doufexi, S. Armour 'Design Consideration and Physical Layer Performance Results for a 4G OFDMA System employing Dynamic Subcarrier Allocation', *in Proceedings of Personal, Indoor and Mobile Radio Communications (PIMRC)*,Berlin, September 2005, pp. 351-361

[25] R1-071104, "Uplink Overhead for CQI and MIMO Feedback in E-UTRA', Huawei, RAN1 meeting #48, St. Louis, USA, February, 2007

[26] S.Sesia, I.Toufik, M.Baker, ' LTE The Long Term Evolution: From Theory to Practice,' John Wiley & Sons Ltd., 2009, pp243-282

[27] Y.Li,J.Chuang, N.Sollenberger, ' Transmitter Diversity for OFDM Systems and Its Impact on High Rate Data Wireless Networks', *IEEE Journal on Selected Areas in Communications*, Vol. 17, pp. 1233-1243, July 1999

[28] P.Mogensen, et. al. , 'LTE Capacity compared to the Shannon Bound', *in Proceedings of Vehicular Technology Conference*, April 2007 , pp. 1234-1238

[29] S.Benedetto, G.Montorsi, 'Unveiling turbo codes: some results on parallel concatenated codingschemes', *IEEE Transaction on Information Theory*, vol. 42, March 1996, pp 409-428

[30] E. Dahlman,S. Parkvall, J. Skold, P. Beming,' 3G Evolution: HSPA and LTE for Mobile Broadband', Academic Press, 2008

[31] K.Zhang and Z.Niu, 'Multiuser MIMO Downlink Transmission Over Time-Varying Channels', *Proc. in International Conference on Communications*, June 2007, pp 5514-5518

[32] J.Zhu, J.Liu, X. She, L.Chen, ' Investigation on Precoding Techniques in E-Utra and Proposed Adaptive Precoding Schemes for MIMO Systems', *in Proc. of Asia Pacific Conference on Communications*, Oct 2008, pp1-5

Chapter 8

Conclusion

The world of communication is moving at a rapid pace. LTE was first conceived in 2004 and the feasibility studies started soon after. Over the past few years, attention and contributions from both industry and academia had been overwhelming. At the end of 2008, LTE specifications were finalized and frozen to be released as 3GPP *Release 8*. Several key players in cellular communications such as Ericsson and Samsung will be producing world first LTE equipment in the year 2010. It took only 6 years from the conception to the commercial deployment, which is a relatively short cycle compared to the previous generations. It is astonishing how telecommunications experts from all over the world are working together and making this possible in such a short period.

Most of the work in this thesis encompasses LTE, especially in the aspect of scheduling and resource allocation. While the signalling to support the scheduling is specified in the standard, the choice of the scheduling algorithm is not. This allows for operator specific algorithms to be developed which can be optimized for different scenarios and purposes. Thus it is intended that the output of this thesis could be helpful to the development of mobile communication industry especially in the aspect of resource allocation and scheduling in LTE.

This chapter will summarize the work that has been done over the past few years. Some key contributions of this thesis will be identified and presented. Lastly, some related work will be outlined for future consideration.

8.1 Summary of Work

This thesis started with a brief introduction of the development of mobile radio communication in Chapter 1. The evolution from the first generation to pre-4G system as

well as the timeline was described in detail. In addition, the motivation of the research in this thesis was also outlined.

Chapter 2 briefly described radiowave propagation and the associated fading characteristics. The discussion helps a reader to understand the selection of the physical transmission technique that is being used in LTE. Besides that, the 3GPP Spatial Channel Model Extension (SCME) was briefly described and this channel model was used throughput the thesis. This channel model is one of the most commonly used channel model to evaluate a 3GPP platform.

In addition to that, the channel capacity of SISO and MIMO channels were presented. It was also shown how the spatial correlation can affect the MIMO channel capacity. At the end of Chapter 2, the potential gain of a multiuser system was analysed. When there is more than one user in a wireless system, multiuser diversity gain can be achieved. Significant multiuser gain can be achieved in Rayleigh fading channels when there are sufficient users in the system and the CSI information is available at the transmitter.

In Chapter 3, an overview description of LTE was first given. A simulator was developed in Matlab to simulate the performance of the LTE downlink. A detailed description of each module of the simulator was given. Through complex simulation and rigorous investigation, the downlink performance of an LTE OFDM system was presented. Considering a highest modulation and coding scheme of 64QAM ¾ rate, a maximum spectral efficiency of 3.78dbits/Hz/s can be achieved at an average SNR of 27dB in a SISO scenario. However the spectral efficiency of 3.78bits/Hz/s could not meet the required peak data rate of LTE, therefore MIMO techniques need to be included.

Another important topic considered in Chapter 3 is Hybrid ARQ. Several Hybrid ARQ techniques were described and evaluated for the LTE downlink. Simulation results showed that the full incremental redundancy scheme offers the best throughput performance and outperforms the partial incremental redundancy and Chase Combining schemes. However, the gain comes at the cost of higher memory requirement. Simulations also showed that an advanced retransmission technique which adopts frequency diversity and constellation diversity can provide an enhancement to the conventional Hybrid ARQ technique. In particular, the simulation results showed that the Chase combining scheme can exploit most diversity gain from frequency diversity and

constellation diversity and that this leads to a narrower gap in term of performance compared to the incremental redundancy schemes.

The performance analysis in Chapter 4 has shown that it is important to consider the underlying HARQ operation in order to optimise the mapping between SNR and MCS. The proposed mapping has shown a significant improvement especially in the case of the full incremental redundancy scheme. In addition to that, simulation results have shown that a modified proportionally fair scheduler which incorporates retransmission information to compute a more accurate effective data rate outperforms a conventional proportionally fair scheduler.

In addition, the potential gain achievable through joint scheduling in both frequency domain and time domain to exploit diversity in both domains has been investigated for LTE with HARQ. Simulation results have shown that joint time frequency proportionally fair schedulers achieve significant improvements in performance compared to a frequency-blind, time-domain-only proportionally fair scheduler. For the scenario considered, in order to balance the diversity gain from both time and frequency domains, approximately 50-70% of all multiplexing users should be selected to transmit in each time slot to best exploit the diversity available in the time and frequency domains. Two variants of a combination of proportionally fair scheduling in time and frequency domains achieve good performance in terms of both throughput and fairness. The proposed combination of time domain proportionally fair and frequency domain dynamic allocation scheme achieves similar fairness but superior throughput.

In chapter 5, two low complexity dynamic resource allocation algorithms based on a maximal ratio weighted metric were proposed and evaluated in the downlink of 3GPP LTE system. The proposed algorithms eliminate the need to perform sort and swap iterations and therefore the complexity of the algorithms are greatly reduced. The computational complexity is as low as DSA algorithm but with considerable performance enhancement. Simulation results showed that the proposed allocation algorithms can achieve a near optimal performance, similar to the iterative algorithm (MGSS) but with much lower computational complexity.

An analytical model was presented to derive the optimal threshold for a 1 bit feedback scheme for users with Rayleigh distributed fading channels. This model can be easily extended to a more general class of fading distributions. Simulation results have shown a

perfect match with the analytical model. In addition to that, it was observed from the simulation results that the proposed algorithms were also less susceptible to the 1 bit feedback scheme and performed better than other sub-optimal schemes e.g. MGSS.

Chapter 6 presented a detailed link level simulation for two MIMO techniques, SFBC and SM. SFBC is a transmit diversity technique which aims to increase the reliability and robustness of a transmission. SM on the other hand aims to increase the spectral efficiency by transmitting independent data streams over the spatial layers. From the simulations results, it was shown that SFBC performs exceptionally well at low SNRs. However at higher SNRs, parallel data streams transmission of the SM begins to overshadow the diversity gain of the SFBC. Simulation results showed that the SM outperforms the SFBC to achieve a better throughput performance at approximately 20dB SNR. However, it was shown that SM is more vulnerable to the spatial correlation of the channels. Therefore, for highly correlated spatial channels, the crossover point for two the MIMO techniques is increased to 28dB in the SCM urban macro scenario.

In addition to that, the performance of several hybrid ARQ schemes was also presented in a MIMO scenario. It was shown that incremental redundancy schemes remain the best option for LTE due to the significant gain that can be achieved, especially at high modulation and coding schemes. It is also worth noting that simulation results have shown that SFBC achieved less diversity gain from the retransmission mechanism than SM due to the diversity exploiting nature of the SFBC scheme.

Chapter 7 presented a thorough analysis of LTE downlink with codebook based unitary precoding. Simulation results showed that the performance gain of unitary precoding in a conventional single user MIMO scenario is limited. However, a significant gain can be achieved when multi-user diversity is exploited. Further gain can be achieved in MU-MIMO when additional diversity gain in spatial dimension can be achieved. Two feedback schemes were considered. MU-MIMO with full feedback achieved a better performance than the partial feedback scheme but the gain came at a cost of higher signalling overhead and scheduling complexity.

The MU-MIMO with partial feedback scheme is proposed in the literature due to the ability to trade-off between the performance and signalling overhead. However, the performance of the MU-MIMO partial feedback scheme is compromised especially for a small number of users. A modified partial feedback scheme was proposed. By offsetting

the received CQI, the proposed partial feedback scheme was shown to achieve a good performance that is close to the performance of the full feedback scheme but without any additional signalling overhead.

8.2 Key Contributions

- A detailed performance analysis of the physical layer of LTE downlink [1] has been presented. The performance analysis is useful in helping the design of the link budget, network planning, and resource management. The analysis also enables a comparison with other wireless standards such as WIMAX and etc.

- A detailed performance analysis of several popular HARQ schemes [1] has been performed in the downlink of LTE. The analysis includes the SISO and MIMO scenarios. The performance analysis of the HARQ in different scenarios helps to optimize the transmission parameters in the base station. An advanced scheme incorporating frequency diversity and constellation diversity was also suggested. In addition to that, the performance analysis of the HARQ leads to a modified proportionally fair scheduler which can further improve the system throughput.

- A joint time-frequency domain scheduler is proposed [2][7]. The proposed scheduler combines a proportionally fair scheduler in the time domain with an aggressive frequency domain resource allocation algorithm. The proposed scheduler can perform better than a time domain only scheduler and a joint time-frequency scheduler which employs proportionally fair algorithm in both domains. The joint time frequency scheduler concept can be deployed with various resource allocation algorithms in the frequency domain to achieve different QoS requirements.

- Two heuristic resource allocation algorithms have been proposed [3] to maximise the throughput given an equal share constraint. The algorithms works exceptional well with a maximal ratio weighted metric and achieve a near optimal performance with low computational complexity.

- A detailed performance analysis on the performance of SU-MIMO and MU-MIMO in the downlink of LTE has been presented [4][5]. The simulation results

match with the theoretical expectation and provide a good reference for comparison purposes.

- A modified partial feedback scheme for MU-MIMO has been proposed [6]. The proposed algorithm exploits the difference of the received SINR of different precoding matrices. The modified algorithm can achieve a good performance that is near to the full feedback algorithm.

8.3 Future Work

Due to time constraint, there is some interesting work that cannot be accomplished in the limited time frame. In this section, some related work is outlined for possible future work.

- Further performance analysis can be done in spatially correlated channels for MU-MIMO scheme. It is envisaged that more gain can be obtained in comparison to the SU-MIMO in an uncorrelated scenario due to the ability of MU-MIMO scheme to avoid transmission at the weaker spatial layers. Further analysis in spatially correlated channels would better justify and quantify the gain of MU-MIMO.

- Cyclic Delay Diversity (CDD) is another feature that is new to LTE. CDD transmits the same set of OFDM symbols on the same set of OFDM subcarriers from multiple transmit antennas, however with a different delay on each antenna. Therefore, each subcarrier will experience a different beamforming pattern and diversity can be achieved due to frequency selectivity. It is expected the CDD will improve the performance of spatial multiplexing scheme especially in spatially correlated channels. Further analysis would help to better evaluate the throughput performance of LTE system.

- Performance analysis has shown that significant performance gain in dB can be achieved by the MU-MIMO scheme. However, further work can be done in term of defining the gain of MU-MIMO with a more useful metric. Our early work [8] uses an Energy Consumption Gain (ECG) metric [9] as a comparison metric. Further analysis is needed to define a more effective way of quantifying the

power consumption and power reduction by MU-MIMO or other transmission schemes.

- Another possible extension of the current work would be to further investigate the modified proportionally fair scheduler which takes into account the retransmission information. It was shown that significant gain can be achieved by considering the underlying HARQ scheme in the modified proportionally fair scheduler. However, it was further shown in Chapter 3 and Chapter 6 that different gain can be achieved in retransmissions for SISO, SFBC and SM schemes. Therefore, by adding different weights for different transmission schemes while calculating the effective rate for the proportionally fair scheduler, more gain cmight possibly be achieved.

- Several enhancements could be made to the current simulator. One of the assumptions that were made in the simulator is the static channel condition, which means that a channel response remains the same during a packet transmission. For future work, this could be extended to include a time varying channel model in the simulator. This would be helpful to better evaluate the performance of the pilot structure in LTE.

- To consider a more realistic scenario, a multi-cell scenario including inter-cell interference can be considered. Currently in the simulation model, only a single cell scenario is considered. By considering the multi-cell scenario, it could better model the throughput performance of the users in the cell edge. In addition to that, a sectorised cell can also be considered, with 3 sectors per cell be the possible option.

- LTE specifications were finalized and frozen to be released as 3GPP Release 8. However, LTE still does not qualify as a 4G system. In 2008, an extension to LTE was already proposed [10]. LTE-Advanced was proposed and several enabling technologies are suggested for the new release. Two important features that are proposed in the LTE-Advanced are support for relays and repeaters as well as support for coordinated multipoint transmission [11][12]. These features are currently still under intensive attention by the research community. By including these features, the scheduler design might become more complicated and challenging. This is an interesting direction for future work. It is hoped that

further work can help to incorporate the new features while maintaining if not exceeding the diversity gain that can be possibly achieved.

References

[1] K.C.Beh, A.Doufexi, S.Armour, 'Performance Evaluation of Hybrid ARQ Schemes of 3GPP LTE ODFMA System', *in Proceedings of International Symposium on Personal, Indoor and Mobile Radio Communications* (PIMRC), September 2007, pp 1-5

[2] K.C.Beh, S.Armour ,A.Doufexi, 'Joint Time-Frequency Domain Proportional Fair Scheduler with HARQ for 3GPP LTE Systems', *in Proceedings of Vehicular Technology Conference*, Calgary, October 2008, pp1-5

[3] K.C.Beh, A.Doufexi, S.Armour, 'A Low Complexity Dynamic Resource Allocation Algorithm for 3GPP LTE Based on a Maximal Ratio Weighted Metric with Limited Feedback', *in Proceedings of NEWCOM++/COST2100 Workshop on Radio Resource Assignment for LTE'*, Vienna, September 2009

[4] K. C. Beh, C. Han, M. Nicolaou, S. Armour, A. Doufexi, "Power Efficient MIMO Techniques for 3GPP LTE and Beyond," *invited paper at special session on Green Radio at Vehicular Technology Conference*, Alaska, September 2009

[5] K.C.Beh, A.Doufexi, S.Armour, 'On the Performance of SU-MIMO and MU-MIMO in 3GPP LTE Downlink', *in Proceedings of International Symposium on Personal, Indoor and Mobile Radio Communications* (PIMRC), Tokyo, September 2009

[6] K.C.Beh, S.Armour ,A.Doufexi, 'A Modified Partial Feedback scheme for Multi-User MIMO' *submitted to VTC 2010 Spring*

[7] C. Han, K. C. Beh, M. Nicolaou, S. Armour, A. Doufexi, 'Dynamic Resource Scheduling and Allocation Algorithms for LTE', *submitted to VTC 2010 Spring*

[8] M. Nicolaou, C. Han, K. C. Beh, S. Armour, A. Doufexi, 'MIMO Techniques for Green Radio Guaranteeing QoS', *submitted to JCN Special Issue On Green Radio: Energy Efficiency In Wireless*

[9] B. Badic, T. O'Farrell, P. Loskot, J. He, "Energy Efficient Radio Access Architectures for Green Radio: Large versus Small Cell Size Deployment," *IEEE VTC Fall*, September. 2009.

[10] Parkvall, S.; Dahlman, E.; Furuskar, A.; Jading, Y.; Olsson, M.; Wanstedt, S.; Zangi, K., "LTE-Advanced - Evolving LTE towards IMT-Advanced," *Vehicular Technology Conference, 2008. VTC 2008-Fall. IEEE 68th* , vol., no., pp.1-5, 21-24 Sept. 2008

[11] Sendonaris, A.; Erkip, E.; Aazhang, B., "User cooperation diversity. Part I. System description," *Communications, IEEE Transactions on* , vol.51, no.11, pp. 1927-1938, Nov. 2003

[12] Karakayali, M.K.; Foschini, G.J.; Valenzuela, R.A., "Network coordination for spectrally efficient communications in cellular systems," Wireless Communications, IEEE , vol.13, no.4, pp.56-61, Aug. 2006

Appendix A.1: Error Performance Analysis for Hybrid ARQ Schemes in Short Term Static Model

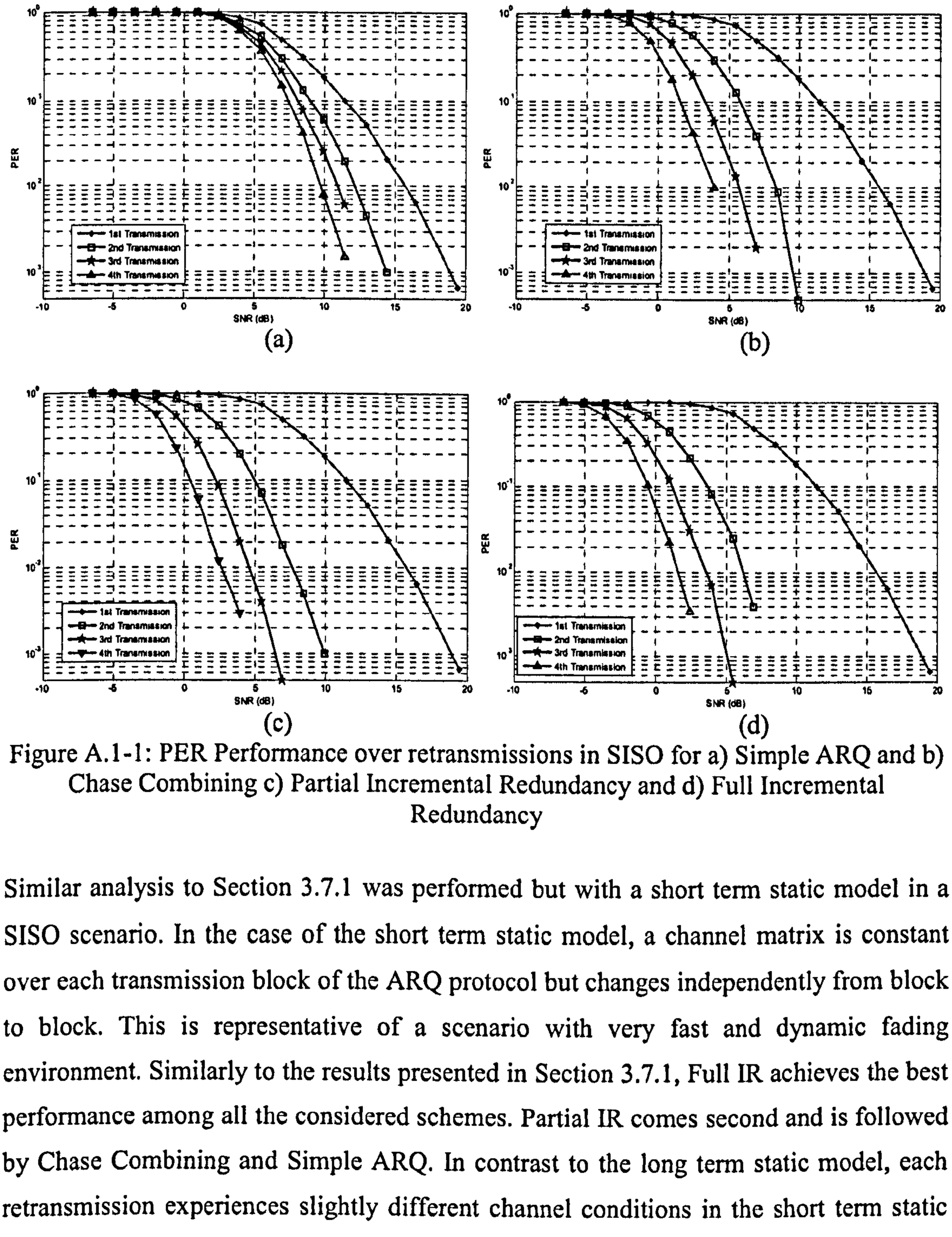

Figure A.1-1: PER Performance over retransmissions in SISO for a) Simple ARQ and b) Chase Combining c) Partial Incremental Redundancy and d) Full Incremental Redundancy

Similar analysis to Section 3.7.1 was performed but with a short term static model in a SISO scenario. In the case of the short term static model, a channel matrix is constant over each transmission block of the ARQ protocol but changes independently from block to block. This is representative of a scenario with very fast and dynamic fading environment. Similarly to the results presented in Section 3.7.1, Full IR achieves the best performance among all the considered schemes. Partial IR comes second and is followed by Chase Combining and Simple ARQ. In contrast to the long term static model, each retransmission experiences slightly different channel conditions in the short term static model. Therefore it is likely that a retransmission will occur at a better channel condition than the previous transmission. Thus in the short term static model, diversity in the time

domain can be observed on top of the soft combining gain and coding gain of the HARQ schemes. From Figure A.1-1, it can be seen that all the schemes achieve more performance gain in the retransmissions compared to the long term static models, particularly for Simple ARQ and Chase Combining schemes. Up to 5dB improvement can be observed in both the Simple ARQ and Chase Combining schemes. Having said that, Simple ARQ scheme is still much inferior to other schemes, as this scheme does not exploit any soft combining gain and coding gain. Nonetheless, the performance gap between Chase Combining scheme and incremental redundancy schemes is narrowed down to approximately 1-2dB.

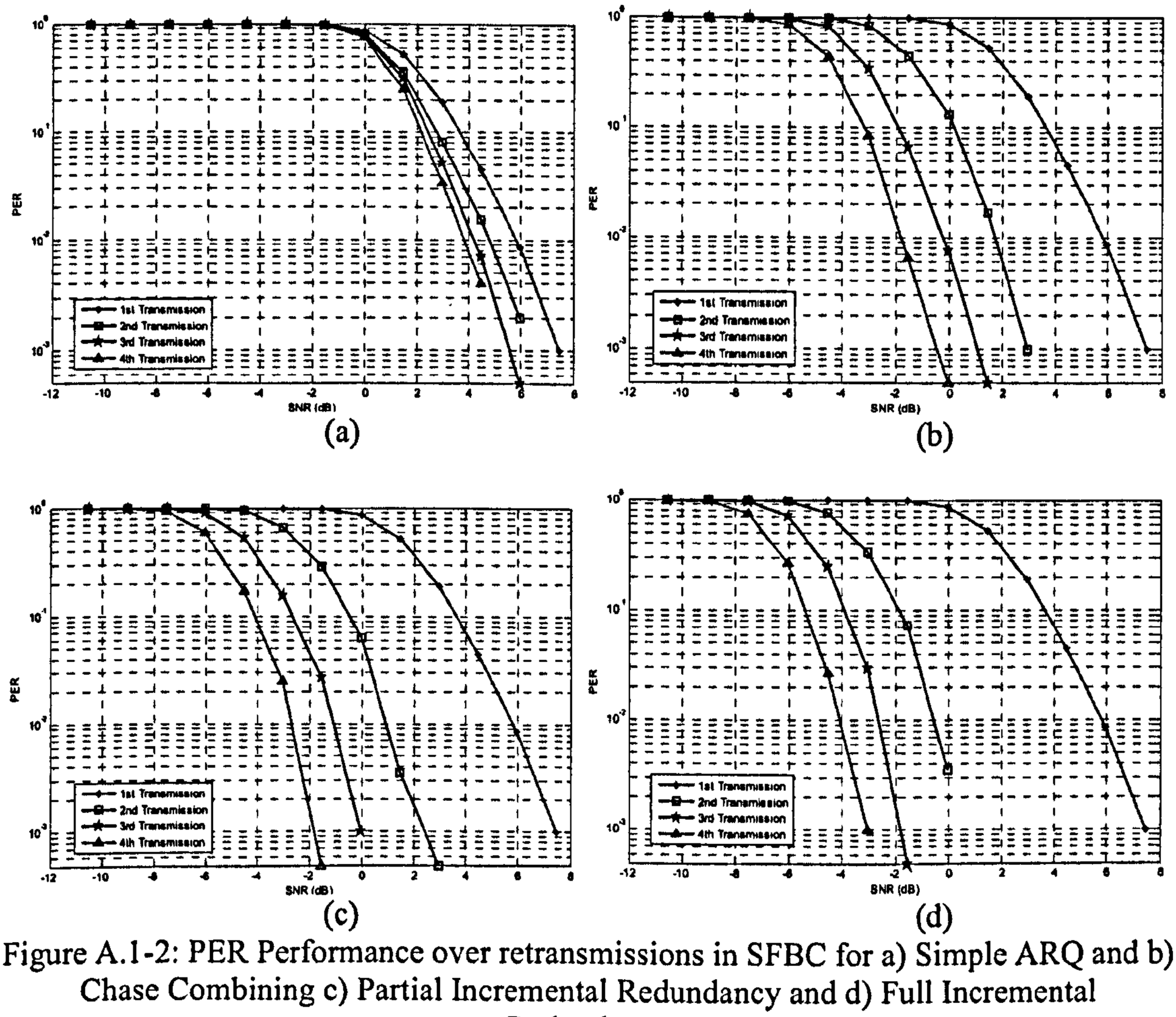

Figure A.1-2: PER Performance over retransmissions in SFBC for a) Simple ARQ and b) Chase Combining c) Partial Incremental Redundancy and d) Full Incremental Redundancy

Similar analysis is performed in MIMO scenarios, for both the SFBC and SM schemes. As it can be seen in from Figure A.1-2a-d, not much improvement can be observed in the short term static model for SFBC. Since the SFBC scheme (using Alamouti code) aims to maximise the diversity order, the additional diversity in the time domain (via

retransmissions) does not seem to further increase the performance significantly. Nevertheless, up to 1-2 dB can still be seen achieved.

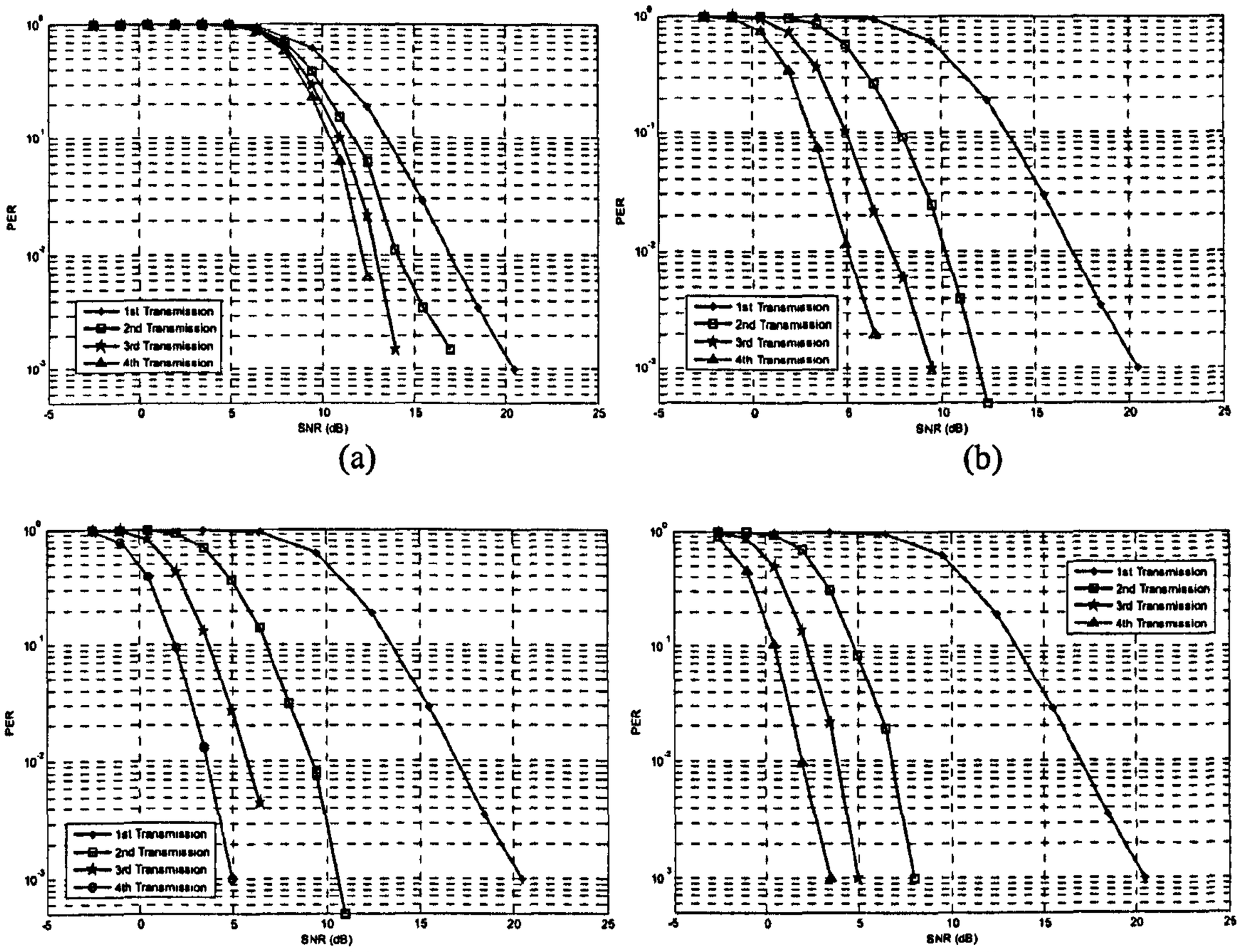

Figure A.1-3: PER Performance over retransmissions in SM for a) Simple ARQ and b) Chase Combining c) Partial Incremental Redundancy and d) Full Incremental Redundancy

On the other hand, significant gain can be observed by the SM scheme in the short term static model, as seen in Figure A.1-3. Simple ARQ achieves considerable improvement due to the time diversity gain that can be exploited in the retransmissions. Still the gain of Simple ARQ is limited due the inability to exploit soft combining and coding gain. Chase combining achieves a huge gain of up to 8dB in the short term static model in comparison to the long term static model. Both the incremental redundancy schemes achieve an additional of 1-2dB in the short term static model. The choice of incremental redundancy scheme is obvious since this scheme achieves better performance in different environments, be it a fast or slow changing environments.

Appendix A.2: Constellation Diagrams, CRC Polynomial Generator and Turbo Code Encoder

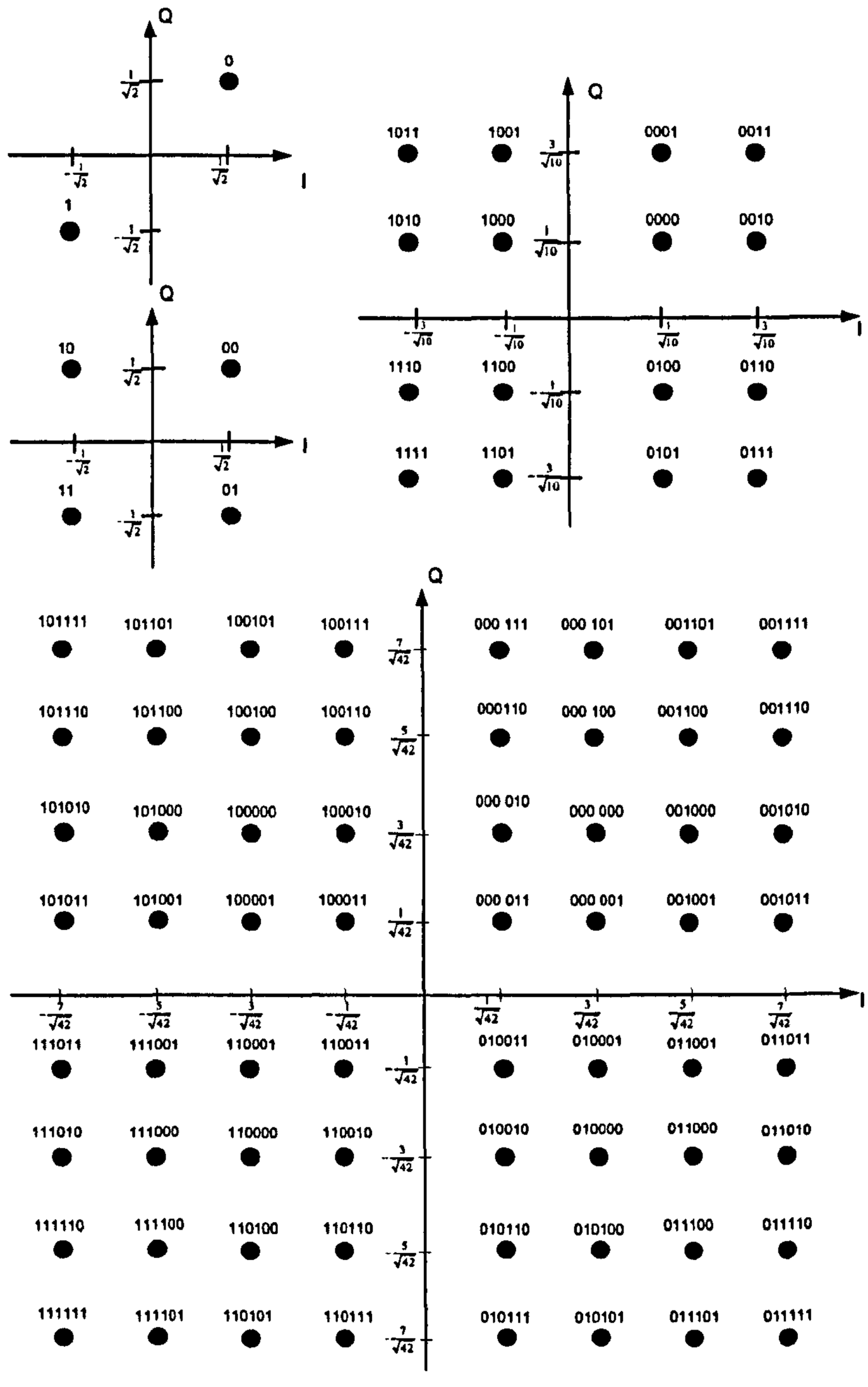

Figure A.2-1: BPSK, QPSK, 16QAM, and 64QAM constellation diagrams

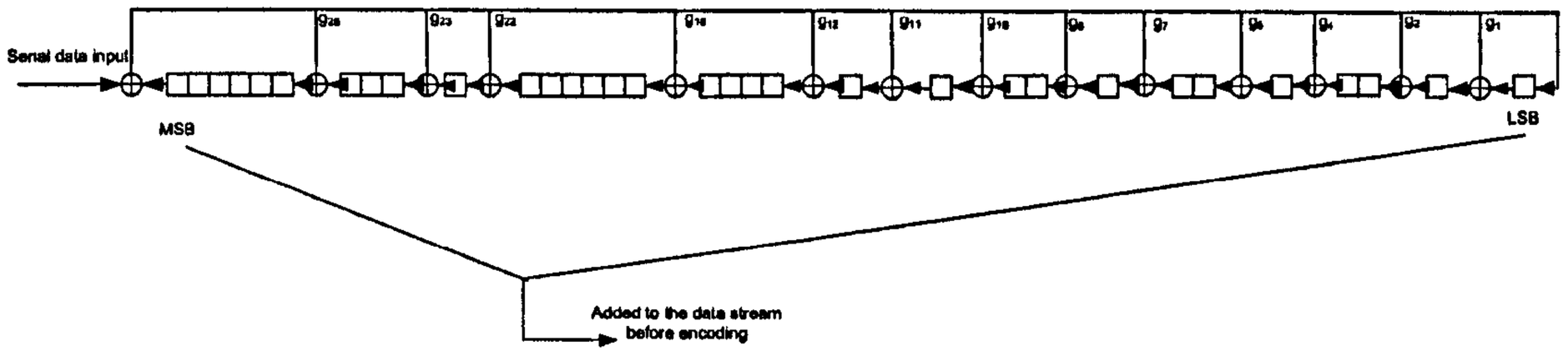

Figure A.2-2: CRC Polynomial Generator, $G(X) = x^{32} + x^{26} + x^{23} + x^{22} + x^{16} + x^{12} + x^{11} + x^{10} + x^8 + x^7 + x^5 + x^4 + x^2 + x + 1$

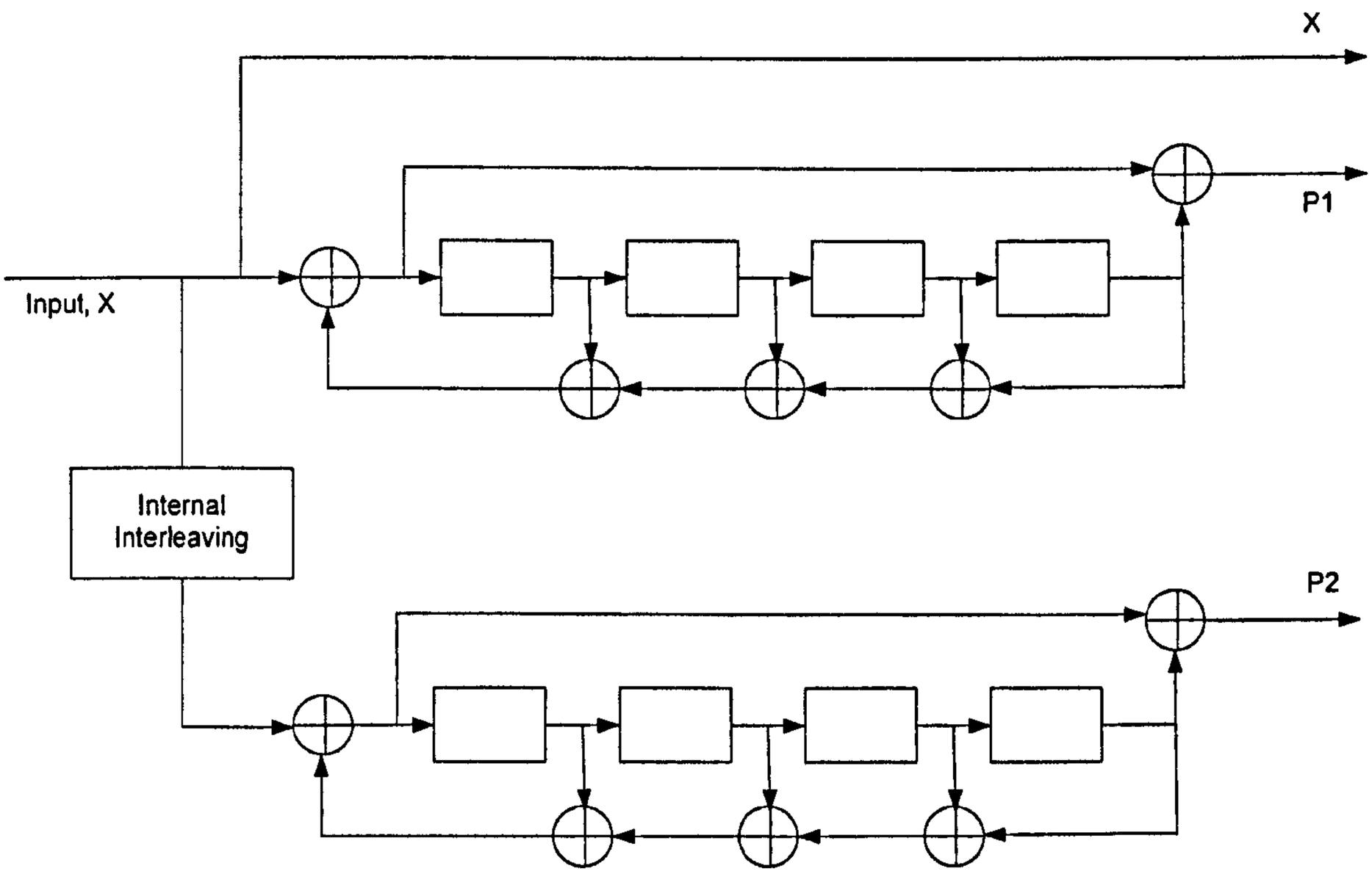

Figure A.2-3: Structure of the 1/3 rate Turbo Encoder

The structure of the Turbo encoder is shown in Figure A2-3. The RSC generator polynomial is [1 ,$G_1(D)/G_0(D)$] where $G_1(D)$ is $1+D^4$ and $G_0(D)$ is $1 +D1+D2+D3+D4$.

Appendix A.3: SNR Mapping Thresholds for Incremental Redundancy Schemes

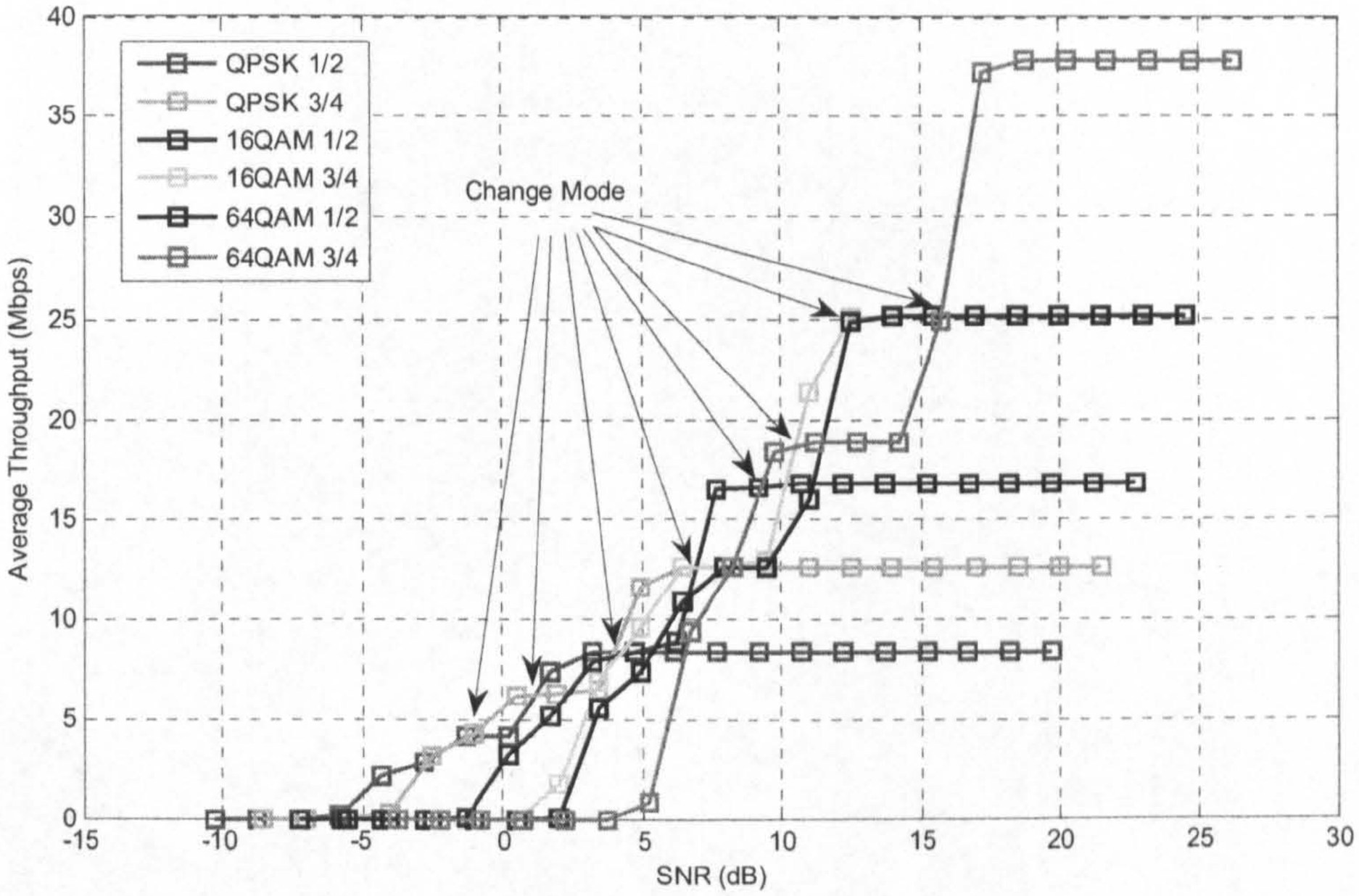

Figure A.3-1: Throughput performance for Partial Incremental Redundancy in AWGN

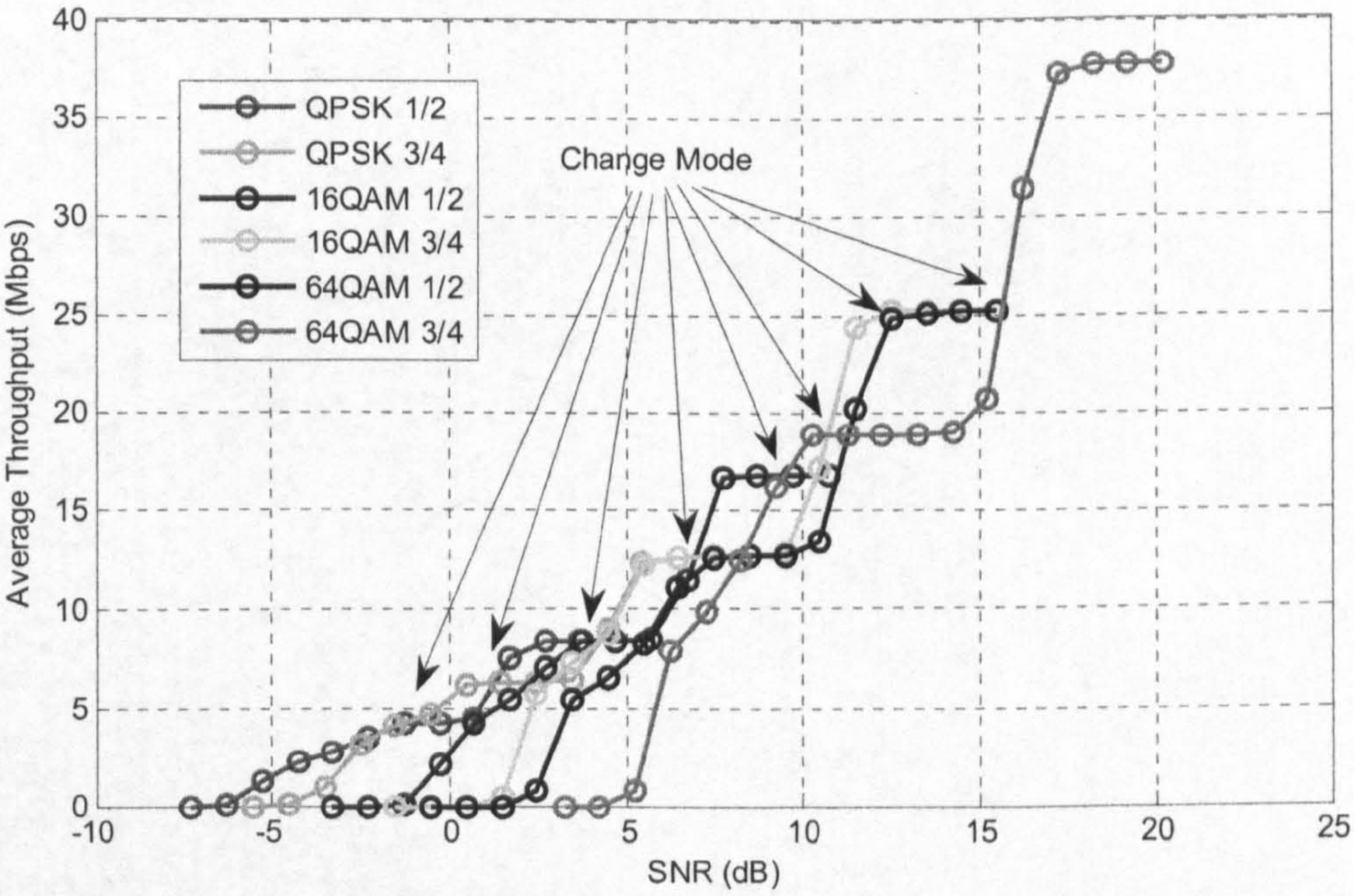

Figure A.3-2: Throughput performance for Full Incremental Redundancy in AWGN